UNIVERSITÀ
DI PAVIA

PhD IN BIOMEDICAL SCIENCES

DEPARTMENT OF BRAIN AND BEHAVIORAL SCIENCES

UNIT OF NEUROPHYSIOLOGY

Staphylococcus aureus iron-regulated surface determinant B (IsdB) protein interacts with von Willebrand factor and promotes adherence to endothelial cells

PhD Tutor: Giampiero Pietrocola

PhD dissertation of
Mariangela Jessica Alfeo

a.a. 2020/2021

TABLE OF CONTENT

ABSTRACT

Staphylococcus aureus is a major human opportunistic pathogen and the leading cause of life-threatening infections, including bacteremia, infective endocarditis, skin, and soft tissue infections. The burden of staphylococcal bloodstream infection has been notably increasing in industrialized countries and *S. aureus* now represents the most common cause of infective endocarditis (IE) worldwide.

In the early stages of infection, the bacterium needs to adhere to endothelial cells (ECs) which constitute the outermost layer of the heart and vessel wall. *S. aureus* has developed sophisticated mechanisms to attach to endothelial cells lining the heart and vessel wall and to the extracellular matrix exposed when the endothelium is damaged. For this purpose, the bacterium expresses a repertoire of cell wall-anchored (CWA) surface proteins that mediate adhesion to the tissue structures. The archetype of such interaction is the bacterial binding to endothelium under flow *via* von Willebrand factor (vWF), a large blood glycoprotein produced by endothelial cells and megakaryocytes and then stored in Weibel-Palade bodies (WPBs) and α-granules of platelets, respectively. The mature 2,050 amino acid long monomer consists of four homologous units which are arranged in the following sequence: D1-D2-D′-D3-A1-A2-A3-D4-B1-B2-B3-C1-C2-CK. Each domain can specifically bind several ligands. The D′D3 domain interacts with factor VIII, the A1 domain binds to the platelet GPIb receptor, heparin, and collagen type IV and VI, the A2 domain contains a cryptic cleavage site for ADAM13 protease, the A3 domain binds fibril-forming collagens I and III, and C1 is the binding domain for integrin αIIbβ3 and $\alpha_v\beta_3$ through an RGD motif. In the intracellular environment, vWF is organized in compact multimers stored in organelles called Weibel-Palade bodies. vWF multimerization is triggered by the sequential formation of disulfide bonds between C-terminal domains of two protomers leading to tail-to-tail homodimerization followed by disulfide linkage between N-terminal domains of adjacent dimers. Multimers secreted in the plasma may contain up to 40 subunits and can reach a length of around several micrometers. They adopt a globular conformation under normal blood flow conditions. Under high shear flow, multimers undergo a conformational change from a compact to a stretched configuration eventually leading to the exposure of cryptic binding sites for platelet recruitment and extracellular matrix proteins such as collagen.

Staphylococcal interactors of vWF have been found among both surface-exposed, *S. aureus* protein A (SpA), and secreted proteins, vWF binding protein (vWbp). Recently, a fibrinogen-binding protein named vhp, showing significant amino acid identity to vWbp, has been identified in *S. aureus*, but it remains to be determined whether vhp binds to vWF. SpA comprises a tandem array of five separately folded three-helical bundles, each of which can bind several ligands: the interface between helices 1 and 2 binds the A1 domain of vWF. SpA also binds the D'-D3 domain of vWF with lower affinity. vWbp is a multi-domain protein that interacts with a variety of ligands including prothrombin, fibrinogen, fibronectin, and Factor XIII. Importantly, this protein also binds the A1 domain of vWF via a 26 amino acid sequence

located in the C-terminal region. Under shear stress, the binary complex consisting of vWF and vWbp associates with the cell wall-anchored clumping factor A (ClfA). The resulting ternary complex is extremely stable, resisting forces in the 2nN range and mediates the anchoring of *S. aureus* to the blood vessel wall.

Adhesion of *S. aureus* grown in rich medium containing iron to host cells has been extensively studied. Conversely, the *S. aureus* pathophysiology *in vivo*, where the bacterium has restricted access to iron (the plasma iron concentration range is nearly 7-29 μmol/L), remains to be investigated. The deficiency of available iron *in vivo* leads to the upregulation of several genes including those encoding iron regulated-surface determinant (Isd) proteins. An important role of Isd proteins is to capture heme from hemoglobin (Hb) and transport it into the bacterial cell. The Isd system comprises four surface proteins (IsdABCH), a membrane ABC transporter (IsdEF), and two intracellular heme-degrading enzymes (IsdGI). The IsdABCH proteins contain up to three copies of a NEAr transporter (NEAT) motif: a single NEAT domain is present in IsdA and IsdC, whereas IsdB and IsdH contain two and three NEAT modules, respectively. The NEAT domains fold into a beta-sandwich and bind the haem iron atom through a conserved tyrosine located on the eighth beta-strand. Regarding IsdB, no structural data at atomic resolution are available, although the crystallographic structure of the IsdB/hemoglobin (Hb) complex indicates that IsdB has a dumbbell-like shape, with the two NEAT domains laying almost orthogonal to each other and joined by a highly flexible triple helix linker region. Each NEAT domain adopts the characteristic eight-strand immunoglobulin-like β-sandwich fold with a central 3_{10}-helix that forms a hydrophobic cavity. Notably, the two NEAT domains share low sequence identity (about 12%), in line with their known different molecular recognition properties. In fact, NEAT1 preferentially binds Hb, while NEAT2 is involved in heme extraction from the chains of Hb. The NEAT domain is highly conserved among Gram-positive pathogens, such as *S. lugdunensis*, *Streptococcus pyogenes*, *Bacillus anthracis*, and *Listeria monocytogenes*.

Besides acting as hemophores, IsdA, IsdB, and IsdH of *S. aureus* are known to have other biological activities. IsdA binds human proteins including fibrinogen and fibronectin, and is involved in the evasion of the host innate defenses in the skin. IsdH plays a role in *S. aureus* escaping phagocytosis through the inactivation of opsonin C3b. IsdB plays a role in binding to platelets via interaction with the integrin GPIIb/IIIa and promotes staphylococcal adherence to and internalization by non-phagocytic human cells. Furthermore, IsdB acts as a receptor for the host protein vitronectin (Vn) and Vn binding mediates adherence to and invasion of HeLa and HUVEC monolayers.

In this study, focusing on *S. aureus* SH1000 strain and using an array of biochemical assays, a new role as vWF-receptor was discovered for IsdB. A collection of purified recombinant ligand-binding domains of *S. aureus* CWA proteins were screened for the ability to interact with vWF through an ELISA assay.

This preliminary analysis revealed that IsdB NEAT1-NEAT2 has a vWF-binding activity comparable to that of SpA. When grown in iron starvation conditions, IsdB-expressing bacteria bound to both soluble and surface-coated vWF. Moreover, SH1000 WT strain was able to capture about 40% more vWF than a mutant depleted of *isdB*, suggesting that IsdB could have a fundamental role in the overall vWF capture by *S. aureus*.

The binding of recombinant IsdB to vWF was significantly blocked by heparin and reduced at high ionic strength. Furthermore, treatment with ristocetin, an allosteric agent promoting the exposure of the A1 domain in vWF, potentiates the binding of IsdB and IsdB-expressing bacteria to vWF. To verify the hypothesis of the A1 domain being the ligand-binding domain for IsdB on vWF, the isolated A1 domain was cloned and tested for interaction with full-length IsdB, as well as to NEAT1 or NEAT2 domain alone. Both near-iron transporter domains, NEAT1 and NEAT2, individually bound recombinant A1 with K_D values in the micromolar range, although NEAT2 showed a higher affinity for A1 than that observed for IsdB NEAT1-NEAT2 or NEAT1 domain. A structural model for the IsdB/A1 complex formation has been proposed based on the steric and electrostatic complementarity of the structures of the two proteins: the A1 seems to be embraced within NEAT1 and NEAT2, with each domain interacting with the electropositive face of the globular A1 domain *via* the electronegative surfaces in the concave dumbbell structure of IsdB NEAT1-NEAT2.

IsdB was shown to mediate *S. aureus* adhesion to endothelial cells, and this was significantly inhibited by a monoclonal antibody against the A1 domain of vWF, indicating that this ligand-binding domain has a key role in promoting the staphylococcal adherence to vascular endothelium through IsdB. Moreover, bacterial adhesion is blocked by anti-IsdB IgG isolated from patients with staphylococcal endocarditis, suggesting a possible application in immunological therapies to combat the *S. aureus* colonization/infection of the vascular system.

INTRODUCTION

I. *Staphylococcus aureus*

A. Classification and identification

Staphylococcus aureus is the most important pathogenic species of the *Staphylococcus* genus. Bacteria of this genus are typically non-motile, round-shaped, Gram-positive microorganisms, which are about 0.5 to 1.5 µm in diameter and are usually found in grape-like clusters (*Taylor & Unakal, 2020*). The genus name *Staphylococcus* was proposed by Sir Alexander Ogston, who first observed *S. aureus* in slide preparations of pus from post-operative wounds and abscess patients (*Ogston, 1881*). It derives from the Greek words staphylē, "grape", and kókkos, "granule", which means 'bunch of grapes', indicating how these bacteria often appear under the microscope after Gram staining. Later on, Rosenbach gave the formal description of the genus and named the bacteria *Staphylococcus aureus* because of the characteristic yellowish pigmentation of their colonies (*Rosenbach, 1884*), which is due to the production of staphyloxanthin, an orange-red triterpenoid carotenoid that functions as virulence factor and as an antioxidant, protecting bacteria against oxidative stress and the host immune response (*Clauditz et al., 2006; Liu et al., 2005*) (Fig.1).

S. aureus belongs to the phylum *Firmicutes*, class *Bacilli*, order *Bacillales*, family *Staphylococcaceae*, genus *Staphylococcus*. The genus comprises 57 species and 28 subspecies (https://lpsn.dsmz.de/genus/staphylococcus, accessed 06 April 2021). Aside from *S. aureus*, it also includes *S. epidermidis*, *S. hemolyticus*, *S. saprophyticus*, *S lugdunensis*.

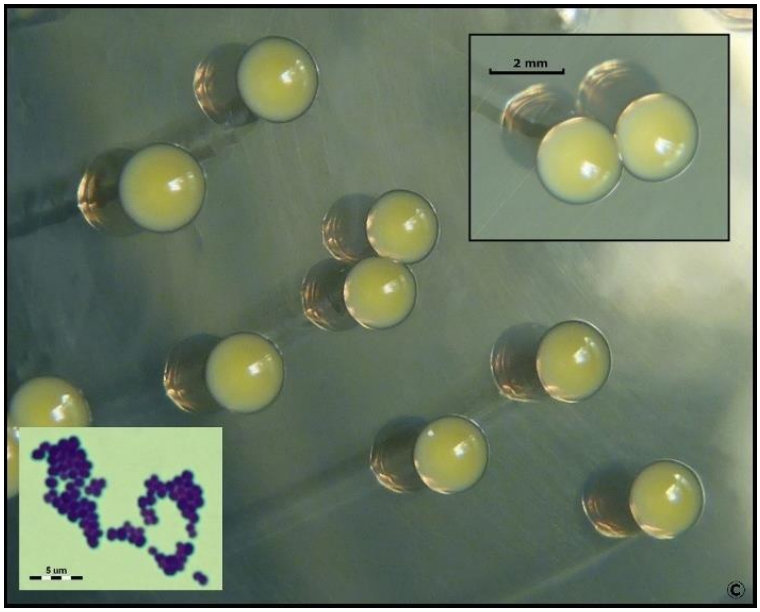

Figure 1. *Staphylococcus aureus*. Gram stain (bottom-left corner); *S. aureus* on Tryptic Soy Agar (TSA) plate, cultivation 24 hours at 37 °C: colonies appear golden-yellow.

1. Structure and morphology

S. aureus is characterized by an optional polysaccharide capsule, a cell wall, and a plasma membrane. Peptidoglycan is the basic component of the cell wall and makes up 50% of the cell wall mass (*Waldvogel et al., 1990*). Peptidoglycan is a large polymer that is constituted of glycan chains made of N-acetylglucosamine acid disaccharide subunits, in which the N-acetylmuramate moiety is linked to highly conserved pentapeptide or tetrapeptide stems consisting of alternating L- and D- amino acids (*Gotz et al., 2006)*.

S. aureus peptidoglycan is characterised by an L-lysine in position 3 of the stem peptide that is cross-linked via a pentaglycine interpeptide bridge. These multiple glycine residues in the cross-bridge cause susceptibility to lysostaphin *(Projan & Novick, 1997)*. Peptidoglycan is integral in the formation of the tight multi-layered cell wall network (Fig. 2), capable of withstanding the high internal osmotic pressure of staphylococci (*Wilkinson & Holmes, 1979*). Moreover, it plays a role in the inflammatory response by stimulating the production of proinflammatory cytokines and chemokines (TNF-α, IL-1β, IL-6, and IL-8) in monocytes and macrophages (*Heumann et al., 1994; Timmermann et al., 1993; Wakabayashi et al., 1991*).

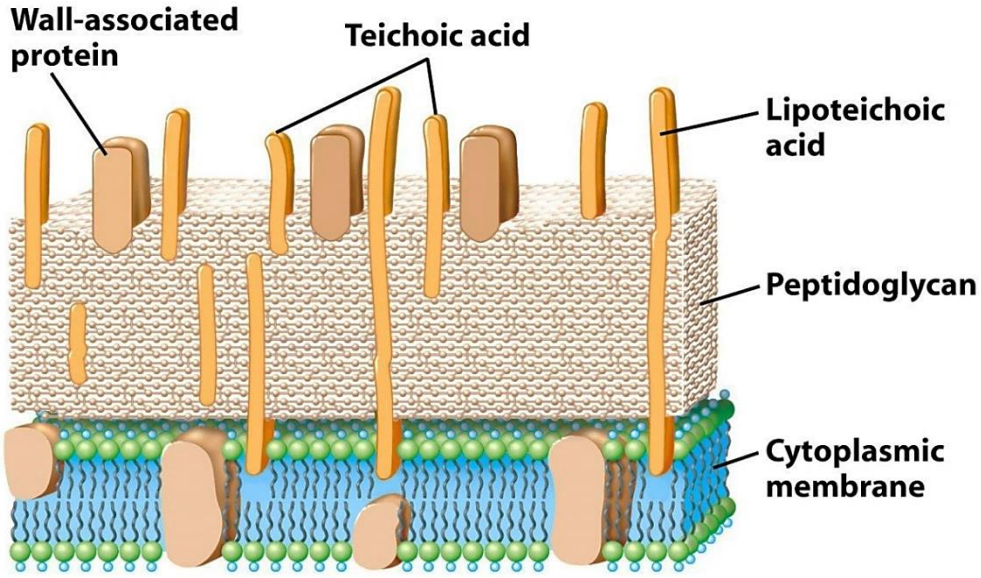

Figure 2. *Staphylococcus aureus* cell wall components and organization (*Madigan et al., 2015*).

The peptidoglycan of actively dividing cells is susceptible to lysostaphin, a glycylglycine endopeptidase that specifically cleaves the pentaglycine cross-bridges found in the staphylococcal peptidoglycan (*Schindler & Schuhardt, 1964*).

Another cell wall constituent is a group of phosphate-containing polymers called teichoic acids (TA), which contributes about 30-40% of cell wall mass (*Knox & Wicken, 1973*). Several crucial roles in *S. aureus* fitness and cell wall maintenance have been assigned to complex TA-polymers, which are either

covalently linked to peptidoglycan (Wall Teichoic Acids, WTA) or the cytoplasmic membrane (LipoTeichoic Acids, LTA) (Fig. 3). Both WTA and LTA are highly charged polymers that concentrate cations at the cell wall surface and associate with proteins to form complexes: they are involved in various biological activities such as cation balance, cell division and regulation of peptidoglycan autolysis (*Ruhland & Fiedler, 1990*).

Several studies have shown that WTA plays a role in host tissue adhesion, but their role in invasive infection and host inflammatory response is unclear (*Majcherczyk et al., 2003*). LTAs have been implicated in inflammation by triggering the release of cytokines by macrophages and other players of the innate immune system (*Deininger et al., 2003)*. Moreover, acting in synergy with peptidoglycan, it can cause septic shock and multiple organ failures (*De Kimpe et al., 1995*).

2. Biochemical and metabolic characteristics

Staphylococci are non-motile, aerobic, or facultative anaerobic microorganisms. They are extremely halotolerant, as they grow at up to 3.5 M NaCl, and they can survive over a broad range of temperatures (18°C to 40°C) (*Murray et al., 2020*). Relatively simple biochemical tests can be used to differentiate *S. aureus* and the other microorganisms.

Given that *S. aureus* is a Gram-positive bacterium, the basic biochemical test available is the Gram-stain, which is based on the differential structure of the cellular membranes and cell walls of the two main groups of bacteria, Gram-positive and Gram-negative. Gram-positive organisms contain a highly cross-linked layer of peptidoglycan that retains the primary dye, crystal violet (CV), following the application of the mordant, iodine (I). The iodine and crystal violet form a complex within the peptidoglycan. When decolourizer is applied to the cells, the CV-I complex remains within the cell, making it appear dark purple to blue (*Bartholomew & Mittwer, 1952*).

Staphylococci are classified into two main groups, «coagulase-positive» and «coagulase-negative» strains, based on the production of coagulase, a secreted zymogen interacting with and activating prothrombin, converting fibrinogen (FBG) into fibrin, and therefore causing clotting of plasma. Based on the coagulase test, it is possible to discriminate «coagulase-positive» staphylococci, the main representative of which is *S. aureus*, from «coagulase-negative» ones, the major representative of which is *S. epidermidis*.

S. aureus is a «catalase-positive» microorganism as well: the catalase test, which screens for the presence of catalase, an enzyme that breaks down hydrogen peroxide into water and oxygen, can be used to distinguish it from other bacteria such as *enterococci* and *streptococci* (*Todar, 2008*).

B. Colonisation and disease

Staphylococcus aureus is a highly successful opportunistic pathogen. Indeed, nearly 20% of healthy subjects are persistently colonised and 60% are intermittent carriers, whereas 20% never carry *S. aureus* (*Kluytmans et al., 1997, van Belkum et al., 2009*). Humans are consistently subjected to *S. aureus* exposure in their environment and an array of ecological niches are provided by the human body for microorganisms to thrive (*Human Microbiome Project Consortium, 2012*). Anyway, not every exposure to staphylococcus results in actual colonisation. *S. aureus* host colonization implies a complex interplay of both bacterium and host factors. Firstly, for colonisation to take place, the bacterium must have the capability to adhere to potential receptors located in such ecological niches. Then, it must also be able to multiply and be resistant to suppression by host defence machinery or the established microbiota (*Weidenmaier et al, 2012, Mulcahy & McLoughlin, 2016*).

1. *S. aureus* sites of colonisation

The nose constitutes the principal ecological niche for *S. aureus* colonization in humans (*Kluytmans et al., 1997*). However, subsidiary colonisation sites have been detected in the skin (*Williams, 1963*), the perineum (*Ridley, 1959*), the vagina (*Guinan, 1982*), the axillae *(Dancer & Noble, 1991*), the pharynx (*Williams, 1963, Guinan, 1982*), the gastrointestinal tract (*Williams, 1963, Acton et al., 2009*), the urinary tract and the throat (*Nilsson & Ripa, 2006*). *S. aureus* colonisation of throat, intestine and pharynx with no nasal carriage has been reported (*Acton et al., 2009, Nilsson & Ripa, 2006, Hamdan-Partida et al., 2010*). Recently, several studies indicate a higher incidence of *S. aureus* prevalence in the throat and pharynx in comparison to the nasal carriage (*Nilsson & Ripa, 2006, Nakamura et al., 2010*). Noteworthy, it appears that *S. aureus* nasal carriage affects the bacterial colonization of other parts of the human body (*Mermel et al., 2011*). This suggests that *S. aureus* nasal carriage allegedly serves as a repository for the staphylococcal dispersal into the environment or colonisation of other body compartments (*White, 1963*). *S. aureus* ability to survive in different ecological niches of the human body reveals its adaptability and heterogeneity in colonising the host.

2. *S. aureus* disease in human

S. aureus is one of the most important bacterial pathogens infecting humans in both healthcare and community settings (*Todar, 2008*). If mucosal barriers are breached or host immunological defences are impaired, *S. aureus* can cause morbidity and mortality. Staphylococcal infection is established through the upregulation of the expression of many virulence factors, which help the organism to evade the host response and promote colonization, tissue damage, and dissemination to distant organs (*Foster, 2019*). The coordination of these mechanisms is under the control of a complex network of global regulators, that control the expression of virulence factors in response to different environmental conditions during infections (*Dunman et al., 2001, Yarwood et al., 2001*). *S. aureus* is the etiological agent of a wide variety of diseases, among which the most frequent are superficial skin infections; when the bacterium gains access to the bloodstream – leading to bacteraemia, it may infect internal tissues, such as heart valves – leading to endocarditis, lungs – leading to pneumonia, bone – leading to osteomyelitis – or joints – leading to septic arthritis (*Tong et al., 2015*). A summary of *S. aureus* infections in humans is given below, with an emphasis on pathophysiological aspects.

a) Bacteraemia and infective endocarditis

Bacteraemia is the presence of a bacterial pathogen in the blood. *S. aureus* bacteraemia may be transient, and asymptomatic, or may result in a bloodstream infection, manifesting as an inflammatory response against the microorganism (*Dayan et al., 2016*). The latter may be successfully treated or may advance, leading to sepsis. Bacteraemia is commonly related to the spreading of a localised infection and it has been shown to progress to sepsis in a rather small proportion of bacteremic infections (*Laupland et al., 2013).* Infective endocarditis (IE), which is an infection of the endocardial surface of the heart valve, may be a complication from *S. aureus* bacteraemia. *S. aureus* has recently emerged as the most common causative agent of IE, affecting both native and prosthetic valves (*Tong et al., 2015*).
The onset of IE implicates stepwise valve colonisation by circulating bacteria, local settling and invasion, and the eventual dissemination to distant organs. In this context, a major role is played by MSCRAMMs, which enhance bacterial adherence to host proteins in endovascular lesions (*Moreillon & Que, 2004*).

b) Skin and soft tissue infections

S. aureus represents a prevalent cause of skin and soft-tissue infections (SSTIs) among hospitalized patients (*DeLeo et al., 2010*). SSTIs often follow minor trauma and are favoured by staphylococcal nasal carriage. The most superficial *S. aureus* skin infection is represented by folliculitis, an infection of the hair follicle manifesting as minute erythematous pustules on the skin (*Tong et al., 2015*).
Impetigo is a common bacterial skin disease caused by *S. aureus*, which affects children usually in exposed areas of the body (*Bangert et al., 2012*). Localized skin infections can spread to soft tissues, causing cellulitis, a skin infection causing redness, swelling, and pain in the infected area, due to bacterial invasion via breaches in

the skin barrier, or even the more severe necrotizing fasciitis, an infection of the deeper tissues that results in progressive destruction of the muscle fascia and overlying subcutaneous fat (*Hatlen & Miller, 2021*).

c) Respiratory tract infections

S. aureus may also be the etiological agent responsible for pneumonia. This arises as a secondary manifestation following a viral infection, often due to the influenza virus. Hematogenous spread from staphylococcal bacteraemia may also develop into staphylococcal pneumonia, and this can also be seen in IE patients (*Tong et al., 2015*). A serious complication of staphylococcal pneumonia is the development of severe necrotizing pneumonia, a lethal infection commonly associated with *S. aureus* strains producing pore-forming toxin Panton-Valentine leucocidin (PVL) (*Gillet et al., 2002*).

d) Osteomyelitis

S. aureus may colonize the bones and joints either as a consequence of a hematogenous infection or it may cause a secondary infection resulting from trauma or the extension of disease from an adjacent area (*Fischetti, 2006, Murray, 2020*). Although gram-negative pathogens have been emerging as causative agents in the past decades, staphylococci are still the most frequent isolated in osteomyelitis patients (*Projan & Novick, 1997*). Moreover, *S. aureus* is the leading cause of septic arthritis in young children and in adults who are being treated with intra-articular injections or who have mechanically abnormal joints. Staphylococcal arthritis usually affects large joints, such as the shoulder, knee, hip, or elbow, which appear as painful and erythematous, with purulent material obtained on aspiration.
The prognosis is usually great in children, whereas it can be tricky in adults, primarily due to underlying medical conditions, and secondary infections often occur (*Murray, 2020*).

e) Toxin-mediated syndromes

Among *S. aureus* virulence factors, toxins are directly responsible for a number of syndromes. These include: (a) toxic shock syndrome (TSS), caused by toxic shock syndrome toxin type 1 (TSST-1), (b) food poisoning, by staphylococcal enterotoxins; and (c) staphylococcal scalded skin syndrome (SSSS), by exfoliative toxins.
Staphylococcal toxic shock syndrome (TSS) is a condition induced by the effects of one or more toxins of S. aureus (*Projan & Novick, 1997*). In particular, the TSS due to toxins-producing *S. aureus* strains is considered as a superantigen-mediated disease, in that the implicated toxins – primarily TSST-1 but also staphylococcal toxins A, B, C, D, E, and H – circumvent certain stages of the antigen-mediated immune response and directly bind MHC class II molecules (*Chuang, 2005*).
Staphylococcal food poisoning is one of the most common foodborne medical conditions and it can be considered as an intoxication more than an infection. This is typically caused by a toxin present in food rather than from a direct effect of the bacterium on the patient. Certain strains of *S. aureus* can also cause enterocolitis, which occurs in patients who have received broad-spectrum antibiotics, that suppress the normal colonic flora and allow *S. aureus* growth (*Murray, 2020*).

Staphylococcal scalded skin syndrome (SSSS) is a disease characterized by denudation of the skin induced by exotoxin producing strains, affecting mainly children or immunocompromised adults. It is characterised by an abrupt onset of localised perioral erythema, with a major potential for widespread peeling, causing the lesion to cover almost the entire body within a couple of days (*Ross & Shoff, 2020*).

C. Antibiotic resistance: emergence and mechanisms

In recent decades, as sequencing technologies have advanced, Staphylococci, and in particular S*taphylococcus aureus*, have become one of the most sequenced bacterial genus. This has clarified how Staphylococci respond to the selective pressure constantly evolving their genomes, exchanging DNA, and leading to the emergence of increasingly successful pathogens. A key theme is the emergence of antibiotic resistance. Penicillin was successfully used to eradicate *S. aureus* soon after its discovery. However, penicillin resistance developed very quickly, due to the production of β-lactamase, an enzyme that cleaves the ß-lactam ring of penicillin (*Kirby, 1944*). The widespread distribution of this enzyme in human isolates was ensured by the presence of its gene, *blaZ*, on transmissible plasmids (*Kernodle, 2000*). *blaZ* is under the control of two adjacent regulatory genes, the antirepressor *blaR1* and the repressor *blaI* (Fig. 3a): when penicillin is absent, BlaI binds to the operator region and represses RNA transcription from *blaZ*, causing very low expression level of ß-lactamase; exposure to penicillin induces the autocatalytic activation of BlaR1, a transmembrane sensor-transducer, which cleaves BlaI and promote transcription from *blaZ*, ensuring ß-lactamase expression (*Lowy, 2003*). The introduction of second-generation ß-lactam antibiotics, such as methicillin, selected for a new type of resistance, mediated by the *mecA* gene, carried on a mobile DNA element, the staphylococcal cassette chromosome *mec* (SCC*mec*). *mecA* encodes for

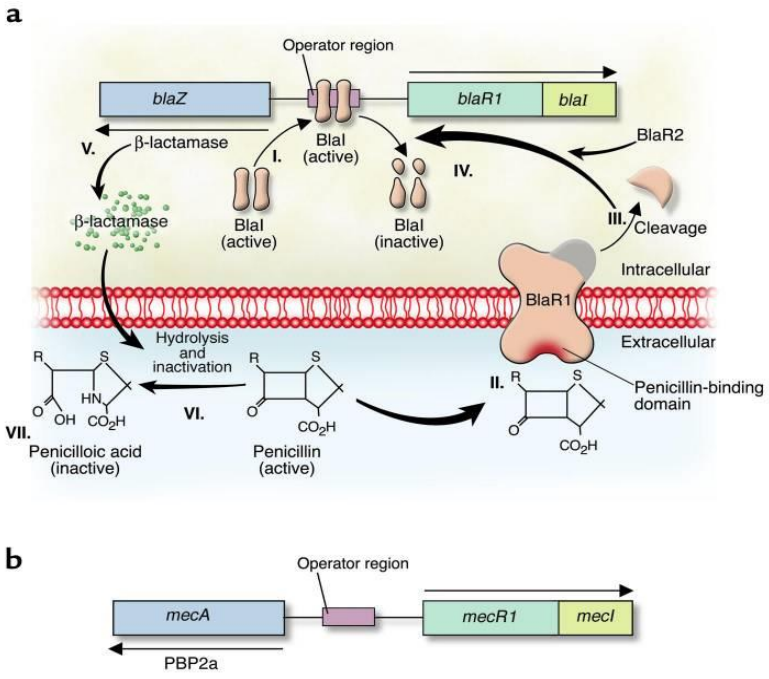

Figure 3. Mechanisms of antibiotic resistance. **A)** Penicillin resistance. **B)** Methicillin resistance (*Lowy, 2003*).

penicillin-binding protein 2a (PBP2a), a peptidoglycan transpeptidase which substitutes for the other PBPs, membrane-bound enzymes whose action is necessary for cross-linkage of peptidoglycan chains, and, because of its very low affinity for β-lactam antibiotics, ensures staphylococcal survival to exposure to these agents (*Lim & Strynadka, 2002*). Production of PBP2a is very similar to that described for β-lactamase (Fig. 3b): when a β-lactam antibiotic is present, the antirepressor MecR1 is synthesized and inactivates the repressor MecI, inducing the synthesis of PBP2a (*Archer & Bosilevac, 2001*).

The SCC*mec* is a novel class of mobile genetic elements and is composed of the *mec* gene complex, encoding for methicillin resistance, the *ccr* gene complex, encoding for recombinases that enable precise integration into and excision from a specific site of the staphylococcal chromosome (*attBscc*), and various resistance genes for non-beta-lactam antibiotics, such as streptomycin, tetracycline, and erythromycin. To date, 12 different SCC*mec* elements have been characterized and classified on the basis of the type of cassette *ccr* complex and the class of the *mec* complex (*Hiramatsu et al., 2013*). Methicillin-resistant *S. aureus* (MRSA) strains have emerged as a result of the acquisition of the SCC*mec* by several multidrug-resistant strains (*Crisóstomo et al., 2001*). MRSA strains were initially isolated in the early 60s, only a few years after the introduction of methicillin into clinical practice. They were first detected in hospitals (healthcare-acquired/associated – HA-MRSA). However, infections have then emerged in the community (community-acquired/associated – CA-MRSA) and from livestock (livestock-associated – LA-MRSA). Consequently, it has developed into a major global health issue due to its pathogenic potential to cause bloodstream infections, pneumonia as well as surgical site infections (*Stefani S. et al., 2012*). The dramatic increase in the use of vancomycin to treat MRSA infections have rapidly selected for a novel antibiotic resistance (*Hiramatsu et al., 1997*). Vancomycin-resistant *S. aureus* (VRSA) strains have probably acquired resistance through the conjugal transfer of the vanA operon from *Enterococcus faecalis*. This operon coordinates the production of a cell-wall precursor that ends in a D-Ala-D-Lac dipeptide rather than a D-Ala-D-Ala one, resulting in a very low affinity for vancomycin (*Showsh et al., 2001*). The emerge of antibiotic resistance *S. aureus* strains has reinforced the need for novel drug targets and for a vaccine to prevent infections.

D. *S. aureus* determinants of colonisation and/or infection

S. aureus may exist as both commensal and pathogenic bacterium in the human host. That demands setting a careful balance between an efficient attachment to the colonization site and the counteracting of the mechanical forces that tend to displace it from such niches. Also, as a pathogen, the microbe should be capable of surviving and establishing itself once the host's barriers have been breached (*Foster, 2005*). Additionally, it should also be able to cause tissue damage and spread to other sites within the host's body so that infection can be established.

S. aureus exhibits a multitude of virulence factors supporting its capacity to interact with the host tissues and the extracellular matrix (ECM) components. The *S. aureus* virulence factors can be broadly classified into secreted factors and surface factors (Fig. 4). Collectively, these factors serve to primarily adhere to the host cell surface and its components, disseminate through the host, circumvent the host's immune system (*Foster et al., 2014, Geoghegan & Foster, 2017*), and, finally, produce toxins and other products capable of causing tissue damage to host cells. In combination with these factors, *S. aureus* also possesses regulatory components and mechanisms designed so that the bacterium expresses these factors only when necessary (*Heilmann, 2011, Cheung et al., 2004*).

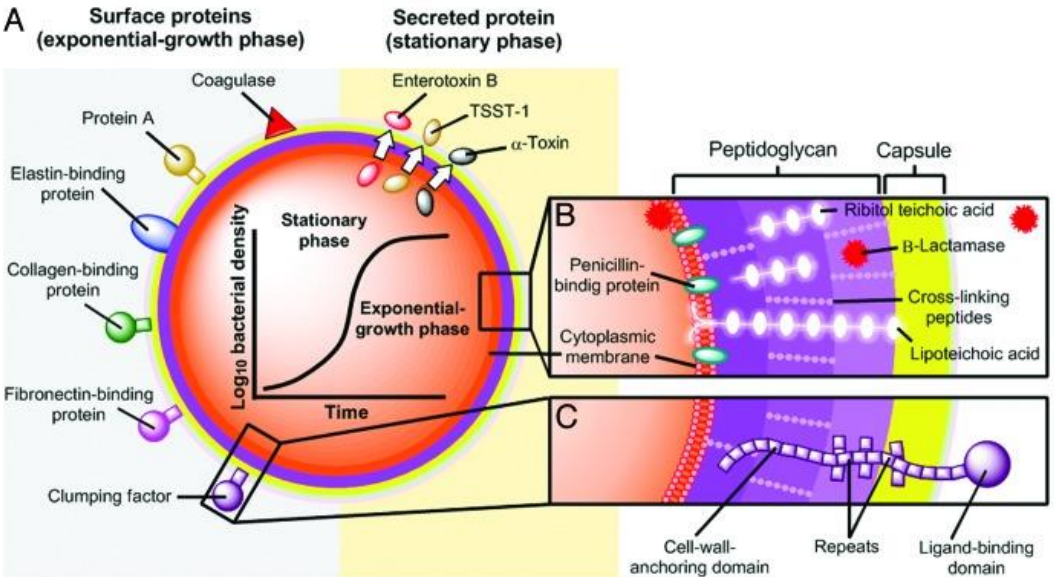

Figure 4. Schematic representation of localization of selected *S. aureus* virulence factors. **(A)** Surface and secreted proteins; **(B and C)** are cross-sections of the cell wall. (*Vatansever et al., 2013*).

1. *S. aureus* secreted factors

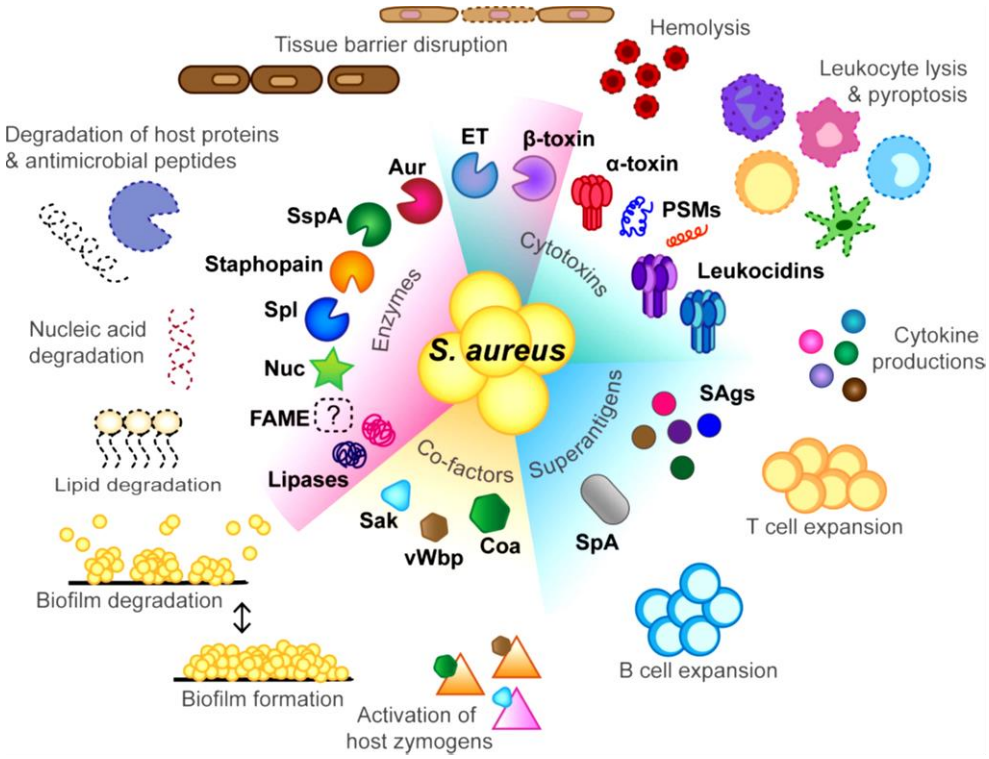

Figure 5. Schematic representation of *S. aureus* secreted toxins and extracellular enzymes (*Tam & Torres, 2019*)

S. aureus produces several factors that are secreted into the extracellular environment (Fig. 5). Of these virulence factors, toxins (exotoxins) account for approximately 10% and can be classified into three groups: cytotoxins, superantigens (SAgs), and cytotoxic enzymes. Cytotoxins target the host cell membranes, leading to cell lysis and consequently inflammation. SAgs initiate the extensive release of cytokines and stimulate T- and B-cell proliferation. Cytotoxic enzymes damage host cells. Collectively, these virulence factors manipulate the host immune response and are critical for the establishment of *S. aureus* infection (*Kusch & Engelmann, 2014*).

Cytotoxins comprise secreted proteins such as Hemolysin-α (α- toxin), Panton-Valentine leukocidin (PVL), γ-toxin (γ-hemolysin, HlgA, HlgB, HlgC) and Phenol-soluble modulins (PSMs), which differ in their mechanisms of action (*Grumann et al., 2014*). For example, α- toxin is a pore-forming toxin (PFT) that specifically binds to ADAM-10 (a disintegrin and metalloprotease 10) and subsequently forms heptameric β-barrel pores in target cell membranes, resulting in cell lysis (*Wilke & Bubeck Wardenburg, 2010*). It specifically targets erythrocytes, platelets, endothelial cells, epithelial cells, and leukocytes, cell types expressing ADAM-10 (*Inoshima et al., 2011, Nygaard et al., 2012*). PVL and γ-toxin are also referred to as bicomponent PFTs as they are very closely related to α- toxin, but their pore formation mechanism requires two subunits, one of which binds to a cell receptor, subsequentially recruits the other subunits for dimerization and finally oligomerizes with additional dimers to form a heptameric pore. As bicomponent PFTs primary target is represented by leukocytes, they are also known as leukocidins

(*Alonzo & Torres, 2014*). PVL target receptors are rabbit and human G-protein-coupled receptors C5aR1 and C5aR2, while γ-toxin ones are human receptors CXCR1, CXCR2, CCR2, and DARC (*Spaan et al., 2017*). Unlike the other cytotoxins described so far, PSMs damage host cells in a receptor-independent manner, playing different roles in staphylococcal pathogenesis, such as cell lysis, biofilm formation, and immune modulation (*Wang et al., 2007*).

Among SAgs, T-cell superantigens are the most prevalent. These proteins have a molecular weight ranging from 19 to 30 kDa and usually fall into three main groups: staphylococcal enterotoxins (SEs), staphylococcal enterotoxin-like (SE-l) SAgs, and toxic shock syndrome toxin-1(TSST-1) (*Spaulding et al., 2013*). The sole representative of B cell superantigens of *S. aureus* is the staphylococcal protein A (SpA). SpA is anchored to the cell wall by sortase A, which recognizes the LPXTG motif at its C-terminus and links the threonyl (T) to the peptidoglycan cross-bridges (*Geoghegan & Foster, 2017*). However, it can be released from the cell wall by LytM, a cell wall hydrolase (*Becker et al., 2014*). The mature protein contains up to five highly conserved immunoglobulin (Ig) binding domains at the N-terminus, which enable SpA to bind the Fcγ portion of Igs to block opsonization (*Kim et al., 2012*).

Such domains also provide the ability to bind B cells by cross-linking the V_H3-expressing B cell receptor, which leads to B cell activation; since this activation is not matched with the costimulatory signals, it culminates in the clonal deletion of B cells (*Goodyear & Silverman, 2003*).
Cytotoxic enzymes produced by *S. aureus* comprise β-toxin and the exfoliative toxins (ETs). β-toxin is a sphingomyelinase, a phospholipase cleaving sphingomyelin to produce ceramide and phosphocholine (*Doery et al., 1963*). ETs are glutamate-specific serine proteases, belonging to the chymotrypsin family, and are the causative agents for staphylococcal scalded skin syndrome (SSSS). These virulence factors are usually involved in immune evasion and survival in the human host (*Bukowski et al., 2010*).

S. aureus also produces a large variety of exoenzymes, which are generally classified into two groups: cofactors activating host zymogens and enzymes degrading tissue components. Among the former, Coagulase (Coa), von Willebrand factor binding protein (vWbp), and staphylokinase (Sak) are the main representatives. Although they do not possess any enzymatic activity, they can activate host zymogens and then subvert different aspects of the host coagulation system (*McAdow et al., 2012*). Coagulase (Coa) is composed of an N-terminal D1D2 domain, involved in prothrombin binding, and a C-terminal tandem repeat domain, involved in FBG binding, kept together by a central linker domain. Coa enables the activation of prothrombin to thrombin by inducing a conformation change in the functional active site of the zymogen, thus promoting blood coagulation. The Coa/prothrombin complex is then able to recognize FBG and convert it to fibrin (*Friedrich et al., 2003*). vWbp, in addition to binding vWF, can associate with prothrombin and convert FBG to fibrin. The sequence of vWbp displays a high degree of homology

with Coa in the N-terminal domain, whereas the C-terminal portion is characterized by a unique vWF and FBG binding site (*Kroh et al., 2009*). The activation of the zymogen mediated by these coagulases induces either the cleavage of complement component C3 or the conversion of C5 into C5a, promoting a bypass of the traditional complement-activation pathways (*McAdow et al., 2012*). Sak is a 136 aa-long bacteriophage-encoded protein expressed by lysogenic strains of *S. aureus*, which can be found in association with the cell surface but can also be secreted in the cell culture environment. Sak is able to bind and convert plasminogen (PLG) to the active serine protease plasmin. The mechanism of PLG activation mediated by Sak significantly differs from those triggered by endogenous PLG activators, such as tissue PLG activator (tPA) and urokinase (Uk). Indeed, rather than inducing a proteolytic activation of the zymogen, Sak forms a complex with plasmin changing its substrate specificity (*Bokarewa et al., 2006*). The ability of *S. aureus* to capture PLG at the bacterial surface through surface-expressed proteins, such as FnBPA and FnBPB, favours the activation of PLG by SAK (*Pietrocola et al., 2016*). Subsequently, surface-bound plasmin elicits the dissolution of fibrin blood clots in human plasma as well as the degradation of opsonins, like human immunoglobulin G (IgG) and human C3b (*Bokarewa et al., 2006*). The enzymes secreted by *S. aureus* include staphylococcal nucleases and proteases. The former act both as endo- and exo-nucleases that break down DNA and RNA substrates through cleavage of the 5′-phosphoryl ester bond, regulating biofilm formation and mediating staphylococcal escape from neutrophil extracellular traps (NETs) (*Cuatrecasas et al., 1967*). The latter comprises three families: metalloproteases, the sole representative of which is Aureolysin (*Nickerson et al., 2008*), cysteine proteases, including Staphopain A and B (*Nickerson et al., 2010*), and serine proteases, such as V8 protease (*Prasad et al., 2004*).

2. Cell-surface factors

The *S. aureus* cell surface is scattered with both proteinaceous and non-proteinaceous molecules (*Dreisbach et al., 2011*, *Heilmann, 2011*). The proteinaceous cell-surface molecules comprise (*a*) Cell Wall-Anchored (CWA) proteins, that are covalently linked to the bacterial cell wall (*Mazmanian et al., 2001*), (*b*) Non-covalently attached cell wall-associated proteins, including proteins with specific cell wall-binding domains, i.e. autolysin (Atl), and (*c*) Membrane spanning proteins, such as the extracellular matrix-binding protein homologue (Ebh) and elastin binding proteins (Ebps) (*Dreisbach et al., 2011*, *Heilmann, 2011*). Among the non-proteinaceous *S. aureus* cell-surface molecules there are the wall teichoic acid (WTA), lipoteichoic acid (LTA), the polysaccharide intracellular adhesin (PIA), and other polysaccharides (*Dreisbach et al., 2011*, *Heilmann, 2011*).

Despite further ongoing investigations to understand the contribution of these cell-surface factors in *S. aureus* colonization and/or virulence, the functions of some of these have already been described

(reviewed in *Foster et al., 2014, Foster, 2019, Heilmann, 2011*). For example, the WTA plays a key role in the early stages of staphylococcal nasal colonization (*Weidenmaier et al., 2012*), the PIA and the LTA are involved in biofilm formation (*Fedtke et al., 2007*) and Ebps interact with elastin, a major component of the ECM (*Downer et al., 2002*).

a) Cell Wall-Anchored proteins

CWA proteins are the main group of *S. aureus* cell surface factors. These surface proteins are crucial to the success of the organism both as a commensal bacterium and as a pathogen. Being exposed on the cell surface, they are in direct contact with the host, and thus, they have evolved to perform crucial functions such as the adhesion to the ECM, the invasion of host cells, the evasion of innate immune responses and biofilm formation (Fig. 6) (*Foster et al., 2014*). About 24 CWA proteins are displayed on the surface of *S. aureus*, a relatively higher number compared to coagulase-negative staphylococci, e.g. *Staphylococcus epidermidis* and *Staphylococcus lugdunensis* (*Heilbronner et al., 2011, Bowden et al., 2005*). Furthermore, their expression varies based on the growth conditions, with some proteins expressed only under iron-limited conditions (*Hammer and Skaar, 2011, Mazmanian et al., 2003*), and others present mostly on cells in the exponential or stationary phases of growth (*McAleese et al., 2001, Bischoff et al., 2004*).

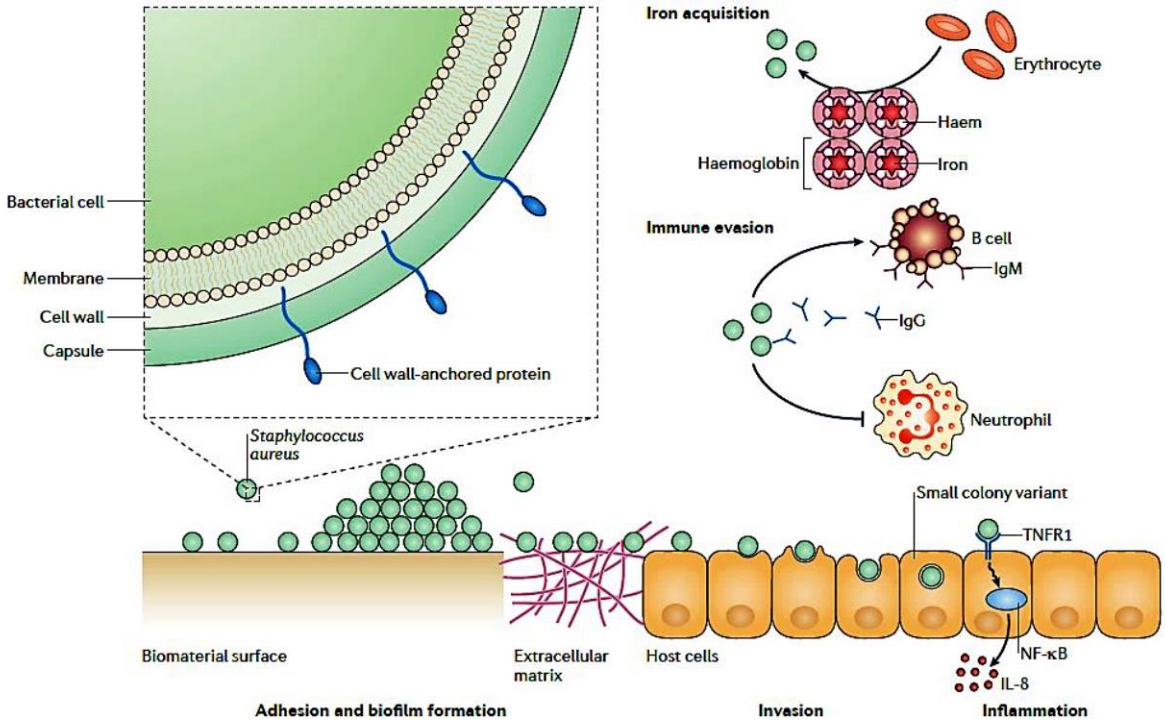

Figure 6. Key functions mediated by CWA proteins in S. aureus. (1) Iron acquisition (2) Immune evasion (3) Inflammation (4) Invasion (5) Adhesion and biofilm formation (*Foster et al., 2014*).

CWA proteins contain a signal sequence peptide at their amino-terminal and a sorting signal at their carboxyl-terminal (*Foster et al., 2014*). The signal sequence directs the translated product to sites within the bacterial peptidoglycan cell wall (*DeDent et al., 2008*). The sorting signal at the carboxyl-terminal facilitates the covalent anchorage of CWA proteins to the dividing peptidoglycan of the *S. aureus* cell wall (*Schneewind et al., 1993*), which is catalyzed by sortases, cysteine transpeptidases. The mechanism of sortase A (SrtA) protein anchoring to *S. aureus* peptidoglycan was the first to be described and is the best understood to date (*Mazmanian et al.,*

2001). During polypeptide secretion via a Sec-dependent pathway, SrtA scans the amino acid chain for a recognition sequence comprising Leu-Pro-XThr-Gly (LPXTG) (*llangovan et al., 2001*). The LPXTG motif is followed by a segment of hydrophobic amino acids and a tail of primarily positively charged residues which presumably retards the export and positions the protein for cleavage by the membrane-associated SrtA. The active site of SrtA nucleophilically attacks the backbone carbonyl carbon of the threonyl residue (T) in the LPXTG motif, breaking T-G peptide bond and forming a thioacyl-linked acyl-enzyme intermediate, and then catalyzes the formation of an amide bond between the carboxyl group of the threonine (T) and the amino group of a glycine (G) residue in peptidoglycan cross-bridges (*Marraffini et al., 2006*).

CWA proteins are classified into five groups on the basis of the presence of motifs that have been defined by structure–function analysis: the microbial surface component recognizing adhesive matrix molecules (MSCRAMM) family, which is defined by tandemly linked IgG-like fold domains – e.g. clumping factor A and B (ClfA, ClfB), serine-aspartate repeat protein (Sdr) C, D and E, and Fibronectin-binding protein A and B (FnBPA, FnBPB); the NEAr iron Transporter (NEAT) motif family, proteins involved in the capture of haem from haemoglobin (Hb) to survive in iron-deficient environments – e.g. Iron-regulated surface determinat (Isd) proteins; the three-helical bundle motif family, that is characterized by tandem repeated three-helical bundles – e.g. Protein A and Sbi; G5-E repeat family, containing G5 (five conserved glycine residues) domains in tandem array that are separated by 50-residues sequences known as E-region – e.g. *S. aureus* surface (Sas) proteins and Plasmin-sensitive surface (Pls) protein; and, finally, the L-lectin/Cadherin-like family, in which a BR region, including a legume lectin-like, a β-grasp fold, a cadherin-like (CHLD) domain, is flanked by serine-rich repeat domains – e.g. serine-rich adhesion for platelet (SraP) protein (Fig. 7) (*Foster, 2019*).

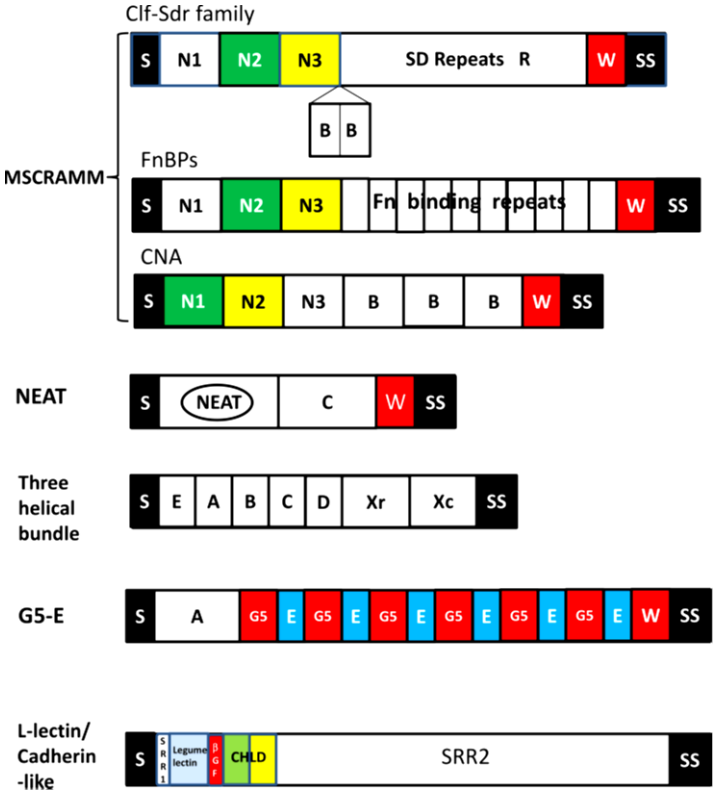

Figure 7. CWA surface proteins classified based on structural motifs (*Foster, 2019*).

(1) The MSCRAMM family

The acronym MSCRAMM was originally reported for surface proteins of *S. aureus* that mediate binding to ECM components of the host cell such as FBG, fibronectin and collagen. However, many bacterial surface proteins are not MSCRAMMs and some MSCRAMMs have additional functions other than promoting adhesion. For this reason, it has been proposed to use the term MSCRAMM to define a family of proteins on the basis of structural similarities and a common mechanism for ligand binding, which is mediated by two adjacent subdomains containing IgG-like folds in the N-terminal A region (*Deivanayagam et al., 2002*). By X-ray structural and biophysical analysis, the A regions were shown to be composed of three separately folded subdomains: N1, N2 and N3. N2 and N3 comprise the IgG-like folds (Fig. 7). Other proteins in this family can be modelled with a high degree of certainty and are predicted to have A domains with a similar structure and similar mechanisms of ligand binding represented by dock-lock-latch (DLL) and the collagen hug (*Foster et al., 2014*). The DLL mechanism was originally described for the *Staphylococcus epidermidis* protein SdrG in the apo form and complex with the β-chain peptide of FBG (*Ponnuraj et al., 2003*). The same mechanism was found to apply to ClfA (*Ganesh et al., 2011*), and the A domains of FnBPA and FnBPB binding to the γ-chain peptide of FBG (*Bingham et al., 2008)* and ClfB binding to cytokeratin-10, loricrin, and the α-chain of FBG (*Xiang et al., 2012*). Basically, the apo form of the protein adopts an open conformation that allows the ligand to access the binding trench between the N2 and N3 domains (Fig. 8). As the ligand docks into the trench, a flexible C-terminal extension of the N3 domain is redirected to cover the ligand and "lock" it in place. The C-terminal part of this extension interacts with the N2 domain by P-strand complementation with a P-sheet in the N2 domain forming a stable complex (*Ganesh et al., 2008, Ponnuraj et al., 2003*).

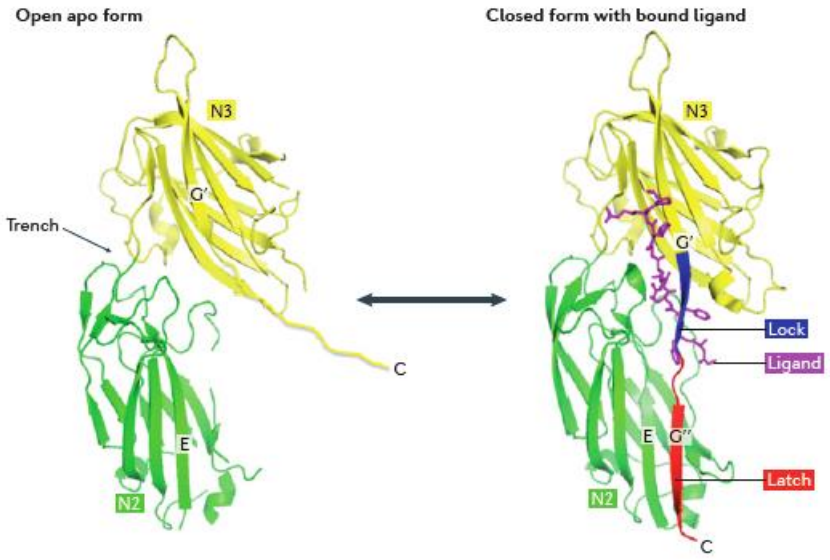

Figure 8. Mechanisms of ligand binding by MSCRAMM proteins: DLL mechanism (*Foster et al., 2014)*.

The collagen-binding protein (CNA) binds collagen by a variation of the DLL mechanism named the collagen hug (*Zong et al., 2005*), where the N1 and N2 subdomains of the A region comprise the IgG-like folds and act as the N2 and N3 subdomains of other MSCRAMMs, with the C-terminal extension of N2 forming the latch (Fig. 9). The long linker region connecting N1 and N2 accommodate the collagen triple helix, with the N2 binding to the ligand and stimulating a conformational change that enables the linker to wrap around collagen. Latching then takes place by β-strand complementation between the C-terminal extension of N2 and a β sheet in subdomain N1 (*Zong et al., 2005*).

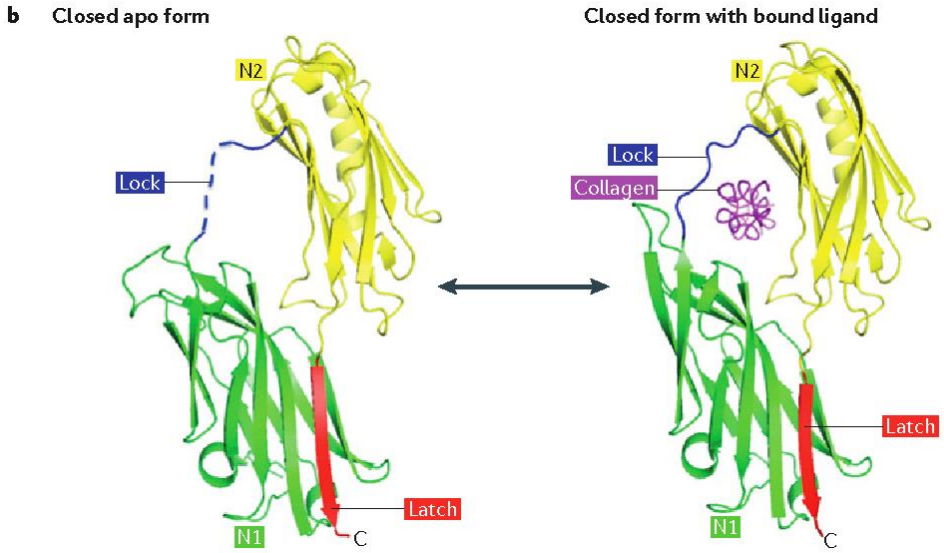

Figure 9. Mechanisms of ligand binding by MSCRAMM proteins: collagen hug (*Foster et al., 2014*).

(2) NEAT motif family

Near-iron transporter (NEAT) domain proteins bind haem or haemoproteins and help bacteria to face the iron-starvation in the host. The *S. aureus* Isd system is encoded within five operons: *isdA*, *isdB*, *isdCDEFsrtBisdG*, *isdH*, and *orfXisdI*, each having an upstream consensus *fur* box. The iron-dependent *f*erric *u*ptake *r*egulator (*fur*) mediates the *S. aureus* protein expression profile in response to an iron-restricted condition. Therefore, all Isd genes are iron-regulated. (*Mazmanian et al., 2000, Reniere & Skaar, 2008*). IsdA, IsdB, IsdH are covalently anchored to the cell wall by SrtA, whereas IsdC anchoring is mediated by another transpeptidase named Sortase B (SrtB), which recognizes NPQTN motif-containing proteins. IsdDEF is a membrane-localized ABC transporter complex transporting iron-containing molecules across the cytoplasmic membrane. IsdG and IsdI encode haem-degrading enzymes in the cytoplasm (*Mazmanian et al., 2000*). The distinctive organization of the Isd CWA proteins comprises one or more NEAT motifs, binding Hb or haem (Fig. 7). The NEAT domains comprise about 125 amino acids and, despite unrelated primary sequences, have a conserved structure forming superimposed IgG-like beta-sandwich folds of 7 or more β-strands in 2 β-sheets (*Andrade et al., 2002, Grigg et al., 2011, Grigg et al., 2010*).

(a) Iron uptake in *S. aureus*

Based on the amino acid sequences, NEAT domains can be distinguished into either haemoprotein or haem binding receptors. The haem binding domains of IsdA, IsdC, IsdB NEAT2, and IsdH NEAT3 make us of a conserved mechanism for the binding of the haem porphyrin ring. They coordinate it in a hydrophobic pocket via a conserved tyrosine residue (*Grigg et al., 2011*). IsdB and IsdH bind Hb through aromatic residues in the loop (β1-β2) for recognition of the chain of Hb (*Krishna Kumar et al., 2011, Pilpa et al., 2006*). The current model for iron uptake in *S. aureus* proposes that IsdA, IsdB, and IsdH are surface-exposed hemoprotein receptors that pass heme to IsdC, which then passes haem through the cell wall to the membrane-localized IsdDEF. Haem is transferred unidirectionally from the NEAT2 domain of IsdB to the NEAT domains of IsdA first, IsdC next, and IsdE lastly (*Muryoi et al., 2008*). Haem is also stripped from the hemoglobin-haptoglobin (Hb-Hp) complex through the sequential activity of the three NEAT domains of IsdH, transferred from its NEAT3 domain to the NEAT2 domain of IsdB, and finally transported to the cell membrane through IsdA and IsdC (*Dryla et al., 2007*). The molecular details regarding heme transport across the membrane have not been fully elucidated yet. The current model suggests that IsdE lipoprotein receives heam from IsdC and then passes it to IsdF, an ABC permease, which then transports haem through the membrane using energy provided by the ATP-hydrolyzing activity of IsdD (*Muryoi et al., 2008*). However, an additional membrane transporter, HtsBC, is involved, the mechanism of which is yet to be explained (*Mason & Skaar, 2009*).

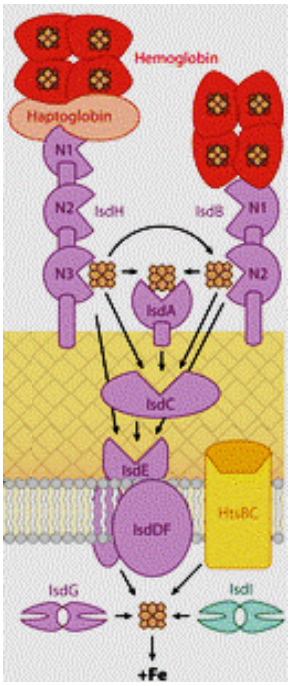

Figure 10. Model of *S. aureus* iron uptake (*Hammer & Skaar, 2011*).

(b) Iron regulated surface determinants – ligand binding and virulence

Beside acting as haemophores, IsdA, IsdB and IsdH are multifunctional proteins acting as virulence factors since they recognize other host ligands and promote bacterial adhesion and resistance to host defences. The details about this aspect are given below in this section.

(i) Iron regulated surface determinant A

IsdA is a multifunctional protein capable of binding to several host ligands promoting host colonisation and invasion. In particular, it mediates adhesion to desquamated epithelial cells of human nares (*Corrigan et al., 2009*), probably interacting with loricrin, cytokeratin-10 and involucrin (*Clarke et al., 2009; Corrigan et al., 2009*). IsdA expression provides resistance to killing by lactoferrin, an abundant peptide in human nasal secretions having an anti-bacterial activity (*Clarke et al., 2008*). Moreover, its C-terminal hydrophilic domain is responsible for decreased cellular hydrophobicity making *S. aureus* resistant to bactericidal human skin fatty acids and peptides and thus promotes bacterial survival on human skin (*Clarke et al., 2007*).

As previously reported, IsdA is involved in haem transfer and therefore can promote *S. aureus* survival in the bloodstream. It contains a single NEAT motif mediating haem-binding via a hydrophobic pocket with propionate groups at the molecular surface. The conserved Tyrl66 (in P6) coordinates haem-iron and forms a hydrogen bond with Tyrl70 which stabilizes the Tyrl66-haem-iron interaction (Fig. 11). Residues located in adjacent loops, additionally coordinate haem by forming hydrogen bonds with haem propionates (*Grigg et al., 2011, Grigg et al., 2007, Pilpa et al., 2006*). The NEAT domain of IsdA also binds to several human plasma glycoproteins including fetuin, fibronectin and the β- and γ-chains of fibrinogen which may further support *S. aureus* host invasion (*Clarke et al., 2004*). IsdA can also act in concert with IsdB in promoting resistance to neutrophil killing. Microbicides of human neutrophils, like hydrogen peroxide (H_2O_2), triggered up-regulation of the *isdA* and *isdB* in *S. aureus* MW2. Mutation of *isdA* and *isdB* resulted in increased susceptibility to H_2O_2 and human neutrophils compared with the wild-type parental strain (*Palazzolo-Ballance et al., 2008*). Inactivation of *isdA* leads to a decrease in bacterial load in murine kidneys five days post-infection in the murine model of abscess formation implying an important role of IsdA in *S. aureus* pathogenesis (*Cheng et al., 2009; Clarke et al., 2007*).

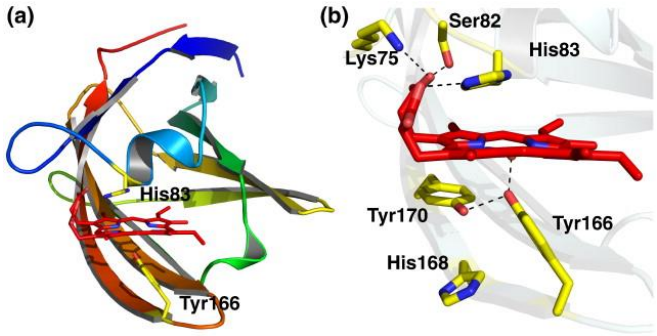

Figure 11. Structure of IsdA NEAT domain and haem-coordinating pocket. **(A)** Structure of the IsdA NEAT domain with highlighted residues involved in haem coordination **(B)** Close-up of the binding pocket. IsdA residues involved in haem coordination are indicated in yellow. The porphyrin ring of haem is indicated in red (*Grigg et al., 2011*).

(ii) Iron regulated surface determinant B

Iron regulated surface determinant B (IsdB) comprises two NEAT domains binding to Hb (NEAT1) and haem (NEAT2), respectively. The deficiency of *isdB* expression results in the inability to use Hb as an iron source. However, this is not true for lack of *isdH*, indicating that in vivo IsdB is the main haemoglobin receptor of the Isd system (*Torres et al., 2006*). IsdB binds human Hb (hHb) with a ca. 20-fold higher affinity than mouse Hb (mHb). This is consistent with the *S. aureus* predilection for hHb over mHb as an iron source, a characteristic of bacteria that are associated with humans, such as *S. aureus*, *S. simulans* and *Corynebacterium diphtheriae*. On the contrary, environmental bacteria infecting diverse hosts like *Acinetobacter baumannii*, *Pseudomonas aeruginosa*, *Bacillus anthracis* and *B. cereus* can use hHb and mHb with the same effectiveness (*Pishchany et al., 2010, Pishchany & Skaar., 2012; Torres et al., 2006*).

IsdB coordinates haem through Tyr440, which forms a hydrogen bond with the phenolate of Tyr444, a prototype interaction for haem binding NEAT domains (*Grigg et al., 2011*). Heam, coordinated by IsdB, is present as a mixture of penta- and hexa-coordinated iron, with the sulphur of Met362 residing in the sixth coordinate position (Fig. 12). This differs from the haem binding mechanism of IsdA. Also, in IsdB the haem propionate groups interact with the hydroxyl group of Ser361 through hydrogen bonds, whereas Val431, Val433, Val 435, Val446, Tyr391 and Trp392 engage hydrophobic contacts (*Gaudin et al., 2011*).

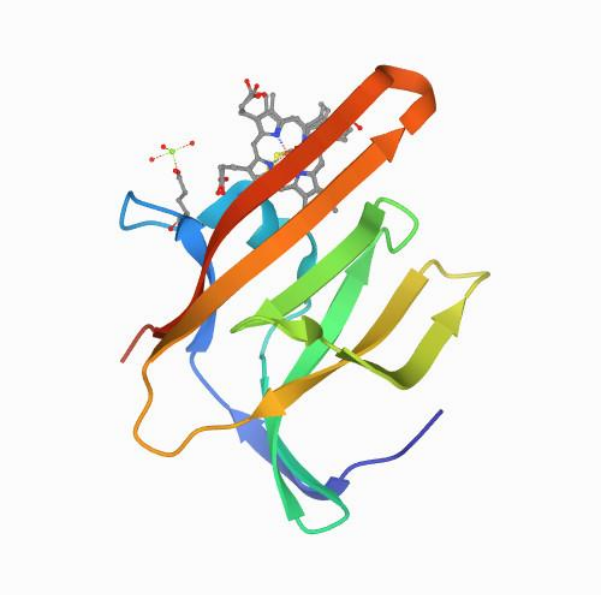

Figure 12. Structure of the IsdB-NEAT2 domain with bound haem. The 1.45 Å resolution X-ray crystal structure of the IsdB-NEAT2-heme complex shows the classical eight-strand β-sandwich fold seen in other NEAT domains; IsdB uses a conserved Tyr residue to coordinate heme-iron, and a Met residue is also involved in iron coordination, resulting in a novel Tyr-Met hexacoordinate heme-iron state (*Gaudin et al., 2011*).

The contribution of IsdB-mediated Hb binding to *S. aureus* pathogenesis infections was evaluated by Torres et al. using a murine model of abscess formation. A considerable decline in the *isdB* mutant load was measured in both the spleen and kidneys of infected animals in comparison to that in the wild-type Newman strain, suggesting a significance of IsdB in *S. aureus* virulence. The *isdH* mutation did not affect the capability of the bacterium to colonize these organs suggesting that, unlike IsdB, IsdH is not required for abscess formation (*Torres et al., 2006*).

IsdB and IsdA are differentially expressed within organs of *S. aureus* infected mice, with IsdB being strongly up-regulated in the hearth and expressed at lower levels in the liver of infected animals (*Pishchany et al., 2009*). The *isdB* mutation led to a severe inability to colonize murine hearts. In accordance with the lower IsdB expression in the murine livers, IsdB-deficient strains have been shown to colonise this organ as efficiently as wild-type strains (*Pishchany et al., 2009*). This also fits with reports on the contribution of IsdB and IsdA to sepsis and abscess formation in mouse models of *S. aureus* infection (*Cheng et al., 2009, Kim et al., 2010, Torres et al., 2006*) but was contradicted by Hurd et al. who pointed to IsdA, IsdB and IsdH protein redundancy in *S. aureus* pathogenesis (*Hurd et al., 2012*).

Nevertheless, these statements were later refuted because the experimental evidence provided by Hurd et al. was impaired by the use of commercial Hb being contaminated with free iron (*Pishchany et al., 2014)*.

Owing to IsdB's elevated affinity for human Hb, the susceptibility of transgenic mice expressing normal adult human Hb to systemic staphylococcal infection was investigated. The $a^{H}\beta^{A}$ mice were more efficiently colonized as compared to wild-type animals, strongly indicating that prior murine models of infection may not fully reflect IsdB's contribution to *S. aureus* virulence (*Pishchany et al., 2010*).

Miajlovic et al. showed that IsdB interacts with platelets *via* direct interaction with the platelet integrin GPIIb/IIIa. Indeed, the lack of IsdB on the cell surface abrogated *S. aureus* adhesion to platelets, whereas strains deficient of either IsdA or IsdH were able to adhere to platelets similarly to the wild-type strain. The direct interaction between IsdB and GPIIb/IIIa was confirmed through a surface plasmon resonance analysis, which gave a KD in the nanomolar range for this interaction. Moreover, this interaction was shown to trigger platelet aggregation not involving any plasma factors, a mechanism that can prove to be essential *in vivo*, where *S. aureus* faces an iron deficiency (*Miajlovic et al., 2010*). IsdB also promotes *S. aureus* adherence to and internalization by non-phagocytic human cells (*Zapotoczna et al., 2012*).
Finally, we recently showed that IsdB acts as a receptor for the host protein vitronectin and vitronectin binding mediates adherence to and invasion of HeLa and HUVEC monolayers (*Pietrocola et al., 2020*).

(iii) Iron regulated surface determinant H

The iron-regulated surface determinant H (IsdH) is made up of three NEAT domains. Of these, the N-terminal NEAT1 and NEAT2 domains share 53% of identity and are responsible for binding Hb, Hp and Hb-Hp complexes. The C-terminal NEAT3 has only 16% identity to NEAT1 and NEAT2 and it accounts for haem trapping by Hb (*Pilpa et al., 2006; Pilpa et al., 2009*).

The initial structure of the IsdH NEAT1 domain was able to demonstrate a β-sandwich IgG fold composed of two antiparallel five-stranded β-sheets (*Pilpa et al., 2006*). A co-crystal structure of IsdH NEAT1 and IsdH NEAT2 with human Hb showed that its domains interact with α (αHb) chains (Fig. 13) (*Krishna Kumar et al., 2011*). A loop 2 at the N-terminus coordinates Hb with a series of aromatic residues uniquely found in Hb-binding NEAT domains. The IsdH NEAT1 loop 2 includes Tyr125, Tyr126, His127, Phe128 and Phe129 that are critical for Hb-binding (Fig. 13). Aromatic side chains form van der Waals contacts with non-polar surfaces on αHb and are buried beneath the solvent. In addition, loops 4 and 6 make up most of the electrostatic interactions with αHb. The Hb interface involves the α-chain residues of Lys7, Lys 11, and Gly18 (Fig. 13). Loops 2 and 4 constitute the largest proportion of IsdH NEAT1 interactions with Hb and are broadly conserved in IsdH NEAT2 and IsdB NEAT1, indicating that they bind αHb similarly to IsdH NEAT1 (Fig. 13).
It has been shown that IsdH induces enhanced degradation of serum opsonin C3b resulting in reduced uptake of *S. aureus* by human neutrophils. Expression of IsdH by *S. aureus* also promoted bacterial survival in human blood (*Smith et al., 2011, Visai et al., 2009*) and virulence in a mouse model of sepsis (*Visai et al., 2009*).

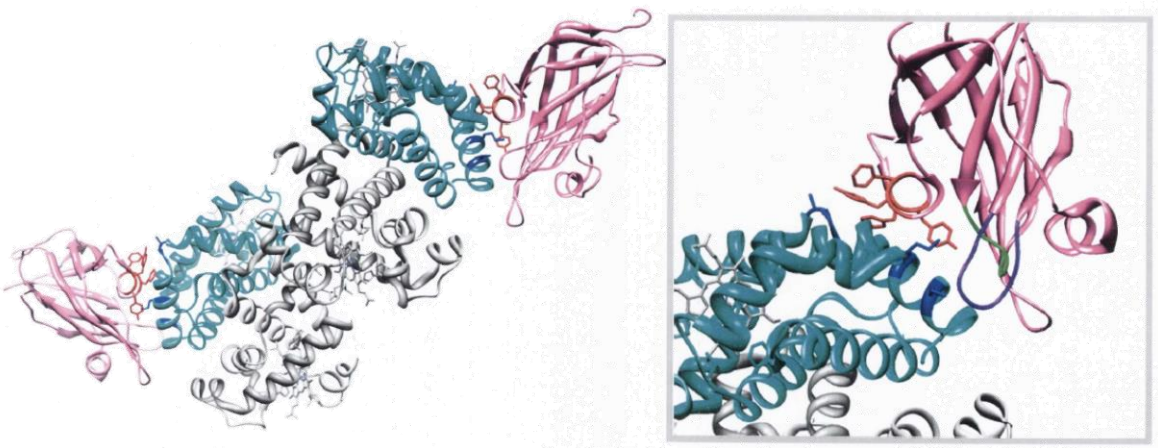

Figure 13. The crystal structure of IsdH NEAT1-haemoglobin complex. Tetrameric Hb comprises two α- (light blue) and two β- (grey) chains. NEAT1 domain (pink) interacts with αHb. On the right, a zoom in on the interaction: the aromatic side chains in loop 2 of IsdH NEAT1 (red) and α-chain residues Lys7, Lys 11, and Gly18 in Hb (blue). Loops 4 and 6 are showed in green and purple, respectively (*Krishna Kumar et al., 2011*).

(3) Three-helical bundle motif family: Protein A and Sbi

Protein A is a multifunctional CWA protein that is ubiquitously expressed in *S. aureus* and is often used in strain typing based on variation in the DNA sequence-encoding region Xr. The N terminal region includes five homologous modules (known as EABCD; Fig. 7), and each module consists of single separately folded three-helical bundles (*Deisenhofer, 1981, Cedergren et al.,1993*) that represent the binding sites for several distinct ligands. Protein A is the only CWA protein of *S. aureus* that has the repeated three-helical bundles; however, the *S. aureus* binder of IgG protein (Sbi), which is non-covalently associated with lipoteichoic acid in the cell wall (*Smith et al., 2012*), contains four three-helical bundles, two of which have sequence similarity to protein A (*Burman et al., 2008*). Sbi protein at C-terminus comprises the proline-rich region Wr and the tyrosine-rich region Y, which is assumed to mediate Sbi association with the cell envelope. The D1 and D2 domains located at the N-terminus show a degree of sequence similarity with the IgG-binding domains of protein A. Domains D3 and D4 are on the other hand implicating in the binding of the complement protein C3, promoting the conversion of C3 to C3b, which would represent an effective immune evasion system if the protein were extracellular (*Smith et al., 2012*) (Fig. 14).

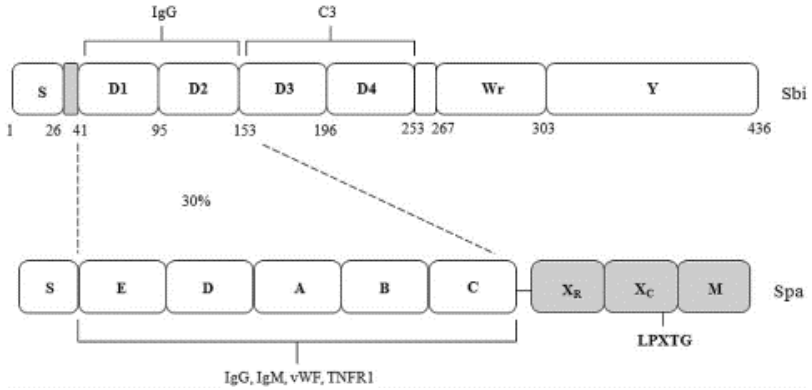

Figure 14. Schematic representation of Sbi and Spa (in order of appearance). S - signal sequence; D1D2 - Sbi IgG-binding domains showing sequence similarity to Spa IgG-binding domains (E, D, A, B, C); D3D4 - Sbi complement factor C3-binding domains; Wr and Xr - proline-rich C-terminal domains; Y - C-terminal domain; LPXTG - wall-anchoring motif; M -transmembrane domain and positively charged C-terminus. Spa ligands are indicated (*Smith et al., 2012*)

According to Smith et al., Sbi would be associated with the surface of the bacterium through a bond with lipoteichoic acid and exposing the N-terminal domain D1D2 that interact with the IgG. The extracellular part of Sbi does not bind to the wall and is available and likely triggers the metabolism of C3 as described by Burman et al. (*Burman et al., 2008*). The protein is present as freely released and in the LTA-associated form, both being necessary for full protection from host defence systems. The binding of IgG to D1D2 domains would be biologically active when Sbi is associated with the bacterial cell surface, while the D3D4 domains would fold at C3 only in the case the protein is secreted (*Smith et al., 2012*).

(4) G5-E Repeat Family

The *S. aureus* surface protein SasG is very similar in structure and organisation to the accumulation-associated protein Aap of *S. epidermidis* (*Gruszka et al., 2012, Conrady et al., 2013*). Both proteins promote cell aggregation and biofilm formation. SasG has multiple alternating repeats of G5-E domains that are identical in sequence and form similar flat single-layered β-sheets lacking a compact hydrophobic core (Fig. 7). The alternation of G5 and E regions is a device that prevents misfolding that would otherwise occur in a tandem array of identical or very similar sequences. The unique structural organisation of the G5-E repeats provides mechanical strength, allowing the protein to maintain both its length and stability. This is due to the E domains forming stable interfaces (clamps) that couple non-adjacent G5 domains by forming H bonds between β-strands in flanking G5 domains (*Gruszka et al., 2015*).

The G5-E domains become exposed by proteolytic removal of the N-terminal A domain (Aap) (*Rohde et al., 2005*) or by limited cleavage within the G5-E domain (SasG) (*Geoghegan et al., 2010*). This allows a specific homophilic interaction to occur between proteins located on adjacent cells, which promotes cell aggregation and biofilm accumulation.

(5) L-lectin/Cadherin-like Family

Serine-rich adhesin of platelets (SraP) is a member of a family of Gram-positive glycoproteins (*Lizcano et al., 2012*). The structural gene sraP is located in a locus including genes that code for glycosyltransferases (GtfA and GtfB) and accessory secretion factors (SecY2 and SecA2). The CWA protein presents a short serine-rich repeat region (SSR1) located at the N-terminus, which is followed by the BR ligand-binding domain (Fig. 7). The latter consists of four separately folded subdomains forming a rigid bent rod (*Yang et al., 2014*). Two cadherin-like domains and a β-grasp fold domain function to project the legume-lectin domain. This bears a structural similarity to legume lectins and binds to glycoproteins containing N-acetyl neuraminic acid (Neu5Ac) which are attached to the mammalian cell surface. It even binds to gp340 salivary glycoprotein, containing a 5NeuAc trisaccharide (*Kukita et al., 2013*). SraP has been shown to facilitate bacterial attachment to and invasion of mammalian cells (*Yang. et al., 2014*). This was evident by running an experimental system where little or no fibronectin was available and using a strain expressing low levels of FnBPs. As such, minimal engagement of highly efficient FnBP-mediated uptake was involved. Thus, SraP, similar to IsdB, could act as an accessory invasin. The cadherin-like domains dimerise in solution and enhance cell-cell build-up and biofilm formation (*Yang et al., 2014*).

E. *S. aureus* and host interaction

As outlined above, more than 20 different proteins decorate *S. aureus* surface, all covalently anchored to the peptidoglycan by the action of sortase A. Many functions are attributed to these surface proteins, involving adhesion and invasion of host cells and tissues, biofilm formation and escape of host immune system responses (*Foster et al., 2014*). More details about the CWA-mediated staphylococcal interaction with the human host are given below.

1. CWA-mediated interaction with host ligands

Nearly 20% of the population is permanently colonised by *S. aureus* in the nares, along with the rest being intermittently colonised (*Kluytmans et al., 1997, van Belkum et al., 2009*). *S. aureus* colonization of the nares occurs through adherence to both ciliated epithelial cells in the posterior region of the nares and to squamous epithelial cells in the anterior nares (*Weidenmaier et al., 2012*). The primary player in this scenario is represented by the zwitterionic bacterial wall teichoic acid (WTA), which mediates the binding to the scavenger receptor SREC-1 (*Baur et al., 2014*), but the CWA proteins are also known to support staphylococcal attachment to corneocytes. Indeed, it has been demonstrated that ClfB and IsdA promote nasal colonisation in rodents and, as far as ClfB is concerned, human models (*Mulcahy et al., 2012, Clarke et al., 2006, Wertheim et al., 2008*). SdrC, SdrD, SasG, Pls and SasX have been shown to contribute to bacterial adhesion to corneocytes in vitro, and SasX can also promote colonisation in the nostrils of mice (*Roche et al., 2003, Corrigan et al., 2009, Li et al., 2012*).

ClfB has been well documented to be able to bind to cytokeratin-10 and loricrin, which are both exclusively present in corneocytes (*Ganesh et al., 2011, Xiang et al., 2012, Walsh et al., 2004*). Loricrin appears to be the major *in vivo* ligand; loricrin knock-out mice have a defect in colonisation (*Mulcahy et al., 2012*). ClfB binds to loricrin via the high-affinity DLL mechanism (*Mulcahy et al., 2012*). IsdA also binds to loricrin, cytokeratin-10 and involucrin, but there is no evidence about the mechanisms underlying these apparently weak connections (*Clarke et al., 2009*). SdrD can bind to desmoglein 1, which is a constituent of the desmosomes holding together keratinocytes and corneodesmosons governing desquamation in the stratum corneum (*Askarian et al., 2016*, 121).

S. aureus is considered a relatively minor or temporary resident of healthy skin. Nevertheless, in patients with atopic dermatitis (AD) experiencing a flare-up, the normal skin microbiota diversity is impaired and *S. aureus* proliferates (*Kong et al., 2012*). The bacterium secretes several proteins that may aggravate the inflammatory situation in AD skin (*Ong P.Y. & Leung D.Y., 2016*). The colonization of AD skin is at least partially driven by the bacterial capacity to attach to corneocytes in a ClfB-dependent manner (*Fleury et al., 2017*). The attachment to loricrin and/or ligands which become exposed on the surface of misfolded corneocytes where the corneodesmosome proteins are located on villus-like prominences is an essential preliminary colonization step (*Riethmuller et al., 2015*).

While it is still not understood how the human immune system manages to combat *S. aureus*, it would appear to depend on innate rather than acquired immunity. Over the last few years, an understanding has emerged that the coagulation system is an essential element of innate immunity. Pathogens or tissue damage initiate an inflammatory response and simultaneously turn on the coagulation cascade (*Verhamme & Hoylaerts, 2009*). However, thanks to the extensive arsenal of virulence factors, *S. aureus* devised a highly efficient countermeasure to manage the haemostatic system. As previously mentioned, the bacterium is able to directly activate thrombin by secreting two coagulases, Coa and vWbp. Because of this direct prothrombin activation, anticoagulants and bivalent thrombin inhibitors are not efficient in blocking *S. aureus*-mediated thrombin activity (*Vanassche et al., 2010*). During colonisation, Coa remains localised to the site of infection, where it establishes a dense fibrin layer surrounding staphylococcal colonies, as opposed to vWbp which is seemingly dispersed and responsible for a widespread fibrin network enclosing the capsule (*Cheng et al., 2010*). A finely tuned balance drives fibrin formation, which can alternately be exploited by the host and by the bacterium. Thrombin supports the containment of infection by trapping invading pathogens in a tight network of fibrin filaments. However, fibrin formation can be turned to the advantage of the bacterium. Indeed, *S. aureus* can rely on the fibrin network to produce biofilms and abscesses (*Vanassche et al., 2013*).

S. aureus is also able to modulate the coagulation system by interfering with the activity of host clotting factors. For example, in addition to acting as a coagulase, vWbp remains in part attached to the bacterial surface and also functions as an adhesin, binding to vWF and mediating adhesion to vascular endothelium (*Claes et al., 2017*), similarly to SpA, which was first identified as an adhesin for vWF (*Hartleib et al., 2000*). However, the most well-known because of their role in this scenario are the clumping factors ClfA and ClfB and the fibronectin-binding proteins FnBPA and FnBPB.

We have seen already that both ClfA and ClfB are able to bind fibrinogen by the DLL mechanism (*Ganesh et al., 2011*). Both adhesins, upon binding fibrinogen, result in the formation of small aggregates that shield the bacterium by protecting it from phagocytosis. In addition, these aggregates are retained longer in the circulation and cause metastasis. For these reasons, they have a significant role in sepsis and endocarditis (*McAdow et al., 2012*). On the other hand, FnBPA and FnBPB interact with several structurally different host extracellular matrix/plasma proteins. They possess N-terminal domains that are analogous to that of ClfA and therefore also bind the fibrinogen γ-chain through the DLL mechanism. Furthermore, the FnBP N-terminus also binds to PLG and elastin. Binding to PLG occurs by a mechanism different from the DLL and involving a single subdomain (*Pietrocola et al., 2016*). The capture of PLG from serum and its conversion to plasmin by the host or bacterial activators promotes degradation of opsonins and facilitates the spreading of bacteria in infected tissue (*Pietrocola et al., 2016*).

Moreover, both the A domains of FnBPA and FnBPB promote adhesion of *S. aureus* to tropoelastin (*Roche et al., 2003*), but the mechanism underlying this interaction is still unknown. In addition, FnBPB binds histones, most likely by DLL, with an affinity that is 20-fold higher than for FBG, indicating that FnBPB will bind preferentially histones. FnBPB could simultaneously bind H3 histone and PLG and activation of bound PLG resulted in cleavage of H3. Thus, FnBPB neutralizes the bactericidal activity of histones by direct capture of histones and prevention of their access to the surface. Alternatively, FnBPB can bind to PLG which, when activated to plasmin, can cleave the sequestered histone. Also, FnBPB expression was shown to be responsible for protecting *S. aureus* from the bactericidal effect of the total histones released by neutrophils in the form of NETs (*Pietrocola et al., 2019*). The C-terminal region of FnBP adhesins is responsible for high-affinity binding to fibronectin through a mechanism known as tandem β-zipper (*Burke et al., 2010*).

SdrC, FnBPA and FnBPB MSCRAMMs can promote cell-cell attachment and biofilm formation (*Geoghegan et al., 2013, O'Neill et al., 2008*). In both instances, the A-domains on neighbouring cells engage in homophilic connections. Subdomain N2 of SdrC contains two interaction sites that have been identified through screening of phage display libraries for inhibitory peptides (*Barbu et al., 2014*). The molecular modelling demonstrated that a β-neurexin peptide binding to SdrC obstructs one of the interaction sites and thus prevents biofilm formation (*Feuillie et al., 2017, Barbu et al., 2010*). Investigations using bacterial cells expressing FnBPs or derivatives have shown that A-domains are necessary for biofilm formation and that for FnBPA, the DLL is not involved (*Geoghegan et al., 2013*). For SdrC, the A-domain also supports attachment to hydrophobic surfaces and could therefore be implicated in both adhesion to indwelling medical devices and biofilm accumulation (*Feuillie et al., 2017*).

2. *S. aureus* immune evasive strategies

S. aureus has developed mechanisms of evasion or other strategies designed to elude host immune responses against the bacteria. Such strategies are enabled by secreted or surface-associated virulence factors, helping it to interrupt the normal function of host defences, thus providing an environment in which the bacteria can better survive and prosper. Staphylococcal immune evasion strategies are manifested in a number of forms (*Foster, 2005*). The most significant of these being the ability of *S. aureus* to evade phagocytosis and intracellular killing of neutrophils function. Indeed, SpA is a multifunctional staphylococcal CWA protein that promotes innate response evasion through its ability to bind serum IgG (Fig. 15). Bacterial cells coat themselves with IgG that is misbound so that the Fc region of the antibody is not recognised by the Fc receptor of neutrophils (*Forsgren & Quie, 1974, Cedergren et al., 1993*). In order to activate the classical complement fixation pathway, the complement protein C1q needs to bind to the Fc region of bound IgG (*Thielens et al., 2017, Tosi, 2005*). In this way, opsonophagocytosis is completely inhibited by denying detection of IgG and C3b opsonins by either the Fc receptor or the complement receptor on neutrophils. Cna also prevents the onset of the classical complement fixation pathway as it binds to the C1q collagen triple helix structures, shifting C1r-C1s and inhibiting complement activation (*Kang et al., 2013*). In addition to this, *S. aureus* is capable of reducing the efficacy of antimicrobial peptides, inhibit TLR signalling and complement activation and opsonization (*Foster, 2005, Askarian et al., 2018*).

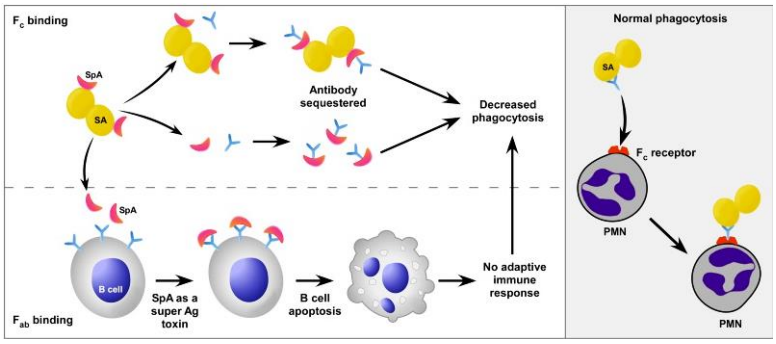

Figure 15. Mechanisms of SpA-mediated immune evasion. (Left panel) SpA present on the surface of *S. aureus* or secreted SpA binds the Fc region of antibody, thereby preventing normal phagocytosis (right panel). Alternatively, SpA binds the Fab regions of the B-cell receptor (lower left panel), which induces B-cell death and prevents the production of antibody specific for *S. aureus*. SA, *S. aureus*; Ab, antibody; Ag, antigen; PMN, polymorphonuclear leukocyte (*Kobayashi & DeLeo, 2013*).

II. von Willebrand Factor

A. vWF overview

A hereditary blood disease, which differed from other well-known disorders, was first recognised in 1924 by the Finnish doctor Erich von Willebrand in a young woman who bled to death during her fourth menstrual period. He failed to define whether the patient's defect lied in her platelets, blood plasma or vasculature. The bleeding disorder is now known as von Willebrand disease (vWD) and the defective protein as vWF. The protein is found in platelets, blood plasma, neighbouring vascular endothelial cells, and the extracellular matrix.

vWF was first characterised in the 70s, and the complete sequence recorded, and the gene cloned in the 80s. By the late 90s, the molecular background and the biosynthesis of several of vWF's procoagulant activities were identified (*Sadler, 1998, Wagner, 1990*). A hallmark of vWF is its large size, acquired in biosynthesis via disulphide bonding among vWF monomers. Particular domains of the vWF monomers associate with receptors on platelets' surface and with collagens displayed within the subendothelial matrix; the large size of the vWF protein allows the recruitment of platelets to the site of vascular injury. vWF also binds the coagulation factor FVIII, enhancing its half-life and facilitating the delivery of this constituent of secondary haemostasis to the site of vascular injury and the platelet plug.

A protease with the ability to cleave vWF was identified in 2001 (*Tsai & Lian, 1998, Furlan et al., 1998*) and named ADAMTS13 (*Fujikawa et al., 2001, Zheng et al., 2001*). ADAMTS13 cleaves vWF at the specific Y1605-M1606 bond in the A2 domain of vWF (*Tsai et al., 1994*). ADAMTS13 interaction, in contrast to other defined vWF binding partners, has a clot-disrupting effect that lowers the haemostatic potential of vWF. The relevance of the interplay between vWF and ADAMTS13 is emphasised in the thrombotic condition known as thrombocytopenic purpura (TTP) (*Kaushansky, 2016*). In TTP, a defect in the ADAMTS13-mediated proteolysis of vWF triggers the build-up of 'unusually large' or “ultra-large” vWF (UL-vWF). UL-vWF has the potential to self-interact with platelets in the absence of vascular injury resulting in microvascular thrombosis (*Sadler, 2008*).

As shown in Fig. 16, The vWF gene is located on chromosome 12 (12p13.2) and comprises 52 exons spanning ~180kb. Its translation product is 2813 amino acids (aa) long and incorporates a signal peptide of 22aa, a propeptide of 741aa and a mature subunit of 2050aa. The peptide sequence includes a large number of cysteine residues (234/2813) and 17 N-linked and 10 O-linked glycosylation sites (*Titani et al., 1986, Canis et al., 2010*). Recently, advances in homology modelling in conjunction with electron microscopy imaging of the vWF protein gave rise to the domain/structure annotation of vWF as follows: D1-D2-D'D3-A1-A2-A3-D4-C1-C2-C3-C4-C5-C6-CK (*Zhou et al., 2012*).

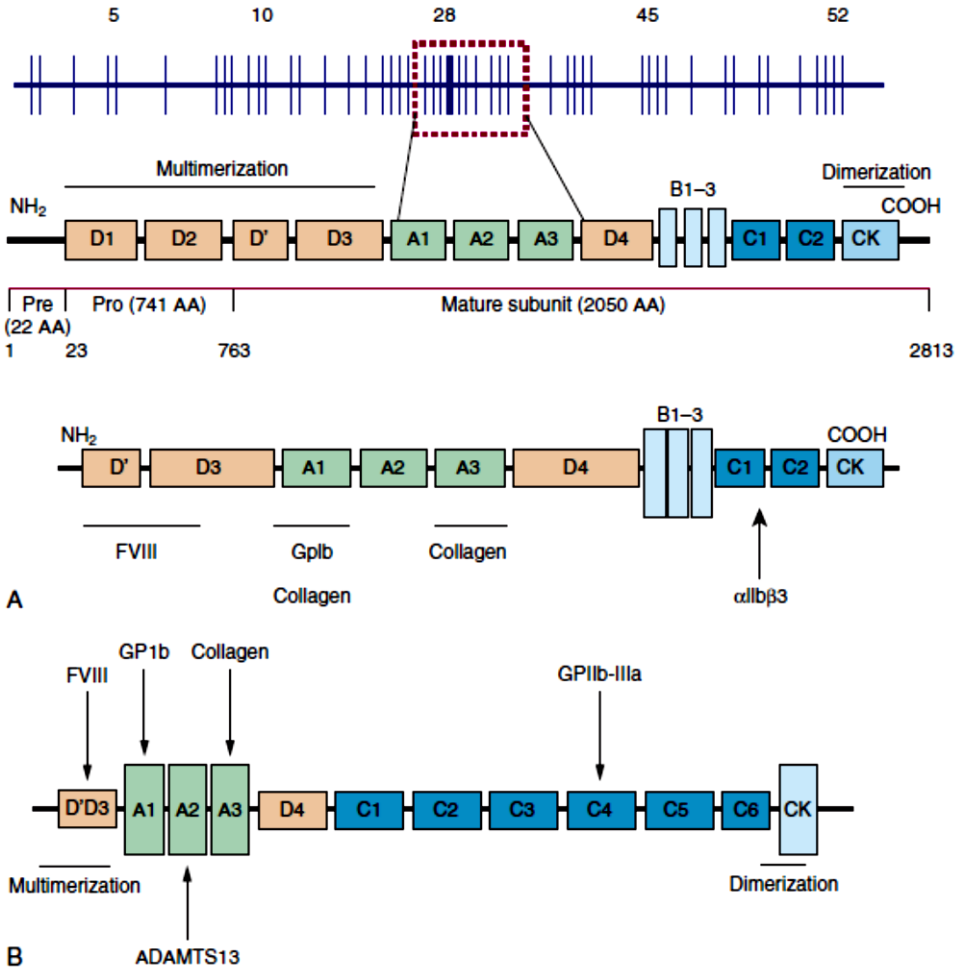

Figure 16. von Willebrand Factor gene, mRNA and protein. *A*, The VWF gene is located on chromosome 12 at p13.3 and spans 178 kb and includes 52 exons. The mRNA is 8.8 kb in length. Prepro-VWF contains 2813 amino acids (AA) with a 22-AA signal peptide, a 741-AA propeptide, and a 2050-AA mature subunit. The mature subunit consists of repeated domains (A–D), several of which have distinct functions and binding sites. *B*, Diagram showing the revised annotation of the VWF subunit that was derived from electron microscopy. ADAMTS13, A Disintegrin And Metalloproteinase with a Thrombospondin Member 13; FVIII, Factor VIII; GP, Glycoprotein, mRNA, Messenger RNA (*James & Rydz, 2018*).

There are four distinct sites for vWF in the vasculature: the subendothelial matrix, blood plasma, endothelial cells and the platelet α-granule (derived from the megakaryocyte). There is little or no contribution from vWF expressed in the megakaryocyte (MK) to vWF detected in blood plasma and the subendothelial matrix. On the other hand, endothelial cell-expressed vWF is secreted into the plasma and the subendothelial matrix. Its structure and domain organisation are also key to its synthesis, intracellular processing, storage, secretion and function.

B. vWF synthesis, secretion, and storage

A distinctive aspect of vWF is the very large multimeric complexes it produces. The mature vWF monomer exhibits a molecular weight (MW) of ~250kDa and the largest circulating vWF multimers may have a MW of up to ~20,000kDa, indicating that the largest multimeric species of VWF must incorporate at least 40-80 monomeric vWF subunits. Throughout synthesis, vWF polymerises via "head-to-tail" and "tail-to-tail" disulphide bonds, guaranteeing the linear disposition of its subunits (*Springer, 2011*).

During biosynthesis by an endothelial cell, vWF secretion is controlled to keep the plasma concentration stable, and also to enable the secretion of vWF to the underlying ECM, thus allowing platelets to attach to sites of vascular injury. In addition to the secreted vWF pools, endothelial cells also accumulate VWF in vesicles called Weibel-Palade bodies (WPBs) for release following inflammatory or thrombotic stimuli.

After vWF gene transcription and translation, the 22aa signal peptide is excised from the 2813aa gene product in the endoplasmic reticulum (ER). The protein then undergoes a series of post-translational modifications, starting in the ER with the attachment of N-linked glycans at 17 positions in the pro-vWF monomer. Still in the ER, the great majority of cysteine residues in vWF are cross-linked by disulphide bonds to produce the tertiary structure of the defined vWF domains (*Lenting et al., 2015*).

As the first step in vWF multimerization, tail-to-tail bonding is established between the CK C-terminal domains of pro-vWF monomers. Three cysteine residues form the disulphide bonds between the paired CK domains (C2771, C2773 and C2811), two reciprocal C2771-C2773 and one C2811-C2811 bonds, form the three disulphide bridges between the two CK domains (*Zhou & Springer, 2014*). Upon glycosylation of the pro-vWF monomer and disulphide bond formation, the now "pro-vWF dimer" is trafficked out of the ER. The exit from the ER is believed to be the rate-limiting step in vWF synthesis (*Wagner, 1990*). More unusually in a mammalian cell, the successive steps of vWF multimerization take place outside the ER. The ER is the 'traditional' site of polymerisation for many other proteins given its redox potential and chaperones that regulate disulphide bond formation (*Frand et al., 2000*).

After being released from the ER, pro-vWF dimers are carried to the cis-Golgi. On passage of vWF through the Golgi network, additional post-translational modifications are carried out. The 17 N-linked glycans of pro-vWF are processed and further edited, for example by sialylation, sulphation and by adding blood ABO(H) antigens (*Matsui et al., 1992*). There are more than 300 different variations in glycan structure across the 17 N-linked glycan sites in plasma vWF (*Canis et al., 2012*). In addition to the modification of the 17 N-linked glycans, 10 O-linked glycans are also attached in the Golgi. Once vWF advances to the lower pH of the trans-Golgi, the vWF propeptide domains (D1-D2) also play a crucial role. It is believed that the propeptide possesses 'protein disulphide isomerase' activity as a result of the two CxxC motifs at positions 159-162 and 521-524 (*Mayadas & Wagner, 1989, Purvis & Sadler, 2004)*. The D1-D2 domains are responsible for the formation of two disulphide bonds (C1099-C1099 and C1142-C1142) between adjacent D3 domains in the trans-pro-vWF dimers (*Sadler, 2009*). Such a process is then repeated, connecting further pro-vWF dimers into 4-mers, 6-mers, 8-mers and up to a maximum of 50-mers, the size of which is limited by the size of the pathway taken through the trans-Golgi (*Ferraro et al., 2014*). The lower pH of the trans-Golgi triggers a zipping of the cis-pro-vWF dimers by coupling the C-terminal domains of the vWF monomers (*Zhou et al., 2011, Zhou et al., 2012*). A second role of the D1-D2 propeptide domains is to associate in helices forming the characteristic WPB tubules. Multimerised pro-vWFs with 'zipped' C-termini are then assembled in “mini-stacks” around the D1-D3 domains. Finally, the propeptide is cleaved by Furin (after a dibasic amino acid pair at position 763) (*Rehemtulla & Kaufman, 1992*) but stays non-covalently bound to the D'D3 domains of the now mature vWF monomer at a lower intracellular pH (*Vischer & Wagner, 1994*). A further feature of the propeptide is to arrange mini-stacks in the larger multimers found in WPBs (*Sadler, 2009*). A non-covalent connection between Arg416 of the propeptide and Thr869 in mature VWF favours VWF trafficking in the WPB (*Haberichter et al., 2003*). Limited-sized VWF mini-stacks gem out of the trans-Golgi and a protein complex of AP1/clathrin serves as a scaffold to fuse the mini-stacks into a nascent WPB (*Ferraro et al., 2014*). Nascent WPBs then dock to filamentous actin and mature (*Rojo Pulido et al., 2011*). VWF is the major constituent of the WPB in terms of both cargo and organelle formation. A functional VWF is essential for generating a WPB (*Haberichter et al., 2005*). Other proteins that occur in the WPB are most likely trafficked because of their interaction with VWF, including P-selectin, galectins and osteoprotegerin (*Michaux et al., 2006, Saint-Lu et al., 2012, Shahbazi et al., 2007*). VWF-mediated chaperoning of proteins in the WPB is also further highlighted by the overexpression and subsequent incorporation of the coagulation factor FVIII into the WPB of endothelial cells (*Shi et al., 2010*), and also by the expression and storage of FVIII from a subset of endothelial cells (*Jacquemin et al., 2006*).

Other WPB residents like cytokines and tissue plasminogen activator seem to occur due to a random inclusion process (*Knipe et al., 2010*). WPB protein cargoes are thus positioned to function in haemostasis or inflammation (*Rondaij et al., 2006*).

Since endothelial cells direct vWF in three directions, outside in the circulating blood and subendothelial matrix, and internally in the WPB, it would appear that separate secretion pathways are required. It was previously thought that 90-95% of the secretion of newly synthesised vWF was via the "constitutive secretory pathway" (*Sporn et al., 1986*). In this case, vWF was transported directly to the endothelial cell membrane for secretion and never participated in or entered the formation of a WPB. Only 5-10% of the newly synthesised vWF went into the "regulated secretory pathway" and participated in WPB formation.

The latest findings suggest that the constitutive secretory pathway's contribution to circulating vWF levels is insignificant in cultured endothelial cells (*Giblin et al., 2008*). Most of the unstimulated release of vWF into the circulation is accounted for by "basal secretion". Basal secretion is referred to as "the unstimulated secretion of a regulated secretory cargo", denoting that the bulk of vWF goes into an immature WPB independently of whether it will be secreted directly or stored in a WPB for stimulated secretion. The "basal" secretion mechanism is probably due to the fortuitous movement of a cohort of nascent WPBs, which eventually brings them into contact with the membrane of endothelial cells causing them to fuse and then secrete their contents (*de Wit et al., 2003*). Crucial to vWF function in the circulation is the large size of the multimers it forms. The secretion of lower MW vWF goes to the ECM via the constitutive secretory pathway (*Lopes da Silva & Cutler, 2016*).

vWF stimulated release is one of several responses to endothelial cell activation. Physiological activators triggering vWF secretion from endothelial cells comprise thrombin, histamine, epinephrine and vasopressin (*Levine et al., 1982, Hamilton & Sims, 1987, Vischer & Wollheim, 1997, Kaufmann et al., 2000*). These secretion agents act by elevating Ca^{2+} levels or increasing cAMP (*Rondaij et al., 2006*). Following stimulation, mature WPBs translocate to the perinuclear area, more WPBs fuse to form "secretory pods" that result in the delivery of large volumes of UL-vWF (*Lenting et al., 2015*, *Valentijn et al., 2010*). Central to the organised delivery of these multimers of UL-vWF is the pH shift as the WPBs fuse with the extracellular environment, causing the tightly packed tubules to unwind (*Michaux et al., 2006*). The vWF released on endothelial cell stimulation is considerably larger and more thrombotic than that released during basal secretion (*André et al., 2000*).

Most studies on vWF synthesis, storage and secretion focus on the endothelial cell. However, vWF synthesis also takes place in MKs, and the processes of vWF synthesis and multimerisation seem to be analogous to those described for endothelial cells (*Sporn et al., 1985*). The major discrepancy between these two cell types producing vWF is that no constitutive/ basal secretion from MKs occurs. Instead, the

entire amount of vWF is channelled into the storage granules. The storage granule is the α granule of the MK and then the α granule of the MK-derived platelet. vWF is released from the platelet's α-granule upon platelet activation. vWF synthesised by the MK has a different glycosylation pattern from endothelial cell vWF. The platelet vWF lacks the ABO blood group antigens that are found on endothelial vWF and has fewer sialylated glycan structures (*McGrath et al., 2010, McGrath et al., 2013*). This variation in glycosylation may account for the different affinities that platelet-derived VWF has for GpIbα and GpIIbIIIa (*Williams et al., 1994*), and its reduced proteolysis by ADAMTS13 (*McGrath et al., 2013*).

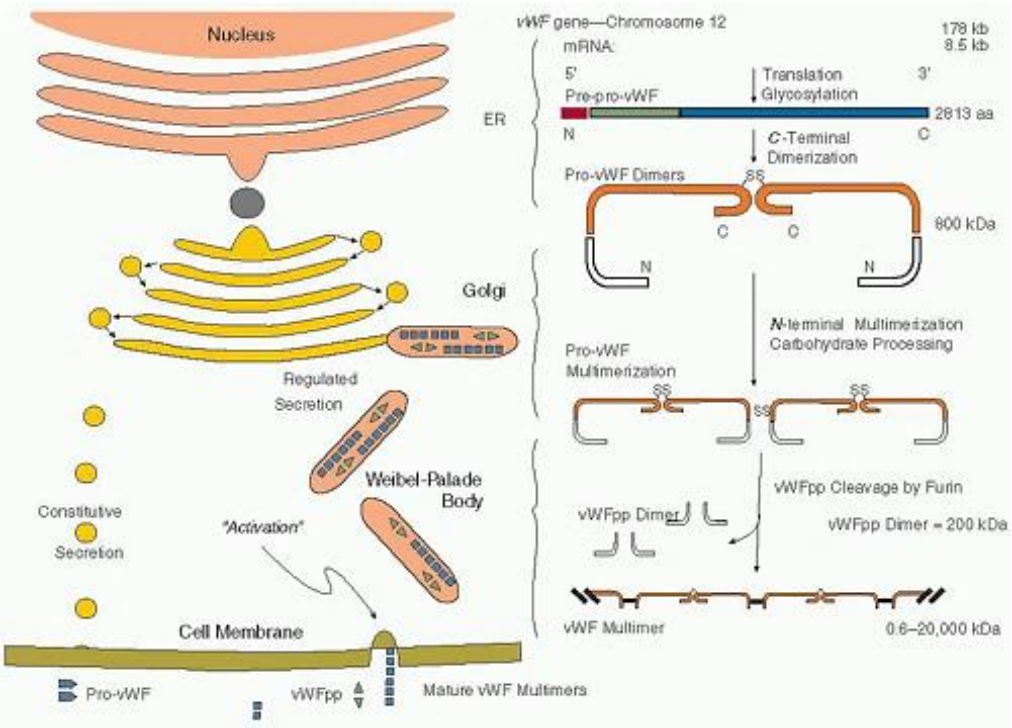

Figure 17. Overview of VWF synthesis and secretion in an endothelial cell. vWF protomer is synthesized as a pre-pro-vWF C-terminal disulphide-bonded dimer within the ER. The 22aa signal peptide is then cleaved and processed into complex sugars within the Golgi compartment. N-Linked multimerization by virtue of the self-association of the vWF propeptide (vWFpp) occurs in the acidic compartment of the late-Golgi, and the vWFpp is cleaved from the mature vWF by furin. A pH-dependent association between vWFpp and vWF enables the packaging of both proteins into WPbs. After endothelial cell activation, the regulated secretion of these proteins occurs, but at the neutral pH in plasma, there is no longer an association of vWFpp with vWF. A similar pathway is assumed to occur in MKs, but the α-granule contains more different types of proteins. In the absence of vWF, WPbs are not formed, but the α-granule is still present. (*McGrath et al., 2010*).

C. Structure and function of the vWF domains

vWF harbours a large number of cysteine residues (234 out of 2813aa) accounting for 8.3% of the total AA composition. This is higher than the average cysteine content of mammalian proteins, 2.3% (although no direct comparison exists between vWF and the cysteine content of other secreted plasma proteins). A feature of cysteine residues is that they form strong covalent disulphide bonds between pairs of cysteines. These disulphide bonds contribute to maintaining the stability and structural integrity of vWF domains and modular groups under the rheological and proteolytic stresses of the vasculature. Most vWF cysteines are located outside the vWF A domains. The vWF A domains cover 600aa of the vWF peptide sequence but contain only 6 cysteine residues. Cysteine residues are not only engaged in interchain disulphide bonds but also in intrachain disulphide bonds (*Miseta & Csutora, 2000*).

The amino acid sequence of vWF includes four homologous repeating segments, called A to D, which constitute approximately 90% of the precursor. They are also found in many unrelated proteins. For example, vWF A domains are found in up to 22 human genes, including human leukocyte adhesion receptors, collagen receptors and cartilage matrix proteins. Similarly, homologues of vWF B, C, D and CK domains appear throughout the genome and can be found in proteins with various functions. That is evidence that the vWF gene is the product of a complex series of partial gene duplications (*Whittaker & Hynes, 2002*).

Based on four homologous repeated segments, A to D, the structure of the vWF domain has been annotated in the following sequence: S-D1-D2-D′-D3-A1-A2-A3-D4-B1-B2-B3-C1-C2-CK (*Zhou et al., 2012*).

The annotation of the protein structure of vWF has recently been revised according to the structures seen by electron microscopy. A-domains can be seen as globular structures and are the principal sites of vWF, platelets and collagen. The previously known B and C domains are re-annotated as six-tandem von Willebrand C (vWC) and vWC-like domains. Such domains stretch and give flexibility to the vWF protein, an essential property for vWF to function under different shear stresses within the circulation (*Zhou et al., 2012*).

Fundamental domains responsible for multimerisation, cleavage and binding were identified. The signal peptide (S) directs prepro-vWF to the endoplasmic reticulum (ER), where it is readily cleaved. The cysteine knot (CK) domains of adjacent vWF monomers create disulfide bonds, resulting in tail-to-tail dimers. The vWF propeptide (D1-D2 domains) has an important role in the vWF multimer by encouraging the formation of head-to-tail oligomers through disulphide bonds that involves D3. Domain A2 harbours the Tyr1605-Met1606 cleavage site for ADAMTS13 (*Haberichter et al., 2003*).

The vWF subunit has several binding sites, almost entirely encoded by exon 28 and comprising the D′-D3-A1-A2-A3 domains. In addition, the C1 domain, encoded by exons 42-44, contains one binding site. The D′ and D3 domains carry the FVIII binding site, which also interacts with the N-terminal portion of the FVIII light chain (*Jacquemin et al., 2006*).

vWF interacts with platelets through two platelet receptors: GPIbα and GPIIb/IIIa, which facilitate platelet adhesion to the damaged subendothelium and aggregation of activated platelets, respectively. The binding site for GPIbα is situated within the large disulfide ring of A1, while the binding site for GPIIb/IIIa is found in the RGD sequence of C1. vWF binds to collagen I and III via domains A1 and A3 and collagen VI via domain A1. Even though the main binding site for collagen is within the A3 domain, the two sites probably have complementary roles and shear stress-mediated flux is important for the conformation and function of both (*McGrath et al., 2010*).

D. The role of vWF in haemostasis

Platelet deposition at the site of vascular injury is the main step in repairing vascular damage to avoid bleeding. vWF is fundamental for platelet attachment to the subendothelium. The basal and induced release of vWF from the secretagogue enables vWF deposition on the cell surface and ECM. On the cell surface, vWF is docked by integrin αvβ3 and P-selectin (*Cheresh and Spiro, 1987, Padilla et al., 2004*). In the presence of flow, vWF unfolds and reveals platelet binding sites, thereby triggering platelet capture. In ECM, the exposed fibrillar collagen from vascular injury binds to vWF (*Romijn et al., 2001, Mazzucato et al., 1999*). As circulating vWF does not bind to platelets, the immobilization of plasmatic VWF to the ECM reveals the A1 domain of VWF that carries the binding site for the platelet GbIbα glycoprotein receptor (*Peyvandi et al., 2011, Savage et al., 1996*). This initial interaction between platelets and vWF is a key player in the rolling of platelets at the site of vascular injury. Moreover, other ECM constituents as fibronectin recruit integrin α5β1 to platelets to promote stable arrest. The initial engagement of vWF-GpIb results in an increase in intracellular Ca^{2+} levels (*Kroll et al., 1991*), which is critical for activating integrin αIIbβ3 (GpIIb-IIIa) on platelets. This gives the second crucial step in platelet activation as it facilitates further platelet aggregation. Furthermore, the firm adhesion of platelets to the site of vascular injury leads to conformational changes and to the release of α-granules which ultimately triggers the production of various pro-thrombotic agents such as thromboxane A2 (TxA2).

A stable fibrin clot is important for the successful completion of haemostasis. Tissue factor (TF) delivered from impaired vessels binds to and then activates coagulation factor VII (FVII). Activated FIX employs activated FVIII (FVIIIa) as a cofactor for FX conversion, which in turn favours prothrombin activation and fibrinogenesis (*Palta et al., 2014*). The key to this terminal step is the availability of FVIII as a substrate. FVIII covalently binding to vWF upon release from the endothelial cells preserves it from proteolytic degradation by protein C. Recent reports indicate that vWF-FVIII interaction may also occur intracellularly in some endothelial beds (*Turner and Moake, 2015*). This shows why in early reports of vWD, patients exhibited haemophilia-like symptoms and low levels of FVIII. Subsequent studies showed that mutations in the FVIII binding domain (D'-D3) of vWF could lead to a subtype of vWD that is characterised by low FVIII levels and normal vWF levels.

E. The effect of shear on platelet adhesion and vWF conformation

Platelets are produced in the bone marrow by MKs and are atypical cells as they form out of MK cytoplasmic fragments and do not possess a nucleus. In a healthy human adult, a total of ~$3x10^{11}$ platelets/litre of blood and ~$1x10^{9}$ produced/day (*Kaushansky, 2006*). Platelets are essential for primary haemostasis, constituting the core of the haemostatic plug. During normal conditions, the surface of endothelial cells delivers an anti-coagulant milieu and also suppresses platelet activation (*Cines et al., 1998*). The high content of platelets results in their engagement in additional events including inflammation, angiogenesis and immunity (*Semple et al., 2011*). Concerning haemostasis, the activation of platelets may be triggered by a wide range of stimuli and the outcome is a shift in platelet morphology and the delivery of molecules promoting platelet aggregation (*Broos et al., 2011*). *Ex vivo* measurement of platelet function frequently involves the assessment of adhesion and aggregation as separate platelet functions; while *in vivo*, adhesion and aggregation both involve the capture of platelets from the circulation to the site of injury with related receptor and ligand pairs involved in both processes (*Ruggeri, 2009*).

An important aspect of blood flow dynamics, as well as platelet adhesion and aggregation, is the role of shear gradients in generating haemostatic plug formation (*Nesbitt et al., 2009*). In a simplified overview of a blood vessel, the rapidity of blood flow is maximal at the centre and declines to zero at the wall. Thus, blood flow through a vessel can be conceived as "an infinite number of infinitesimal laminae sliding over each other" (*Kroll et al., 1996*). Each lamina undergoes frictional interaction with adjacent layers, with the shear stress described as the force per unit between the laminae. Vessel radius and operating pressure affect shear stress, and this is defined by the unit: dynes per square cm (dynes/cm^2). The most widely used variable to depict the flow conditions of a blood vessel is the "shear rate", quantified in inverse seconds (s^{-1}).

The "shear rate" is distinct from the “shear stress” as the shear rate represents the change in speed relative to the distance measured perpendicular to the flow direction. The shear rate is maximum closer to the vessel wall and zero in the centre, in contrast to the speed. Shear rate shows a distinct correlation with shear stress and can be used to calculate shear forces in different vessels *in vivo* (*Kroll et al., 1996*) and application to microfluidic devices *in vitro* (*Sarvepalli et al., 2009, Roest et al., 2011*).

Platelet adhesion mechanism strongly relies on the local shear rate: at low shear rates (<500-1000s^{-1}) it can occur regardless of vWF (*Ruggeri, 2007*) and is directly intermediated via resting platelet surface receptors and exposed ECM. The major receptor engaged in low-shear adhesion is GP VI (predominant on α2β1) which interacts with collagens in the ECM (*Nieswandt & Watson, 2003*). Additional adhesive interactions have been demonstrated with fibronectin, laminin and vitronectin through other platelet surface receptors (*Ruggeri, 2009*). Above 1000s^{-1}, platelet adhesion is dependent on vWF (*Savage et al., 1998*). Increased shear forces shorten the contact time between the platelet receptor and the potential adhesive ligand. Only the interaction of the A1 domain of vWF with GpIbα has a sufficiently fast on-rate to make platelet adhesion easier at higher shear rates (*Savage et al., 1996*). Multiple binding and breakage events cause platelets to roll through the vWF, reducing their speed, ultimately resulting in more stable adhesive interactions and subsequent aggregation (*Fredrickson et al., 1998*).

The impact of shear forces on the entire conformation of vWF multimers is crucial for its haemostatic function. Early experiments with atomic force microscopy (AFM) were employed to visualise vWF purified from plasma immobilised on a hydrophobic surface: the unperturbed vWF multimers adopted a globular shape. When shear force was applied (7-19 pN using the AFM needle), a brief extension of the globular conformation was seen. The application of >35 dyne/cm^2 shear force (using a rotating disc) resulted in further extension of the vWF (*Siedlecki et al., 1996*) multimer conformation. It is now well recognised that shear-induced conformational change is an important aspect of vWF function (*Springer, 2014, Schneider et al., 2007*). The nature of the shifts in the molecular structures of single vWF domains and monomers and the way they shape the overall structure and function of vWF multimers is still an intriguing question, attracting interest from the research fields of biology, biochemistry, bioengineering, biophysics and polymer physics (*Gogia & Neelamegham, 2015*, *Sing & Alexander-Katz, 2010, Andrews & Berndt, 2008).*

The well-known effects of shear-dependent vWF conformational change are vWF A1 domain exposure and its consequential interaction with GpIbα, vWF A2 domain unfolding leading to ADAMTS13 proteolysis and self-association of vWF multimers in long fibres (although there is no defined molecular mechanism). The required force to cause the conformational change varies depending on the multimeric size of the vWF (larger multimers are more sensitive to haemodynamic forces) and on if the vWF multimers are in solution or immobilised on a surface (*Springer, 2011*). In addition, the type of surface on which vWF is immobilised may affect the force demanded. This has been demonstrated with vWF fibres being formed at lower shear rates on endothelial cells (*Dong et al., 2002*) compared to collagen-bound vWF (*Colace & Diamond, 2013*). Variations in the in vitro morphology of vWF arise upon adsorption onto surfaces with a different hydrophobic or hydrophilic nature (*Raghavachari et al., 2000, Tronic et al., 2016*).

Single-molecule pulling tests performed on recombinant vWF fragments disclosed regions of vWF that may behave as "resistance points" to pulling stresses, shifting conformation over a specific force threshold. The most evident example is the A2 domain of the vWF. Pulling trials with vWF domain A2 in isolation have shown that the domain experiences a dramatic conformational change at forces >10 pN.

The spacing between the N and C termini extends from 1nm to 60nm over pulling, thereby assisting the proteolysis of the vWF A2 domain by ADAMTS13 (*Zhang et al., 2009*). The distinct unfolding signature (length span of ~60 nm) of the vWF A2 domain was also observed with single-molecule unfolding studies of the isolated vWF A2 domain, similarly to that of large fragments of vWF (*Müller et al., 2016, Jakobi et al., 2011, Wijeratne et al., 2013*).

A feature of the shear-guided conformational change is the following exposure of the A1 domain of vWF and its interplay with platelets via their surface receptor GpIbα. The interaction fails to occur under static, low-shear conditions. The function of forces in controlling the interaction is apparently three-fold. Primarily, forces propagate the vWF conformational change from its globular "bird's nest" to a stretched conformation (*Schneider et al., 2007*), and expose the previously concealed vWF A1 domain. The "resistance points" that preclude vWF A1 domain exposure are most likely: intra-multimer self-association of vWF domains (*Ulrichts et al., 2005*), shielding of the vWF A1-GpIbα binding site by the D'D389 domain, O-linked glycan-containing regions (*Nowak et al., 2012, Madabhushi et al., 2014, Ju et al., 2013*) and vWF A1-A290 domain interactions (*Aponte-Santamaría et al., 2015*). The question of if the exposure of the vWF A1 domain involves forces that are comparable to those required to unravel the vWF A2 domain and whether the events take place concomitantly is not fully defined. In addition to the exposure of the vWF A1 domain, the shear forces dictate the nature of the bond between vWF A1 and GpIbα.

There are two different states of the bond. At initial low interaction forces, 'slip' binding appears, in that binding duration diminishes and strength augments (a general rule for most receptor-ligand interactions) (*Sokurenko et al., 2008, Thomas, 2008*). At initial stronger forces, the bond nature changes, lengthening the bond duration and boosting the breaking force from ~10 to 20pN (*Kim et al., 2010*). vWF's capacity to fine-tune mechanically stabilised bond formation/catch with rapidly mobilizing platelets is a key part of its haemostatic role. A third influence of force lies in regulating the vWF A1 domain conformation. When traction forces are applied through the vWF A1 domain, they are expected to subtly change the conformation of the domain. Once these forces exceed a specific force threshold, the vWF A1 domain is presumed to enter a high-affinity state. This is probably at the basis of the enhanced binding strength seen at higher forces (*Springer, 2014, Kim et al., 2010*). The inspection of the crystal structure of the WT vWF A1 domain suggests that there is a network of hydrogen bonds around the disulfide bond crossing the domain. When force is applied to the A1 domain these interactions break down, virtually favouring conversion to a high-affinity state (*Springer, 2014*). Molecular engineering of the A1 domain of vWF to yield a high-affinity interaction with GpIbα resulted in an A1 variant (Y1271C/C1458R), with the disulfide expanding domain displaced by one residue (*Blenner et al., 2014*).

This variant bound to GpIbα with an affinity similar to that of the vWD type2B mutations identified in the vWF A1 domain (*Blenner et al., 2014*), whereby the high-affinity state (induced by the mutation) was present at low strengths, which likely underlies the increased interaction with GpIbα under static conditions (*Yago et al., 2008*).

A less mechanistically delineated role of shear forces is in vWF self-association. Mismatched cysteine residues in the C-terminal vWF segment were found to be involved in vWF self-association (*Ganderton et al., 2011*). Shear forces have been shown to play a key function in the self-association that likely takes place following vWF A1 domain interaction with GpIbα (*Choi et al., 2007, Shankaran et al., 2003, Dayananda et al., 2010*). The shear-driven conformational changes resulting in lateral association of vWF are unclear. It remains to be determined if there are conformational changes in vWF that promote lateral association across distinct domains or if indiscriminate twinning of vWF multimers occurs. As with other conformational changes in vWF, there is likely a “resistance point” that vWF overcomes to engage in self-association. Recent tensile experiments have identified that a strong interaction occurs between the D4 domains of vWF dimers (requiring forces of ~50pN to explain, compared to ~10pN to explain the A2 vWF domain) and keeps vWF if a “closed conformation” (*Müller et al., 2016*). It could be inferred that after this interaction is overcome, exposed regions of the C-terminal tail could engage in lateral self-association.

III. Impact of von Willebrand Factor on Staphylococcal Pathogenesis

vWF release from the endothelial WPBs is induced by host-directed hormones including epinephrine and histamine along with other plasma factors but is also elicited by pathogenic bacteria (*van Mourik et al., 2002*). For instance, the intracellular pathogen *Rickettsia rickettsii*, the major cause of Rocky Mountain spotted fever, triggers vWF secretion from WPBs of cultured endothelial cells (*Sporn et al., 1991*). It is also well-established that vWF secretion from human pulmonary endothelial cell WPBs is markedly up-regulated in the presence of pneumococcal adherence and response to the cytotoxic effects of the pneumococcal toxin pneumolysin (*Lüttge et al., 2012*). These findings provide a strong suggestion that in vivo, the interplay of circulating bacteria in the bloodstream and with the endothelial vasculature could directly contribute to elevated plasma vWF levels.

In this context, a scientific debate on whether the released vWF is used directly by the bacteria for their advantage, in that it serves as a binding site to the host endothelium, for platelet aggregation or to interfere with host coagulation, has been raised. As a matter of fact, *S. aureus* bacteria have been shown to bind to vWF-coated surfaces and vWF in suspension (*Herrmann et al., 1997*). A heparin-susceptible bacterial adhesion to soluble vWF has also been described for coagulase-negative Staphylococcus species, frequently linked to prosthetic device infections (*Li et al., 2000*).

The adhesion of bacteria to the vascular endothelium is of considerable significance for the pathology of blood-borne infections, as this fosters bacterial establishment, prompts inflammatory responses and favours bacterial transmigration and dissemination to deeper tissue locations. Therefore, it became evident that the bloodstream-induced conformational changes of the vWF molecule, being crucial for the physiological function of vWF in the bloodstream, could also be very relevant for vWF-mediated bacterial adhesion. Indeed, it has already been proved that, under defined flow conditions, staphylococci adhere directly to vWF multimers and also attach to collagen of the exposed subendothelium in blood-borne infections (*Mascari & Ross, 2003*). *S. aureus* adhesion to cell-exposed vWF has also been recorded *in vivo* (*Liesenborghs et al., 2019*), providing evidence for vWF-mediated bacterial adhesion to vascular endothelium. Furthermore, there is direct evidence that *in vivo* attachment of bacteria to multimeric vWF strings in the circulation results in an enhanced resistance to shear-stress driven clearance by blood flow (*Pappelbaum et al., 2013*).

The bacterial interplay with components of haemostasis *in vivo* would suggest the existence of dedicated bacterial surface proteins, mediating vWF binding. SpA from *S. aureus* is a vWF-binding receptor on the bacterial surface. SpA elicits binding activity to both soluble and surface-immobilised vWF (*Viela et al., 2019*). Subsequently, the sites for vWF binding within SpA were restricted to the IgG-binding domain (*O'Seaghdha et al., 2006*). By employing single-molecule atomic force microscopy (AFM), Viela et al. provided extensive evidence that vWF binds very strongly to SpA employing a force-sensitive capture binding mechanism, implying force-dependent structural changes in the SpA domains (*Viela et al., 2019*). Besides SpA, an additional staphylococcal vWF-binding protein (vWbp) with a coagulase function was detected (*Bjerketorp et al., 2002, Bjerketorp et al., 2004*). Apparently, vWbp appears to have significant relevance for vWF recruitment rather than under static conditions (*Thomer et al., 2013*). Similarly, pneumococci bind vWF under static conditions and also recruit circulating globular vWF through surface-exposed enolase (*Jagau et al., 2019*).

On the basis of the clinical symptoms, various functional aspects of the interaction of bacteria with vWF may be linked directly or indirectly to a minimum of three major infection pathologies: infective endocarditis, bacterial sepsis and cardiovascular complications. Heart valves infection begins when circulating bacteria attach to the endocardium and form bacterial vegetations, that are incorporated within fibrin and platelets (*Guerrero et al., 2011*). The resulting inflammatory processes cause, among other things, vWF deposition on vascular endothelial cells. Also, as it also generates extensive shear stress, vWF stretches and exposes cryptical binding sites for bacterial adhesins, which in turn mediates bacterial adhesion to the hearth valve (*Liesenborghs et al., 2019*). Note that of the staphylococci, *S. aureus* and *S. lugdunensis* are the only ones capable of binding vWF, and this may, perhaps, partially clarify the reason why these bacteria are more efficient at causing endocarditis than other staphylococci (*Liesenborghs et al., 2016*).

The vWF is a central player in coagulation and thrombosis as a response to vascular damage and inflammation. The bacterial interplay with vWF has great medical and scientific relevance as it is closely related to clinical manifestations and long-term consequences of infectious diseases. The binding of *S. aureus* and *S. pneumoniae* to vWF strings has been proven to be governed by hydrodynamic flow conditions. Hitherto, the following pathogenic bacterial mechanisms engaging host-derived vWF have been designated: multimeric vWF string binding facilitates bacterial adhesion to endothelial surfaces in the bloodstream - the main precondition for bacterial colonisation, inflammation and dissemination; vWF recruitment promotes bacterial entrapment inside coagulated blood, which in turn precludes bacterial elimination by immunothrombosis; the intravascular vWF recruitment prompts the formation of bacterial aggregates, which ultimately results in microcapillaries occlusion and reduced blood supply.

While several sophisticated technologies like microfluidic systems and binding force determinations have largely delivered in-depth insights within the biological and biochemical details of cells, the multifaceted complex nature of the bacterial interplay with vWF is still a demanding topic of current scientific investigation.

IV. Rationale for this study

In the early stages of infection, *S. aureus* needs to adhere to endothelial cells which constitute the outermost layer of the heart and vessel wall. For this purpose, the bacterium has developed sophisticated mechanisms to attach to endothelial cells lining the heart and vessel wall and to the extracellular matrix exposed when the endothelium is damaged. It has been shown that von Willebrand Factor (vWF) is the host mediator of staphylococcal vascular endothelial cell binding under flow (*Herrmann M. et al., 1997*). SpA has been then recognized as a ligand for vWF (*Hartleib J. et al., 2000*) and the molecular mechanisms of this interaction revealed (*O'Seaghdha M. et al., 2006*). Moreover, *S. aureus* expresses a von Willebrand factor binding protein (vWbp) mediating staphylococcal deposition on the blood vessel. Claes et al. showed that adhesion under high shear conditions was significantly reduced using a strain not expressing vWbp or by blocking the A1 domain of vWF (*Claes J. et al., 2014*). However, nearly 40% of residual shear-dependent adhesion was retained, suggesting that other vWF ligands may be expressed by *S. aureus*.

On this basis, this study aimed to identify the putative additional interactor/s of vWF expressed on the surface by *S. aureus*. The search for these was carried out in iron starvation conditions, a situation faced by the bacterium *in vivo* where it has restricted access to iron (the plasma iron concentration range is nearly 7-29 μmol l^{-1}) (*Sherwood, 2005*). Indeed, the deficiency of available iron induces the iron-dependent *fur* regulator, which controls the transcription of genes belonging to the Isd system exploited by the bacterium to overcome *in vivo* iron limitation (*Hammer & Skaar, 2011*). IsdB was identified as a new vWF receptor on the surface of *S. aureus*, and the biochemical and molecular mechanisms underlying the interaction were investigated in greater detail in this study.

MATERIAL AND METHODS

I. Bacterial Strains and Culture Conditions

All strains used in this study are listed above in Table 1. *S. aureus* cells (*Pietrocola et al., 2020, Horsburgh et al., 2002, Claro et al., 2011*) were grown overnight in brain heart infusion (BHI) (VWR International Srl, Milan, Italy) or RPMI 1640 (Sigma-Aldrich, MO, USA) medium at 37°C with shaking. *L. lactis* cells carrying the expression vector alone (pNZ8037) (*De Ruyter et al., 1996*) or harboring the *isdB* gene (pNZ8037::*isdB*) (*Zapotoczna et al., 2013*) were grown overnight in BHI medium supplemented with chloramphenicol (10 μg/ml) at 30°C without shaking. Cultures of *L. lactis* were diluted 1:100 in the same medium and allowed to reach exponential phase. Nisin (6.4 ng/ml) was added, and cultures were allowed to grow overnight as above. In experiments where a defined number of cells were used, bacteria were harvested from the cultures by centrifugation, washed, and suspended in phosphate-buffered saline (PBS), at OD_{600nm}=1.0. *Escherichia coli* BL21 (DE3) strain (Invitrogen, CA, USA) transformed with vector pQE30 or pET28a (Integrated DNA Technologies, Leuven, Belgium) was grown in Luria agar and Luria broth (VWR International Srl, Milan, Italy) containing 100 μg/ml ampicillin or kanamycin respectively at 37°C with shaking.

Table 1.

Abbreviations used are as follows: Cm^r, chloramphenicol resistance, Tc^r, tetracycline resistance.

Bacterial strain	Relevant properties	Reference
S. aureus		
SH1000 WT	Laboratory strain. rsbU $^+$ derivative of *S. aureus* 8325-4	(*Horsburgh et al., 2002*)
SH1000 *spa*	*spa*:: Tc^r transduced from 8325-4 *spa ::Tc^r*	(*Claro et al., 2011*)
SH1000 *isdB*	*isdB gene deleted by allelic exchange*	(*Pietrocola et al., 2020*)
L. lactis		
NZ9800 (pNZ8037)	Expression vector with a nisin-inducible promoter, *Cm^r*	(*Zapotoczna et al., 2013*)
NZ9800 (pNZ8037::*isdB*)	isdB gene cloned in pNZ8037, *Cm^r*	(*Pietrocola et al., 2020*)
E. coli		
XL1-Blue	*E. coli* cloning host	*Stratagene*
BL21 (DE3)	*E. coli* cloning host	*Invitrogen*

II. Plasmid and DNA Manipulation

Plasmid DNA (Table 2) was isolated using the NucleoSpin Plasmid kit (Macherey-Nagel GmbH & Co. KG, Düren, Germany), according to the manufacturer's instructions, and transformed into *E. coli* XL1-Blue or BL21 (DE3) cells using standard procedures (*Sambrook, 2001*). Transformants were screened by restriction analysis and verified by DNA sequencing (Eurofins Genomics, Milan, Italy). Cloning of IsdB NEAT1-NEAT2 (aa residues 48–480) was performed as reported before (*Miajlovic et al., 2010*).

Table 2.

Abbreviations used as follows: Amp^R, ampicillin resistance; Kan^R, kanamycin resistance.

Plasmid	Feature	Marker	Reference
pQE30	*E. coli* vector for the expression of hexa-His-tagged recombinant proteins	Amp^R	*Qiagen*
pQE30::isdB NEAT1-NEAT2	pQE30 encoding the NEAT1-NEAT2 domains of IsdB protein from *S. aureus* SH1000	Amp^R	(*Miajlovic et al., 2010*)
pQE30::IsdB-NEAT1	pQE30 derivative encoding the NEAT1 domain of IsdB protein from *S. aureus* SH1000	Amp^R	(*Pietrocola et al., 2020*)
pQE30::IsdB NEAT2	pQE30 derivative encoding the NEAT2 domain of IsdB protein from *S. aureus* SH1000	Amp^R	(*Pietrocola et al., 2020*)
pET28a	*E. coli* vector for the expression of hexa-His-tagged recombinant proteins	Kan^R	*MilliporeSigma*
pET28a::vWF-A1	pET28a derivative encoding the A1 domain of the human von Willebrand factor	Kan^R	*This study*

The synthetic gene fragment corresponding to the A1 domain of human vWF and modified based on a protocol already described in literature (*Chudapongse et al., 2011*) was purchased by Eurofins Genomics (Milan, Italy). Cloning of the A1 domain (aa residues 460-730) and IsdB NEAT1 (aa residues 144–270) and IsdB NEAT2 (aa residues 334–458) domains was performed following the NEBuilder® HiFi DNA Assembly according to the manufacturer's instructions (New England Biolabs, MA, USA). The primers used to amplify the A1 domain, IsdB NEAT1, and IsdB NEAT2 domains, and pET28a and pQE30 vectors (Table 3) were purchased from Integrated DNA Technologies (Leuven, Belgium). The assembly reaction was transformed into *E. coli* BL21 (DE3) cells, for the A1 domain, and into *E. coli* XL1-Blue, for IsdB NEAT1 and IsdB NEAT2, as reported above. Transformed colonies were selected and verified by colony PCR. DNA purification was carried out using the NucleoSpin Gel and PCR Clean-up kit (Macherey-Nagel GmbH & Co. KG, Düren, Germany) and transformants were then verified by DNA sequencing (Eurofins Genomics, Milan, Italy).

Table 3

Primer	Sequence (5'-3')	5' restriction site
A1 (460-730) F	agcaaatgggtcgcggatccgatgttgtcaacctcacctctgaagc	BamHI
A1 (460-730) R	tgtcgacggagctcgaattcTCAcaagagccccgggcc	EcoRI
pET28a-A1 F	gaattcgagctccgtcgac	EcoRI
pET28a-A1 R	ggatccgcgacccatttg	BamHI
IsdB-NEAT1 (144-270) F	tcacggatccacaaatacagaagcacaac	BamHI
IsdB-NEAT1 (144-270) R	tggctgcaggtttttcaggaagtttatcttgaattttatttaattc	PstI
pQE30-NEAT1 F	tcctgaaaaacctgcagccaagcttaattag	PstI
pQE30-NEAT1 R	ctgtatttgtggatccgtgatggtgatg	BamHI
IsdB-NEAT2 (334-458) F	tcacggatccttaaaggctgagtacaag	BamHI
IsdB-NEAT2 (334-458) R	tggctgcaggagtagcttccttcttagc	PstI
pQE30-NEAT2 F	ggaagctactcctgcagccaagcttaattag	PstI
pQE30-NEAT2 R	cagcctttaaggatccgtgatggtgatg	BamHI

III. Expression and purification of recombinant proteins

Recombinant proteins IsdB NEAT1-NEAT2, IsdB NEAT1, and IsdB NEAT2 were expressed from pQE30 (Qiagen, Hilden, Germany) in *E. coli* XL1-Blue (Agilent Technologies, CA, USA). Recombinant A1 domain was expressed from pET28a (Millipore-Sigma, MA, USA) in *E. coli* BL21 (DE3) (Invitrogen, CA, USA). Overnight starter cultures were diluted at 1:40 in Luria broth containing the appropriate antibiotics (see above) and incubated with shaking until the culture reached the exponential phase (A_{600} = 0.4-0.6). Recombinant protein expression was induced by the addition of 1mM (final concentration) isopropyl 1-thio-β-D-galactopyranoside (IPTG) (Inalco, Milan, Italy) to the culture. After 4 h, bacterial cells were harvested by centrifugation and frozen at -80°C. Cells were re-suspended in lysis buffer (50 mM NaH_2PO_4, 300 mM NaCl, pH 8.0) containing 1 mM phenyl-methane-sulfonyl-fluoride (PMSF) (Sigma-Aldrich) and 20 µg/mL DNase (Sigma-Aldrich, St. Louis, MO, USA) and lysed by sonication (70% amplitude, 12 x 30″ on/off, 1′30″ interval between sonication steps). The cell debris was removed by centrifugation and proteins purified from the supernatants by Ni^{+2}-affinity chromatography on a HiTrap chelating column (GE Healthcare, Buckinghamshire, UK). Protein purity was assessed by 10% SDS-PAGE and Coomassie Brilliant Blue staining. A bicinchoninic acid protein assay (Pierce, Rockford, IL, USA) was used to measure the concentration of purified proteins.

Recombinant proteins FnBPA$_{194-511}$ (*Keane et al., 2007*), FnBPB$_{163-480}$ (*Burke et al., 2011*), IsdA$_{47-313}$ (*Clarke et al., 2004*), IsdH$_{41-660}$ (*Visai et al., 2009*), ClfA$_{221-559}$ (*O'Connell et al., 1998*), ClfB$_{201-542}$ (*Mulcahy et al., 2012*), CNA$_{31-344}$ (*Valotteau et al., 2017*), SdrE$_{53-606}$ (*Josefsson et al., 1998*), SdrD$_{36-568}$ (*Josefsson et al., 1998*), kindly provided by Prof. Timothy J. Foster and Prof. Joan A. Geoghegan of the Microbiology Department, Moyne Institute of Preventive Medicine, Trinity College, Dublin, Ireland, were all expressed with His_6 N-terminal affinity tags and purified as reported above.

IV. Reagents, proteins, and antibodies

BSA (bovine serum albumin), Protease-free DNase I, Skim milk, von Willebrand factor, Heparin, Chondroitin sulphate, Heparan sulphate, Lysostaphin, Nisin, Protein A (SpA$_{37-485}$), Biotin, Avidin-HRP, Trypsin, Calcium ionophore A23187 were purchased from Sigma-Aldrich. Collagens type I, type III, type IV, and type VI were purchased by Merck (Darmstadt, Germany). Ristocetin was from Hyphen BioMed (Neuville-sur-Oise, France). IgG were isolated from patients with infective endocarditis as previously reported by Rindi *et al*. (*Rindi et al., 2006*). Anti-A1 6D1 monoclonal antibody was raised as previously described (*Claes et al., 2014*). αThrombin and PPACK were bought from Haematologic Technologies (Essex Junction, VT, USA). Sensor Chip NTA and Ni^{2+} Sepharose 6 Fast Flow resin were purchased by Cytiva Lifesciences (Washington, USA). IsdB antibody was raised in rabbit by routine immunization procedure using purified IsdB NEAT1-NEAT2 as antigen. Anti-*L. lactis* antibody was raised in rabbit by routine immunization procedure using heat-inactivated *L. lactis* NZ9800 cells as antigen. Rabbit anti-human von Willebrand factor antibody and rabbit anti-mouse or goat anti-rabbit Horseradish Peroxidase (HRP)-conjugated secondary antibodies were purchased from Dako Cytomation (Glostrup, Denmark). Monoclonal mouse HRP-conjugated α-polyHistidine antibody were purchased from Abcam (Cambridge, UK).

V. Validation of isdB gene expression by quantitative RT-PCR (qRT-PCR)

Total RNA was extracted from *S. aureus* SH1000 *spa* cells during the exponential (OD_{600nm} of 0.4-0.6) and stationary phases (OD_{600nm} of 1.0) of growth in BHI and RPMI media. Cells were harvested and total RNA was stabilized with RNeasy Protect Bacteria Reagent (Qiagen, Hilden, Germany) according to the manufacturer's instructions. Total RNA was extracted using the Quick-RNA Fungal/Bacterial Miniprep Kit (Zymo Research, CA, USA) following the manufacturer's recommendations. DNA was removed by DNase I treatment by using the TURBO DNA-free kit (Invitrogen, CA, USA). The RNA concentration was >100 ng/µL, and the A260/A280 ratio was >1.8. qRT-PCR was performed with iTAq Universal SYBR Green One-Step Kit (Bio-Rad) using 4 ng of RNA in 20 µl volumes carried out on three replicates and all reactions were performed in 20 µL volumes according to the manufacturer's protocol. The cDNA was analyzed using primers relative to the *isdB* coding sequence. The conditions for thermal cycling were as follows: 50°C for 10 mins and 95 °C for 1 min, then 35-40 cycles with 95 °C for 10 sec and then 60 °C for 10-30 sec, followed by a slow increase of temperature by 0.5 °C per cycle to 95 °C, with continuous measurement of the fluorescence.

Four ng of total RNA from each sample were used in a qRT-PCR experiment performed using a CFX Connect Real-Time PCR Detection System (Bio-Rad) and iTAq Universal SYBR Green One-Step Kit (Bio-Rad). Expression of isdB was analyzed using primers isdBF (GCAGGCGTTTTGTCTTTACC) and isdBR (GCCTAGCAAACCAACACCAT). Target gene expression was normalized using the reference gene rpoC which was amplified using primers SAurpoCF (CCGCACCATCTGGTAAGATTAT) and SAurpoCR (GCTGTATCGGCAAGACCTTTA). No-template and no-RT controls were run for each assay, and the specificity of each amplification product was verified using dissociation curve analysis. Standard curves were generated from serial dilutions of chromosomal DNA spanning at least six orders of magnitude. All reactions proceeded within 90% to 110% efficiency. Gene expression analysis was performed using the CFX Manager Software (Bio-Rad). Three technical replicates were performed for each experiment.

VI. Release of CWA proteins from *S. aureus* and detection of vWF-binding activity

Lysostaphin digestion. To release CWA proteins from *S. aureus*, bacteria were grown to the stationary phase, either in RPMI or BHI medium, harvested by centrifugation at 7000×*g* for 15 min at 4 °C, washed three times with PBS, and resuspended to an A_{600} = 2.0 in lysis buffer (50 mM Tris-HCl, 20 mM $MgCl_2$, pH 7.5) supplemented with 30% (w/v) raffinose. Cell wall proteins were solubilized from *S. aureus* by incubation with lysostaphin (200 µg/ml) for 20 min at 37 °C in the presence of protease inhibitors (Complete Mini; Sigma-Aldrich). Protoplasts were recovered by centrifugation at 6000 ×*g* for 20 min, while the supernatant taken as the wall fraction was concentrated by treatment with 20% (v/v) trichloroacetic acid (TCA) for 30 min at 4 °C. The precipitated proteins were washed twice with ice-cold acetone and dried overnight.

SDS-PAGE and Western blotting. Proteins released by lysostaphin digestion were boiled for 10 min in sample buffer (0.125 M Tris-HCl, 4% (w/v) SDS, 20% (v/v) glycerol, 10% (v/v) β-mercaptoethanol, 0.002% (w/v) bromophenol blue), separated by 10% (w/v) SDS-PAGE and electroblotted onto a nitrocellulose membrane (GE Healthcare). After blocking with 5% (w/v) skim milk (Sigma-Aldrich) in PBS overnight at 4 °C, the membrane was probed with either 2 µg/ml of human von Willebrand factor in PBS for 1h at 22°C followed by rabbit polyclonal anti-vWF antibody (1:5000) and HRP-conjugated goat anti-rabbit antibody (1:10000) in 1% (w/v) skim milk (Ligand Western Blotting) or with rabbit polyclonal anti-IsdB antibody (1:5000) and HRP-conjugated goat anti-rabbit antibody (1:10000) in 1% (w/v) skim milk (Western Immunoblotting). Blots were developed using the ECL Advance Western blotting detection kit (GE Healthcare), and images of the bands were captured by an ImageQuantTM LAS 4000 mini-biomolecular imager (GE Healthcare).

ELISA-type solid-phase binding assays

Binding of vWF to IsdB and blocking experiments. The ability of soluble vWF to bind to immobilized recombinant CWA proteins (SpA_{37-485}, $FnBPA_{194-511}$, $FnBPB_{163-480}$, $IsdA_{47-313}$, $IsdB_{48–480}$, $IsdH_{41-660}$, $ClfA_{221-559}$, $ClfB_{201-542}$, CNA_{31-344}, $SdrE_{53-606}$, $SdrD_{36-568}$) was determined by ELISA assay. Microtiter wells were coated overnight at 4 °C with 1 µg/well of each protein in 0.1 M sodium carbonate, pH 9.5. The plates were washed three times with 0.5% (v/v) Tween 20 in PBS (PBST). To block additional protein-binding sites, the wells were treated for 1 h at 22 °C with 2% (v/v) BSA in PBS and incubated for 1 h at 22 °C with 1 µg/well of vWF in PBS. The plates were incubated with a rabbit polyclonal anti-human von Willebrand factor IgG (1:1000 in 1% (v/v) BSA) and incubated for 1 h at 22 °C.

The wells were then incubated with an HRP-conjugated goat anti-rabbit antibody (1:1000 in 1% (v/v) BSA) for 45 min at 22°C. After washing, *o*-phenylenediamine dihydrochloride was added to the wells and the absorbance at 490 nm was determined using an ELISA plate reader (BioRad, CA, USA).

To determine the effect of vWF ligands (heparin, and different types of collagens) on IsdB-vWF interaction, microtiter wells, coated with 1 μg of vWF, were incubated with 1 μg of IsdB in the presence or absence of 10 μg/well of each ligand. IsdB-binding to vWF was detected by the addition of a rabbit polyclonal anti-IsdB IgG (1:2000) followed by HRP-conjugated goat anti-rabbit antibody (1:1000).

The binding of 1 μg of IsdB to surface coated vWF (1 μg/well) in presence of increasing concentrations (from 0 to 10 μg/well) of heparin, chondroitin sulfate, or heparan sulphate was detected with IsdB antibody as reported above.

To assess the effect of ionic strength on the IsdB-vWF interaction, microtiter wells coated with 1 μg of vWF were incubated with 1 μg of IsdB in presence of increasing concentrations of NaCl (from 0 to 1 M). Complex formation was detected by incubation of the wells with the IsdB antibody.

The dose-dependent binding of IsdB to surface-coated human vWF or A1 domain (1 μg/well) was evaluated by incubation of the plates with increasing concentrations of IsdB (from 0 to 5 μg/well). Bound protein was revealed as reported before.

Binding of increasing concentrations of the A1 domain (from 0 to 5 μg/well) to immobilized IsdB NEAT1-NEAT2 or its subregions NEAT1 and NEAT2 (1 μg/well) was also assessed and detected by the addition of anti-human von Willebrand factor IgG.

To assess the allosteric conformational change and the A1 domain exposure by ristocetin treatment, vWF (10 μg /ml) was treated with 0.5 mg/ml of ristocetin and the complex used to coat microtiter wells (100 μl). The A1 domain exposure was evaluated by the addition of the anti-A1 domain monoclonal antibody 6D1 (250 ng/well) followed by HRP-conjugated rabbit anti-mouse antibody (1:1000) to the wells.

The impact of the conformational change of the ristocetin-treated vWF was evaluated by measuring the binding of soluble vWF (1 μg/well) to immobilized IsdB (1 μg/well). The complex formation was detected using anti-human vWF IgG as previously reported.

Bacterial adhesion to surface-coated vWF. The ability of *S. aureus* or *L. lactis* ectopically expressing IsdB, to adhere to surface-coated vWF was evaluated by ELISA-based assay. Microtiter wells coated with vWF were incubated with cells (A_{600}=1.0) of *S. aureus* SH1000 and its *isdB* mutant obtained from cultures grown to stationary phase in RPMI and suspended in 0.5% (v/v) BSA. The wells were extensively washed with PBST, blocked with 2% (v/v) BSA, and incubated with 100 µl bacterial suspensions for 1 h at 22°C. Bacterial adhesion was detected by incubating the plates for 45 min with an HRP-conjugated rabbit anti-mouse antibody (1:1000). Adhesion of *L. lactis* to vWF was performed by incubating plates coated with vWF with cells of *L. lactis* expressing IsdB (*L. lactis* pNZ8037::*isdB)* and the strain carrying the empty vector (*L.lactis* pNZ8037) obtained from cultures grown in BHI. *L. lactis* binding to surface-coated vWF was detected by incubating 1 h at 22 °C with a rabbit polyclonal anti-*L. lactis* IgG (1 µg/well) followed by an HRP-conjugated goat anti-rabbit antibody (1:1000).

Reactivity of IgG from patients with infective endocarditis against IsdB. To test the reactivity of IgG from the collection of IE sera IsdB NEAT1-NEAT2 was immobilized onto microtiter wells (1 µg/well). After blocking with BSA, the wells were incubated with antibodies (1 µg/well) from patients and healthy donors. The binding of antibodies was revealed by the addition of a polyclonal rabbit anti-human IgG (1:1000).

VII. Capture of vWF by *S. aureus* cells

Cells of *S. aureus* strain SH1000 or the *isdB* mutant, grown to stationary phase in RPMI, were harvested by centrifugation at 7000×*g* at 4 °C for 15 min, washed three times with PBS, and resuspended to an A_{600} =1.0 in PBS. Cells were then incubated with human vWF (5 µg/mL) for 1 h at 22 °C under constant shaking. Bacteria, harvested by centrifugation, were washed with PBS and treated with the extraction buffer (125 mM Tris-HCl, pH 7.0, 2% (w/v) SDS) for 3 min at 95°C and finally centrifuged at 10.000 ×*g* for 3 min. The supernatants were subjected to 5% (w/v) SDS-PAGE under reducing conditions, and the proteins were electrotransferred to a nitrocellulose membrane. The membrane was incubated with a rabbit polyclonal vWF antibody followed by HRP-conjugated goat anti-rabbit IgG. The band intensities were quantified with Quantity One software (Bio-Rad).

VIII. Surface plasmon resonance

For performing SPR measurements on an NTA-Ni^{2+} sensor chip (see below), the recombinant 6xHis-tag-A1 was treated with α-thrombin to remove the 6xHis tag and yield the A1 domain sequence with an additional 17-amino acid segment at the N-terminus. The fused protein (1 mg/ml, 0.5 ml) was treated at an enzyme:substrate molar ratio of 1:200 in PBS, for 1h at 25 °C. The reaction was quenched by adding 1 μM (D)-Phe-Pip-Arg-chloromethylketone, as an irreversible thrombin inhibitor, while A1 was purified by the batch mode procedure. Briefly, the reaction mixture was incubated with 25 μl of Ni^{2+}-Sepharose-6 Fast Flow resin at 22°C for 1 h under gentle stirring on an orbital shaker. The supernatant, containing the purified A1, was then collected and protein purity and chemical identity were assessed by nonreducing 4-12% (w/v) SDS-PAGE, high-resolution mass spectrometry, and by Dot Blot analysis (not shown), using anti-His tag antibody as a probe, all conforming the removal of the 6xHis-tag.

SPR analyses were carried out on a dual flow-cell Biacore X-100 instrument (Cytiva, Uppsala, Sweden). 6xHis-tag-IsdB proteins (i.e., the ligands) were noncovalently immobilized onto a Ni^{2+}-chelated nitrilotriacetate (NTA) carboxymethyldestrane sensor chip, and incremental concentrations of A1 domain (i.e., the analyte) lacking the 6xHis-tag were loaded at incremental concentrations in the mobile phase, following the single-cycle operation mode. The Ni^{2+}-NTA/6xHis-IsdB chip assembly was prepared as follows: the NTA chip (Cytiva) was first washed (flow-rate: 30 μl/min) with 0.35 M EDTA, pH 8.3 (contact time: 60 sec) and then loaded with 0.5 mM $NiCl_2$ solution (120 μl, contact time: 240 sec); excess Ni^{2+} was removed by injecting 3 mM EDTA solution (contact time: 180 sec); finally, a solution of 6xHis-IsdB (130μl, 2μg/ml) was injected on the sensor chip (contact time: 180 sec) to yield a final immobilization level of 655 response units (RU). Next, the Ni^{2+}-NTA/6xHis-IsdB chip was challenged (flowrate: 30 μl/min; contact time: 120 sec) with increasing concentrations of vWF A1. All measurements were carried out at 25°C in HBS-EP+ buffer (10 mM HEPES, pH 7.4, 0.15 M NaCl, 50 μM EDTA, 0.005% v/v polyoxyethylene sorbitan). After each set of measurements, the NTA chip was regenerated by a pulse of regeneration buffer (350 mM EDTA). Each sensogram was subtracted for the corresponding baseline, obtained on the reference flow cell, and accounting for nonspecific binding, i.e., typically less than 2% of RU_{max}. The binding data were analyzed using the BIAevaluation software vs 2.0. The sensorgrams (Fig. 25, black curves) were fitted with theoretical curves obtained by simulations based on several different 1:1 stoichiometric binding models: i) simple analyte-ligand interaction, ii) bivalent analyte, and iii) heterogeneous ligand binding model (*Morton et al., 1995; Myszka, 1997*). The best fit, as evaluated from the χ^2 values of experimental and simulated sensorgrams, was obtained using the heterogeneous ligand binding model, which assumes the existence of two populations/orientations (i.e., L1 and L2) of the immobilized ligand, allowing the exposure of different ligand surfaces which are

variably accessible for interaction with the analyte. This is even more likely to occur with highly charged IsdB proteins bound on the NTA sensor chip, formed by the negatively charge chelating agent NTA and the positive Ni^{2+} ions. The relative abundance of L_1 and L_2 were estimated from their RU_{max} values, obtained as a fitting parameter, e.g. $L_1 = [RU_{max1}/(RU_{max1} + RU_{max2})] \times 100$ (*Morton et al., 1995; Myszka, 1997*).

IX. Computational methods

Electrostatic potential calculations were carried out using the APBS (*Baker et al., 2001*) program, run on the crystallographic structure of IsdB_E chain (5vmm.pdb) (*Bowden et al., 2018*), after removal of Hb coordinates, and on the crystallographic structure of the A1 domain bound to platelets thrombin receptor GpIbα (1u0n.pdb) (*Fukuda et al., 2005*), after removal of the receptor coordinates. Calculations were performed using a solvent dielectric of 78.14 and a protein dielectric of 2.0 at 310K in 150 mM NaCl.

X. Binding and Adhesion assays to endothelial cells

IsdB binding to endothelial cells. To examine the binding of recombinant IsdB to endothelial cells, human umbilical vein endothelial (HUVEC) cells were cultured onto microtiter wells. Monolayers ($8x10^4$ cells/well) were treated with 0,1mM calcium ionophore A23187 (Sigma-Aldrich) for 10 min at 22°C, washed three times with PBS, and then fixed with 3% (w/v) paraformaldehyde in PBS for 10 min. The wells were thoroughly rinsed with PBS, blocked with BSA (v/v) 2% in PBS for 1 h, and then incubated with increasing concentrations of recombinant IsdB (0.63 – 2.5 µg/well) in PBS for 1h. After extensive washing, IsdB-binding to the wells was detected by addition to the wells of a rabbit polyclonal IsdB antibody followed by HRP-conjugated goat anti-rabbit IgG.

Bacterial adherence to endothelial cells. The ability of *S. aureus* cells to adhere to HUVEC cells was assessed by an ELISA-based assay. 100 µl of bacterial suspensions (A_{600}=1.0) of *S. aureus* strain SH1000 WT and its isogenic *isdB* mutant obtained from cultures grown in RPMI were added to ionophore-treated HUVEC monolayers and the wells incubated for 1h. The attached bacteria were detected by incubating the wells with an HRP-conjugated rabbit anti-mouse antibody (1:1000) for 45 min at 22°C. To test the effect of the anti-A1 monoclonal antibody (mAb) 6D1 on the adhesion of *S. aureus* SH1000 to HUVEC monolayers, the assay was performed in the presence of 250 ng/well of the 6D1 or an unrelated mAb and bacterial attachment determined as above.

Inhibitory activity of patients' IgG on the interaction of IsdB with vWF expressed on endothelial cells. The ability of the patients' IgG to interfere with the binding of recombinant IsdB NEAT1-NEAT2 to ionophore-treated and fixed endothelial cells was determined by incubating the wells with 2.5 μg IsdB in the presence of the indicated IgG (10 μg/well) for 1h at 22°C. The binding of IsdB to the cells was detected as reported above. To analyze the effect of patients' IgG on adherence of staphylococci to ionophore-treated HUVEC cells, 100 ml of an *S. aureus* SH1000 suspension (A_{600}=1.0) were added to the monolayers and the wells incubated for 1 h at 22°C. Bacterial adherence was detected by incubating the wells with an HRP-conjugated rabbit anti-mouse antibody (1:1000). A similar adhesion protocol was used to test the effect of patients' IgG on adhesion *of L. lactis* pNZ8037::isdB and *L. lactis* pNZ8037 to the monolayers. *L. lactis* adherence to the cells was determined by adding to the wells a rabbit anti-*L. lactis* IgG (1 μg/well) followed by an HRP-conjugated goat anti-rabbit antibody (1:1000).

XI. Statistical methods.

Two-group comparisons were performed by Student's t-test. Analyses were performed using Prism 4.0 (GraphPad). Two-tailed P values < 0.05 were considered statistically significant.

RESULTS

isdB gene expression is growth-phase dependent

The expression of the *isdB* gene in cells grown both in BHI or RPMI media to mid-exponential and stationary phases of growth was analyzed by qRT-PCR (Fig. 18A). Expression of *isdB* in cells grown to stationary phase in RPMI medium was about 5-fold higher than in cells grown in BHI or cells grown to mid-exponential phase in either media.

To validate this finding, lysostaphin-solubilized cell-wall fractions of *S. aureus* SH1000 *spa* cells were subjected to SDS-PAGE and immunoblotting and probed with an IsdB antibody (Fig. 18B). While IsdB was virtually undetectable in material released from bacteria grown to both the mid-exponential and stationary phases in BHI, the protein was abundant in material released from bacteria grown to the stationary phase in RPMI (Fig. 18B, lane 3).

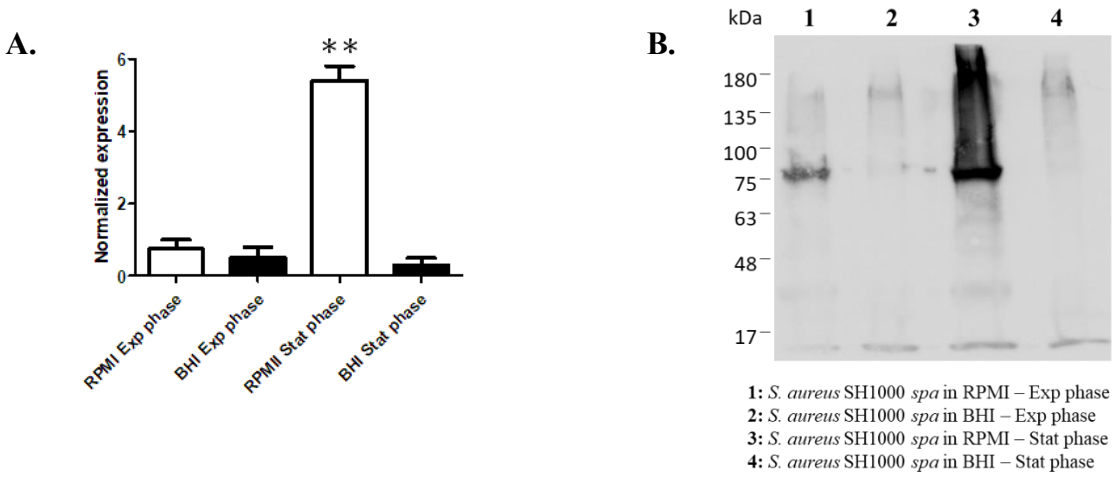

Figure 18. Expression levels of *isdB* in *S. aureus* strain SH1000 *spa*. ***A***, The expression of *isdB* gene was measured by qRT-PCR. *S. aureus* SH1000 spa cells were grown either in BHI or RPMI to both mid-exponential and stationary phases. Expression of *isdB* was normalized relative to the housekeeping reference gene *rpoC*. The reported data are the mean values ± SD from three independent experiments. Statistically significant differences are indicated (Student's t test; **, P<0.01). ***B***, Detection of IsdB expressed by *S. aureus* SH1000 *spa* grown either in BHI and RPMI to both mid-exponential and stationary phases by Western immunoblotting. Material released by lysostaphin digestion of bacteria (A_{600} of 2.0) was subjected to SDS-PAGE, transferred to nitrocellulose membrane, and sequentially probed with mouse IsdB antibody and HRP-conjugated rabbit anti-mouse IgG.

A. Identification of a novel *S. aureus* vWF-binding protein expressed in iron-limited conditions

A property of *S. aureus*, shared with other Gram-positive bacteria, is the ability to use several different CWA proteins to interact with a specific host component. As an example of this redundancy, *S. aureus* can adhere to fibrinogen via clumping factors, ClfA (*McDevitt et al., 1997*) and ClfB (*Ní Eidhin et al., 1998*), and fibronectin-binding proteins, FnBPA (*Wann et al., 2000*) and FnBPB (*Fitzgerald et al., 2006*). To date, the only CWA protein known to interact with vWF is SpA (*Hartleib et al., 2000*). In the search for new *S. aureus* surface component(s) potentially involved in vWF binding, SH1000 *spa* deletion mutant cells were grown either in iron-rich (BHI) or iron-poor (RPMI) medium. They were digested with lysostaphin, and the released material was subjected to SDS-PAGE under reducing conditions and analyzed for vWF-binding by far Western blotting. A 75 kDa vWF-binding protein was detected in material released from cells grown in RPMI (Fig. 19A, lane 1), whereas no significant signal was detected in proteins originating from cells grown in BHI (Fig. 19A, lane 2) suggesting that binding depends on a protein that is induced by iron starvation. Additional low molecular weight molecules (12–25 kDa) were observed in the material released from bacteria grown in both media.

In iron starvation conditions, *S. aureus* expresses several iron-regulated surface proteins. Among these, IsdB with a molecular weight of 75 kDa is a potential candidate receptor for vWF. To confirm that IsdB is the putative vWF-ligand, purified recombinant ligand-binding domains of several *S. aureus* CWA proteins were screened for the ability to bind vWF by an ELISA-type assay. In particular, vWF showed a binding activity for IsdB NEAT1-NEAT2 comparable to that already reported for SpA, whereas no binding to the N-terminal domains of the other proteins tested was detectable (Fig. 19B). The specificity of IsdB binding to vWF was confirmed by the finding that IsdA and IsdH did not interact with vWF.
The binding of vWF to recombinant IsdB was also observed by far Western ligand blotting (Fig.19B, inset). Altogether, these data provide evidence that IsdB is a novel surface receptor of vWF.

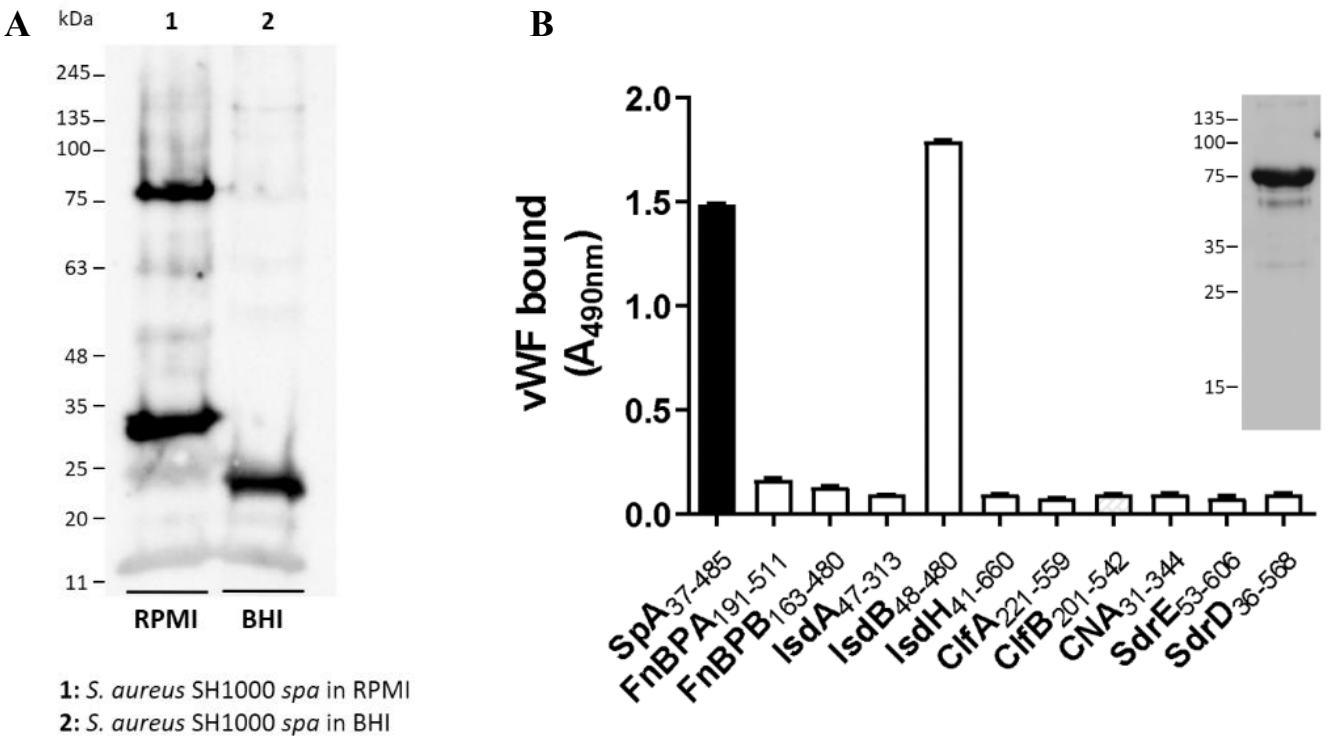

Figure 19. Identification of vWF receptor in *S. aureus* SH1000 *spa*. ***A***, Lysostaphin-released material from *S. aureus* SH1000 *spa* grown in RPMI (lane 1) and BHI (lane 2) was subjected to Far Western Blotting. The nitrocellulose membrane was probed with human vWF followed by polyclonal rabbit vWF antibody and HRP-conjugated goat anti-rabbit IgG. ***B***, Binding of vWF to surface proteins from *S. aureus*. Microtiter wells were coated with purified recombinant A regions of the indicated CWA proteins of *S. aureus* and incubated with human vWF. Ligand bound to the wells was detected with a polyclonal rabbit vWF antibody followed by HRP-conjugated goat anti-rabbit IgG. The data points are the means ±SD of two independent experiments. In the inset, binding of the vWF to purified recombinant IsdB NEAT1-NEAT2 protein in a Western blotting assay is shown.

B. Capture of vWF by *S. aureus*

To investigate the role of IsdB in promoting the recruitment of soluble vWF, *S. aureus* SH1000 WT and its isogenic *spa* or *isdB* mutants were grown in iron-deficient conditions, incubated with vWF, and the amount of ligand captured was quantified by Western blotting and densitometry. Isogenic *spa* or *isdB* mutants captured 23% and 42% less vWF than the wild type strain, respectively, suggesting that under static conditions IsdB and SpA together contribute about two-thirds to the overall vWF capture by *S. aureus* SH1000 and that other unidentified receptors could be involved in vWF-binding (Fig. 20A-B). The mutual involvement of each receptor in vWF capture would likely depend on the copy number of the protein expressed by a particular strain, the stoichiometry of the interaction as well as the environmental conditions (e.g., static versus dynamic conditions).

When human plasma was used as a source of vWF no capture of vWF was observed (data not shown). This contrasts with our ability to detect IsdB-promoted capture of vitronectin from plasma (*Pietrocola et al., 2020*). This difference is likely to be due to the different plasma concentrations of vWF and Vn (10 µg versus 300 µg per ml).

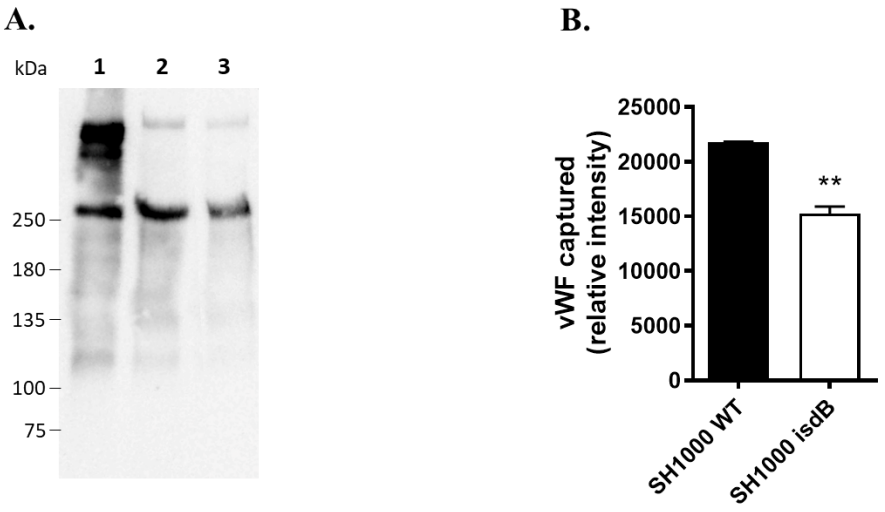

1: 2 µg vWF
2: *S. aureus* SH1000 WT + vWF (5 µg/mL)
3: *S. aureus* SH1000 *isdB* + vWF (5 µg/mL)

Figure 20. Capture of vWF by *S. aureus* cells. ***A***, *S. aureus* SH1000 WT and its *isdB* mutant were grown in RPMI to a stationary phase. The staphylococcal cells were incubated with purified human vWF (5 µg/ml) and bacteria-bound protein was released by extraction buffer and subjected to SDS-PAGE and Western Immunoblotting. 2 µg of purified vWF was loaded as control. The membrane was probed with a polyclonal rabbit vWF antibody followed by HRP-conjugated goat anti-rabbit IgG. Molecular masses of standard proteins are indicated on the left. ***B***, Densitometric analysis of vWF bound to *S. aureus* WT and its isogenic *isdB* mutant. The reported data are the mean values ± SD from three independent experiments. Statistically significant differences as indicated (Student's test; *, $p \leq 0.05$, **, $p \leq 0.01$).

C. IsdB-mediated adhesion of bacteria to immobilized vWF

To evaluate the role of IsdB in bacterial adhesion to vWF, we compared the ability of SH1000 WT and its *isdB* mutant to bind immobilized vWF in an ELISA-type assay. A significantly higher attachment of the WT strain compared to the deletion mutant was observed, indicating the important role of IsdB in bacterial adhesion to vWF (Fig. 21A). The ability of IsdB to promote adhesion to vWF was also investigated using the surrogate host strain of *L. lactis* expressing IsdB from a gene cloned into the plasmid vector pNZ8037 (*L. lactis*$_{\text{pNZ8037::}isdB}$). When lactococci were tested for adhesion to surface-coated vWF, significantly higher adhesion of *L. lactis*$_{\text{pNZ8037::}isdB}$ was observed compared to that of *L. lactis* harboring the empty vector (Fig. 21B).

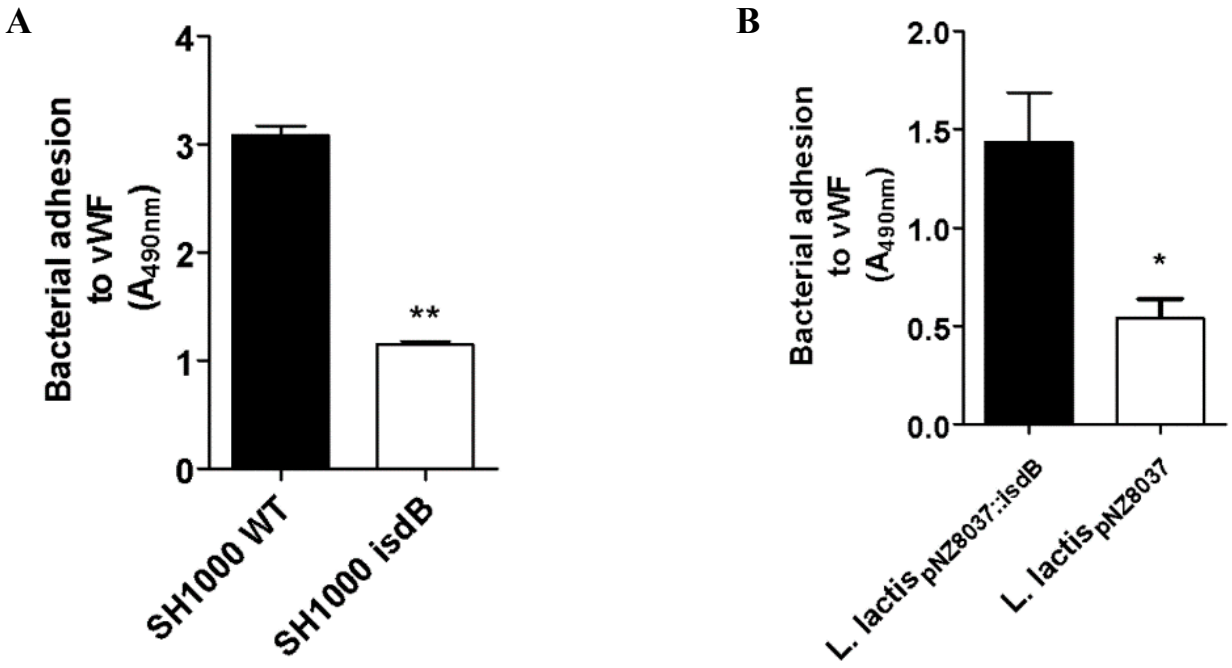

Figure 21. Adhesion of *S. aureus* and *L. lactis* ectopically expressing IsdB to immobilized vWF. ***A***, Adhesion of *S. aureus* SH1000 and its isogenic *isdB* mutant to immobilized vWF. Microtiter wells coated with vWF were incubated with cells of S. aureus SH1000 WT and its *isdB* mutant obtained from cultures grown in RPMI. Bacteria bound to vWF were detected by the addition of HRP-conjugated rabbit anti-mouse antibody to the wells. ***B***, Adhesion of *L. lactis* expressing IsdB to immobilized vWF. Microtiter wells coated with vWF were incubated with *L. lactis* ectopically expressing IsdB (*L. lactis*$_{\text{pNZ8037::}isdB}$) or *L. lactis* carrying the empty vector (*L. lactis*$_{\text{pNZ8037}}$). Bacteria bound to vWF were detected incubating the wells with a polyclonal rabbit anti-L. lactis IgG and HRP-conjugated goat anti-rabbit antibody. The data points are the means ± SD from three independent experiments, each performed in triplicate. Statistically significant differences are indicated (Student's test; *, $p \leq 0.05$, **, $p \leq 0.01$).

D. Interference of vWF binding ligands on the interaction of IsdB with vWF

A competitive inhibition assay was developed to investigate the effect of heparin and other specific vWF-ligands (collagen type I, type III, type IV, and type VI) (*Fujimura et al., 1987, Bryckaert et al., 2015*) on the binding of IsdB to vWF. Heparin and collagen type IV and VI, each of which interacts with the A1 domain, reduced IsdB binding to vWF by 80% and 50%, respectively. In contrast, collagen type I, which binds to the A3 domain, showed a marginal inhibitory effect (Fig. 22A). We also compared the dose-dependent inhibition of IsdB binding to vWF by the glycosaminoglycans, including heparin, heparan sulfate, and chondroitin sulfate. Unlike heparan sulfate and chondroitin sulfate, heparin inhibited the IsdB-vWF interaction up to 80% at the highest concentration (Fig. 22B). A further clue of the involvement of the A1 domain in IsdB binding came from the treatment of vWF with ristocetin, an allosteric effector that promotes elongation/stretching and exposure of cryptic regions including the A1 domain (*Papi et al., 2010*). Ristocetin induced a threefold higher reactivity of immobilized vWF with the anti-A1 domain mAb 6D1 (*Claes et al., 2014*) as compared to the untreated protein in an ELISA assay (Fig, 23A). The binding of ristocetin-treated vWF to immobilized IsdB was increased by nearly 40% compared to the binding of untreated vWF (Fig. 23B). Together these results indicate that IsdB binds the A1 domain of vWF.

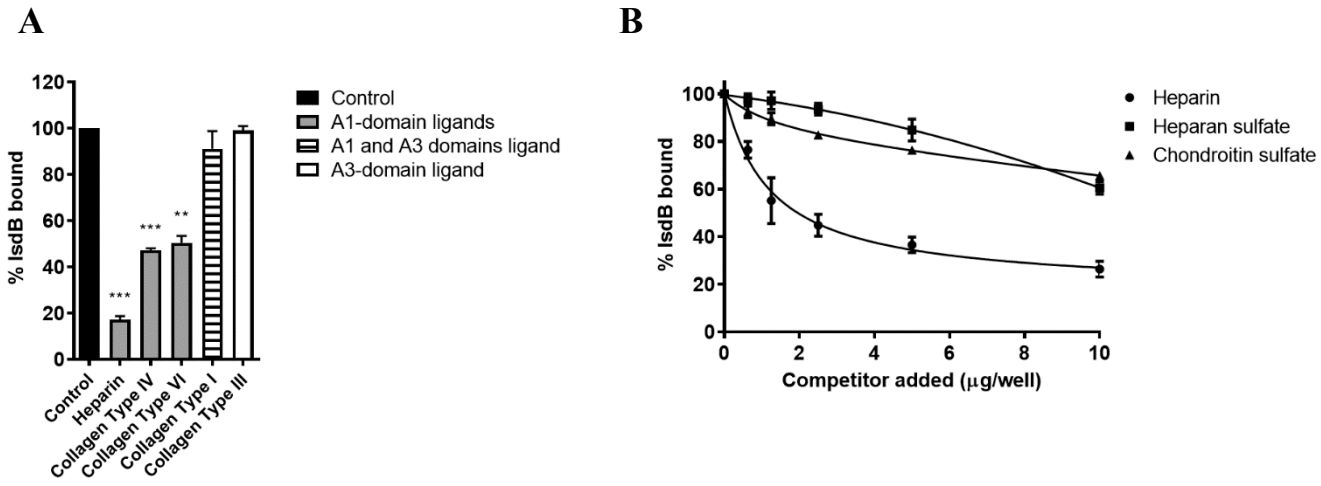

Figure 22. Interference of vWF ligands on VWF/IsdB interaction. ***A***, The effect of vWF ligands on the binding of IsdB NEAT1-NEAT2 to immobilized vWF. Microtiter wells coated with vWF were incubated with IsdB NEAT1-NEAT2 in the presence of the indicated potential competitors. IsdB NEAT1-NEAT2 binding to the wells was detected by the addition of a polyclonal rabbit anti- IsdB antibody followed by HRP-conjugated goat anti-rabbit IgG. Binding data are expressed as a percentage of the control, i.e. incubation performed in the absence of any potential IsdB competitor. ***B***, The effect of polyanionic compounds on the binding of IsdB NEAT1-NEAT2 to immobilized vWF. Microtiter wells coated with vWF were incubated with IsdB NEAT1-NEAT2 in the presence of increasing concentrations of heparin, heparan sulfate, and chondroitin sulfate. Binding was detected as reported in A The data points are the means ± SD from three independent experiments, each performed in triplicate. Statistically significant differences are indicated (Student's test; **, $p \leq 0.01$, ***, $p \leq 0.001$).

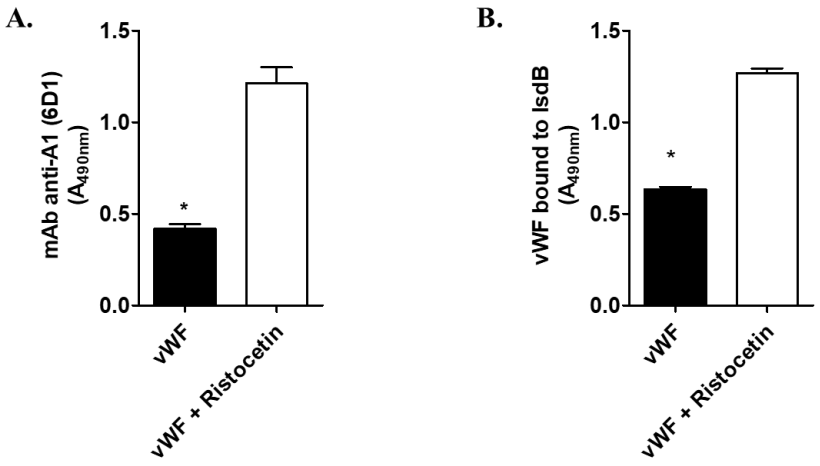

Figure 23. Binding of IsdB NEAT1-NEAT2 to ristocetin-treated vWF. ***A***, Binding of the monoclonal antibody 6D1 to vWF treated with ristocetin (0.5 mg/ml) for 30 min at 37 °C. Ristocetin-treated vWF was immobilized onto microtiter wells and incubated with the mAb 6D1. The binding of the antibody was detected by the addition of an HRP-conjugated rabbit anti-mouse antibody. The binding of 6D1 to untreated vWF is reported as a control. ***B***, Binding of ristocetin-treated vWF to immobilized IsdB NEAT1-NEAT2. Surface-coated IsdB NEAT1-NEAT2 was incubated with ristocetin-treated vWF (as reported above). The binding of the ligand to immobilized protein was detected by the addition of a rabbit polyclonal vWF antibody followed by HRP-conjugated goat anti-rabbit IgG. Data are expressed as means ± SD of triplicate tests (Student's test; ***, $p \leq 0.001$).

E. Localization of binding sites in IsdB and vWF and affinity studies

To directly show that the A1 domain of vWF carries the IsdB-binding region, the isolated A1 domain of vWF was expressed in *E. coli* and tested by ELISA-type binding assays (Fig. 24). First, the interaction between immobilized vWF or the A1 domain and IsdB NEAT1-NEAT2 was examined. IsdB bound to the A1 domain in a saturable and dose-dependent manner and the binding profile appeared to be very similar to that obtained for the binding of IsdB to the full-length vWF (Fig. 24A). This implies that there is a single binding site for IsdB in vWF. To map the vWF-binding region(s) within the IsdB protein, the binding of the A1 domain to immobilized IsdB NEAT1-NEAT2 and the IsdB NEAT1 or IsdB NEAT2 modules was assessed. Our data indicate that the A1 domain bound dose-dependently and saturably to each recombinant module and with a binding pattern resembling that exhibited by IsdB NEAT1-NEAT2 (Fig. 24B).

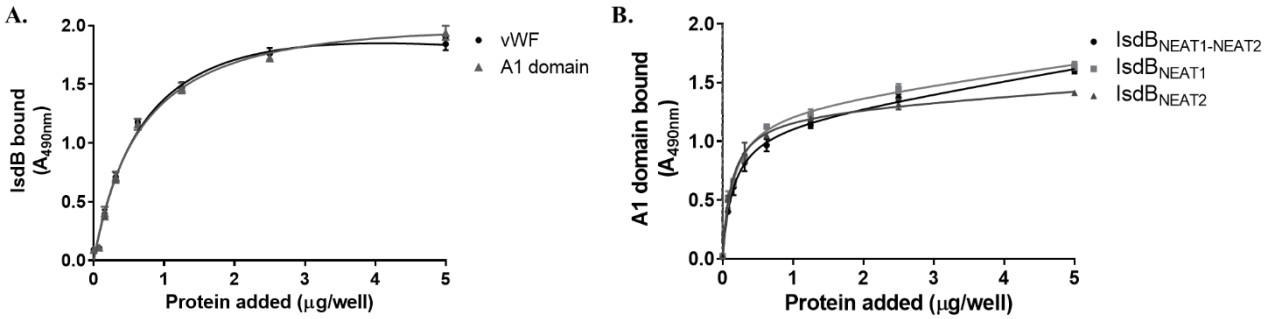

Figure 24. Localization of the binding sites involved in the interaction of IsdB with vWF. ***A***, concentration dependent-binding of IsdB NEAT1-NEAT2 to immobilized vWF or A1 domain. vWF and the recombinant A1 domain were immobilized onto microtiter wells and incubated with increasing concentrations of IsdB NEAT1-NEAT2. Complex formation was detected by addition to the wells of a polyclonal rabbit anti-IsdB IgG followed by HRP-conjugated goat anti-rabbit IgG. ***B***, Binding of A1 domain to IsdB proteins. IsdB NEAT1-NEAT2 protein and its NEAT1 and NEAT2 subregions were immobilized onto microtiter wells and incubated with increasing concentrations of the A1 domain. Ligand binding was detected as reported in Fig. 1C. The data points are the means ± SD from three independent experiments, each performed in duplicate.

To determine the affinity of the A1 domain for IsdB proteins by surface plasmon resonance (SPR), IsdB NEAT1-NEAT2 and the single NEAT domains were immobilized on an NTA-Ni^{+2} sensor chip and incubated with increasing amounts of A1 domains (from 0.08 to 1.25 μM) in a single-cycle operation mode. The sensorgrams shown in Fig. 25 revealed a complex binding system and were fitted within the framework of a 1:1 stoichiometric heterogeneous ligand binding model (*Morton et al., 1995; Myszka, 1997*), to yield the equilibrium dissociations constants (K_D) of the macromolecular complex formed between vWF A1 domain and IsdB proteins (Fig. 25). From this analysis, dissociation constant (K_D) values in the low micromolar range for the A1/IsdB protein complexes were obtained (Fig. 25). However, the A1 domain showed a higher affinity for the NEAT2 domain than that observed for the IsdB NEAT1-

NEAT2 or NEAT1 domain. Comparative analysis of the affinities of IsdB NEAT1-NEAT2 and NEAT1 and NEAT2 revealed a nonadditive behavior of the isolated domains in binding to the A1 domain. More specifically, the affinity of IsdB NEAT1-NEAT2 for A1 is much lower than the sum of the affinities of isolated NEAT1 and NEAT2. This finding is suggestive of a different binding mechanism that the two NEAT domains likely exploit for interacting with A1 in the isolated form or when they are embedded in the single-chain IsdB NEAT1-NEAT2 protein.

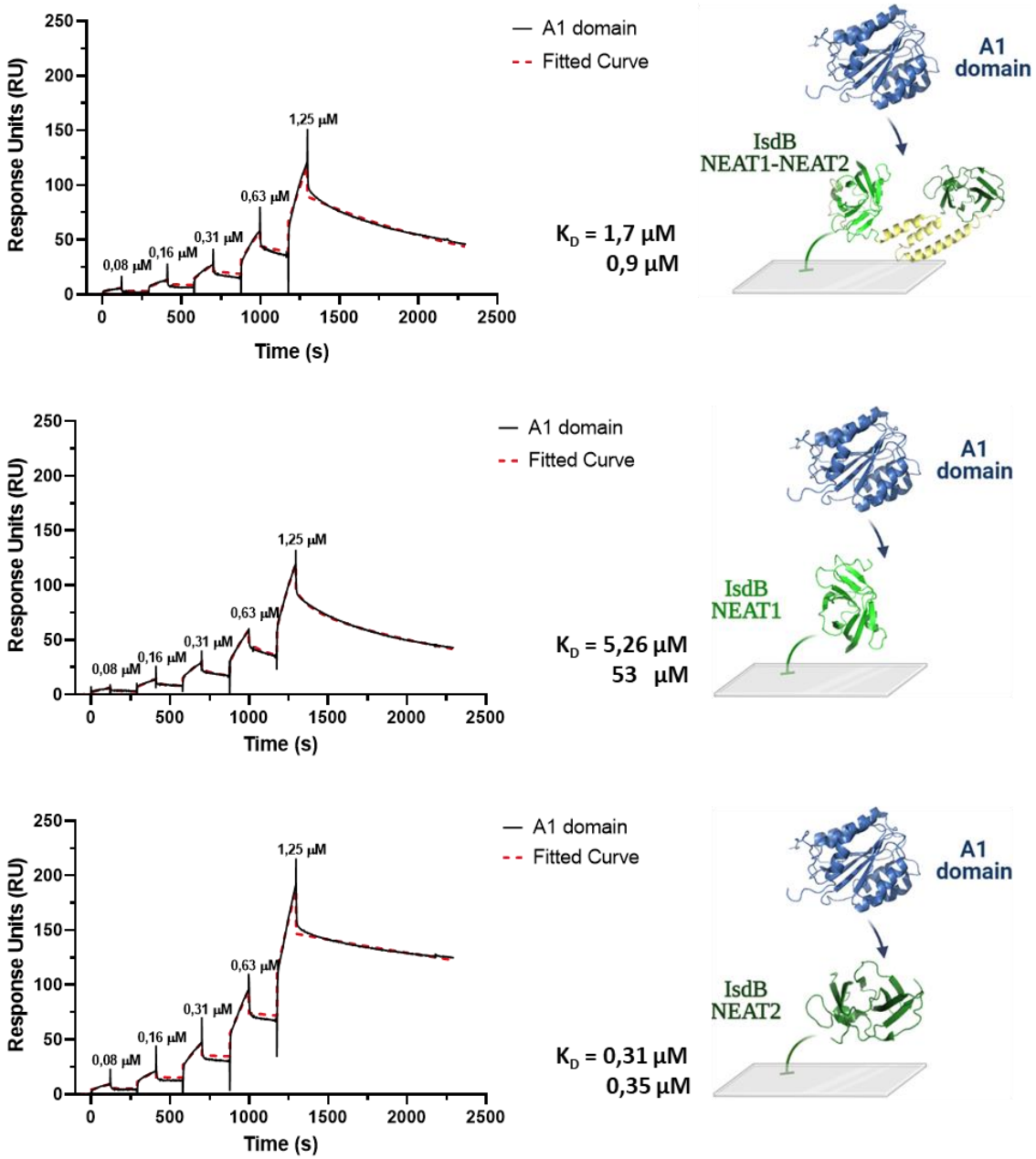

Figure 25. BIAcore analysis of A1 binding to IsdB proteins. 6xHis-tagged IsdB NEAT1-NEAT2 or isolated NEAT1 and NEAT2 were immobilized on an NTA-Ni^{2+} sensor chip, while increasing concentrations of recombinant A1 (0-1.25 µM), lacking the 6xHis tag, were loaded in the mobile phase, following the single-cycle operation mode. Sensograms were subtracted from reference flow cell data and then fitted with the equation describing the heterogeneous ligand binding model to obtain the values of K_D and RU_{max} for the two ligand populations considered (L_1 and L_2) along with their relative abundance. IsdB NEAT1-NEAT2: K_{D1} = 1.7±0.3 µM; K_{D2} = 0.9±0.2 µM; RU_{max1} = 354±21; RU_{max2} = 355±23; L_1 and L_2 = 50%. NEAT1: K_{D1} = 53±2 µM; K_{D2} = 5.3±0.3 µM; RU_{max1} = 948±40; RU_{max2} = 2705±125; L_1 = 26, L_2=74. NEAT2: K_{D1} = 0.3±0.1 µM; K_{D2} = 0.4±0.1 µM; RU_{max1} = 529±51; RU_{max2} = 527±39; L_1 and L_2 = 50%. All measurements were carried out at 25 °C, in PBS containing 0.005% v/v Tween 20.

F. Electrostatic properties of IsdB and A1 domain

To determine whether ionic forces play a role in the interaction of IsdB with vWF, the effect of increasing NaCl concentrations on IsdB binding was assessed. The addition of salt significantly reduced the binding of IsdB to immobilized vWF. At 0.5M NaCl IsdB binding was reduced by > 70% (Fig. 26A). These results provide indirect evidence that charge-charge interactions play a role in IsdB-vWF complex formation.

Electrostatic potential calculations (Fig. 26B, panels *a* - *d*), obtained from the crystallographic structure of IsdB deduced from the IsdB/Hb complex (*Bowden et al., 2018*), indicate that the linker region is highly electropositive whereas the NEAT domains display an asymmetric distribution of charges. This is more pronounced in NEAT2, where a predominantly negative face could be identified. On the other hand, NEAT1 is mainly electropositive, with some interspersed negative spots encompassing the β-strand 153-156 and α-helix 163-169.

The A1 domain has a cuboid shape, with a central hydrophobic parallel, eight-stranded parallel β-sheet flanked by three α-helices on each side of the β-sheet (*Emsley et al., 1998*). Electrostatic potential calculations carried out on the A1 domain (Fig. 26B, panels *e* - *h*) identified two distinct faces of opposite charges, i.e. a strongly electropositive face covering helices α4 and α5 and an electronegative face encompassing helices α1 and α7. Thus, the highly charged nature of both IsdB and A1 suggests that ionic forces may play an important role in macromolecular complex formation. The steric and electrostatic complementarity of the IsdB and A1 structures (Fig. 26B) suggest that the highly electropositive face of the globular A1 domain can preferentially couple with the electronegative surfaces in the concave dumbbell structure of IsdB NEAT1-NEAT2, as observed in the X-ray structure of the IsdB-hemoglobin complex (*Bowden et al., 2018)*.

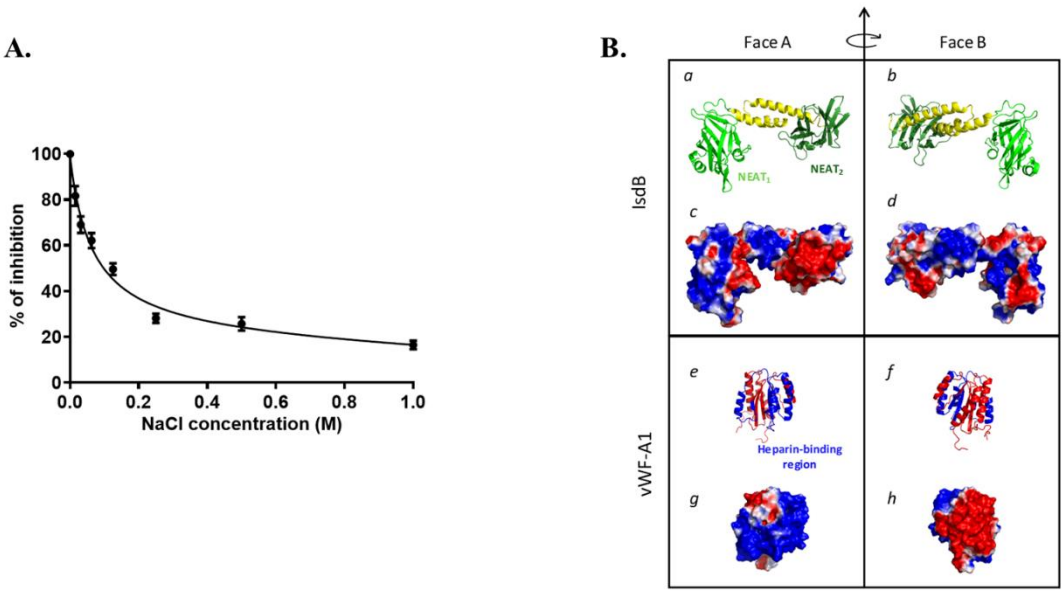

Figure 26. Role of electrostatic forces on the interaction of IsdB with vWF. ***A***, the effect of ionic strength on the binding of IsdB NEAT1-NEAT2 to vWF. The binding of IsdB NEAT1-NEAT2 to immobilized vWF was tested under increasing concentrations of NaCl. Binding of the ligand was detected by addition to the wells of a rabbit anti-IsdB IgG . Error bars show S.D. of the means from three independent determinations, each performed in triplicate. ***B***, Surface electrostatic properties of vWF-A1 and IsdB. Ribbon drawings and surface electrostatic potential of IsdB (5vmm.pdb) (*a,b,c,d*) and A1 (1u0n.pdb) (*e,f,g,h*). The protein surfaces are color-coded according to their electrostatic potential, from −1 kcal/mol/e− (deep red) to +1 kcal/mol/e− (deep blue). Electrostatic potential calculations were carried out using the APBS program.

G. IsdB binding to vWF mediates adhesion of *S. aureus* to endothelial cells

Endothelial cells (ECs) and megakaryocytes are the only cells that synthesize vWF. Thus, we asked whether *S. aureus* expressing IsdB can adhere to vWF associated with the ECM of ECs. Increasing amounts of IsdB NEAT1-NEAT2 were incubated with monolayers of human umbilical vein endothelial cells (HUVEC) pre-treated with the calcium ionophore A23187, a compound that induces the fusion of Weibel-Palade bodies with the plasma membrane and secretion of vWF. IsdB bound dose-dependently to activated cells and significantly more than to untreated cells (Fig. 27A). The mechanism of the IsdB binding to resting endothelial cells is unknown.

The adhesion of the SH1000 WT and its isogenic *isdB* mutant to activated HUVEC cells was explored. The WT strain showed a level of adhesion to the monolayers nearly three times higher than the *isdB* mutant (Fig. 27B), indicating the active involvement of IsdB in the process.
To demonstrate the role of the A1 domain of vWF in promoting adherence of *S. aureus* to HUVEC cells *via* IsdB, a bacterial adhesion assay was performed in the presence of mAb 6D1, which inhibits the binding of IsdB to the A1 domain (data not shown). The mAb 6D1, but not a control antibody, significantly decreased the adhesion of the WT strain to activated HUVEC cells (Fig. 27B). Conversely, no effect by the mAb 6D1 on adhesion of SH1000 *isdB* mutant to the monolayers was observed.

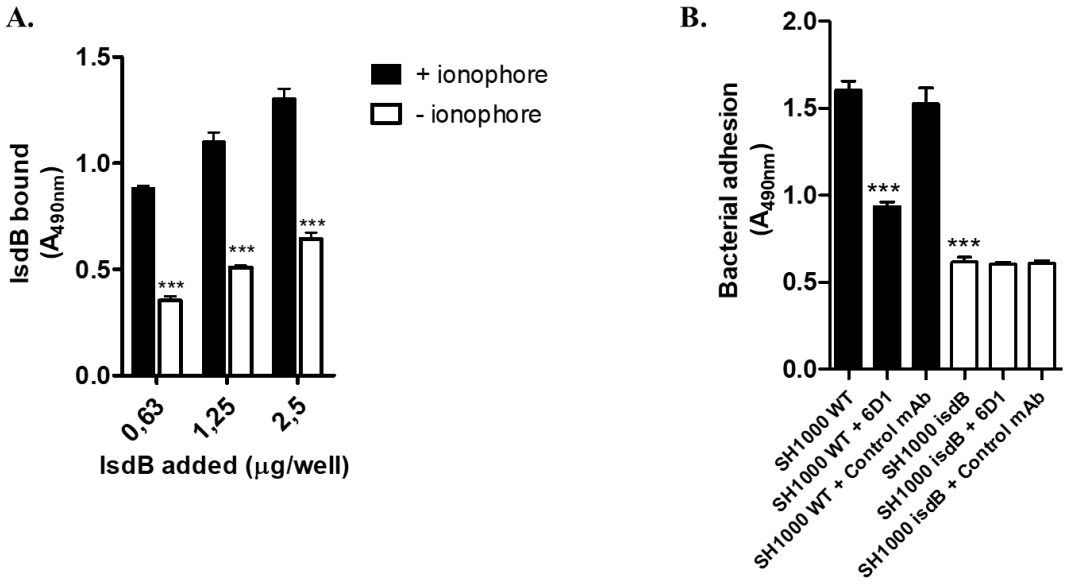

Figure 27. IsdB-mediated adhesion to HUVEC cell monolayers. ***A***, confluent umbilical vein endothelial cell (HUVEC) monolayers were incubated with calcium ionophore A23187 and fixed with paraformaldehyde. The monolayers were incubated with the indicated amounts of IsdB NEAT1-NEAT2 and binding of the ligand to the cells was detected by addition to the wells of a rabbit polyclonal IsdB antibody followed by an HRP-conjugated goat anti-rabbit IgG. The binding of IsdB NEAT1-NEAT2 to the ionophore-untreated cells is also reported. ***B***, endothelial cell monolayers treated as reported in A were incubated with *S. aureus* SH1000 WT and *isdB* mutant bacteria. Adherence to the monolayers was detected by the addition of HRP-conjugated rabbit anti-mouse IgG to the wells. The effect of antibodies on the adhesion of bacteria to endothelial cells was tested by incubating *S. aureus* cells with monolayers in the presence of an anti-A1 6D1 antibody or an unrelated mAb. Error bars show S.D. of the means from three independent determinations, each performed in triplicate (Student's *t*-test; ***, $p \leq 0.001$).

H. Effect of IgG from patients with infective endocarditis on adhesion of *S. aureus* to HUVEC cells

Considering the role of adhesion to and invasion of endothelia by *S. aureus* and the consequent cardiovascular-associated pathologies such as sepsis and endocarditis, a study was designed where the role of IgG against IsdB on bacterial adhesion to HUVEC cells was investigated. A collection of IgG, previously isolated from patients with *S. aureus* endocarditis (*Rindi et al., 2006*), was tested for reactivity to IsdB NEAT1-NEAT2. Although the response varied among the individual IgG preparations, the majority of IgG from patients exhibited a reactivity for IsdB that was higher than that of IgG from sera of healthy donors (Fig. 28A). This observation underlines the *in vivo* relevance of IsdB as an antigen.

Following this, IsdB was pre-incubated with either IgG from the most reactive patients (P14 and P19) or healthy donors (C2 and C7) and then tested for binding to activated HUVEC cells. Patients' IgG showed a strong blocking effect, while the control IgG affected the binding marginally (Fig. 28B). When SH1000 WT was tested for adhesion to activated HUVEC cells in the presence of IsdB IgG and control IgG, a low but significant blocking effect on adhesion by patients' IgG was noticed, while no action by the control IgG was recorded (Fig. 28C). The limited inhibitory effect of IsdB IgG can be explained by considering both the action of SpA as a vWF receptor and its activity as an agent capturing the antibodies. Along this line, we investigated the effect of patients' IgG on IsdB-mediated bacterial adhesion to activated HUVEC by *L. lactis* pNZ8037::*isdB*. The *L. lactis* heterologously expressing IsdB exhibited a level of adhesion increased by 40% compared to *L. lactis* harboring the empty vector (Fig. 28D). Moreover, pre-incubation of *L. lactis* pNZ8037::*isdB* with patients' IgG almost completely reduced bacterial adhesion to the monolayers, whereas controls' IgG did not affect the adhesion.

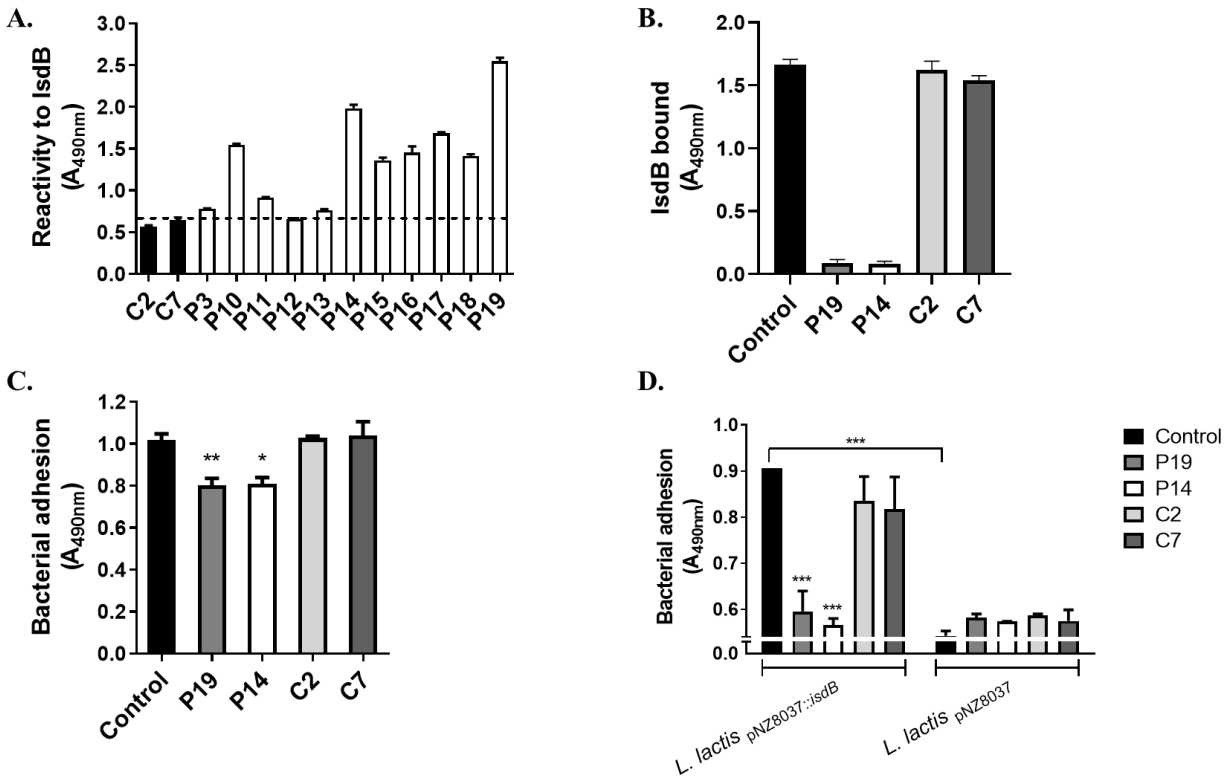

Figure 28. Reactivity of IsdB antibodies from human sera and their effect on IsdB-mediated adhesion to HUVEC monolayers. ***A***, patients' sera reactivity for IsdB protein. Microtiter wells coated with IsdB NEAT1-NEAT2 were probed with IgG isolated from sera of patients with staphylococcal endocarditis. IgG from healthy donors were used as controls. Bound antibody was detected by the addition of rabbit anti-human HRP-conjugated IgG to the wells. Data are expressed as means ± S.D. of triplicate tests. ***B***, Effect of IgG isolated from patients' sera on IsdB NEAT1-NEAT2 binding to HUVEC monolayers. Confluent HUVEC monolayers were treated with calcium ionophore A23187 and incubated with recombinant IsdB NEAT1-NEAT2 in the presence of the indicated IgG isolated from patients' sera. Bound IsdB NEAT1-NEAT2 was detected by the addition of a rabbit polyclonal IsdB antibody followed by HRP-conjugated goat anti-rabbit IgG. The binding of IsdB NEAT1-NEAT2 to the monolayers in the presence of control IgG is also reported. Binding observed in the absence of antibodies was set as 100 % binding. ***C***, adhesion of *S. aureus* SH1000 to HUVEC monolayers in the presence of IgG isolated from patients' sera. HUVEC cell monolayers treated with ionophore A23187 were incubated with cells of *S. aureus* SH1000 WT in the presence of the indicated IgG isolated from patients' sera or healthy human sera. Adhesion was determined by the addition of an HRP-conjugated rabbit anti-mouse IgG. Bacterial attachment observed in the absence of antibodies was set as 100 % adhesion. ***D***, adhesion of *L. lactis* ectopically expressing IsdB to HUVEC monolayers in the presence of IgG isolated from patients' sera. HUVEC cell monolayers treated with ionophore A23187 were incubated with cells of *L. lactis* pNZ8037 or *L. lactis* pNZ8037::*isdB* in the presence of the indicated IgG isolated from patients' sera or healthy human donors. Adhesion of bacteria to HUVEC monolayers was detected through rabbit anti-*L. lactis* IgG followed by an HRP-conjugated goat anti-rabbit IgG. Bars reported in B, C and D represent means ± SD of triplicate tests. Statistically significant differences are indicated (Student's test; *, $p \leq 0.05$, **, $p \leq 0.01$, ***, $p \leq 0.001$).

DISCUSSION

The ability of *S. aureus* to adhere to and colonize the endothelia is strongly associated with the severity of cardiovascular diseases. Several *S. aureus* surface proteins are involved in attachment to endothelial cells or the surface-associated ECM. The fibronectin-binding proteins FnBPA and FnBPB recognize fibronectin in the ECM, and FnBPA/B-mediated adhesion is the prerequisite for endothelial cell invasion by *S. aureus* (*Speziale & Pietrocola, 2020*). In contrast, ClfA binds to surface-anchored integrin $\alpha_V\beta_3$ via fibrinogen (*Viela et al., 2019*). Furthermore, IsdB binds to Vn (*Pietrocola et al., 2020*) and SpA interacts with vWF (*Hartleib et al., 2000*) in the ECM or with gC1qR on the surface of activated endothelial cells (*Sethi et al., 2011*). However, the bacterial and host determinants of endothelial binding have not been fully elucidated. Here we identified vWF as a ligand for *S. aureus* IsdB and provide a comprehensive analysis of the interaction between the bacterial protein and its host binding partner. As reported for Vn, vWF binding to IsdB was strictly related to the conditions required for the optimal expression of the protein (stationary phase of growth and iron-starvation).

Thus, IsdB-expressing bacteria captured soluble vWF and adhered to the immobilized molecule. *L. lactis* ectopically expressing IsdB also attached to surface-coated vWF. The observation that heparin blocked IsdB binding to vWF and the finding that IsdB directly interacted with the A1 domain clearly indicated that the A1 contains the IsdB-binding site. Thus, IsdB and SpA share the same binding site on vWF. It is noteworthy that SpA-mediated adhesion of *S. aureus* to vWF has been demonstrated in conditions of low shear stress (*O'Seaghdha et al., 2006*), whereas our findings regarding IsdB-binding to vWF were performed in static conditions. However, it cannot be ruled out that IsdB may also play a role in mediating staphylococcal adhesion under shear stress conditions. IsdB binding to vWF significantly increased when the protein was treated with ristocetin, a compound that reproduces *in vivo* high shear stress-induced conformational change of vWF. Thus, it can be concluded that the IsdB binding site is partially hidden in the compact conformation of vWF.

The importance of IsdB-mediated adhesion of *S. aureus* to vWF could be even more relevant *in vivo* considering that the role of SpA as vWF receptor could be of minor impact in a milieu such as blood where the immunoglobulins could successfully compete with vWF for binding to SpA expressed on the surface of bacteria (*Hartleib et al., 2000*).

To localize the vWF-binding site(s) on IsdB, the recombinant NEAT1 and NEAT2 modules were tested for their ability to interact with the A1 domain by ELISA. The A1 domain bound dose-dependently to the individual modules and with a binding profile resembling that exhibited using IsdB NEAT1-NEAT2.
As determined by SPR, each module interacted with the A1 domain with an affinity comparable to that of the IsdB NEAT1-NEAT2. However, the NEAT2 module showed an affinity for A1 that was higher than that of NEAT1 that is consistent with the low sequence identity and the different functionality of the modules.

The ability of A1 to bind both the modules is reminiscent of Vn binding to each NEAT domain. However, Vn did not compete with the binding of A1 to IsdB (data not shown), indicating that A1 and Vn recognize and bind to different subsites within the IsdB domains and, possibly, with different binding mechanisms. The evidence that high ionic strength significantly reduced the IsdB interaction with the A1 domain, as well as molecular docking analysis, provide clues that electrostatic bonds could be involved in the vWF-IsdB interaction.

We also demonstrated that IsdB mediates *S. aureus* adhesion to vWF on activated HUVEC cells. Furthermore, we show that adhesion directly involves the A1 domain as indicated by the specific inhibitory effect of the A1 mAb named 6D1 on the process. Thus, a scenario can be envisaged where activated endothelial cells secrete ultra large vWF fibers that run parallel to the direction of the flow in the blood (*Huang et al., 2009*). vWF multimers can also rebind to the endothelial surface via integrin $\alpha_v\beta_3$ (*Huang et al., 2009*) or, in case of endothelial damage or inflammation, to subendothelial matrix molecules such as fibrin monomers (*Miszta et al., 2014*), collagens (*Pareti et al., 1987; Denis et al., 1993; Flood et al., 2015*) or fibronectin (*Keesler et al., 2021*). Due to the effect of shear stress, the globular, concealed A1 domain in vWF fibers becomes exposed and allowed to interact with *S. aureus* via specifically up-regulated IsdB in the iron-limited conditions of the blood. These events allow the pathogen to withstand the strong current of the blood flow and create the prerequisite of vascular infections such as infective endocarditis. In support of the crucial role of A1 in bacterial adherence, in the presence of heparin, a binder of A1, both fiber formation and bacterial adhesion are simultaneously reduced (*Pappelbaum et al., 2013*).

The importance of bacterial receptor/vWF interaction in vascular infections is underlined by the consideration that, among the staphylococci, only *S. aureus* and the coagulase-negative *Staphylococcus lugdunensis* are able to bind vWF and are more effective in causing endocarditis compared to other staphylococcal species (*Liesenborghs et al., 2016*). The nature of the vWF receptor in *S. lugdunensis* remains elusive, despite its potential importance in the pathogenesis associated with this bacterium (*Nilsson et al., 2004; Heilbronner & Foster, 2020*). Perhaps the IsdB orthologue of *S. lugdunensis* binds vWF and promotes endothelial colonization and invasion.

The functional aspects of *S. aureus* binding to vWF can be correlated with the pathophysiological consequences of this interaction such as infective endocarditis, sepsis, and cardiovascular complications. Infection of the heart valves is triggered by the attachment of circulating bacteria to the endocardium and the formation of bacterial vegetations, which are embedded in fibrin and platelets. Bacterial growth occurs within cells and the matrix inside vegetations, making it difficult for the host immune system to control or eradicate the ongoing infection. Therefore, in the perspective of future therapeutic interventions, the acquisition of information on the immune response by the host remains essential.

Along this line, we examined the reactivity of IgG isolated from patients with *S. aureus* endocarditis and their possible interference with the vWF/IsdB interaction. A considerable proportion of isolated IgG from a collection of human sera showed a significant reactivity to IsdB. Moreover, anti-IsdB antibodies blocked the binding of recombinant IsdB to activated endothelial cells and interfered with the adhesion of *L. lactis* ectopically expressing IsdB to HUVEC cells. On the other hand, the antibodies affected less, although significantly, *S. aureus* adhesion to endothelial cells. The reduced efficacy of immune IgG on adhesion of SH1000 to HUVEC cells may be attributable to the action of SpA as vWF receptor *per se* and/or to its IgG neutralizing activity. Moreover, the involvement of other staphylococcal vWF-binding partners in the process cannot be excluded. In summary, a therapeutic approach based on a multivalent vaccine that includes IsdB warrants further investigation.

REFERENCES

1. Acton D.S., Plat-Sinnige M.J., van Wamel W., de Groot N., van Belkum A. (2009) Intestinal carriage of *Staphylococcus aureus*: how does its frequency compare with that of nasal carriage and what is its clinical impact? *Eur. J. Clin. Microbiol. Infect. Dis*. 28(2):115-27. doi: 10.1007/s10096-008-0602-7
2. Alonzo F. 3rd & Torres V. J. (2014). The bicomponent pore-forming leucocidins of *Staphylococcus aureus*. *Microbiol. Mol. Biol. Rev.*, 78(2), 199–230. doi: 10.1128/MMBR.00055-13
3. Andrade M.A., Ciccarelli F.D., Perez-lratxeta C., Bork P. (2002). NEAT: a domain duplicated in genes near the components of a putative Fe3-i- siderophore transporter from Gram-positive pathogenic bacteria. *Genome Biol*, 3 (9): 118-137.
4. André P., Denis C.V., Ware J., Saffaripour S., Hynes R.O., Ruggeri Z.M., Wagner D.D. (2000). Platelets adhere to and translocate on von Willebrand factor presented by endothelium in stimulated veins. *Blood*, 96(10), 3322–3328.
5. Andrews R.K. & Berndt M.C. (2008) Platelet adhesion: a game of catch and release. *J Clin Invest*, 118, 3009-3011.
6. Aponte-Santamaría C., Huck V., Posch S., Bronowska A.K., Grässle S., Brehm M.A., Obser T., Schneppenheim R., Hinterdorfer P., Schneider S.W., Baldauf C., Gräter F. (2015). Force-sensitive autoinhibition of the von Willebrand factor is mediated by interdomain interactions. *Biophys J*, 108(9), 2312–2321. doi: 10.1016/j.bpj.2015.03.041.
7. Archer G. L. & Bosilevac J. M. (2001). Signaling antibiotic resistance in staphylococci. *Science*, 291(5510), 1915–1916. doi: 10.1126/science.1059671
8. Askarian F., Uchiyama S., Valderrama J.A., Ajayi C., Sollid J.U., van Sorge N.M., Nizet V., van Strijp J.A., Johannessen M. (2016). Serine-aspartate repeat protein D increases *Staphylococcus aureus* virulence and survival in blood. *Infect Immun* 85:85.
9. Askarian F., Wagner T., Johannessen M., Nizet, V. (2018). *Staphylococcus aureus* modulation of innate immune responses through Toll-like (TLR), (NOD)-like (NLR) and C-type lectin (CLR) receptors. *FEMS Microbiol Rev.*, 42(5), 656–671. doi: 10.1093/femsre/fuy025
10. Baker N.A., Sept D., Joseph S., Holst M.J., McCammon J.A. (2001). Electrostatics of nanosystems: application to microtubules and the ribosome. *PNAS.* 98, 10037–10041 doi: 10.1073/pnas.181342398.
11. Bangert S., Levy M., Hebert A.A. (2012) Bacterial resistance and impetigo treatment trends: a review. *Pediatr. Dermatol*. 29(3):243-8. doi: 10.1111/j.1525-1470.2011.01700.x
12. Barbu E.M., Ganesh V.K., Gurusiddappa S., Mackenzie R.C., Foster T.J., Sudhof T.C., Höök M. (2010) beta-Neurexin is a ligand for the *Staphylococcus aureus* MSCRAMMSdrC. *PLoS Pathog* 6:e1000726. doi: 10.1371/journal.ppat.1000726.
13. Barbu E.M., Mackenzie C., Foster T.J., Höök M. (2014). SdrC induces staphylococcal biofilm formation through a homophilic interaction. *Mol Microbiol* 94:172–185 doi: 10.1111/mmi.12750.
14. Bartholomew J.W. & Mittwer T. (1952) The Gram stain. *Bacteriol Rev.* 16(1):1-29. PMID: 14925025; PMCID: PMC180726.

15. Baur S., Rautenberg M., Faulstich M., Grau T., Severin Y., Unger C., Hoffmann W.H., Rudel T., Autenrieth I.B., Weidenmaier C. (2014). A nasal epithelial receptor for *Staphylococcus aureus* WTA governs adhesion to epithelial cells and modulates nasal colonization. *PLoS Pathog* 10: e1004089 doi: 10.1371/journal.ppat.1004089.
16. Becker S., Frankel M. B., Schneewind O., Missiakas D. (2014). Release of protein A from the cell wall of *Staphylococcus aureus*. *Proc. Natl. Acad. Sci. U S A*., 111(4), 1574–1579. doi: 10.1073/pnas.1317181111
17. Bingham R.J., Rudiño-Piñera E., Meenan N.A., Schwarz-Linek U., Turkenburg J.P., Höök M., Garman E.F., Potts J.R. (2008). Crystal structures of fibronectin-binding sites from *Staphylococcus aureus* FnBPA in complex with fibronectin domains. *Proc. Natl. Acad. Sci. U.S.A.*, 105(34), 12254–12258. doi: 10.1073/pnas.0803556105
18. Bischoff M., Dunman P., Kormanec J., Macapagal D., Murphy E., Mounts W., Berger-Bächi B., Projan S. (2004). Microarray-based analysis of the *Staphylococcus aureus* σB regulon. *J. Bacteriol.*, 186(13), 4085–4099. doi: 10.1128/JB.186.13.4085-4099.2004
19. Bjerketorp J, Jacobsson K, Frykberg L. (2004) The von willebrand factor-binding protein (vWbp) of *Staphylococcus aureus* is a coagulase. *FEMS Microbiol Lett*. 234:309–14. doi: 10.1111/j.1574-6968.2004.tb09549.x.
20. Bjerketorp J, Nilsson M, Ljungh A, Flock JI, Jacobsson K, Frykberg L. A novel von willebrand factor binding protein expressed by *Staphylococcus aureus*. *Microbiology*. (2002) 148:2037–44. doi: 10.1099/00221287-148-7-2037.
21. Blenner M.A., Dong X., Springer T.A. (2014) Structural basis of regulation of von Willebrand factor binding to glycoprotein Ib. *J Biol Chem*, 289, 5565-79.
22. Bokarewa M. I., Jin T., Tarkowski A. (2006). *Staphylococcus aureus*: Staphylokinase. *Int. J. Biochem. Cell. Biol.*, 38(4), 504–509. doi: 10.1016/j.biocel.2005.07.005
23. Bowden C.F.M, Chan A.C.K., Li E.J.W., Arrieta A.L., Eltis L.D., Murphy M.E.P. (2018). Structure-function analyses reveal key features in *Staphylococcus aureus* IsdB-associated unfolding of the heme-binding pocket of human hemoglobin. *J. Biol. Chem*. 5;293(1):177-190. doi: 10.1074/jbc.M117.806562.
24. Bowden M.G., Chen W., Singvall J., Xu Y., Peacock S.J., Valtulina V., Speziale P., Höök M., (2005). Identification and preliminary characterization of Cell-Wall-Anchored proteins of *Staphylococcus epidermidis*. *Microbiology*, 151(Pt 5):1453-64.
25. Broos K., Feys H.B., De Meyer S.F., Vanhoorelbeke K., Deckmyn H. (2011) Platelets at work in primary hemostasis. *Blood Rev,* 25, 155-67.
26. Bryckaert M., Rosa J.P., Denis C.V., Lenting P.J. (2015). Of von Willebrand factor and platelets, *Cell. Mol. Life Sci*., vol. 72, no. 2, pp. 307–326.
27. Bukowski M., Wladyka B., Dubin G. (2010). Exfoliative toxins of *Staphylococcus aureus*. *Toxins*, 2(5), 1148–1165. doi: 10.3390/toxins2051148
28. Burke F.M., Di Poto A., Speziale P., Foster T.J. (2011). The A domain of fibronectin-binding protein B of *Staphylococcus aureus* contains a novel fibronectin binding site. *FEBS J,* 278, 2359-2371. doi: 10.1111/j.1742-4658.2011.08159.x.

29. Burke F.M., McCormack N., Rindi S., Speziale P., Foster T. J. (2010). Fibronectin-binding protein B variation in *Staphylococcus aureus*. *BMC Microbiol*., 10, 160. doi: 10.1186/1471-2180-10-160
30. Burman J.D., Leung E., Atkins K.L., O'Seaghdha M.N., Lango L., Bernadó P., Bagby S., Svergun D.I., Foster T.J., Isenman D.E., van den Elsen J.M. (2008). Interaction of human complement with Sbi, a Staphylococcal Immunoglobulin-binding protein: indications of a novel mechanism of complement evasion by *Staphylococcus aureus*. *J. Biol. Chem*., 283(25):17579–17593.
31. Canis K., McKinnon T.A., Nowak A., Haslam S.M., Panico M., Morris H.R., Laffan M.A., Dell A. (2012). Mapping the N-glycome of human von Willebrand factor. *Biochem J.*, 447(2), 217–228. doi: 10.1042/BJ20120810.
32. Canis K., McKinnon T.A., Nowak A., Panico M., Morris H.R., Laffan M., Dell A. (2010). The plasma von Willebrand factor O-glycome comprises a surprising variety of structures including ABH antigens and disialosyl motifs. *J. Thromb. Haemost*., 8(1), 137–145. doi: 10.1111/j.1538-7836.2009.03665.x.
33. Cedergren L., Andersson R., Jansson B., Uhlen M., Nilsson B., (1993). Mutational analysis of the interaction between staphylococcal protein A and human IgG1. *Protein Eng*., 6:441–448.
34. Cheng A.G., Kim H.K., Burts M.L., Krausz T., Schneewind O., Missiakas D.M. (2009). Genetic requirements for *Staphylococcus aureus* abscess formation and persistence in host tissues. *FASEB J*., 23(10), 3393–3404. doi: 10.1096/fj.09-135467
35. Cheng A.G., McAdow M., Kim H.K., Bae T., Missiakas D.M., Schneewind O. (2010). Contribution of coagulases towards *Staphylococcus aureus* disease and protective immunity. *PLoS Pathog*., 6(8), e1001036. doi: 10.1371/journal.ppat.1001036
36. Cheresh D.A. & Spiro R.C. (1987). Biosynthetic and functional properties of an Arg-Gly-Asp-directed receptor involved in human melanoma cell attachment to vitronectin, fibrinogen, and von Willebrand factor. *J Biol Chem*., 262(36), 17703–17711.
37. Cheung A. L., Bayer A. S., Zhang G., Gresham H., Xiong Y. Q. (2004). Regulation of virulence determinants in vitro and in vivo in *Staphylococcus aureus*. *FEMS Immunol. Med. Microbiol.*, 40(1), 1–9. doi: 10.1016/S0928-8244(03)00309-2
38. Choi H., Aboulfatova K., Pownall H.J., Cook R., Dong J.F. (2007) Shear-induced disulfide bond formation regulates adhesion activity of von Willebrand factor. *J Biol Chem,* 282, 35604-35611.
39. Chuang Y.Y., Huang Y.C. Lin T.Y. (2005) Toxic Shock Syndrome in Children. *Pediatr-Drugs* 7, 11–24. doi: 10.2165/00148581-200507010-00002
40. Chudapongse N., Krubphachaya P., Leelayuwat C., Kermode J.C. (2011). Expression and Purification of a Soluble Recombinant A1 Domain of Human von Willebrand Factor in Bacteria. *Biotechnol. Equip.,* 25(4), 2658-2662. doi: 10.5504/BBEQ.2011.0087.
41. Cines D.B., Pollak E.S., Buck C.A., Loscalzo J., Zimmerman G.A., McEver R.P., Pober J.S., Wick T.M., Konkle B.A., Schwartz B.S., Barnathan E.S., McCrae K.R., Hug B.A., Schmidt A.M., Stern D.M. (1998). Endothelial cells in physiology and in the pathophysiology of vascular disorders. *Blood*, 91(10), 3527–3561.

42. Claes J, Liesenborghs L, Peetermans M, Veloso TR, Missiakas D, Schneewind O, Mancini S, Entenza JM, Hoylaerts MF, Heying R, Verhamme P, Vanassche T. (2017) Clumping factor A, von Willebrand factor-binding protein and von Willebrand factor anchor *Staphylococcus aureus* to the vessel wall. *J Thromb Haemost*, 15: 1009–19.
43. Claes J., Vanassche T., Peetermans M., Liesenborghs L., Vandenbriele C., Vanhoorelbeke K., Missiakas D., Schneewind O., Hoylaerts M.F., Heying R., Verhamme P. (2014). Adhesion of *Staphylococcus aureus* to the vessel wall under flow is mediated by von Willebrand factor-binding protein. *Blood*, 124(10), 1669–1676. doi: 10.1182/blood-2014-02-558890.
44. Clarke S.R. & Foster S.J. (2008). IsdA protects *Staphylococcus aureus* against the bactericidal protease activity of apolactoferrin. *Infect. Immun.*, 76(4), 1518–1526. doi: 10.1128/IAI.01530-07
45. Clarke S.R., Andre G., Walsh E.J., Dufrêne Y.F., Foster T.J., Foster S.J. (2009). Iron-regulated surface determinant protein A mediates adhesion of *Staphylococcus aureus* to human corneocyte envelope proteins. *Infect. Immun*., 77(6), 2408–2416. doi: 10.1128/IAI.01304-08
46. Clarke S.R., Brummell K.J., Horsburgh M.J., McDowell P.W., Mohamad S.A., Stapleton M.R., Acevedo J., Read R.C., Day N.P., Peacock S.J., Mond J.J., Kokai-Kun J.F., Foster S.J. (2006). Identification of *in vivo*-expressed antigens of *Staphylococcus aureus* and their use in vaccinations for protection against nasal carriage. *J Infect Dis* 193:1098–1108 doi: 10.1086/501471.
47. Clarke S.R., Mohamed R., Bian L., Routh A.F., Kokai-Kun J.F., Mond J.J., Tarkowski A., Foster S.J. (2007). The *Staphylococcus aureus* surface protein IsdA mediates resistance to innate defenses of human skin. *Cell. Host Microbe*., 1(3), 199–212. doi: 10.1016/j.chom.2007.04.005
48. Clarke S.R., Wiltshire M.D., Foster S.J. (2004). IsdA of Staphylococcus aureus is a broad spectrum, iron-regulated adhesin. *Mol. Microbiol.*, 51(5):1509-1519. doi: 10.1111/j.1365-2958.2003.03938.x
49. Claro T., Widaa A., O'Seaghdha M., Miajlovic H., Foster T.J., O'Brien F.J., Kerrigan S.W. (2011). *Staphylococcus aureus* protein A binds to osteoblasts and triggers signals that weaken bone in osteomyelitis. *PloS one*, 6(4), e18748. doi: 10.1371/journal.pone.0018748.
50. Clauditz A., Resch A., Wieland K.P., Peschel A., Götz F., (2006). Staphyloxantin plays a role in the fitness of *Staphylococcus aureus* and its ability to cope with oxydative stress. *Infect. Immun.*, 74(8):4950- 3.
51. Colace T.V. & Diamond S.L. (2013) Direct observation of von Willebrand factor elongation and fiber formation on collagen during acute whole blood exposure to pathological flow. *Arterioscler Thromb Vasc Biol,* 33, 105-13.
52. Corrigan R.M. & Foster T.J. (2009). An improved tetracycline-inducible expression vector for *Staphylococcus aureus*. *Plasmid*, 61(2), 126–129. doi: 10.1016/j.plasmid.2008.10.001
53. Corrigan R.M., Miajlovic H., Foster T.J. (2009). Surface proteins that promote adherence of *Staphylococcus aureus* to human desquamated nasal epithelial cells. *BMC Microbiol* 9:22 doi: 10.1186/1471-2180-9-22.
54. Crisóstomo M. I., Westh H., Tomasz A., Chung M., Oliveira D. C., de Lencastre H. (2001). The evolution of methicillin resistance in *Staphylococcus aureus*: similarity of genetic backgrounds in historically early methicillin-susceptible and -resistant isolates and contemporary epidemic clones. *Proc. Natl. Acad. Sci. U. S. A.*, 98(17), 9865–9870. doi: 10.1073/pnas.161272898

55. Cuatrecasas P., Fuchs S., Anfinsen C. B. (1967). Catalytic properties and specificity of the extracellular nuclease of *Staphylococcus aureus*. *J. Biol. Chem.*, 242(7), 1541–1547.
56. Dancer S. J. & Noble W. C. (1991) Nasal, axillary, and perineal carriage of *Staphylococcus aureus* among women: identification of strains producing epidermolytic toxin. *J. Clin. Pathol.* 44, 681–4.
57. Dayan G.H., Mohamed N., Scully I.L., Cooper D., Begier E., Eiden J., Jansen K.U., Gurtman A., Anderson A.S. (2016) *Staphylococcus aureus*: the current state of disease, pathophysiology and strategies for prevention. *Expert. Rev. Vaccines*. 15(11):1373-1392. doi: 10.1080/14760584.2016.1179583
58. Dayananda K.M., Singh I., Mondal N., Neelamegham S. (2010) von Willebrand factor selfassociation on platelet GpIbalpha under hydrodynamic shear: effect on shear-induced platelet activation. *Blood*, 116, 3990-8.
59. De Kimpe S.J., Kengatharan M., Thiemermann C., Vane J.R. (1995). The cell wall components peptidoglycan and lipoteichoic acid from *Staphylococcus aureus* act in synergy to cause shock and multiple organ failure. *Proc. Natl. Acad. Sci. U. S. A.*, 92(22):10359-63
60. De Ruyter P.G., Kuipers O.P., de Vos W.M. (1996). Controlled gene expression systems for *Lactococcus lactis* with the food-grade inducer nisin. *Appl Environ Microbiol*., 62(10), 3662–3667. doi: 10.1128/aem.62.10.3662-3667.1996.
61. de Wit T.R., Rondaij M.G., Hordijk P.L., Voorberg J., van Mourik J.A. (2003).Real-time imaging of the dynamics and secretory behavior of Weibel-Palade bodies. *Arterioscler Thromb Vasc Biol,* 23, 755-761.
62. DeDent A., Bae T., Missiakas D. M., Schneewind, O. (2008). Signal peptides direct surface proteins to two distinct envelope locations of *Staphylococcus aureus*. *EMBO J.*, 27(20), 2656–2668. doi: 10.1038/emboj.2008.185
63. Deisenhofer J., (1981). Crystallographic refinement and atomic models of a human Fc fragment and its complex with fragment B of protein A from *Staphylococcus aureus* at 2.9- and 2.8-Å resolution. *Biochemistry*, 20:2361–2370.
64. Deivanayagam C.C., Wann E.R., Chen W., Carson M., Rajashankar K.R., Höök M., Narayana S.V. (2002). A novel variant of the immunoglobulin fold in surface adhesins of *Staphylococcus aureus*: crystal structure of the fibrinogen-binding MSCRAMM, clumping factor A. *EMBO J.*, 21(24), 6660–6672. doi: 10.1093/emboj/cdf619
65. DeLeo F.R., Otto M., Kreiswirth B.N., Chambers H.F. (2010) Community-associated meticillin-resistant *Staphylococcus aureus*. *Lancet*. 375(9725):1557-68. doi: 10.1016/S0140-6736(09)61999-1
66. Denis C., Baruch D., Kielty C.M., Ajzenberg N., Christophe O., Meyer D. (1993). Localization of von Willebrand factor binding domains to endothelial extracellular matrix and to type VI collagen. *Arterioscler. Thromb. Vasc. Biol*., 13(3), 398–406. doi: 10.1161/01.atv.13.3.398.
67. Doery H. M., Magnusson B. J., Cheyne I. M., Sulasekharam J. (1963). A phospholipase in staphylococcal toxin which hydrolyses sphingomyelin. *Nature*, 198, 1091–1092. doi: 10.1038/1981091a0
68. Dong J.F., Moake J.L., Nolasco L., Bernardo A., Arceneaux W., Shrimpton C.N., Schade A.J., McIntire L.V., Fujikawa K., López J.A. (2002). ADAMTS-13 rapidly cleaves newly secreted ultralarge von Willebrand factor

multimers on the endothelial surface under flowing conditions. *Blood*, 100(12), 4033–4039. doi: 10.1182/blood-2002-05-1401.

69. Downer R., Roche F., Park P. W., Mecham R. P., Foster, T. J. (2002). The elastin-binding protein of *Staphylococcus aureus* (EbpS) is expressed at the cell surface as an integral membrane protein and not as a cell wall-associated protein. *J. Biol. Chem*., 277(1), 243–250. doi: 10.1074/jbc.M107621200
70. Dreisbach A., van Dijl J. M., Buist G. (2011). The cell surface proteome of *Staphylococcus aureus*. *Proteomics*, 11(15), 3154–3168. doi: 10.1002/pmic.201000823
71. Dunman P.M., Murphy E., Haney S., Palacios D., Tucker-Kellogg G., Wu S., Brown E.L., Zagursky R.J., Shlaes D., Projan S.J. (2001) Transcription profiling-based identification of *Staphylococcus aureus* genes regulated by the agr and/or sarA loci. *J. Bacteriol*. 183(24):7341-53. doi: 10.1128/JB.183.24.7341-7353.2001
72. Emsley J., Cruz M., Handin R., Liddington R. (1998). Crystal structure of the von Willebrand Factor A1 domain and implications for the binding of platelet glycoprotein Ib. *J. Biol. Chem*., 273(17), 10396–10401. doi: 10.1074/jbc.273.17.10396.
73. Fedtke I., Mader D., Kohler T., Moll H., Nicholson G., Biswas R., Henseler K., Götz F., Zähringer U., Peschel A. (2007). A *Staphylococcus aureus* ypfP mutant with strongly reduced lipoteichoic acid (LTA) content: LTA governs bacterial surface properties and autolysin activity. *Mol. Microbiol.*, 65(4), 1078–1091. doi: 10.1111/j.1365-2958.2007.05854.x
74. Ferraro F., Kriston-Vizi J., Metcalf D.J., Martin-Martin B., Freeman J., Burden J.J., Westmoreland D., Dyer C.E., Knight A.E., Ketteler R., Cutler D.F. (2014). A two-tier Golgi-based control of organelle size underpins the functional plasticity of endothelial cells. *Dev Cell*., 29(3), 292–304. doi: 10.1016/j.devcel.2014.03.021.
75. Feuillie C., Formosa-Dague C., Hays L.M., Vervaeck O., Derclaye S., Brennan M.P., Foster T.J., Geoghegan J.A., Dufrêne Y.F. (2017). Molecular interactions and inhibition of the staphylococcal biofilm-forming protein SdrC. *PNAS* 114:3738–3743 doi: 10.1073/pnas.1616805114.
76. Fischetti V. A., Novick R. P., Ferretti J. J., Portnoy D. A., Rood J. I. (2006). *Gram-Positive Pathogens*. (2nd ed.) American Society for Microbiology.
77. Fitzgerald J.R., Loughman A., Keane F., Brennan M., Knobel M., Higgins J., Visai L., Speziale P., Cox D., Foster T.J. (2006). Fibronectin-binding proteins of *Staphylococcus aureus* mediate activation of human platelets via fibrinogen and fibronectin bridges to integrin GPIIb/IIIa and IgG binding to the FcgammaRIIa receptor. *Mol. Microbiol.*, 59(1), 212–230. doi: 10.1111/j.1365-2958.2005.04922.x.
78. Fleury O.M., McAleer M.A., Feuillie C., Formosa-Dague C., Sansevere E., Bennett D.E., Towell A.M., McLean W.H.I., Kezic S., Robinson D.A., Fallon P.G., Foster T.J., Dufrêne Y.F., Irvine A.D., Geoghegan J.A. (2017). Clumping factor B promotes adherence of *Staphylococcus aureus* to corneocytes in atopic dermatitis. Infect Immun 85:85 doi: 10.1128/IAI.00994-16.
79. Flood V.H., Schlauderaff A.C., Haberichter S.L., Slobodianuk T.L., Jacobi P.M., Bellissimo D.B., Christopherson P.A., Friedman K.D., Gill J.C., Hoffmann R.G., Montgomery R.R., Zimmerman T.S. (2015). Crucial role for the VWF A1 domain in binding to type IV collagen. *Blood*, 125(14), 2297–2304. doi: 10.1182/blood-2014-11-610824.

80. Forsgren A. & Quie P.G. (1974). Effects of staphylococcal protein A on heat labile opsonins. *J Immunol* , 112:1177–1180.
81. Foster T. J. (2005). Immune evasion by staphylococci. *Nat. Rev. Microbiol.*, 3(12), 948–958. doi: 10.1038/nrmicro1289
82. Foster T. J., Geoghegan J. A., Ganesh V. K., Höök M. (2014). Adhesion, invasion and evasion: the many functions of the surface proteins of *Staphylococcus aureus*. *Nat. Rev. Microbiol.*, 12(1), 49–62. doi: 10.1038/nrmicro3161
83. Foster T.J. (2019) Surface proteins of *Staphylococcus aureus*. *Microbiol. Spectrum.* 7(4):GPP3-0046-2018. doi: 10.1128/microbiolspec.GPP3-0046-2018
84. Frand A.R., Cuozzo J.W., Kaiser C.A. (2000). Pathways for protein disulphide bond formation. *Trends Cell. Biol*. 10, 203-210.
85. Fredrickson B.J., Dong J.F., McIntire L.V., Lopez, J.A. (1998) Shear-dependent rolling on von Willebrand factor of mammalian cells expressing the platelet glycoprotein Ib-IX-V complex. *Blood*, 92, 3684-93.
86. Friedrich R., Panizzi P., Fuentes-Prior P., Richter K., Verhamme I., Anderson P. J., Kawabata S., Huber R., Bode W., Bock P. E. (2003). Staphylocoagulase is a prototype for the mechanism of cofactor-induced zymogen activation. *Nature*, 425(6957), 535–539. doi: 10.1038/nature01962
87. Fujikawa K., Suzuki H., McMullen B. Chung D. (2001). Purification of human von Willebrand factor-cleaving protease and its identification as a new member of the metalloproteinase family. *Blood* 98, 1662-1666.
88. Fujimura Y., Titani K., Holland L.Z., Roberts J.R., Kostel P., Ruggeri Z.M., Zimmerman T.S. (1987). A Heparin-binding Domain of Human von Willebrand Factor, *J. Biol. Chem*., 262(4):1734-1739.
89. Fukuda K., Doggett T., Laurenzi I.J., Liddington R.C., Diacovo T.G. (2005). The snake venom protein botrocetin acts as a biological brace to promote dysfunctional platelet aggregation. *Nat. Struct. Mol.*, 12(2), 152–159. doi: 10.1038/nsmb892.
90. Furlan M., Robles R., Galbusera M., Remuzzi G., Kyrle P. A., Brenner B., Krause M., Scharrer I., Aumann V., Mittler U., Solenthaler M., Lämmle, B. (1998). von Willebrand factor-cleaving protease in thrombotic thrombocytopenic purpura and the hemolytic-uremic syndrome. *N Engl J Med*., 339(22), 1578–1584. doi: 10.1056/NEJM199811263392202 5.
91. Ganderton T., Wong J.W.H., Schroeder C., Hogg, P.J. (2011) Lateral self-association of VWF involves the Cys2431-Cys2453 disulfide/dithiol in the C2 domain. *Blood*, 118, 5312-5318.
92. Ganesh V.K., Barbu E.M., Deivanayagam C.C., Le B., Anderson A.S., Matsuka Y.V., Lin S.L., Foster T.J., Narayana S.V., Höök M. (2011). Structural and biochemical characterization of *Staphylococcus aureus* clumping factor B/ligand interactions. *J. Biol. Chem.*, 286(29), 25963–25972. doi: 10.1074/jbc.M110.217414
93. Ganesh V.K., Rivera J.J., Smeds E., Ko Y.P., Bowden M.G., Wann E.R., Gurusiddappa S., Fitzgerald J.R., Höök M. (2008). A structural model of the *Staphylococcus aureus* ClfA-fibrinogen interaction opens new avenues for the design of anti-staphylococcal therapeutics. *PLoS Pathog.*, 4(11), e1000226. doi: 10.1371/journal.ppat.1000226

94. Gaudin C.F., Grigg J.C., Arrieta A.L., Murphy M.E. (2011). Unique heme-iron eoordination by the hemoglobin receptor IsdB of *Staphylococcus aureus*. *Biochemistry* 50 (24): 5443-5452. doi: 10.1021/bi200369p

95. Geoghegan J. A. & Foster T. J. (2017). Cell Wall-Anchored Surface Proteins of *Staphylococcus aureus*: Many Proteins, Multiple Functions. *Curr. Top. Microbiol. Immunol.*, 409, 95–120. doi: 10.1007/82_2015_5002

96. Geoghegan J.A, Monk I.R., O'Gara J.P., Foster T.J. (2013). Subdomains N2N3 of fibronectin binding protein A mediate *Staphylococcus aureus* biofilm formation and adherence to fibrinogen using distinct mechanisms. *J Bacteriol* 195:2675–2683 doi: 10.1128/JB.02128-12.

97. Geoghegan, J.A. Corrigan R.M., Gruszka D.T., Speziale P., O'Gara J.P., Potts J.R., Foster T.J. (2010). Role of surface protein SasG in biofilm formation by *Staphylococcus aureus*. *J. Bacteriol*., 192, 5663–5673.

98. Giblin J.P., Hewlett L.J., Hannah, M.J. (2008). Basal secretion of von Willebrand factor from human endothelial cells. *Blood*, 112, 957-964.

99. Gillet Y., Issartel B., Vanhems P., Fournet J.C., Lina G., Bes M., Vandenesch F., Piémont Y., Brousse N., Floret D., Etienne J. (2002) Association between *Staphylococcus aureus* strains carrying gene for Panton-Valentine leukocidin and highly lethal necrotising pneumonia in young immunocompetent patients. *Lancet*. 359(9308):753-9. doi: 10.1016/S0140-6736(02)07877-7

100. Gogia S. & Neelamegham S. (2015) Role of fluid shear stress in regulating VWF structure, function and related blood disorders. *Biorheology,* 52, 319-35.

101. Goodyear C. S. & Silverman, G. J. (2003). Death by a B cell superantigen: In vivo VH-targeted apoptotic supraclonal B cell deletion by a Staphylococcal Toxin. *J. Exp. Med.*, 197(9), 1125–1139. doi: 10.1084/jem.20020552

102. Gotz F., Bannerman T., Schleifer K.H. (2006) The genera *Staphylococcus* and *Macrococcus*. In: Balows A, Truper AG, Dworkin M, et al, eds. *The Prokaryotes*. ed. 3. New York*: Springer Science+Business Media*, 1-75.

103. Grigg J.C., Mao C.X., Murphy M.E. (2011). Iron-coordinating tyrosine is a key determinant of NEAT domain heme transfer. *J. Mol. Biol*., 413 (3): 684-698.

104. Grigg J.C., Ukpabi G., Gaudin C.F., Murphy M.E. (2010). Structural biology of heme binding in the *Staphylococcus aureus* Isd system. *J. Inorg. Biochem*., 104 (3):341-348.

105. Grigg J.C., Vermeiren C.L., Heinrichs D.E., Murphy M.E. (2007). Haem recognition by a *Staphylococcus aureus* NEAT domain. *Mol. Microbiol.*, 63(1), 139–149. doi: 10.1111/j.1365-2958.2006.05502.x

106. Grumann D., Nübel U., Bröker B. M. (2014). *Staphylococcus aureus* toxins--their functions and genetics. *Infect. Genet. Evol.*, 21, 583–592. doi: 10.1016/j.meegid.2013.03.013

107. Gruszka D.T., Whelan F., Farrance O.E., Fung H.K., Paci E., Jeffries C.M., Svergun D.I., Baldock C., Baumann C.G., Brockwell D.J., Potts J.R., Clarke J. (2015). Cooperative folding of intrinsically disordered domains drives assembly of a strong elongated protein. *Nat. Commun.*, 6:7271

108. Gruszka D.T., Wojdyla J.A., Bingham R.J., Turkenburg J.P., Manfield I.W., Steward A., Leech A.P., Geoghegan J.A., Foster T.J., Clarke J., Potts, J.R. (2012). Staphylococcal biofilm-forming protein has a contiguous rod-like structure. *Proc. Natl Acad. Sci. U.S.A*, 109:E1011–E1018.

109. Guerrero M.L., Aldamiz G., Bayon J., Cohen V.A., Fraile J. (2011) Long-term survival of salvage cardiac transplantation for infective endocarditis. *Ann Thorac Surg*. 92:e93–94. doi: 10.1016/j.athoracsur.2011.05.048.

110. Guinan M.E., Dan B.B., Guidotti R.J., Reingold A.L., Schmid G.P., Bettoli E.J., Lossick J.G., Shands K.N., Kramer M.A., Hargrett N.T., Anderson R.L., Broome C.V. (1982) Vaginal colonization with *Staphylococcus aureus* in healthy women: a review of four studies. *Ann. Intern. Med*. 96(6 Pt 2):944-7. doi: 10.7326/0003-4819-96-6-944

111. Haberichter S.L., Jacobi P., Montgomery R.R. (2003). Critical independent regions in the VWF propeptide and mature VWF that enable normal VWF storage. *Blood*, 101, 1384-1391.

112. Haberichter S.L., Merricks E.P., Fahs S.A., Christopherson P.A., Nichols T.C., Montgomery R.R. (2005). Re-establishment of VWF-dependent Weibel-Palade bodies in VWD endothelial cells. *Blood*, 105(1), 145–152. doi: 10.1182/blood-2004-02-0464.

113. Hamdan-Partida A., Sainz-Espuñes T., Bustos-Martínez J. (2010). Characterization and persistence of *Staphylococcus aureus* strains isolated from the anterior nares and throats of healthy carriers in a Mexican community. *J. Clin. Microbiol*. 48(5), 1701–1705. doi:10.1128/JCM.01929-09

114. Hamilton K.K. & Sims P.J. (1987). Changes in cytosolic Ca2+ associated with von Willebrand factor release in human endothelial cells exposed to histamine. Study of microcarrier cell monolayers using the fluorescent probe indo-1. *J Clin Invest,* 79, 600-8.

115. Hammer N.D and Skaar E.P. (2011). Molecular mechanisms of *Staphylococcus aureus* iron acquisition. *Annu. Rev. Microbiol*., 65:129–147.

116. Hartleib J, Kohler N, Dickinson RB, Chhatwal GS, Sixma JJ, Hartford OM, Foster TJ, Peters G, Kehrel BE, Herrmann M. (2000) Protein A is the von Willebrand factor binding protein on *Staphylococcus aureus*. *Blood*; 96: 2149–56.

117. Hatlen T.J. & Miller L.G. (2021) Staphylococcal Skin and Soft Tissue Infections. *Infect. Dis. Clin. North. Am*. 35(1):81-105. doi: 10.1016/j.idc.2020.10.003

118. Heilbronner S., Foster T.J. (2020). *Staphylococcus lugdunensis*: a Skin Commensal with Invasive Pathogenic Potential. *Clin. Microbiol. Rev*., 34(2), e00205-20. doi: 10.1128/CMR.00205-20.

119. Heilbronner S., Holden M.T., van Tonder A., Geoghegan J.A., Foster T.J., Parkhill J., Bentley S.D. (2011). Genome sequence of *Staphylococcus lugdunensis* N920143 allows identification of putative colonization and virulence factors. *FEMS Microbiol. Lett.*, 322:60–67.

120. Heilmann C. (2011). Adhesion mechanisms of staphylococci. *Adv. Exp. Med. Biol.*, 715, 105–123. doi: 10.1007/978-94-007-0940-9_7

121. Herrmann M., Hartleib J., Kehrel B., Montgomery R.R., Sixma J.J., Peters G. (1997) Interaction of von willebrand factor with *Staphylococcus aureus*. *J Infect Dis*. 176:984–91. doi: 10.1086/516502.

122. Heumann D., Barras C., Severin A., M.P. Glauser, Tomasz A. (1994). Gram-positive cell walls stimulate synthesis of tumor necrosis fator alpha and interleukin-6 by human monocytes. *Infect. Immun.*, 62:2715- 2721.

123. Hiramatsu K., Hanaki H., Ino T., Yabuta K., Oguri T., Tenover F. C. (1997). Methicillin-resistant *Staphylococcus aureus* clinical strain with reduced vancomycin susceptibility. *J. Antimicrob. Chemother.*, 40(1), 135–136. doi: 10.1093/jac/40.1.135

124. Hiramatsu K., Ito T., Tsubakishita S., Sasaki T., Takeuchi F., Morimoto Y., Katayama Y., Matsuo M., Kuwahara-Arai K., Hishinuma T., Baba T. (2013). Genomic Basis for Methicillin Resistance in *Staphylococcus aureus*. *Infect. Chemother.*, Jun;45(2):117-136. doi: 10.3947/ic.2013.45.2.117

125. Horsburgh M.J., Aish J.L., White I.J., Shaw L., Lithgow J.K., Foster S.J. (2002). sigmaB modulates virulence determinant expression and stress resistance: characterization of a functional rsbU strain derived from *Staphylococcus aureus* 8325-4. *J Bacteriol*., 184(19), 5457–5467. doi: 10.1128/JB.184.19.5457-5467.2002.

126. Huang J., Roth R., Heuser J.E., Sadler J.E. (2009). Integrin alpha(v)beta(3) on human endothelial cells binds von Willebrand factor strings under fluid shear stress. *Blood*, 113(7), 1589–1597. doi: 10.1182/blood-2008-05-158584.

127. Human Microbiome Project Consortium. (2012) Structure, function and diversity of the healthy human microbiome. *Nature*. 486(7402):207-14. doi: 10.1038/nature11234

128. Hurd A. F., Garcia-Lara J., Rauter Y., Cartron M., Mohamed R., Foster S. J. (2012). The iron-regulated surface proteins IsdA, IsdB, and IsdH are not required for heme iron utilization in *Staphylococcus aureus*. FEMS microbiology letters, 329(1), 93–100. doi: 10.1111/j.1574-6968.2012.02502.x

129. Ilangovan U., Ton-That H., Iwahara J., Schneewind O., Clubb R. T. (2001). Structure of sortase, the transpeptidase that anchors proteins to the cell wall of *Staphylococcus aureus*. *Proc. Natl. Acad. Sci U.S.A.*, 98(11), 6056–6061. doi: 10.1073/pnas.101064198

130. Inoshima I., Inoshima N., Wilke G. A., Powers M. E., Frank K. M., Wang Y., Bubeck Wardenburg J. (2011). A *Staphylococcus aureus* pore-forming toxin subverts the activity of ADAM10 to cause lethal infection in mice. *Nat. Med.*, 17(10), 1310–1314. doi: 10.1038/nm.2451

131. Jacquemin M., Neyrinck A., Hermanns M.I., Lavend'homme R., Rega F., Saint-Remy J.M., Peerlinck K., Van Raemdonck D., Kirkpatrick C.J. (2006). FVIII production by human lung microvascular endothelial cells. *Blood*, 108(2), 515–517. doi: 10.1182/blood-2005-11-4571.

132. Jagau H., Behrens I.K., Lahme K., Lorz G., Köster R.W., Schneppenheim R., Obser T., Brehm M.A., König G., Kohler T.P., Rohde M., Frank R., Tegge W., Fulde M., Hammerschmidt S., Steinert M., Bergmann S. (2019). Von Willebrand Factor Mediates Pneumococcal Aggregation and Adhesion in Blood Flow. *Front. Microbiol*., 10, 511. doi: 10.3389/fmicb.2019.00511.

133. Jakobi A.J., Mashagh, A., Tans S.J., Huizinga, E.G. (2011) Calcium modulates force sensing by the von Willebrand factor A2 domain. *Nature Communications*, 2, 385.

134. James P. & Rydz N. (2018). Structure, Biology, and Genetics of von Willebrand Factor. *Hematology (Seventh Edition*), 138, 2051-2063. doi: 10.1016/B978-0-323-35762-3.00138-4.

135. Josefsson E., McCrea K.W., Eidhin D.N., O'Connell D., Cox J., Hook M., Foster T.J. (1998). Three new members of the serine-aspartate repeat protein multigene family of *Staphylococcus aureus*. *Microbiology (Reading)*, 144 (12), 3387–3395. doi: 10.1099/00221287-144-12-3387.

136. Ju L., Dong J.F., Cruz M.A., Zhu, C. (2013) The N-terminal flanking region of the A1 domain regulates the force-dependent binding of von Willebrand factor to platelet glycoprotein Ibalpha. *J Biol Chem,* 288, 32289-301.

137. Kang M., Ko Y.P., Liang X., Ross C.L., Liu Q., Murray B.E., Höök M. (2013). Collagen-binding microbial surface components recognizing adhesive matrix molecule (MSCRAMM) of Gram-positive bacteria inhibit complement activation via the classical pathway. *J Biol Chem* , 288:20520–20531 doi: 10.1074/jbc.M113.454462.

138. Kaufmann J.E., Oksche A., Wollheim C.B., Günther G., Rosenthal W., Vischer U.M. (2000). Vasopressin-induced von Willebrand factor secretion from endothelial cells involves V2 receptors and cAMP. *J Clin Invest.*, 106(1), 107–116. doi: 10.1172/JCI9516.

139. Kaushansky K. (2006). Lineage-specific hematopoietic growth factors. *N Engl J Med,* 354, 2034-45.

140. Kaushansky K. (2016). Blood's 70th anniversary: the elusive von Willebrand factor-cleaving protease. *Blood*, 127, 2163-4.

141. Keane F.M., Loughman A., Valtulina V., Brennan M., Speziale P., Foster T.J. (2007). Fibrinogen and elastin bind to the same region within the A domain of fibronectin binding protein A, an MSCRAMM of *Staphylococcus aureus*. *Mol. Microbiol*., 63(3), 711–723. doi: 10.1111/j.1365-2958.2006.05552.x.

142. Keesler D.A., Slobodianuk T.L., Kochelek C.E., Skaer C.W., Haberichter S.L., Flood V.H. (2021). Fibronectin binding to von Willebrand factor occurs via the A1 domain. *Res. Pract. Thromb. Haemost*., 5(5), e12534. doi: 10.1002/rth2.12534.

143. Kernodle D.S. (2000) Mechanisms of resistance to β-lactam antibiotics. In Gram-positive pathogens. V.A. Fischetti, R.P. Novick, J.J. Ferretti, D.A. Portnoy, J.I. Rood, editors. American Society for Microbiology. Washington, DC, USA. 609–620.

144. Kim H. K., DeDent A., Cheng A. G., McAdow M., Bagnoli F., Missiakas D. M., Schneewind O. (2010). IsdA and IsdB antibodies protect mice against *Staphylococcus aureus* abscess formation and lethal challenge. *Vaccine*, 28(38), 6382–6392. doi: 10.1016/j.vaccine.2010.02.097

145. Kim H. K., Thammavongsa V., Schneewind O., Missiakas D. (2012). Recurrent infections and immune evasion strategies of *Staphylococcus aureus*. *Curr. Opin. Microbiol.*, 15(1), 92–99. doi: 10.1016/j.mib.2011.10.012

146. Kim J., Zhang C.-Z., Zhang X., Springer T.A. (2010) A mechanically stabilized receptor-ligand flexbond important in the vasculature. *Nature,* 466, 992-U123.

147. Kirby W. M. (1944) Extraction of a highly potent penicillin inactivator from penicillin resistant staphylococci. *Science*, 99(2579), 452–453. doi: 10.1126/science.99.2579.452

148. Kluytmans J., van Belkum A., Verbrugh H. (1997) Nasal carriage of *Staphylococcus aureus*: epidemiology, underlying mechanisms, and associated risks. *Clin. Microbiol. Rev*. 10(3):505-20. doi: 10.1128/CMR.10.3.505-520.1997

149. Knipe L., Meli A., Hewlett L., Bierings R., Dempster J., Skehel P., Hannah M.J., Carter T. (2010). A revised model for the secretion of tPA and cytokines from cultured endothelial cells. *Blood*, 116(12), 2183–2191. doi: 10.1182/blood-2010-03-276170.

150. Knox K.W. & Wicken A.J. (1973). Immunological properties of teichoic acids. *Bacteriol Rev.*, 37(2):215-57.

151. Kobayashi S. D. & DeLeo F. R. (2013). *Staphylococcus aureus* protein A promotes immune suppression. *mBio*, 4(5), e00764-13. doi: 10.1128/mBio.00764-13

152. Kong H.H., Oh J., Deming C., Conlan S., Grice E.A., Beatson M.A., Nomicos E., Polley E.C., Komarow H.D., Murray P.R., Turner M.L., Segre J.A. (2012). Temporal shifts in the skin microbiome associated with disease flares and treatment in children with atopic dermatitis. *Genome Res* 22:850–859 doi: 10.1101/gr.131029.111.

153. Krishna Kumar K., Jacques D.A., Pishchany G., Caradoc-Davies T., Spirig T., Malmirchegini G.R., Langley, D.B., Dickson, C.F., Mackay, J.P., Clubb, R.T., Skaar, E.P., Guss, J.M., Gell, D.A. (2011). Structural basis for hemoglobin capture by *Staphylococcus aureus* cell-surface protein, IsdH. *J. Biol. Chem.,* 286 (44): 38439-38447.

154. Kroh H. K., Panizzi P., Bock P. E. (2009). Von Willebrand factor-binding protein is a hysteretic conformational activator of prothrombin. *Proc. Natl. Acad. Sci. U.S.A.*, 106(19), 7786–7791. doi: 10.1073/pnas.0811750106

155. Kroll M.H., Harris T.S., Moake J.L., Handin R.I. & Schafer A.I. (1991). von Willebrand factor binding to platelet GpIb initiates signals for platelet activation. *J. Clin. Investig*., 88, 1568-1573.

156. Kroll M.H., Hellums J.D., McIntire L.V., Schafer A.I., Moake, J.L. (1996) Platelets and shear stress. *Blood*, 88, 1525-1541.

157. Kukita K., Kawada-Matsuo M., Oho T., Nagatomo M., Oogai Y., Hashimoto M., Suda Y., Tanaka T., Komatsuzawa H. (2013). *Staphylococcus aureus* SasA is responsible for binding to the salivary agglutinin gp340, derived from human saliva. *Infect Immun,* 81:1870–1879. doi: 10.1128/IAI.00011-13.

158. Kusch H. & Engelmann S. (2014). Secrets of the secretome in *Staphylococcus aureus*. *Int. J. Med. Microbiol.*, 304(2), 133–141. doi: 10.1016/j.ijmm.2013.11.005

159. Laupland K.B., Lyytikäinen O., Søgaard M., Kennedy K.J., Knudsen J.D., Ostergaard C., Galbraith J.C., Valiquette L., Jacobsson G., Collignon P., Schønheyder H.C.; International Bacteremia Surveillance Collaborative. (2013) The changing epidemiology of *Staphylococcus aureus* bloodstream infection: a multinational population-based surveillance study. *Clin. Microbiol. Infect*. 19(5):465–471. doi: 10.1111/j.1469-0691.2012.03903.x

160. Lenting P.J., Christophe O.D. Denis C.V. (2015). von Willebrand factor biosynthesis, secretion, and clearance: connecting the far ends. *Blood*, 125, 2019-2028.

161. Levine J.D., Harlan J.M., Harker L.A., Joseph M.L. Counts R.B. (1982). Thrombin-mediated release of factor VIII antigen from human umbilical vein endothelial cells in culture. *Blood*, 60, 531-4.

162. Li D.Q., Lundberg F., Ljungh A. (2000) Binding of von willebrand factor by coagulase-negative staphylococci. *J Med Microbiol*. 49:217–25. doi: 10.1099/0022-1317-49-3-217.

163. Li M., Du X., Villaruz A.E., Diep B.A., Wang D., Song Y., Tian Y., Hu J., Yu F., Lu Y., Otto M. (2012). MRSA epidemic linked to a quickly spreading colonization and virulence determinant. *Nat Med* 18:816–819 doi: 10.1038/nm.2692.

164. Liesenborghs L., Meyers S., Lox M., Criel M., Claes J., Peetermans M., Trenson S., Vande Velde G., Vanden Berghe P., Baatsen P., Missiakas D., Schneewind O., Peetermans W.E., Hoylaerts M.F., Vanassche T., Verhamme P. (2019). *Staphylococcus aureus* endocarditis: distinct mechanisms of bacterial adhesion to damaged and inflamed heart valves. *Eur Heart J*., 40(39), 3248–3259. doi: 10.1093/eurheartj/ehz175.

165. Liesenborghs L., Peetermans M., Claes J., Veloso T.R., Vandenbriele C., Criel M., Lox M., Peetermans W.E., Heilbronner S., de Groot P.G., Vanassche T., Hoylaerts M.F., Verhamme P. (2016). Shear-Resistant Binding to von Willebrand Factor Allows *Staphylococcus lugdunensis* to Adhere to the Cardiac Valves and Initiate Endocarditis. *J Infect Dis*., 213(7), 1148–1156. doi: 10.1093/infdis/jiv773.

166. Lim D. & Strynadka N. C. (2002). Structural basis for the beta lactam resistance of PBP2a from methicillin-resistant *Staphylococcus aureus*. *Nat. Struct. Biol.*, 9(11), 870–876. doi: 10.1038/nsb858

167. Liu G.Y., Essex A., Buchanan J.T., Datta V., Hoffman H.M., Bastian J.F., Fierer J., Nizet V., (2005). *Staphylococcus aureus* golden pigment impairs neutrophil killing and promotes virulence through its antioxidant activity. *J. Exp. Med.*, 202(2): 209–215.

168. Lizcano A., Sanchez C.J., Orihuela C.J. (2012). A role for glycosylated serine-rich repeat proteins in Gram-positive bacterial pathogenesis. *Mol Oral Microbiol*, 27:257–269. doi: 10.1111/j.2041-1014.2012.00653.x.

169. Lopes da Silva M. & Cutler D.F. (2016). von Willebrand factor multimerization and the polarity of secretory pathways in endothelial cells. *Blood*, 128(2), 277–285. doi: 10.1182/blood-2015-10-677054.

170. Lowy F. D. (2003). Antimicrobial resistance: the example of *Staphylococcus aureus*. *J. Clin. Investig.*, 111(9), 1265–1273. doi: 10.1172/JCI18535

171. Lüttge M., Fulde M., Talay S.R., Nerlich A., Rohde M., Preissner K.T., Hammerschmidt S., Steinert M., Mitchell T.J., Chhatwal G.S., Bergmann S. (2012). *Streptococcus pneumoniae* induces exocytosis of Weibel-Palade bodies in pulmonary endothelial cells. *Cell. Microbiol*., 14(2), 210–225. doi: 10.1111/j.1462-5822.2011.01712.x.

172. Madabhushi S.R., Zhang C.J., Kelkar A., Dayananda K.M., Neelamegham, S. (2014) Platelet Gplb alpha Binding to von Willebrand Factor Under Fluid Shear: Contributions of the D'D3-Domain, A1-Domain Flanking Peptide and O-Linked Glycans. *J. Am. Heart Assoc*., 3, 21.

173. Majcherczyk P.A., Rubli E., Heumann D., Glauser M.P., Moreillon P. (2003). Teichoic acids are not required for *Streptococcus pneumoniae* and *Staphylococcus aureus* cell walls to trigger the release of tumor necrosis factor by peripheral blood monocytes. *Infect. Immun.*, 71:3707-3713.

174. Marraffini L.A., Dedent A.C., Schneewind O., (2006). Sortases and the art of anchoring proteins to the envelopes of gram-positive bacteria. *Microbiol. Mol. Biol. Rev.*, 70(1):192-221.

175. Mascari L.M. & Ross J.M. (2003) Quantification of staphylococcal-collagen binding interactions in whole blood by use of a confocal microscopy shear-adhesion assay. *J Infect Dis*. 188:98–107. doi: 10.1086/375826.

176. Mason W.J. & Skaar E.P. (2009). Assessing the contribution of heme-iron acquisition to *Staphylococcus aureus* pneumonia using computed tomography. *PLoS One*., 4(8), e6668. doi: 10.1371/journal.pone.0006668

177. Matsui T., Titani K., Mizuochi T. (1992). Structures of the asparagine-linked oligosaccharide chains of human von Willebrand factor. Occurrence of blood group A, B, and H(O) structures. *J Biol Chem*, 267, 8723-31.

178. Mayadas T.N. & Wagner D.D. (1989). In vitro multimerization of von Willebrand factor is triggered by low pH. Importance of the propolypeptide and free sulfhydryls. *J Biol Chem,* 264, 13497-503.

179. Mazmanian S. K., Ton-That H., Schneewind O. (2001). Sortase-catalysed anchoring of surface proteins to the cell wall of *Staphylococcus aureus*. *Mol. Microbiol.*, 40(5), 1049–1057. doi: 10.1046/j.1365-2958.2001.02411.x

180. Mazmanian S.K., Liu G., Jensen E.R., Lenoy E., Schneewind O. (2000). *Staphylococcus aureus* sortase mutants defective in the display of surface proteins and in the pathogenesis of animal infections. PNAS, 97:5510–15. doi: 10.1073/pnas.080520697

181. Mazzucato M., Spessotto P., Masotti A., De Appollonia L., Cozzi M.R., Yoshioka A., Perris R., Colombatti A. & De Marco L. (1999). Identification of Domains Responsible for von Willebrand Factor Type VI Collagen Interaction Mediating Platelet Adhesion under High Flow. *J Biol Chem*., 274, 3033-3041.

182. McAdow M., Missiakas D. M., Schneewind O. (2012). *Staphylococcus aureus* secretes coagulase and von Willebrand factor binding protein to modify the coagulation cascade and establish host infections. *J. Innate Immun.*, 4(2), 141–148. doi: 10.1159/000333447

183. McAleese F.M., Walsh E.J., Sieprawska M., Potempa J., Foster T.J. (2001). Loss of clumping factor B fibrinogen binding activity by *Staphylococcus aureus* involves cessation of transcription, shedding and cleavage by metalloprotease. *J. Biol. Chem.*, 276:29969–29978.

184. McDevitt D., Nanavaty T., House-Pompeo K., Bell E., Turner N., McIntire L., Foster T., Höök M. (1997). Characterization of the interaction between the *Staphylococcus aureus* clumping factor (ClfA) and fibrinogen. *Eur. J. Biochem*., 247(1), 416–424. doi: 10.1111/j.1432-1033.1997.00416.x.

185. McGrath R.T., McRae E., Smith O.P., O'Donnell, J.S. (2010). Platelet von Willebrand factor structure, function and biological importance. *Br. J. Haematol*., 148, 834-843.

186. McGrath R.T., van den Biggelaar M., Byrne B., O'Sullivan J.M., Rawley O., O'Kennedy R., Voorberg J., Preston R.J., O'Donnell J.S. (2013). Altered glycosylation of platelet-derived von Willebrand factor confers resistance to ADAMTS13 proteolysis. *Blood*, 122(25), 4107–4110. doi: 10.1182/blood-2013-04-496851.

187. Mermel L.A., Cartony J.M., Covington P., Maxey G., Morse D. (2011) Methicillin-resistant *Staphylococcus aureus* colonization at different body sites: a prospective, quantitative analysis. *J. Clin. Microbiol.* 49(3):1119-21. doi: 10.1128/JCM.02601-10

188. Miajlovic H., Zapotoczna M., Geoghegan J. A., Kerrigan S. W., Speziale P., Foster T. J. (2010). Direct interaction of iron-regulated surface determinant IsdB of *Staphylococcus aureus* with the GPIIb/IIIa receptor on platelets. *Microbiology (Reading),* 156(Pt 3), 920–928. doi: 10.1099/mic.0.036673-0

189. Michaux G., Abbitt K.B., Collinson L.M., Haberichter S.L., Norman K.E., Cutler D.F. (2006). The physiological function of von Willebrand's factor depends on its tubular storage in endothelial Weibel-Palade bodies. *Dev. Cell*, 10(2), 223–232. doi: 10.1016/j.devcel.2005.12.012.

190. Michaux G., Pullen T.J., Haberichter S.L., Cutler, D.F. (2006). P-selectin binds to the D '-D3 domains of von Willebrand factor in Weibel-Palade bodies. *Blood,* 107, 3922-3924.

191. Miseta A. & Csutora P. (2000) Relationship between the occurrence of cysteine in proteins and the complexity of organisms. *Mol. Biol. Evol*., 17, 1232-1239.

192. Miszta A., Pelkmans L., Lindhout T., Krishnamoorthy G., de Groot P.G., Hemker C.H., Heemskerk J.W., Kelchtermans H., de Laa, B. (2014). Thrombin-dependent Incorporation of von Willebrand Factor into a Fibrin Network. *J. Biol. Chem*., 289(52), 35979–35986. doi: 10.1074/jbc.M114.591677.

193. Morton T.A., Myszka D.G., Chaiken, I. M. (1995). Interpreting complex binding kinetics from optical biosensors: a comparison of analysis by linearization, the integrated rate equation, and numerical integration. *Anal. Biochem*., 227(1), 176–185. doi: 10.1006/abio.1995.1268.

194. Mulcahy M.E. & McLoughlin R.M. (2016) Host-Bacterial Crosstalk Determines *Staphylococcus aureus* Nasal Colonization. *Trends. Microbiol.* 24(11):872-886. doi: 10.1016/j.tim.2016.06.012

195. Mulcahy M.E., Geoghegan J.A., Monk I.R., O'Keeffe K.M., Walsh E.J., Foster T.J., McLoughlin R.M. (2012). Nasal colonisation by *Staphylococcus aureus* depends upon clumping factor B binding to the squamous epithelial cell envelope protein loricrin. *PLoS Pathog* 8:e1003092 doi: 10.1371/journal.ppat.1003092.

196. Müller J.P., Mielke S., Löf A., Obser T., Beer C., Bruetzel L.K., Pippig D.A., Vanderlinden W., Lipfert J., Schneppenheim R., Benoit M. (2016) Force sensing by the vascular protein von Willebrand factor is tuned by a strong intermonomer interaction. *Proc Natl Acad Sci U S A.*, 113, 1208-1213.

197. Murray P.R., Rosenthal K.S., Pfaller M.A., (2020). Medical Microbiology (9th edition). *Mosby Inc.*, Philadelphia, PA, USA.

198. Muryoi N., Tiedemann M.T., Pluym M., Cheung J., Heinrichs D.E., Stillman M.J. (2008). Demonstration of the iron-regulated surface determinant (Isd) heme transfer pathway in *Staphylococcus aureus*. *J. Biol. Chem*., 283(42), 28125–28136. doi: 10.1074/jbc.M802171200

199. Myszka, D.G. (1997). Kinetic analysis of macromolecular interactions using surface plasmon resonance biosensors. *Curr. Opin. Biotechnol*., 8(1), 50-57. doi: 10.1016/S0958-1669(97)80157-7.

200. Nakamura M.M., McAdam A.J., Sandora T.J., Moreira K.R., Lee G.M. (2010) Higher prevalence of pharyngeal than nasal *Staphylococcus aureus* carriage in pediatric intensive care units. *J. Clin. Microbiol*. 48(8):2957-9. doi: 10.1128/JCM.00547-10

201. Nesbitt W.S., Westein E., Tovar-Lopez F.J., Tolouei E., Mitchell A., Fu J., Carberry J., Fouras A., Jackson S.P. (2009). A shear gradient-dependent platelet aggregation mechanism drives thrombus formation. *Nature medicine*, 15(6), 665–673. doi: 10.1038/nm.1955.

202. Ní Eidhin D., Perkins S., Francois P., Vaudaux P., Höök M., Foster T.J. (1998). Clumping factor B (ClfB), a new surface-located fibrinogen-binding adhesin of *Staphylococcus aureus*. *Mol. Microbiol*., 30(2), 245–257. doi: 10.1046/j.1365-2958.1998.01050.x.

203. Nickerson N. N., Joag V., McGavin M. J. (2008). Rapid autocatalytic activation of the M4 metalloprotease aureolysin is controlled by a conserved N-terminal fungalysin-thermolysin-propeptide domain. *Mol. Microbiol.*, 69(6), 1530–1543. doi: 10.1111/j.1365-2958.2008.06384.x

204. Nickerson N., Ip J., Passos D. T., McGavin M. J. (2010). Comparison of Staphopain A (ScpA) and B (SspB) precursor activation mechanisms reveals unique secretion kinetics of proSspB (Staphopain B), and a different interaction with its cognate Staphostatin, SspC. *Mol. Microbiol.*, 75(1), 161–177. doi: 10.1111/j.1365-2958.2009.06974.x

205. Nieswandt B. & Watson S.P. (2003) Platelet-collagen interaction: is GPVI the central receptor? *Blood*, 102, 449-61.

206. Nilsson M., Bjerketorp J., Wiebensjö A., Ljungh A., Frykberg L., Guss B. (2004). A von Willebrand factor-binding protein from *Staphylococcus lugdunensis*. *FEMS Microbiol. Lett*., 234(1), 155–161. doi: 10.1016/j.femsle.2004.03.024.

207. Nilsson P. & Ripa T. (2006) *Staphylococcus aureus* throat colonization is more frequent than colonization in the anterior nares. *J. Clin. Microbiol*. 44, 3334–3339.

208. Nowak A.A., Canis K., Riddell A., Laffan M.A., McKinnon T.A.J. (2012) O-linked glycosylation of von Willebrand factor modulates the interaction with platelet receptor glycoprotein Ib under static and shear stress conditions. *Blood,* 120, 214-222.

209. Nygaard T. K., Pallister K. B., DuMont A. L., DeWald M., Watkins R. L., Pallister E. Q., Malone C., Griffith S., Horswill A. R., Torres V. J., Voyich J. M. (2012). Alpha-toxin induces programmed cell death of human T cells, B cells, and monocytes during USA300 infection. *PloS one*, 7(5), e36532. doi: 10.1371/journal.pone.0036532

210. O'Neill E., Pozzi C., Houston P., Humphreys H., Robinson D.A., Loughman A., Foster T.J., O'Gara J.P. (2008). A novel *Staphylococcus aureus* biofilm phenotype mediated by the fibronectin-binding proteins, FnBPA and FnBPB. *J Bacteriol* 190:3835–3850 doi: 10.1128/JB.00167-08.

211. O'Connell D.P., Nanavaty T., McDevitt D., Gurusiddappa S., Höök M., Foster T.J. (1998). The fibrinogen-binding MSCRAMM (clumping factor) of *Staphylococcus aureus* has a Ca^{2+}-dependent inhibitory site. *J Biol Chem.*, 273(12), 6821–6829. doi: 10.1074/jbc.273.12.6821.

212. Ogston A. (1881) Report upon micro-organisms in surgical diseases. *B. M. J.* 1, 369–377.

213. Ong P.Y. & Leung D.Y. (2016). Bacterial and viral infections in atopic dermatitis: a comprehensive review. *Clin Rev Allergy Immunol* 51:329–337 doi: 10.1007/s12016-016-8548-5.

214. O'Seaghdha M., van Schooten C.J., Kerrigan S.W., Emsley J., Silverman G.J., Cox D., Lenting P.J., Foster T.J. (2006). *Staphylococcus aureus* protein A binding to von Willebrand factor A1 domain is mediated by conserved IgG binding regions. *FEBS J.*, 273(21), 4831–4841. doi: 10.1111/j.1742-4658.2006.05482.x.

215. O'Seaghdha M., van Schooten C.J., Kerrigan S.W., Emsley J., Silverman G.J., Cox D., Lenting P.J., Foster T.J. (2006). *Staphylococcus aureus* protein A binding to von Willebrand factor A1 domain is mediated by conserved IgG binding regions. *FEBS J*, 273(21), 4831–4841. doi: 10.1111/j.1742-4658.2006.05482.x.

216. Padilla A., Moake J.L., Bernardo A., Ball C., Wang Y., Arya M., Nolasco L., Turner N., Berndt M.C., Anvari B., Lopez J.A. & Dong J.F. (2004). P-selectin anchors newly released ultralarge von Willebrand factor multimers to the endothelial cell surface. *Blood*, 103, 2150-6.

217. Palazzolo-Ballance A.M., Reniere M.L., Braughton K.R., Sturdevant D.E., Otto M., Kreiswirth B.N., Skaar E.P., DeLeo, F.R. (2008). Neutrophil microbicides induce a pathogen survival response in community-associated methicillin-resistant *Staphylococcus aureus*. *J. Immunol.,* 180(1), 500–509. doi: 10.4049/jimmunol.180.1.500

218. Palta S., Saroa R. & Palta A. (2014). Overview of the coagulation system. *Indian J Anaesth*., 58(5), 515–523. doi: 10.4103/0019-5049.144643.

219. Papi M., Maulucci G., De Spirito M., Missori M., Arcovito G., Lancellotti S., Di Stasio E., De Cristofaro R., Arcovito A. (2010). Ristocetin-induced self-aggregation of von Willebrand factor, *Eur. Biophys. J.*, 39:1597–1603. doi: 10.1007/s00249-010-0617-8.

220. Pappelbaum K.I., Gorzelanny C., Grässle S., Suckau J., Laschke M.W., Bischoff M., Bauer C., Schorpp-Kistner M., Weidenmaier C., Schneppenheim R., Obser T., Sinha B., Schneider S.W. (2013). Ultralarge von Willebrand factor fibers mediate luminal *Staphylococcus aureus* adhesion to an intact endothelial cell layer under shear stress. *Circulation*, 128(1), 50–59. doi: 10.1161/CIRCULATIONAHA.113.002008.

221. Pareti F.I., Niiya K., McPherson J.M., Ruggeri Z.M. (1987). Isolation and characterization of two domains of human von Willebrand factor that interact with fibrillar collagen types I and III. *J. Biol. Chem*., 262(28), 13835–13841.

222. Peyvandi F., Garagiola I. & Baronciani L. (2011). Role of von Willebrand factor in the haemostasis. *Blood Transfus*, 9 Suppl 2, s3-8.

223. Pietrocola G., Nobile G., Alfeo M.J., Foster T.J., Geoghegan J.A., De Filippis V., Speziale P. (2019). Fibronectin-binding protein B (FnBPB) from *Staphylococcus aureus* protects against the antimicrobial activity of histones. *J Biol Chem*., 294(10), 3588–3602. doi: 10.1074/jbc.RA118.005707

224. Pietrocola G., Nobile G., Gianotti V., Zapotoczna M., Foster T. J., Geoghegan J. A., Speziale P. (2016). Molecular Interactions of Human Plasminogen with Fibronectin-binding Protein B (FnBPB), a Fibrinogen/Fibronectin-binding Protein from *Staphylococcus aureus*. *J. Biol. Chem.*, 291(35), 18148–18162. doi: 10.1074/jbc.M116.731125

225. Pietrocola G., Pellegrini A., Alfeo M. J., Marchese L., Foster T. J., Speziale P. (2020). The iron-regulated surface determinant B (IsdB) protein from *Staphylococcus aureus* acts as a receptor for the host protein vitronectin. *J. Biol. Chem*., 295(29), 10008–10022. doi: 10.1074/jbc.RA120.013510

226. Pilpa R.M., Fadeev F.A., Villareal V.A., Wong M.L., Phillips M., Clubb R.T. (2006). Solution structure of the NEAT (NEAr Transporter) domain from IsdH/HarA: the human hemoglobin receptor in *Staphylococcus aureus*. *J. Mol. Biol.*, 360 (2): 435-447.

227. Pilpa R.M., Robson S.A., Villareal V.A., Wong M.L., Phillips M., Clubb R.T. (2009). Functionally distinct NEAT (NEAr Transporter) domains within the *Staphylococcus aureus* IsdH/HarA protein extract heme from methemoglobin. *J. Biol. Chem*., 284(2), 1166–1176. doi: 10.1074/jbc.M806007200

228. Pishchany G. & Skaar E. P. (2012). Taste for blood: hemoglobin as a nutrient source for pathogens. *PLoS Pathog*., 8(3), e1002535. doi: 10.1371/journal.ppat.1002535

229. Pishchany G., Dickey S.E., Skaar E.P. (2009). Subcellular localization of the *Staphylococcus aureus* heme iron transport components IsdA and IsdB. *Infect. Immun*., 77 (7): 2624-2634. doi: 10.1128/IAI.01531-08

230. Pishchany G., McCoy A. L., Torres V. J., Krause J. C., Crowe J. E., Jr, Fabry M. E., Skaar E. P. (2010). Specificity for human hemoglobin enhances *Staphylococcus aureus* infection. *Cell. Host Microbe*., 8(6), 544–550. doi: 10.1016/j.chom.2010.11.002

231. Pishchany, G., Sheldon, J. R., Dickson, C. F., Alam, M. T., Read, T. D., Gell, D. A., Heinrichs, D. E., Skaar, E. P. (2014). IsdB-dependent hemoglobin binding is required for acquisition of heme *by Staphylococcus aureus*. *J. Infect. Dis*., 209(11), 1764–1772. doi: 10.1093/infdis/jit817

232. Ponnuraj K., Bowden M.G., Davis S., Gurusiddappa S., Moore D., Choe D., Xu Y., Hook M., Narayana S.V. (2003). A "dock, lock, and latch" structural model for a staphylococcal adhesin binding to fibrinogen. *Cell*, 115(2), 217–228. doi: 10.1016/s0092-8674(03)00809-2

233. Prasad L., Leduc Y., Hayakawa K., Delbaere L. T. (2004). The structure of a universally employed enzyme: V8 protease from *Staphylococcus aureus*. *Acta Crystallogr. D. Biol. Crystallogr.*, 60(Pt 2), 256–259. doi: 10.1107/S090744490302599X

234. Projan S.J. & Novick R.P. (1997). The molecular basis of pathogenicity. In K.B. Crossley & G.L. Archer, The *staphylococci* in human disease. *Churchill Livingstone*, New York, NY.

235. Purvis A.R. & Sadler J.E. (2004). A covalent oxidoreductase intermediate in propeptide-dependent von Willebrand factor multimerization. *J Biol Chem*, 279, 49982-49988.

236. Raghavachari M., Tsai H., Kottke-Marchant K., Marchant, R.E. (2000) Surface dependent structures of von Willebrand factor observed by AFM under aqueous conditions. *Colloids Surf B Biointerfaces,* 19, 315-324.

237. Rehemtulla A. & Kaufman R.J. (1992). Preferred sequence requirements for cleavage of pro-von Willebrand factor by propeptide-processing enzymes. *Blood,* 79, 2349-55.

238. Reniere M. L. & Skaar E. P. (2008). *Staphylococcus aureus* haem oxygenases are differentially regulated by iron and haem. *Mol. Microbiol*., 69(5), 1304–1315. doi: 10.1111/j.1365-2958.2008.06363.x

239. Ridley M. (1959) Perineal carriage of *S. aureus*. *B.M.J*. 1, 270–273.

240. Riethmuller C., McAleer M.A., Koppes S.A., Abdayem R., Franz J., Haftek M., Campbell L.E., MacCallum S.F., McLean W.H., Irvine A.D., Kezic S. (2015). Filaggrin breakdown products determine corneocyte conformation in patients with atopic dermatitis. *J Allergy Clin Immunol* 136:1573–80e1-2.

241. Rindi S., Cicalini S., Pietrocola G., Venditti M., Festa A., Foster T.J., Petrosillo N., Speziale P. (2006). Antibody response in patients with endocarditis caused by *Staphylococcus aureus*. *Eur J Clin Invest.*, 36(8), 536–543. doi: 10.1111/j.1365-2362.2006.01675.x.

242. Roche F.M., Meehan M., Foster T.J. (2003). The *Staphylococcus aureus* surface protein SasG and its homologues promote bacterial adherence to human desquamated nasal epithelial cells. *Microbiology* 149:2759–2767 doi: 10.1099/mic.0.26412-0.

243. Roest M., Reininger A., Zwaginga J.J., King M.R., Heemskerk J.W. (2011) Flow chamber-based assays to measure thrombus formation *in vitro*: requirements for standardization. *J Thromb Haemost,* 9, 2322-4.

244. Rojo Pulido I., Nightingale T.D., Darchen F., Seabra M.C., Cutler D.F., Gerke V. (2011). Myosin Va acts in concert with Rab27a and MyRIP to regulate acute von-Willebrand factor release from endothelial cells. *Traffic*, 12(10), 1371–1382. doi: 10.1111/j.1600-0854.2011.01248.x.

245. Romijn R.A.P., Bouma B., Wuyster W., Gros P., Kroon J., Sixma J.J. & Huizinga E.G. (2001). Identification of the Collagen-binding Site of the von Willebrand Factor A3-domain. *J Biol Chem*., 276, 9985-9991.

246. Rondaij M.G., Bierings R., Kragt A., van Mourik J.A. Voorberg J. (2006). Dynamics and plasticity of Weibel-Palade bodies in endothelial cells. *Arterioscler Thromb Vasc Biol,* 26, 1002-1007.

247. Rosenbach, F. J. (1884) Mikro-organismen bei den Wund-Infections-Krankheiten des Menschen.

248. Ross A. & Shoff H.W. (2020) Staphylococcal Scalded Skin Syndrome In: StatPearls [Internet]. Treasure Island (FL): StatPearls Publishing; 2021 Jan–. PMID: 28846262.

249. Ruggeri Z.M. (2007) The role of von Willebrand factor in thrombus formation. *Thromb Res,* 120 Suppl 1, S5-9.

250. Ruggeri Z.M. (2009) Platelet adhesion under flow. *Microcirculation,* 16, 58-83.

251. Ruhland G.J. & Fiedler F. (1990). Occurrence and structure of lipoteichoic acids in the genus *Staphylococcus*. *Arch. Microbiol.*, 154:375-379.

252. Sadler J.E. (1998). Biochemistry and genetics of von Willebrand factor. *Annu Rev Biochem*., 67, 395–424. doi: 10.1146/annurev.biochem.67.1.395

253. Sadler J.E. (2009). von Willebrand factor assembly and secretion. *J. Thromb. Haemost*., 7, 24-27.

254. Sadler, J.E. (2008). Von Willebrand factor, ADAMTS13, and thrombotic thrombocytopenic purpura. *Blood*, 112, 11-18.

255. Saint-Lu N., Oortwijn B.D., Pegon J.N., Odouard S., Christophe O.D., de Groot P.G., Denis C.V., Lenting P.J. (2012). Identification of galectin-1 and galectin-3 as novel partners for von Willebrand factor. *Arterioscler Thromb Vasc Biol*., 32(4), 894–901. doi: 10.1161/ATVBAHA.111.240309.

256. Sambrook J. (2001). Molecular cloning: a laboratory manual. Cold Spring Harbor, N.Y.: Cold Spring Harbor Laboratory Press.

257. Sarvepalli D.P., Schmidtke D.W., Nollert M.U. (2009) Design considerations for a microfluidic device to quantify the platelet adhesion to collagen at physiological shear rates. *Ann Biomed Eng,* 37, 1331-41.

258. Savage B., Almus-Jacobs F., Ruggeri Z.M. (1998) Specific synergy of multiple substrate-receptor interactions in platelet thrombus formation under flow. *Cell*, 94, 657-66.

259. Savage B., Saldivar E. & Ruggeri Z.M. (1996). Initiation of platelet adhesion by arrest onto fibrinogen or translocation on von Willebrand factor. *Cell*, 84, 289-97.

260. Schindler C.A. & Schuhardt V.T. (1964) Lysostaphin: A New Bacteriolytic Agent for the *Staphylococcus*. *Proc. Natl. Acad. Sci. U. S. A.*, 51, 414–421.

261. Schneewind O., Mihaylova-Petkov D., Model P. (1993). Cell wall sorting signals in surface proteins of gram-positive bacteria. *EMBO J.*, 12(12), 4803–4811.

262. Schneider S.W., Nuschele S., Wixforth A., Gorzelanny C., Alexander-Katz A., Netz R.R., Schneider M.F. (2007). Shear-induced unfolding triggers adhesion of von Willebrand factor fibers. *Proc Natl Acad Sci U S A*., 104(19), 7899–7903. doi: 10.1073/pnas.0608422104.

263. Semple J.W., Italiano J.E., Jr. Freedman, J. (2011) Platelets and the immune continuum. *Nat Rev Immunol,* 11, 264-74.

264. Sethi S., Herrmann M., Roller J., von Müller L., Peerschke E.I., Ghebrehiwet B., Bajric I., Menger M.D., Laschke M W. (2011). Blockade of gC1qR/p33, a receptor for C1q, inhibits adherence of *Staphylococcus aureus* to the microvascular endothelium. *Microvasc. Res*., 82(1), 66–72. doi: 10.1016/j.mvr.2011.04.007.

265. Shahbazi S., Lenting P.J., Fribourg C., Terraube V., Denis C.V., Christophe O.D. (2007). Characterization of the interaction between von Willebrand factor and osteoprotegerin. *J Thromb Haemost*., 5(9), 1956–1962. doi: 10.1111/j.1538-7836.2007.02681.x.

266. Shankaran H., Alexandridis P., Neelamegham S. (2003) Aspects of hydrodynamic shear regulating shear-induced platelet activation and self-association of von Willebrand factor in suspension. *Blood*, 101, 2637-45.

267. Sherwood R.A. (2005) Haemoglobins (Hemoglobins). Encyclopedia of Analytical Science (Second Edition), Elsevier, 223-229. doi: 10.1016/B0-12-369397-7/00248-X.

268. Shi Q., Fahs S.A., Kuether E.L., Cooley B.C., Weiler H., Montgomery R.R. (2010). Targeting FVIII expression to endothelial cells regenerates a releasable pool of FVIII and restores hemostasis in a mouse model of hemophilia A. *Blood*, 116(16), 3049–3057. doi: 10.1182/blood-2010-03-272419.

269. Showsh S. A., De Boever E. H., Clewell D. B. (2001). Vancomycin resistance plasmid in *Enterococcus faecalis* that encodes sensitivity to a sex pheromone also produced by *Staphylococcus aureus*. *Antimicrob. Agents. Chemother.*, 45(7), 2177–2178. doi: 10.1128/aac.45.7.2177-2178.2001

270. Siedlecki C.A., Lestini B.J., Kottke-Marchant K.K., Eppell S.J., Wilson D.L., Marchant R.E. (1996). Shear-dependent changes in the three-dimensional structure of human von Willebrand factor. *Blood*, 88(8), 2939–2950.

271. Sing C.E. & Alexander-Katz A. (2010) Elongational Flow Induces the Unfolding of von Willebrand Factor at Physiological Flow Rates. *Biophysical Journal*, 98, L35-L37.

272. Smith E.J., Corrigan R.M., van der Sluis T., Gründling A., Speziale P., Geoghegan J.A., Foster T.J. (2012). The immune evasion protein Sbi of *Staphylococcus aureus* occurs both extracellularly and anchored to the cell envelope by binding lipoteichoic acid. *Mol. Microbiol.*, 83:789–804.

273. Smith E.J., Visai L., Kerrigan S.W., Speziale P., Foster, T.J. (2011). The Sbi protein is a multifunctional immune evasion factor of *Staphylococcus aureus*. *Infect. Immun*., 79(9), 3801–3809. doi: 10.1128/IAI.05075-11

274. Sokurenko E.V., Vogel V., Thomas, W.E. (2008) Catch-bond mechanism of force-enhanced adhesion: counterintuitive, elusive, but ... widespread? *Cell Host Microbe,* 4, 314-23.

275. Spaan A. N., van Strijp J., Torres V. J. (2017). Leukocidins: staphylococcal bi-component pore-forming toxins find their receptors. *Nat. Rev. Microbiol.*, 15(7), 435–447. doi: 10.1038/nrmicro.2017.27

276. Spaulding A. R., Salgado-Pabón W., Kohler P. L., Horswill A. R., Leung D. Y., Schlievert P. M. (2013). Staphylococcal and streptococcal superantigen exotoxins. *Clin. Microbiol. Rev.*, 26(3), 422–447. doi: 10.1128/CMR.00104-12

277. Speziale P., Pietrocola G. (2020). The Multivalent Role of Fibronectin-Binding Proteins A and B (FnBPA and FnBPB) of *Staphylococcus aureus* in Host Infections. *Front Microbiol*., 11, 2054. doi: 10.3389/fmicb.2020.02054.

278. Sporn L.A., Chavin S.I., Marder V.J., Wagner, D.D. (1985). Biosynthesis of von Willebrand protein by human megakaryocytes. *J Clin Invest,* 76, 1102-6.

279. Sporn L.A., Marder V.J., Wagner D.D. (1986). Inducible secretion of large, biologically potent von Willebrand factor multimers. *Cell,* 46, 185-90.

280. Sporn L.A., Shi R.J., Lawrence S.O., Silverman D.J., Marder V.J. (1991) *Rickettsia rickettsii* infection of cultured endothelial cells induces release of large von Willebrand factor multimers from weibel-palade bodies. *Blood*. 78:2595–602. doi: 10.1182/blood.V78.10.2595.bloodjournal78102595.

281. Springer T.A. (2014) von Willebrand factor, Jedi knight of the bloodstream. *Blood,* 124, 1412-1425.

282. Springer, T.A. (2011). Biology and physics of von Willebrand factor concatamers. *J. Thromb. Haemost*., 9, 130-143.

283. Stefani S., Chung D.R., Lindsay J.A., Friedrich A.W., Kearns A.M., Westh H., et al. (2012). Meticillin-resistant Staphylococcus aureus (MRSA): global epidemiology and harmonisation of typing methods. *Int. J. Antimicrob. Agents,* 39(4):273–282.

284. Tam K. & Torres V. J. (2019). *Staphylococcus aureus* Secreted Toxins and Extracellular Enzymes. *Microbiol Spectr.*, 7(2), 10.1128/microbiolspec.GPP3-0039-2018. doi: 10.1128/microbiolspec.GPP3-0039-2018

285. Taylor T.A. & Unakal C.G. *Staphylococcus aureus*. 2020 Aug 23. In: StatPearls [Internet]. *Treasure Island (FL): StatPearls Publishing*; 2021 Jan–. PMID: 28722898.

286. Thielens N.M., Tedesco F., Bohlson S.S., Gaboriaud C., Tenner A.J. (2017). C1q: a fresh look upon an old molecule. *Mol Immunol*, 89:73–83 doi: 10.1016/j.molimm.2017.05.025.

287. Thomas W. (2008) Catch bonds in adhesion. *Annu Rev Biomed Eng,* 10, 39-57.

288. Thomer L., Schneewind O., Missiakas D. (2013) Multiple ligands of von willebrand factor-binding protein (vWbp) promote *Staphylococcus aureus* clot formation in human plasma. *J Biol Chem*. 288:28283–92. doi: 10.1074/jbc.M113.493122.

289. Timmermann C.P., Mattsonn E., Martinez-Martinez L., De Graaf L., Van Strijp J.A., Verbrugh H.A., Verhoef J., Fleer A. (1993). Induction of release of tumor necrosis factor from human monocytes by *staphylococci* and staphylococcal peptidoglycans. *Infect. Immun.*, 61:4167-4172.

290. Titani K., Kumar S., Takio K., Ericsson L.H., Wade R.D., Ashida K., Walsh K.A., Chopek M.W., Sadler J.E., Fujikawa K. (1986). Amino acid sequence of human von Willebrand factor. *Biochemistry*, 25(11), 3171–3184. doi: 10.1021/bi00359a015.

291. Todar K., (2008). *Staphylococcus aureus* and staphylococcal disease. *Todar's Online Textbook of Bacteriology*.

292. Tong S.Y., Davis J.S., Eichenberger E., Holland T.L., Fowler V.G. Jr. (2015) *Staphylococcus aureus* infections: epidemiology, pathophysiology, clinical manifestations, and management. *Clin. Microbiol. Rev*. 28(3):603-61. doi: 10.1128/CMR.00134-14

293. Torres V. J., Pishchany G., Humayun M., Schneewind O., Skaar E. P. (2006). *Staphylococcus aureus* IsdB is a hemoglobin receptor required for heme iron utilization. *J. Bacteriol*., 188(24), 8421–8429. doi: 10.1128/JB.01335-06

294. Tosi M.F. (2005). Innate immune responses to infection. *J Allergy Clin Immunol,* 116:241–249 doi: 10.1016/j.jaci.2005.05.036.

295. Tronic E.H., Yakovenko O., Weidner T., Baio J.E., Penkala R., Castner D.G., Thomas W.E. (2016). Differential surface activation of the A1 domain of von Willebrand factor. *Biointerphases*, 11(2), 029803. doi: 10.1116/1.4943618.

296. Tsai H.M. & Lian E.C. (1998). Antibodies to von Willebrand factor-cleaving protease in acute thrombotic thrombocytopenic purpura. *N Engl J Med* 339, 1585-94 4.

297. Tsai H.M., Sussman I.I., Nagel R. L. (1994). Shear stress enhances the proteolysis of von Willebrand factor in normal plasma. *Blood*, 83(8), 2171–2179.

298. Turner N.A. & Moake J.L. (2015). Factor VIII Is Synthesized in Human Endothelial Cells, Packaged in Weibel-Palade Bodies and Secreted Bound to ULVWF Strings. *PLoS One.*, 10(10), e0140740. doi: 10.1371/journal.pone.0140740.

299. Ulrichts H., Vanhoorelbeke K., Girma J.P., Lenting P.J., Vauterin S., Deckmyn H. (2005). The von Willebrand factor self-association is modulated by a multiple domain interaction. *J Thromb Haemost*., 3(3), 552–561. doi: 10.1111/j.1538-7836.2005.01209.x.

300. Valentijn K.M., van Driel L.F., Mourik M.J., Hendriks G.J., Arends T.J., Koster A.J., Valentijn J.A. (2010). Multigranular exocytosis of Weibel-Palade bodies in vascular endothelial cells. *Blood*, 116(10), 1807–1816. doi: 10.1182/blood-2010-03-274209.

301. Valotteau C., Prystopiuk V., Pietrocola G., Rindi S., Peterle D., De Filippis V., Foster T.J., Speziale P., Dufrêne Y.F. (2017). Single-Cell and Single-Molecule Analysis Unravels the Multifunctionality of the *Staphylococcus aureus* Collagen-Binding Protein Cna. *ACS nano*, 11(2), 2160–2170. doi: 10.1021/acsnano.6b08404.

302. van Belkum A., Verkaik N.J., de Vogel C.P., Boelens H.A., Verveer J., Nouwen J.L., Verbrugh H.A., Wertheim H.F. (2009) Reclassification of *Staphylococcus aureus* nasal carriage types. *J. Infect. Dis*. 15;199(12):1820-6. doi: 10.1086/599119

303. van Mourik J.A., Romani de Wit T., Voorberg J. (2002) Biogenesis and exocytosis of weibel-palade bodies. *Histochem Cell Biol*. 117:113–22. doi: 10.1007/s00418-001-0368-9.

304. Vanassche T., Peetermans M., Van Aelst L.N., Peetermans W. E., Verhaegen J., Missiakas D.M., Schneewind O., Hoylaerts M.F., Verhamme P. (2013). The role of staphylothrombin-mediated fibrin deposition in catheter-related *Staphylococcus aureus* infections. *J Infect Dis.*, 208(1), 92–100. doi: 10.1093/infdis/jit130

305. Vanassche T., Verhaegen J., Peetermans W.E., Hoylaerts M. F., Verhamme P. (2010). Dabigatran inhibits Staphylococcus aureus coagulase activity. *J Clin Microbiol.*, 48(11), 4248–4250. doi: 10.1128/JCM.00896-10

306. Vatansever F., Ferraresi C., de Sousa M. V., Yin R., Rineh A., Sharma S. K., Hamblin M. R. (2013). Can biowarfare agents be defeated with light?. *Virulence*, 4(8), 796–825. doi: 10.4161/viru.26475

307. Verhamme, P. & Hoylaerts M.F. (2009). Hemostasis and inflammation: two of a kind?. *Thromb J.*, 7, 15. doi: 10.1186/1477-9560-7-15

308. Viela F., Prystopiuk V., Leprince A., Mahillon J., Speziale P., Pietrocola G., Dufrêne Y.F. (2019). Binding of *Staphylococcus aureus* Protein A to von Willebrand Factor Is Regulated by Mechanical Force. *mBio*, 10(2), e00555-19. doi: 10.1128/mBio.00555-19.

309. Viela F., Speziale P., Pietrocola G., Dufrene Y.F. (2019) Bacterial pathogens under hightension: Staphylococcus aureus adhesion to von willebrand factor is activated by force. *Microb Cell*. 6:321–3. doi: 10.15698/mic2019.07.684.

310. Visai L., Yanagisawa N., Josefsson E., Tarkowski A., Pezzali I., Rooijakkers S., Foster T.J., Speziale P. (2009). Immune evasion by *Staphylococcus aureus* conferred by iron-regulated surface determinant protein IsdH. *Microbiology (Reading*)., 155(Pt 3), 667–679. doi: 10.1099/mic.0.025684-0

311. Vischer U.M. & Wagner D.D. (1994). von Willebrand factor proteolytic processing and multimerization precede the formation of Weibel-Palade bodies. *Blood,* 83, 3536-44.

312. Vischer U.M. & Wollheim C.B. (1997).Epinephrine induces von Willebrand factor release from cultured endothelial cells: Involvement of cyclic AMP-dependent signalling in exocytosis. *Thromb. Haemost.*, 77, 1182-1188.

313. Wagner D.D. (1990). Cell biology of von Willebrand factor. *Annu Rev Cell Biol*, 6, 217-46.

314. Wakabayashi G., Gelfand J.A., Jung W.K., Connolly R.J., Burke J.F., Dinarello C.A. (1991). *Staphylococcus epidermidis* induces complement activation, tumor necrosis factor and interleukin-1, a shock-like state and tissue injury in rabbits without endotoxemia. Comparison to *Escherichia coli*. *J. Clin. Investig.*, 87:1925-1935.

315. Waldvogel F.A., (1990) *Staphylococcus aureus* (including toxic shock syndrome), In: Mandell GL, Douglas RG, Bennett JE (eds.). *Principles and Practice of Infectious Disease*, 3rd ed. *Churchill Livingston*, London. pp 1489- 1510.

316. Walsh E.J., O'Brien L.M., Liang X., Hook M., Foster T.J. (2004). Clumping factor B, a fibrinogen-binding MSCRAMM (microbial surface components recognizing adhesive matrix molecules) adhesin of *Staphylococcus aureus*, also binds to the tail region of type I cytokeratin 10. *J Biol Chem* 279:50691–50699 doi: 10.1074/jbc.M408713200.

317. Wang R., Braughton K. R., Kretschmer D., Bach T. H., Queck S. Y., Li M., Kennedy A. D., Dorward D. W., Klebanoff S. J., Peschel A., DeLeo F. R., Otto M. (2007). Identification of novel cytolytic peptides as key virulence determinants for community-associated MRSA. *Nat. Med.*, 13(12), 1510–1514. doi: 10.1038/nm1656

318. Wann E.R., Gurusiddappa S., Hook M. (2000). The fibronectin-binding MSCRAMM FnbpA of *Staphylococcus aureus* is a bifunctional protein that also binds to fibrinogen. *J. Biol. Chem*., 275(18), 13863–13871. doi: 10.1074/jbc.275.18.13863.

319. Weidenmaier C., Goerke C., Wolz C. (2012) *Staphylococcus aureus* determinants for nasal colonization. *Trends. Microbiol*. 20(5):243-50. doi: 10.1016/j.tim.2012.03.004

320. Wertheim H.F., Walsh E., Choudhurry R., Melles D.C., Boelens H.A., Miajlovic H., Verbrugh H.A., Foster T., van Belkum A. (2008). Key role for clumping factor B in *Staphylococcus aureus* nasal colonization of humans. *PLoS Med* 5:e17 doi: 10.1371/journal.pmed.0050017.

321. White A. (1963) Increased Infection rates in heavy nasal carriers of coagulase positive Staphylococci. *Antimicrob. Agents. Chemother.* 161, 667–70.

322. Whittaker C.A. & Hynes R.O. (2002). Distribution and evolution of von Willebrand/integrin A domains: widely dispersed domains with roles in cell adhesion and elsewhere. *Mol. Biol. Cell.*, 13(10), 3369–3387. doi: 10.1091/mbc.e02-05-0259.

323. Wijeratne S.S., Botello E., Yeh H.C., Zhou Z., Bergeron A.L., Frey E.W., Patel J.M., Nolasco L., Turner N.A., Moake J.L., Dong J.F., Kiang C.H. (2013). Mechanical activation of a multimeric adhesive protein through domain conformational change. *Phys Rev Lett*., 110(10), 108102. doi: 10.1103/PhysRevLett.110.108102.

324. Wilke G. A. & Bubeck Wardenburg J. (2010). Role of a disintegrin and metalloprotease 10 in *Staphylococcus aureus* alpha-hemolysin-mediated cellular injury. *Proc. Natl. Acad. Sci. U. S. A.*, 107(30), 13473–13478. doi: /10.1073/pnas.1001815107

325. Wilkinson B.J. & Holmes K.M. (1979). *Staphylococcus aureus* cell surface: capsule as a barrier to bacteriophage adsorption. *Infect Immun.*, 23:549-552.

326. Williams R. E. (1963) Healthy carriage of *Staphylococcus aureus*: its prevalence and importance. *Bacteriol. Rev.* 27, 56–71.

327. Williams S.B., McKeown L.P., Krutzsch H., Hansmann K., Gralnick, H.R. (1994). Purification and characterization of human platelet von Willebrand factor. *Br J Haematol,* 88, 582-91.

328. Xiang H., Feng Y., Wang J., Liu B., Chen Y., Liu L., Deng X., Yang M. (2012). Crystal structures reveal the multi-ligand binding mechanism of *Staphylococcus aureus* ClfB. *PLoS Pathog.*, 8(6), e1002751. doi: 10.1371/journal.ppat.1002751

329. Yago T., Lou J., Wu T., Yang J., Miner J.J., Coburn L., López J.A., Cruz M.A., Dong J.F., McIntire L.V., McEver R.P., Zhu C. (2008) Platelet glycoprotein Ibalpha forms catch bonds with human WT vWF but not with type 2B von Willebrand disease vWF. *J Clin Invest.,* 118(9):3195-3207. doi:10.1172/JCI35754.

330. Yang Y.H., Jiang Y.L., Zhang J., Wang L., Bai X.H., Zhang S.J., Ren Y.M., Li N., Zhang Y.H., Zhang Z., Gong Q., Mei Y., Xue T., Zhang J.R., Chen Y., Zhou C.Z. (2014). Structural insights into SraP-mediated *Staphylococcus aureus* adhesion to host cells. *PLoS Pathog*, 10:e1004169. doi: 10.1371/journal.ppat.1004169.

331. Yarwood J.M., McCormick J.K., Schlievert P.M. (2001) Identification of a novel two-component regulatory system that acts in global regulation of virulence factors of *Staphylococcus aureus*. *J. Bacteriol*. 183 (4):1113–1123.

332. Zapotoczna M., Jevnikar Z., Miajlovic H., Kos J., Foster T. J. (2013). Iron-regulated surface determinant B (IsdB) promotes *Staphylococcus aureus* adherence to and internalization by non-phagocytic human cells. *Cell. Microbiol*., 15(6), 1026–1041. doi: 10.1111/cmi.12097

333. Zhang X.H., Halvorsen K., Zhang C.Z., Wong W.P., Springer T.A. (2009) Mechanoenzymatic Cleavage of the Ultralarge Vascular Protein von Willebrand Factor. *Science,* 324, 1330-1334.

334. Zheng X., Chung D., Takayama T. K., Majerus E. M., Sadler J. E., Fujikawa, K. (2001). Structure of von Willebrand factor-cleaving protease (ADAMTS13), a metalloprotease involved in thrombotic thrombocytopenic purpura. *J Biol Chem*., 276(44), 41059–41063. doi: 10.1074/jbc.C100515200.

335. Zhou Y. F., Eng E. T., Nishida N., Lu C., Walz T., Springer T.A. (2011). A pH-regulated dimeric bouquet in the structure of von Willebrand factor. *EMBO J*., 30(19), 4098–4111. doi: 10.1038/emboj.2011.297.

336. Zhou Y.F. & Springer T.A. (2014). Highly reinforced structure of a C-terminal dimerization domain in von Willebrand factor. *Blood,* 123, 1785-1793.

337. Zhou Y.F., Eng E.T., Zhu J., Lu C., Walz T., Springer T.A. (2012). Sequence and structure relationships within von Willebrand factor. *Blood*, 120(2), 449–458. doi: 10.1182/blood-2012-01-405134.

338. Zong Y., Xu Y., Liang X., Keene D.R., Höök A., Gurusiddappa S., Höök M., Narayana S.V. (2005). A 'Collagen Hug' model for *Staphylococcus aureus* CNA binding to collagen. *EMBO J.*, 24(24), 4224–4236. doi: 10.1038/sj.emboj.7600888.

PUBLICATIONS

The experimental evidence presented in this thesis resulted in a manuscript which is scheduled to be published in Scientific Reports on the 23rd of November 2021 at 10 am UK time and henceforth available online at www.nature.com/articles/s41598-021-02065-w. The authors and title of the manuscript are given below:
«Alfeo MJ, Pagotto A, Barbieri G, Foster TJ, Vanhoorelbeke K, De Filippis V, Speziale P, Pietrocola G. *Staphylococcus aureus* iron-regulated surface determinant B (IsdB) protein interacts with von Willebrand factor and promotes adherence to endothelial cells. »

The publications listed below were produced throughout the PhD course and are presented in their published form on the following pages:

- Pietrocola G, Pellegrini A, Alfeo MJ, Marchese L, Foster TJ, Speziale P. The iron-regulated surface determinant B (IsdB) protein from *Staphylococcus aureus* acts as a receptor for the host protein vitronectin. *J Biol Chem*. 2020; 295(29):10008-10022. doi:10.1074/jbc.RA120.013510.
- Mathelié-Guinlet M, Viela F, Alfeo MJ, Pietrocola G, Speziale P, Dufrêne YF. Single-Molecule Analysis Demonstrates Stress-Enhanced Binding between *Staphylococcus aureus* Surface Protein IsdB and Host Cell Integrins. *Nano Lett*. 2020; 20(12):8919-8925. doi:10.1021/acs.nanolett.0c04015.The
- Pietrocola G, Nobile G, Alfeo MJ, Foster TJ, Geoghegan JA, De Filippis V, Speziale P. Fibronectin-binding protein B (FnBPB) from *Staphylococcus aureus* protects against the antimicrobial activity of histones. *J Biol Chem*. 2019; 294(10):3588-3602. doi:10.1074/jbc.RA118.005707.

The iron-regulated surface determinant B (IsdB) protein from *Staphylococcus aureus* acts as a receptor for the host protein vitronectin

Received for publication, March 18, 2020, and in revised form, June 1, 2020 Published, Papers in Press, June 4, 2020, DOI 10.1074/jbc.RA120.013510

Giampiero Pietrocola[1,*], Angelica Pellegrini[1], Mariangela J. Alfeo[1], Loredana Marchese[1], Timothy J. Foster[2], and Pietro Speziale[1,*]

From the [1]Department of Molecular Medicine, Unit of Biochemistry, University of Pavia, Pavia, Italy, [2]Department of Microbiology, Trinity College Dublin, Dublin, Ireland

Edited by Chris Whitfield

Staphylococcus aureus **is an important bacterial pathogen that can cause a wide spectrum of diseases in humans and other animals.** ***S. aureus*** **expresses a variety of virulence factors that promote infection with this pathogen. These include cell-surface proteins that mediate adherence of the bacterial cells to host extracellular matrix components, such as fibronectin and fibrinogen. Here, using immunoblotting, ELISA, and surface plasmon resonance analysis, we report that the iron-regulated surface determinant B (IsdB) protein, besides being involved in heme transport, plays a novel role as a receptor for the plasma and extracellular matrix protein vitronectin (Vn). Vn-binding activity was expressed by staphylococcal strains grown under iron starvation conditions when Isd proteins are expressed. Recombinant IsdB bound Vn dose dependently and specifically. Both near-iron transporter motifs $NEAT_1$ and $NEAT_2$ of IsdB individually bound Vn in a saturable manner, with K_D values in the range of 16–18 nM. Binding of Vn to IsdB was specifically blocked by heparin and reduced at high ionic strength. Furthermore, IsdB-expressing bacterial cells bound significantly higher amounts of Vn from human plasma than did an** ***isdB*** **mutant. Adherence to and invasion of epithelial and endothelial cells by IsdB-expressing** ***S. aureus*** **cells was promoted by Vn, and an $\alpha_v\beta_3$ integrin-blocking mAb or cilengitide inhibited adherence and invasion by staphylococci, suggesting that Vn acts as a bridge between IsdB and host $\alpha_v\beta_3$ integrin.**

Staphylococcus aureus causes a wide range of opportunistic infections that range from superficial skin infections to life-threatening diseases, including endocarditis, pneumonia, and septicemia (1). Adherence of bacteria to host matrix components is the initial critical event in the pathogenesis of most infections. The extracellular matrix (ECM) essentially consists of macromolecules, such as collagens, proteoglycans, and glycoproteins, that serve as a substrate for the adhesion and migration of tissue cells. These processes involve integrins, a family of heterodimeric cell surface receptors that recognize specific ECM proteins (2, 3).

Bacteria, including *S. aureus*, also utilize the ECM as substrata for their adhesion through a family of cell wall-anchored (CWA) adhesins called MSCRAMMs (microbial surface component recognizing adhesive matrix molecules) that specifically recognize host matrix components (4, 5).

Vitronectin (Vn) is a glycoprotein that is synthesized in the liver and secreted into plasma (6) and is also an important component of the ECM (7). Vn is found at a high concentration in plasma (200–700 μg/ml) (8, 9) and is also present in different human tissues (10). The N-terminal portion of mature Vn (43 aa residues) consists of a somatomedin B (SMB) domain followed by the classical integrin-binding motif, Arg-Gly-Asp (RGD). Members of the integrin family that engage in Vn binding include integrin $\alpha3\beta1$, $\alpha_v\beta_3$, $\alpha_v\beta_5$, and $\alpha_5\beta_1$ (11). The next domain comprises four hemopexin-like domains with putative heme-binding motifs. In addition, Vn has three heparin-binding domains (HBD) spanning residues Vn82–137 (HBD-1), Vn175–219 (HBD-2), and Vn348–361 (HBD-3) (12–14) (Fig. S1*A*). Vn is present in the organism in different conformational states: as the native, folded monomer (65–75 kDa, the 65-kDa form being derived from the proteolytic cleavage in the C-terminal region of the protein) in plasma/serum and as a multimeric unfolded form in the ECM (6, 15, 16). Conformational change from the monomeric to the activated, multimeric state is promoted by exposure of Vn to agents, such as urea, or binding to physiological ligands, such as the thrombin-antithrombin complex and the membrane attack complex. Vn conformational activation reveals a number of cryptic sites, including the full exposure of the heparin-binding site at the C-terminal domain of the protein (17, 18) and cell-binding motif (RGD) (19, 20). Vn binds the terminal complement C5b-7 complex. It occupies the metastable membrane binding site and thereby inhibits membrane insertion of the complex (21). It also binds C9 and directly inhibits C9 polymerization (21, 22).

Several bacterial species interact with host cell-bound multimeric Vn, facilitating adherence to epithelial cells and artificial surfaces (23). Simultaneous interaction of Vn with an integrin and bacterial surface proteins results in the formation of a bridge between bacteria and host cells. This leads to internalization of bacteria, as exemplified by *Streptococcus pneumoniae* (24) or *Pseudomonas aeruginosa* (25), resulting in downstream signaling events (24).

Staphylococci contain several Vn-binding proteins, including the autolysins AtlE and Aae from *S. epidermidis* and the homologous proteins AtlA and Aaa from *S. aureus* (26, 27). Also,

This article contains supporting information.

* For correspondence: Giampiero Pietrocola, giampiero.pietrocola@unipv.it; Pietro Speziale, pspeziale@unipv.it.

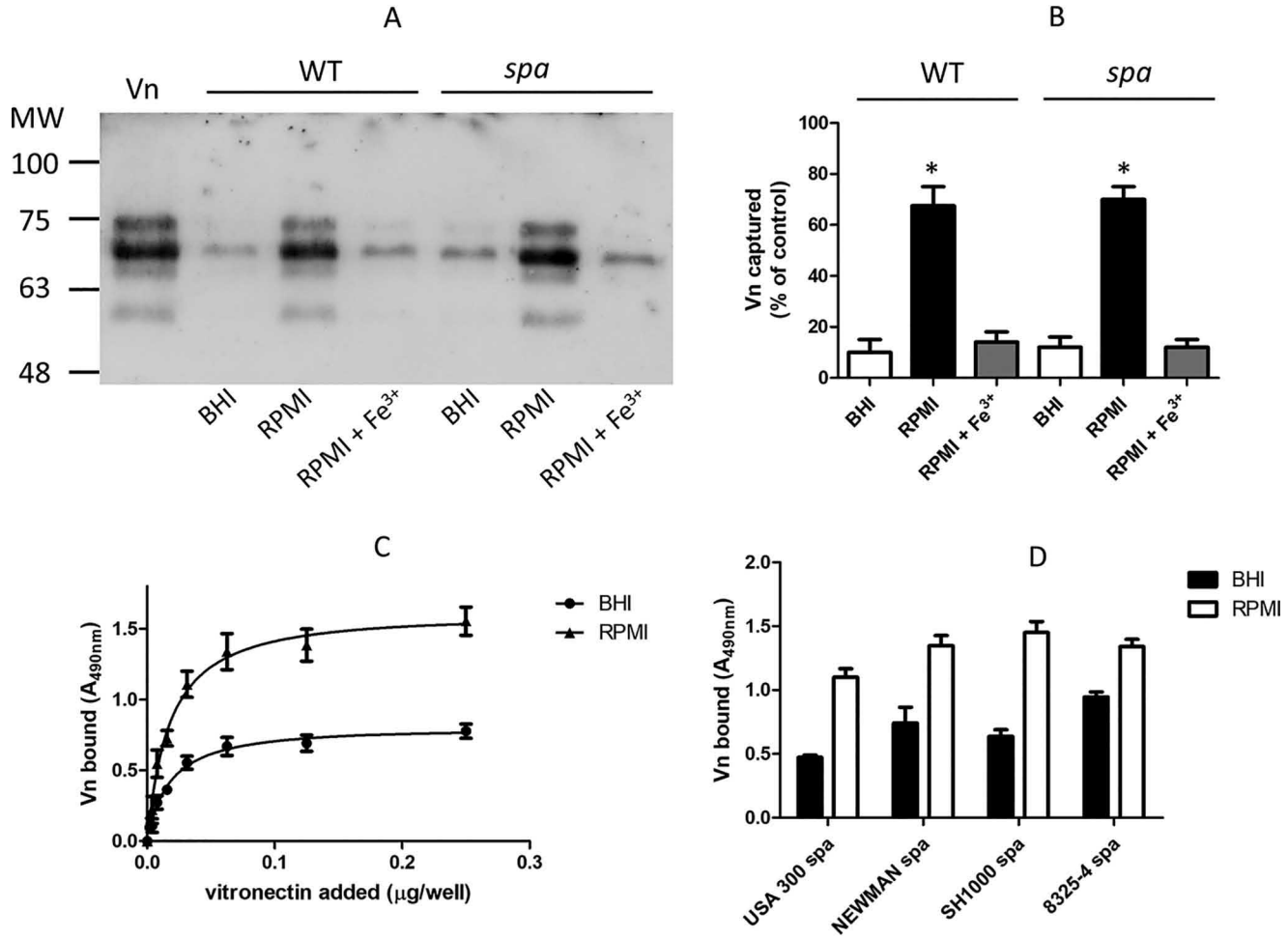

Figure 1. Binding of purified Vn by *S. aureus* cells. *A*, *S. aureus* strain SH1000 and its *spa* mutant grown either in BHI or RPMI medium in the absence/presence of 1 mM $FeCl_3$ were incubated with purified Vn. Bacterium-bound proteins were released by extraction buffer and separated by SDS-PAGE under reducing conditions and analyzed by far Western blotting. The membrane was probed with sheep anti-human Vn, followed by HRP-conjugated rabbit anti-sheep IgG. Molecular masses of standard proteins are indicated on the left. *B*, densitometric analysis of Vn bound to *S. aureus* SH1000 and the *spa* mutant as reported in *panel A*. The band intensity was quantified relative to a sample of purified human Vn (8 μg). The reported data are the mean values ± S.D. from three independent experiments. *C*, binding of increasing concentrations of Vn to immobilized *S. aureus* SH1000 *spa* cells grown in RPMI or BHI medium is shown. Bound Vn was detected as described above. The data points are the means ± S.D. from three independent experiments, each performed in triplicate. A statistically significant difference is indicated (Student's *t* test; *, $p < 0.05$). *D*, binding of Vn to strains of *S. aureus spa.* Microtiter wells coated with *S. aureus spa* strains grown in RPMI or BHI were incubated with Vn. Bound Vn was detected by addition of sheep anti-Vn polyclonal IgG and rabbit HRP-conjugated anti-sheep IgG.

the multifunctional autolysin AtlL from *Staphylococcus lugdunensis* interacts with Vn (28).

Atl autolysins have a similar modular organization (signal peptide, propeptide, amidase activity, three major repeats, R1 to R3, and glucosaminidase activity), share a high degree of sequence similarity, and are functionally interchangeable (29). R1-R2 repeats are critical for autolysin binding to Vn (30). Moreover, the major autolysin, Atl, mediates *S. aureus* internalization via direct interaction with host heat shock protein Hsc70 (31).

Studies on *S. aureus* adhesion to and invasion of host cells have been performed with bacteria grown in rich medium containing iron (4). In contrast, *in vivo S. aureus* has restricted access to iron, and the lack of available iron leads to the upregulation of a number of genes, among which are those that encode surface determinant (Isd) proteins (32). The Isd system contains nine proteins whose expression is coordinately upregulated under iron-depleted conditions (33–36). The primary role of Isd proteins is to capture heme from hemoglobin (Hb) and transport it into the cell (32). These include IsdA, IsdB, IsdC, and IsdH, which are anchored to cell wall peptidoglycan by sortases and are exposed on the cell surface (37, 38). Each protein contains a structurally conserved near iron transporter (NEAT) motif(s) that binds Hb and heme. IsdA and IsdC contain one NEAT domain each, whereas IsdB and IsdH contain two and three NEAT domains, respectively. The NEAT domains adopt a beta sandwich fold that consists of two five-stranded antiparallel beta sheets (39).

Fig. S1*B* shows the organization and primary sequence comparisons between the seven known NEAT domains in *S. aureus*.

Sequence homologs of this class of proteins are found in a number of important human pathogens, such as *S. lugdunensis*, (40–42), *Listeria monocytogenes* (43), *Bacillus anthracis* (44), and *Streptococcus pyogenes* (45).

IsdA, IsdB, and IsdH of *S. aureus* are known to have other biological functions. IsdA interacts with an array of host proteins (36) and confers resistance to the innate defenses of the human

skin (46). IsdH plays a role in the evasion of phagocytosis as a result of accelerated degradation of C3b (47). IsdB binds to platelets via direct interaction with the platelet integrin GPIIb/IIIa and also promotes *S. aureus* adherence to and internalization by nonphagocytic human cells (48). The objective of the current study was to investigate in more detail the binding of Vn to *S. aureus* cells. We show that cells expressing IsdB specifically bind to Vn and analyze the nature and the biological consequences of this interaction.

Results

Vn binding by S. aureus is promoted by growth under iron-restricted conditions

In preliminary experiments, we tested the capture of Vn by *S. aureus* strain SH1000 grown to stationary phase in rich brain heart infusion (BHI) or iron-restricted Roswell Park Memorial Institute 1640 (RPMI) medium with or without $FeCl_3$. Bacteria grown in RPMI showed a higher ability to capture Vn than those grown in iron-rich medium or in RPMI supplemented with $FeCl_3$, suggesting that binding of strain SH1000 depends on proteins induced by iron starvation. Interestingly, a protein A-deficient (*spa*) mutant showed a Vn-binding profile overlapping that of the WT strain, suggesting that Vn binding to the bacterial surface is not related to protein A expression (Fig. 1, *A* and *B*).

To further analyze the interaction of Vn with *S. aureus*, SH1000 *spa* organisms grown in BHI and RPMI medium were immobilized onto microtiter wells and allowed to interact with increasing amounts of soluble Vn (Fig. 1*C*). Under both conditions, Vn bound to bacteria in a dose-dependent and saturable fashion. RPMI-grown bacteria captured significantly larger amounts of Vn, suggesting that *S. aureus* cells express a larger number of receptors on their surface or that novel receptors were induced when grown in iron starvation. To compare the Vn binding potential of different *S. aureus* strains, *spa* mutants of the *S. aureus* laboratory strains Newman, SH1000, and 8325-4 and the clinical strain USA300 grown in BHI or RPMI medium to the stationary phase were immobilized in microtiter wells and tested for binding to soluble Vn. All the strains grown in RPMI medium showed a higher ability to bind Vn when grown under iron starvation conditions than in iron-rich medium (Fig. 1*D*).

Identification of a Vn-binding protein

To identify the surface component(s) involved in Vn binding, SH1000 *spa* cells grown in BHI or RPMI medium were digested with lysostaphin and the released material subjected to SDS-PAGE under reducing conditions and far Western blotting. The nitrocellulose membrane was incubated with Vn, and the bound ligand was detected with anti-Vn IgG. A strong signal corresponding to a molecule of 75 kDa was noted in protein from cells grown in RPMI medium, whereas no significant signal was detected in material released from cells grown in BHI medium (Fig. 2, *lanes 1 and 2*).

To further investigate this issue, proteins were separated by SDS-PAGE under reducing conditions and visualized by staining with Coomassie brilliant blue (Fig. 2, *lane 3*). A candidate protein of 75 kDa was excised from the stained gel, digested with trypsin, and analyzed by MS. The database search unequivocally identified IsdB as the potential Vn-binding protein of *S. aureus* SH1000 (Fig. S2*A*).

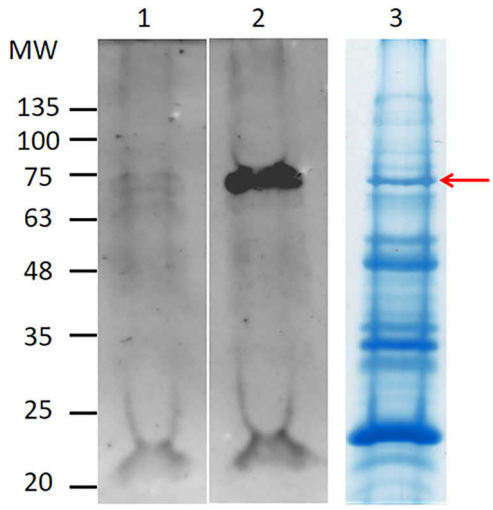

Figure 2. Far Western blotting of lysostaphin-released material from cells of SH1000 *spa*. Cells of SH1000 *spa* grown in BHI (*lane 1*) and RPMI (*lane 2*) were digested with lysostaphin and the released material subjected to far Western blotting. The nitrocellulose membrane was probed with Vn, followed by sheep anti-Vn and HRP-conjugated rabbit anti-sheep IgG. Molecular mass standards are indicated on the *left*. The lysostaphin-released material from cells of SH1000 *spa* grown in RPMI was also subjected to SDS-PAGE and stained with Coomassie blue (*lane 3*). The band corresponding to the 75-kDa bacterial component is marked by an *arrow*.

isdB gene expression is growth-phase dependent

Since *S. aureus* SH1000 *spa* cells grown to stationary phase in BHI medium bound Vn significantly less than when grown in RPMI medium (Fig. 1), we analyzed the expression of the *isdB* gene in cells grown both in BHI or RPMI medium to mid-exponential and stationary phases of growth by quantitative RT-PCR (qRT-PCR). Expression of *isdB* in cells grown to stationary phase in RPMI medium was about 5-fold higher than that in cells grown in BHI medium or cells grown to mid-exponential phase in either medium (Fig. S2*B*).

This finding was validated by comparing the expression levels of the IsdB protein by bacteria grown to mid-exponential and stationary phases in BHI and RPMI media by Western immunoblotting. While IsdB was virtually undetectable in material released from bacteria grown to both the mid-exponential and stationary phases in BHI medium, the protein was abundant in material released from bacteria grown to the stationary phase in RPMI medium (Fig. S2*C*).

Ectopic expression of IsdB by L. lactis and binding to Vn

To study IsdB in isolation from other *S. aureus* CWA proteins, a strain of *L. lactis* expressing IsdB from a gene cloned into the plasmid vector pNZ8037 was used. To validate the expression of IsdB from the bacterium, *L. lactis* pNZ8037::*isdB*

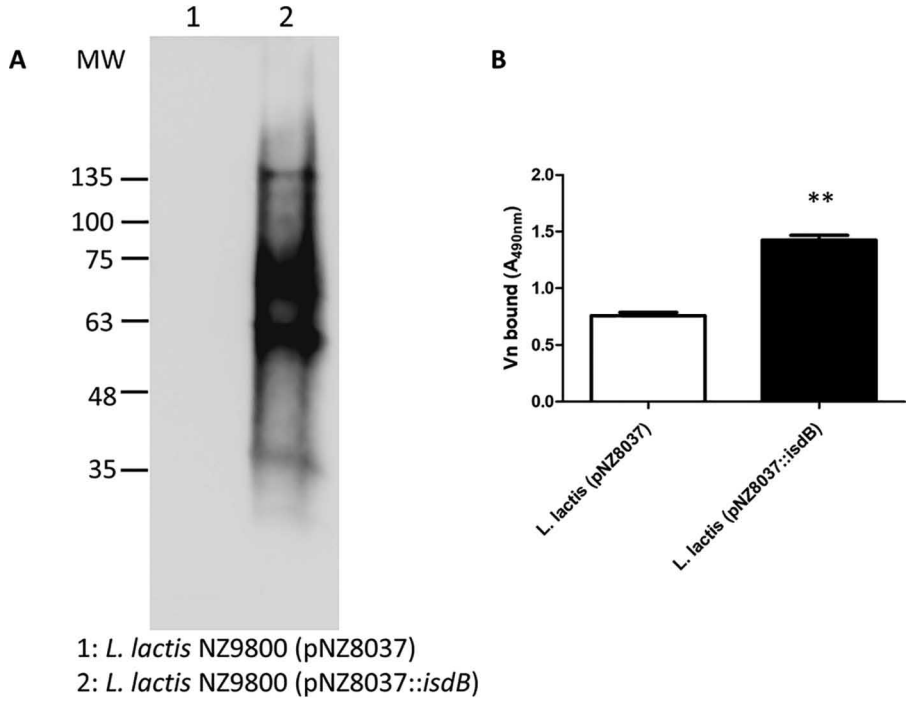

Figure 3. Interaction of *L. lactis*-expressing IsdB with Vn. *A*, cell wall proteins were released by mutanolysin/lysozyme treatment from *L. lactis* expressing IsdB (pNZ8037::*isdB*) and control cells carrying the empty vector. The protein components in the mixture were separated by SDS-PAGE and subjected to far Western blotting. The membrane was probed with Vn, followed by sheep anti-Vn and HRP-conjugated rabbit anti-sheep IgG. The figure is representative of three independent experiments. Molecular mass standards are indicated on the *left*. *B*, interaction of Vn with *L. lactis*-expressing IsdB and cells carrying the empty vector assessed by ELISA. Bacteria were immobilized in microtiter plates and incubated with Vn, followed by addition to the wells of sheep anti-Vn polyclonal IgG and HRP-conjugated rabbit anti-sheep antibody. The data points are the means ± S.D. from three independent experiments, each performed in triplicate. Statistically significant differences are indicated (Student's *t* test; **, $p < 0.01$).

and the isogenic strain carrying the empty vector were treated with mutanolysin and lysozyme, and the released material subjected to far Western blotting. A Vn binding protein of 75 kDa was detected (along with an approximately 60-kDa protein, which may be a breakdown product), whereas the material released from *L. lactis* (pNZ8037) lacked reactivity (Fig. 3*A*). Moreover, the lactococci were immobilized onto microtiter wells, and binding of soluble Vn was examined by ELISA. Significantly higher binding of Vn to *L. lactis* (pNZ8037::*isdB*) was observed compared to that of *L. lactis* harboring the empty vector (Fig. 3*B*).

Specificity of Vn binding to IsdB

To investigate the specificity of Vn binding to IsdB, recombinant IsdB $NEAT_1$-$NEAT_2$ protein was immobilized onto microtiter wells and tested for binding to extracellular matrix proteins, including fibrinogen, fibronectin, collagen, and Vn. Only Vn bound to the surface-coated IsdB, whereas no binding of the other proteins was observed (Fig. 4*A*).

Localization of the binding sites within IsdB

To localize the Vn-binding region within the IsdB protein, the $NEAT_1$ and $NEAT_2$ domains were expressed in *E. coli* and employed in binding studies. First, the binding of soluble Vn to immobilized recombinant $NEAT_1$ and $NEAT_2$ was determined by ELISA. Vn bound dose dependently and saturably to both $NEAT_1$ and $NEAT_2$ fragments and with a binding profile

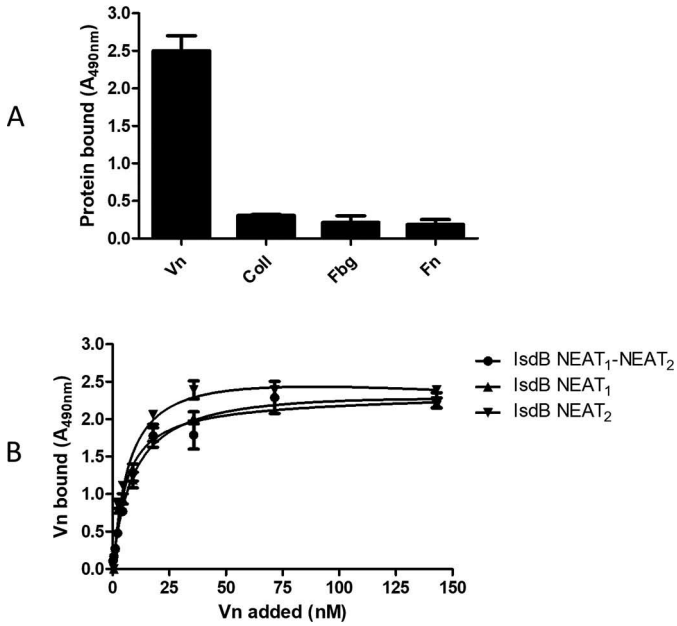

Figure 4. Characterization of Vn-binding activity of IsdB. *A*, specificity of recombinant IsdB interaction with extracellular matrix proteins. Microtiter wells were coated with IsdB NEAT1-NEAT2 and then incubated with the indicated extracellular matrix proteins Vn, collagen type I, fibrinogen, and fibronectin. Each bound protein was detected by the addition of ligand-specific polyclonal antibody and HRP-conjugated secondary IgG. The data points are the means ± S.D. from three independent experiments, each performed in triplicate. *B*, Vn binding to IsdB $NEAT_1$-$NEAT_2$ and its derivatives, $NEAT_1$ and $NEAT_2$. Recombinant IsdB $NEAT_1$-$NEAT_2$ and its derivatives, $NEAT_1$ and $NEAT_2$, were immobilized onto microtiter wells and incubated with increasing amounts of Vn. Bound Vn was detected by the addition of sheep anti-Vn polyclonal IgG and HRP-conjugated rabbit anti-sheep. The data points are the means ± S.D. from three independent experiments, each performed in triplicate.

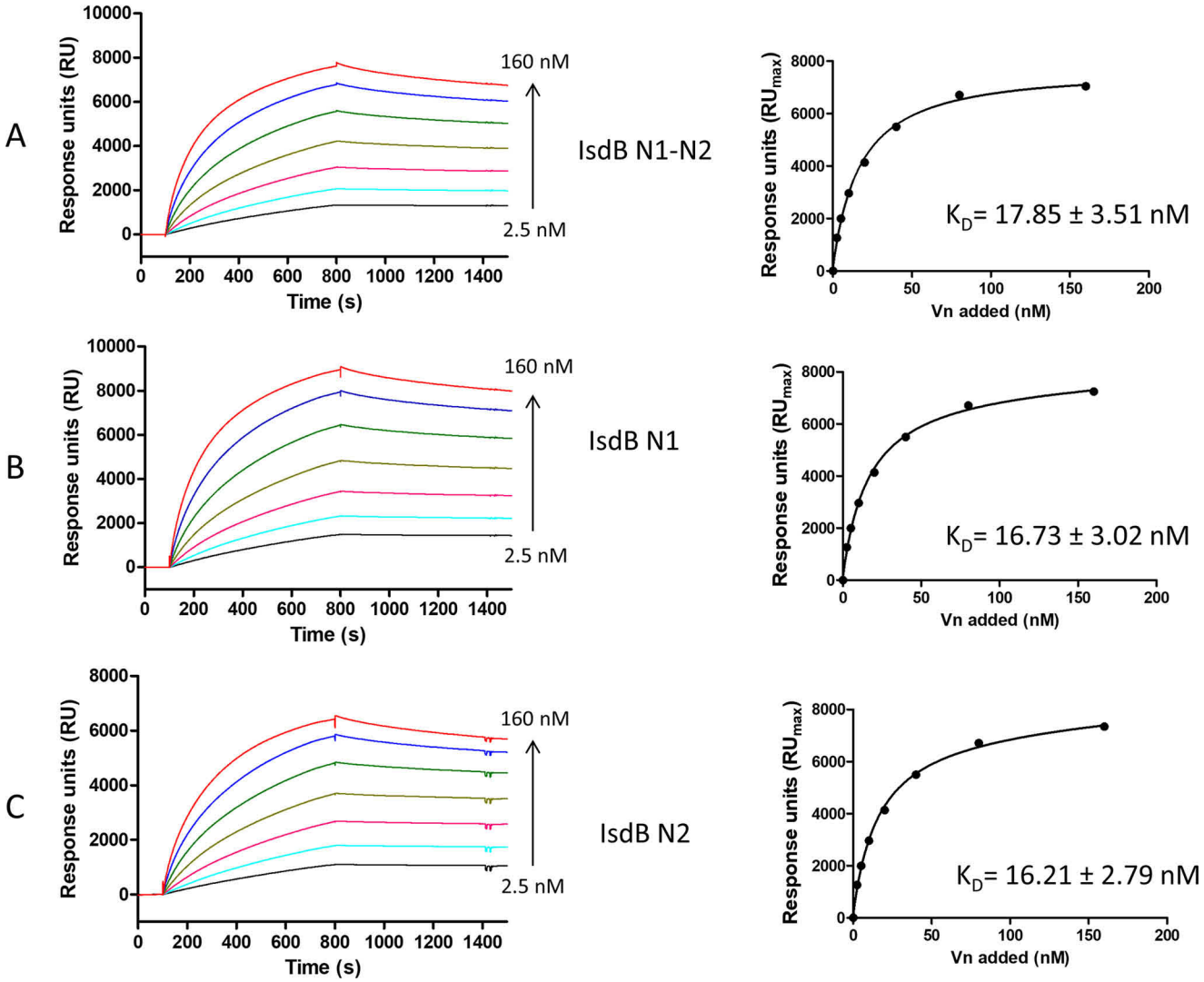

Figure 5. Analysis of the interaction between IsdB $NEAT_1$-$NEAT_2$ and its derivatives, $NEAT_1$ and $NEAT_2$, with Vn by SPR. Twofold linear dilution series (2.5–160 nM) of Vn were injected over the IsdB $NEAT_1$-$NEAT_2$ or its derivatives, $NEAT_1$ and $NEAT_2$, immobilized on the surface of a CM5 sensor chip. The sensorgrams obtained were normalized *versus* the response obtained when Vn was flowed over uncoated chips. The affinity was calculated from curve fitting to a plot of the response unit values at the steady state (RU_{max}) against increasing concentrations of Vn (*left*). Shown is one representative of three experiments.

resembling that exhibited by intact full-length IsdB $NEAT_1$-$NEAT_2$ (Fig. 4*B*).

IsdB $NEAT_1$-$NEAT_2$ and single $NEAT_1$ and $NEAT_2$ domains bind to Vn with high affinity

Surface plasmon resonance (SPR) experiments were performed to compare the binding of Vn to those of immobilized IsdB $NEAT_1$-$NEAT_2$ and single $NEAT_1$ and $NEAT_2$ fragments. Vn displayed a high binding activity, as indicated by the high response values and the slow dissociation of the IsdB-Vn complexes upon removal of the ligand. The best fit of the data points was obtained with the Langmuir isotherm equation describing a one-site binding model. From this analysis, we obtained dissociation constant (K_D) values of 17.85 ± 3.51 nM, 16.73 ± 3.02 nM, and 16.21 ± 2.79 nM for IsdB $NEAT_1$-$NEAT_2$/Vn, $NEAT_1$/Vn, and $NEAT_2$/Vn, respectively (Fig. 5). All these findings show that full-length IsdB contains two separate binding sites that interact with nearly identical high affinities for Vn.

Binding of Vn to IsdB is blocked by heparin and dependent on ionic strength

To investigate whether IsdB competes with glycosaminoglycans for binding to Vn, the effect of heparin, heparan sulfate, and chondroitin sulfate on Vn binding to immobilized IsdB $NEAT_1$-$NEAT_2$ was studied. In contrast to heparan sulfate and chondroitin sulfate, heparin dose dependently inhibited the IsdB-Vn interaction, suggesting that IsdB interacts with the heparin-binding domain(s) of the protein (Fig. S3*A*). To determine if ionic forces play a role in the interaction of IsdB with Vn, the effect of sodium chloride on Vn binding to IsdB was assessed. Addition of NaCl significantly reduced binding of Vn to immobilized IsdB, and at a concentration of 500 mM, NaCl reduced Vn binding to IsdB by almost 80% (Fig. S3*B*).

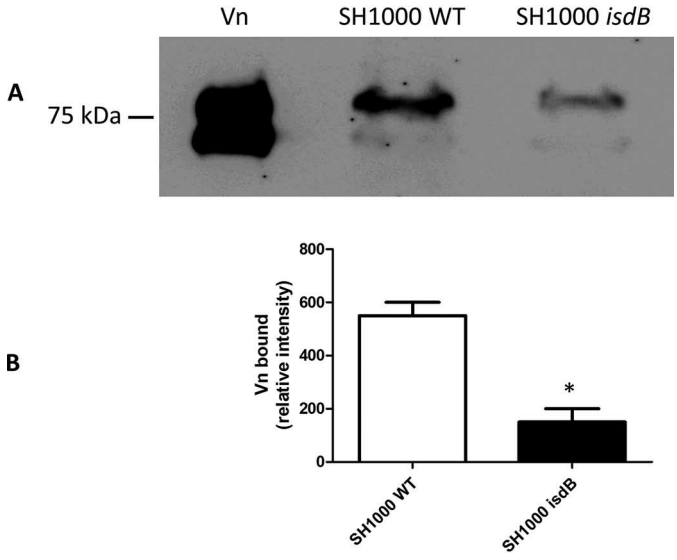

Figure 6. Capture of plasma vitronectin by *S. aureus* strain SH1000. *A*, *S. aureus* SH1000 and its isogenic *isdB* mutant were mixed with 1 ml of human plasma for 60 min. Proteins bound to the cell surface were released by extraction buffer, separated by SDS-PAGE under nonreducing conditions, and analyzed by Western blotting. The membrane was probed with sheep anti-Vn polyclonal IgG and HRP-conjugated rabbit anti-sheep and developed with the ECL Western blotting detection kit. The pure human Vn sample is shown on the *left*. *B*, densitometric analysis of Vn bound to and released from *S. aureus* SH1000 and its isogenic *isdB* mutant. The reported data are the mean values ± S.D. from three independent experiments. Statistically significant differences are indicated (Student's *t* test; *, $p < 0.05$).

S. aureus IsdB captures Vn from plasma

To investigate if *S. aureus* cells expressing IsdB can recruit Vn from plasma, bacteria were incubated with human plasma and the amount of Vn captured was quantified by Western blotting and densitometry. *S. aureus* expressing IsdB captured approximately 4-fold more Vn than the *isdB* mutant. Thus, it can be concluded that IsdB expression is important for *S. aureus* to capture Vn from human plasma. However, it must be pointed out that a substantial amount of Vn bound to the *isdB* mutant, indicating that other Vn receptors are operational on the surface of *S. aureus* cells (Fig. 6).

Vn mediates adherence to and invasion of HeLa and HUVEC monolayers

To investigate the role of the Vn-binding activity of IsdB in promoting adherence of *S. aureus* SH1000 to host cells, bacteria were grown to the stationary phase in BHI or RPMI medium and then tested for attachment to HeLa and human umbilical vein endothelial cell (HUVEC) monolayers (Fig. 7, *A* and *C*) in the absence of Vn. No adherence of the strain grown under either condition was observed. Conversely, the addition of exogenous human Vn to the cell monolayers promoted a high level of adhesion of the RPMI-grown but not the BHI-grown bacteria. Almost complete inhibition of adhesion was observed when the assays were performed in the presence of an integrin $\alpha_v\beta_3$ -binding mAb or the specific $\alpha_v\beta_3$ inhibitor cilengitide, suggesting the involvement of integrin $\alpha_v\beta_3$. To examine whether IsdB/Vn is also involved in the staphylococcal invasion of HeLa cells or HUVECs (Fig. 7, *B* and *D*), BHI- and RPMI-grown bacteria were incubated with cell monolayers in the presence or absence of Vn and then tested for internalization. We found a moderate level of invasion only by RPMI-grown bacteria in the presence of Vn, while no internalization was observed with BHI-grown bacteria even in the presence of Vn. In confirmation of this, neither adhesion nor invasion was observed with the *isdB* mutant (Fig. 7). Together, these data suggest that for promoting efficient adhesion and gaining entry of bacteria into HeLa cells or HUVECs, *S. aureus* can use Vn as a molecular bridge between surface-expressed IsdB and the $\alpha_v\beta_3$ integrin.

Staphylococcal adhesion to HeLa and HUVEC cell lines was similar, while bacterial invasion of HUVECs was 50-fold more effective than that of the HeLa cell line. Variation in expression levels of the $\alpha_v\beta_3$ integrin on the two cell types may contribute to the difference in pathogen invasiveness.

Notably, a persistent, low level of bacterial invasion was observed when bacteria grown in RPMI were incubated with HeLa and HUVECs in the absence of Vn, suggesting that other internalization mechanisms are operational.

Discussion

In our search for *S. aureus* MSCRAMMs with Vn-binding activity, here we show that *S. aureus* IsdB interacts with Vn. As previously demonstrated, IsdB is strongly upregulated under conditions of iron restriction and, in accordance with this property, Vn binding was strictly related to the expression of IsdB by bacterial strains. Bacteria bind Vn when grown under iron starvation conditions and not in an iron-rich medium. Moreover, binding of Vn by bacteria was mostly expressed by cells in the stationary phase of growth.

To characterize this binding to IsdB, we purified and used multimeric Vn, the conformational form of the protein found in the ECM. Notably, we found that bacteria expressing IsdB also captured Vn from plasma, where the monomeric form of the protein prevails. Thus, it seems that IsdB binds to both conformational states of Vn. This is reminiscent of the situation observed with *Moraxella catarrhalis* and *Haemophilus influenzae*, which interact with both isoforms of Vn (23).

The interaction of IsdB with Vn was confirmed using several approaches, including far Western blotting, ELISA, and SPR. Binding of IsdB to Vn was specific and saturable and exhibited a K_D in the nanomolar range, which is comparable to that recorded for high-affinity CWA protein–host protein interactions (49–52).

To narrow down the Vn binding site(s) of IsdB, the $NEAT_1$ and $NEAT_2$ domains were recombinantly produced and tested for their ability to bind the ligand. The individual modules interacted with an affinity for Vn comparable to that of the full-length IsdB, suggesting that each module represents the minimal motif required for efficient interaction of IsdB with Vn and that IsdB potentially can bind two Vn molecules. The finding that both domains interact with Vn is particularly intriguing, in view of the fact that the two NEAT domains of IsdB have very low sequence identity (about 12%) and that they are functionally different. In fact, the $NEAT_1$ domain is involved in Hb binding while $NEAT_2$ plays a role in heme extraction from α and β chains of Hb (53). In view of the discovery that even NEAT motifs with low sequence identity show Vn-binding

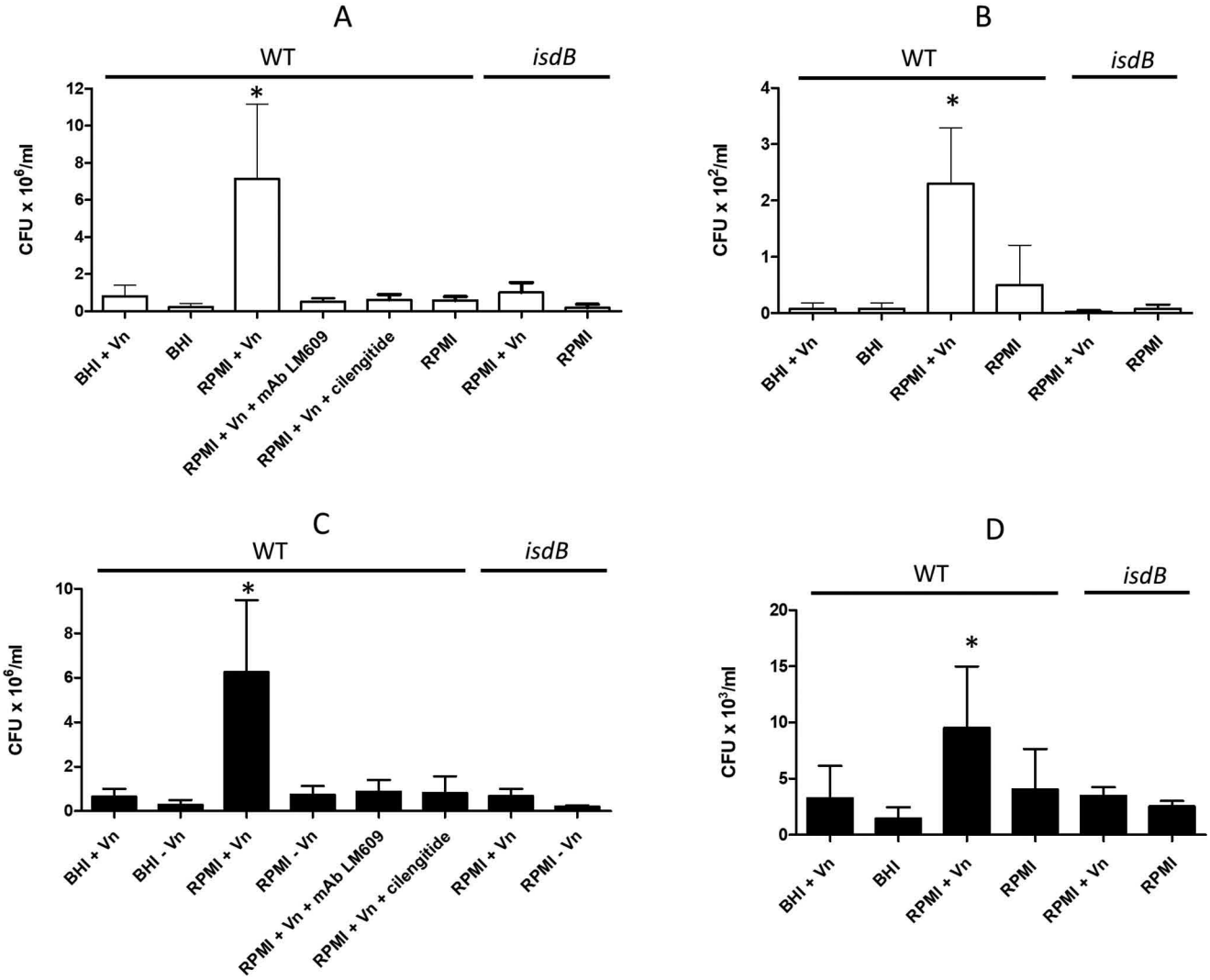

Figure 7. Adhesion and internalization of *S. aureus* cells. Bacterial strains were grown overnight in BHI or RPMI medium, added to HeLa (*A* and *B*) or HUVEC (*C* and *D*) cell monolayers, and tested for adhesion (*A* and *C*) or internalization (*B* and *D*). The experiments were performed in DMEM for 2 h at 37 °C. The effects of $\alpha_v\beta_3$ mAb LM609 and cilengitide on bacterial adherence are also reported. The inocula and adherent and internalized bacteria were quantified by viable counting. Error bars show S.D. of the means from three independent determinations performed in triplicate with similar results (Student's *t* test; *, $p < 0.05$).

activity, other Isd proteins could exhibit Vn-binding activity. The presence of additional Vn receptors on the staphylococcal surface is consistent with the finding that the *isdB* mutant is capable of capturing Vn from human plasma and by the observation that other non-Isd surface proteins of *S. aureus*, such as Atl, have Vn-binding activity (26, 27). In apparent contradiction with these observations, IsdB seems to be the major Vn receptor when material released from bacterial cells was tested by far Western blotting (Fig. 2). This could be due to a higher level of expression of IsdB and/or to a higher affinity of IsdB for Vn compared with that of other potential Vn binders.

In this context, it will be worth investigating the activity of IsdB from *Staphylococcus lugdunensis*, which contains $NEAT_1$ and $NEAT_2$, 60 and 56% identical to *S. aureus* IsdB $NEAT_1$ and $NEAT_2$ domains, respectively (40), and the Vn-binding by other bacterial species expressing Isd proteins, such as *Listeria monocytogenes* and *Bacillus anthracis*.

Increasing the ionic strength had a dramatic effect on Vn binding to IsdB, indicating that Vn/IsdB complex formation is mainly driven by electrostatic interactions. Furthermore, the negatively charged heparin efficiently blocked the IsdB–Vn interaction, suggesting that the IsdB-binding region is located in the heparin-binding domain(s) of Vn. The inhibitory effect of heparin but not of heparan sulfate or chondroitin sulfate is in line with heparin possessing the highest negative charge density of any known biological macromolecule. In fact, although heparin and heparan sulfate are built up of linear chains of repeating disaccharide units, the average heparin disaccharide contains approximately 2.7 sulfate groups, whereas heparan sulfate contains $\geq$1 sulfate group per disaccharide (54).

Related to the finding that electrostatic bonds could be involved in Vn–IsdB interaction is the question of whether Vn and heme compete for the same binding site or have a different location on IsdB. The indication that IsdB uses only a hydrophobic pocket in the $NEAT_2$ domain to bind and extract heme (38) and our observation that Vn binds to both $NEAT_1$ and $NEAT_2$ domains suggest that the binding sites in IsdB for heme and Vn are separate.

Binding of *S. aureus* to Vn contributes to bacterial adhesion to mammalian cells, as demonstrated by attachment of IsdB-expressing staphylococci to HeLa and HUVEC monolayers. The inhibition of the process by an $\alpha_v\beta_3$ mAb and cilengitide strongly suggests that adhesion involves the formation of a Vn bridged complex between IsdB and the integrin. Vn also mediated the internalization of staphylococci into epithelial and endothelial cells. However, due to the modest contribution of Vn to the process, it is possible that Vn-dependent invasion could act as a backup mechanism that becomes operational in the context of tissues where Fn is poorly expressed or under conditions (specific growth medium and/or phase of growth) where bacteria express reduced levels of Fn-binding proteins FnBPA and FnBPB (55, 56).

Binding to Fn by FnBPs allows the formation of a bridge between bacterial cells and the $\alpha_5\beta_1$ integrin on host cells, and this is sufficient to trigger the bacterial uptake. This mechanism is widely acknowledged to be the main internalization process (57). Additional secondary invasion mechanisms have been reported, including, among others, the internalization mediated by EAP (58), Atl (31), and Lpl (59) proteins. Of note, the invasion assays performed in these studies have been carried out with experimental approaches and conditions (different cell lines and strains, absence/presence of serum) that significantly differ from the invasion pathway described in the present investigation. Thus, for an accurate analysis of the contribution of each mechanism to this multifactorial event, individual internalization processes should be evaluated and compared under identical standardized conditions.

It is unclear why the *isdB* deletion mutant, although it can express several Vn receptors (Fig. 6), does not adhere to and invade host cells (Fig. 7). If we hypothesize that non-IsdB receptors bind to Vn in a way that differs from IsdB, we can speculate that these receptors play a role other than adhesin/invasin in bacterial pathogenesis. For example, capture of Vn mediated by receptors could inhibit both assembly and deposition of the terminal complement complex on the bacterial surface. Alternatively, due to the plasminogen (PLG) binding ability of Vn (60), receptor-bound Vn could enhance plasminogen activation to plasmin, thereby contributing to the degradation of fibrin clots and bacterial spreading into the tissues.

IsdB binds directly to β3-containing integrins and promotes platelet activation and invasion of mammalian cells (48, 61). Consistent with this, we found a low level of invasion of both cell lines by bacteria grown in RPMI in the absence of Vn, suggesting that under these conditions the process can be driven by IsdB binding directly to integrins (48). As with many other MSCRAMMs, IsdB is a multivalent virulence factor and contributes in various ways to the pathogenesis of *S. aureus*. Examples of MSCRAMMs that bind to two or more ligands are clumping factor A (ClfA) that, in addition to binding to fibrinogen (62, 63), binds to complement factor I (64, 65), and clumping factor B (ClfB), another CWA protein that interacts with fibrinogen (66, 67), keratin 10 (68, 69), and loricrin (70, 71). These CWA proteins share similar mechanisms of binding (5). In parallel with this, the structural basis of Hb binding to IsdB NEAT motifs has been elucidated (72, 73). From this perspective, X-ray crystal structure analysis of the recombinant IsdB-binding domain of Vn in complex with NEAT motifs could provide clues about the mechanism and function of this important CWA protein in bacterial colonization of and survival within the host. Purified IsdB elicits antibodies that block heme iron scavenging, provide partial protection against *S. aureus* bacteremia in animal models (74–76), and promote opsonophagocytosis of *S. aureus* (75, 77). Although vaccination of humans with IsdB resulted in failure (78, 79), in light of these new findings, the use of IsdB as a vaccine component warrants further investigation.

Experimental procedures

Bacterial strains and culture conditions

All strains used in this study are listed in Table 1. *S. aureus* cells (48, 80–84) were grown overnight in BHI (VWR International Srl, Milan Italy) or in RPMI 1640 (Sigma-Aldrich, MO, USA) medium at 37 °C with shaking. *L. lactis* cells carrying the expression vector alone (pNZ8037) (85) or harboring the *isdB* gene (pNZ8037::*isdB*) (48) were grown overnight in BHI medium supplemented with chloramphenicol (10 μg/ml) at 30 °C without shaking. Cultures of *L. lactis* were diluted 1:100 in the same medium and allowed to reach exponential phase. Nisin (6.4 ng/ml) was added, and cultures were allowed to grow overnight as described above. In experiments where a defined number of cells were used, bacteria were harvested from the cultures by centrifugation, washed, and suspended in PBS at an optical density at 600 nm (OD_{600}) of 1.0. *Escherichia coli* strain XL1-Blue (Agilent Technologies, CA, USA) transformed with vector pQE30 (Stratagene, La Jolla, CA) or derivatives were grown in Luria agar and Luria broth (VWR) containing 100 μg/ml ampicillin at 37 °C with shaking.

Construction of *S. aureus isdB* deletion mutant and *L. lactis* expressing IsdB

Construction of *Lactococcus lactis* expressing IsdB and construction of the *S. aureus isdB* deletion mutant were performed as reported in Table 1.

Plasmid and DNA manipulation

Plasmid DNA (Table 2) was isolated using the WizardPlus SV miniprep kit (Promega, WI, USA), according to the manufacturer's instructions, and transformed into *E. coli* XL1-Blue cells using standard procedures (86). Transformants were screened by restriction analysis and verified by DNA sequencing (Eurofins Genomics, Milan, Italy). Chromosomal DNA was extracted using the bacterial genomic DNA purification kit (Edge Biosystems, MD, USA). Cloning of IsdB $NEAT_1$-$NEAT_2$ (aa residues 48–480) was performed as reported by Miajlovic *et al.* (61). Cloning of IsdB $NEAT_1$ (aa residues 144–270) and IsdB $NEAT_2$ (aa residues 334–458) domains was performed following the NEBuilder® HiFi DNA assembly according to the manufacturer's instructions (New England Biolabs, MA, USA). The primers used to amplify IsdB $NEAT_1$ and IsdB $NEAT_2$ domains and the pQE30 vector (Table S1) were purchased from Integrated DNA Technologies (Leuven, Belgium). DNA

Table 1
Bacterial strains

Bacterial strain	Relevant properties[a]	Reference or source
S. aureus		
LAC *spa*	Strain derivative of LAC* deficient in protein A; constructed by transduction of *spa*::Kan^r by phage 85 into strain LAC*	80
Newman *spa*	Strain containing a null mutation in protein A obtained through transduction from *S. aureus* 8325-4 spa::Kan^r (81) by generalized phage transduction using phage 85	82
8325-4 *spa*	*spa* gene inactivated by substituting part of the *spa* coding sequence for a DNA fragment specifying resistance to ethidium bromide. *In vitro*-constructed *spa*::EtBrr substitution mutation was introduced into the *S. aureus* chromosome by recombinational allele replacement	81
SH1000	Laboratory strain. *rsbU* + derivative of *S. aureus* 8325-4 *rsbU* + derivative of *S. aureus* 8325-4	83
SH1000 *spa*	*spa*::Tc^r transduced from 8325-4 *spa*::Tc^r	84
SH1000 *isdB*	*isdB* gene deleted by allelic exchange	48
L. lactis		
NZ9800 (pNZ8037)	Expression vector with nisin-inducible promoter, Cm^r	85
NZ9800 (pNZ8037::*isdB*)	*isdB* gene cloned in pNZ8037, Cm^r	48
E. coli		
XL1-Blue	*E. coli* cloning host	Stratagene

[a] Cm^r, chloramphenicol resistance; Kan^r, kanamycin resistance; Tc^r, tetracycline resistance.

purification was carried out using the WizardSV gel and PCR clean-up system (Promega).

Expression and purification of recombinant proteins

Recombinant proteins IsdB $NEAT_1$-$NEAT_2$, IsdB-$NEAT_1$, and IsdB-$NEAT_2$ were expressed from pQE30 (Qiagen, Hilden, Germany) in *E. coli* XL1-Blue (Agilent Technologies, CA, USA). Overnight starter cultures were diluted 1:40 in Luria broth containing ampicillin (100 μg/ml) and incubated with shaking until the culture reached the exponential phase (optical density at 600 nm of 0.4–0.6). Recombinant protein expression was induced by the addition of 1 mM (final concentration) isopropyl 1-thio-β-D-galactopyranoside (IPTG) (Inalco, Milan, Italy) to the culture. After 4 h, bacterial cells were harvested by centrifugation and frozen at −80 °C. Cells were resuspended in lysis buffer (50 mM NaH_2PO_4, 300 mM NaCl, pH 8.0) containing 1 mM PMSF (Sigma-Aldrich) as the protease inhibitor and 20 μg/ml DNase (Sigma-Aldrich) and lysed by freezing with liquid nitrogen and subsequent defrosting with warm water. The lysis procedure was repeated twice. The cell debris was removed by centrifugation, and proteins were purified from the supernatants by Ni^{+2}-affinity chromatography on a HiTrap chelating column (GE Healthcare, Buckinghamshire, UK).

Protein purity was assessed by 15% SDS-PAGE and Coomassie brilliant blue staining (Fig. S4*A*). A bicinchoninic acid protein assay (Pierce, Rockford, IL, USA) was used to measure the concentration of purified proteins.

Reagents, proteins, and antibodies

BSA, hemoglobin, protease-free DNase I, skim milk, heparin, chondroitin sulfate, heparan sulfate, cilengitide, lysostaphin, trypsin, sheep anti-Vn polyclonal IgG, and HRP-conjugated rabbit anti-sheep IgG were purchased from Sigma-Aldrich. Human fibronectin (Fn) was purified from plasma by a combination of gelatin- and arginine-Sepharose affinity chromatography (87). The human Fn rabbit antibody was purchased from Pierce. Human fibrinogen (Fbg) was obtained from Calbiochem (Darmstadt, Germany). Collagen (Coll) type I was a generous gift of Professor R. Tenni (Department of Molecular Medicine, Pavia, Italy). Coll type I rabbit antibody was from Merck (Rome, Italy). $\alpha_v\beta_3$ integrin mAb LM609 was from Abcam (Cambridge, UK). Vn mAb 8E6 was purchased from Merck. IsdB and Fbg antibodies were raised in mice by a routine immunization procedure using purified IsdB $NEAT_1$-$NEAT_2$ and Fbg as the antigen, respectively. Rabbit anti-mouse HRP-conjugated secondary antibody was purchased from Dako Cytomation (Glostrup, Denmark).

Human plasma

Normal human plasma was prepared from freshly drawn blood obtained from healthy volunteers with informed consent and permission of the ethical board of the University of Pavia (permit no. 19092013). The study also abides by the Declaration of Helsinki principles. After centrifugation, the plasma fraction was frozen in aliquots and stored at −20 °C.

Isolation of Vn from human plasma

Human Vn was purified from human plasma on a heparin-Sepharose Hi-Trap^{TM} column (GE Healthcare) by following the protocol described by Akiyama (88). The method takes advantage of the observation that the monomeric plasma Vn must be activated or "opened" with 8 M urea before it can bind well to heparin. Thus, the plasma is first depleted of compounds such as fibronectin that bind specifically or nonspecifically to heparin-Sepharose and then treated with 8 M urea to activate the heparin-binding activity of Vn, which is subsequently bound to a heparin affinity column and eluted in a multimeric conformation.

The purity of the isolated Vn was checked with 12.5% (w/v) SDS-PAGE under reducing conditions and Coomassie brilliant blue staining (Fig. S4*B*, *lane 1*) and its concentration quantified with the BCA assay. The multimeric conformation of the isolated Vn was assessed by 12.5% PAGE performed in the absence of SDS (Fig. S4*B*, *lane 2*) and by determination of the reactivity with the mAb 8E6, which preferentially recognizes the multimeric, activated form of Vn (data not shown).

Vn binding to S. aureus

To test binding of Vn, microtiter wells were coated overnight at 37 °C with 100 μl/well of stationary-phase *S. aureus* cells

Table 2
Plasmids

Plasmid	Feature	Marker[a]	Source or reference
pQE30	*E. coli* vector for the expression of hexa-His-tagged recombinant proteins	Amp^r	Qiagen
pQE30::*isdB* $NEAT_1$-$NEAT_2$	pQE30 encoding residues 48–480 of IsdB $NEAT_1$-$NEAT_2$ protein	Amp^r	61
pQE30::rIsdB-NEAT1 (144–270)	pQE30 derivative encoding the NEAT1 domain of IsdB $NEAT_1$-$NEAT_2$ protein from *S. aureus* SH1000	Amp^r	This study
pQE30::rIsdB-NEAT2 (334–458)	pQE30 derivative encoding the NEAT2 domain of IsdB protein from *S. aureus* SH1000	Amp^r	This study

[a] Amp^r, ampicillin resistance.

(OD_{600} of 1) in PBS. The plates were washed with PBS. To block free protein binding sites, the wells were treated for 1 h at 22 °C with BSA (2%, v/v) in PBS. The plates were then incubated for 1 h with increasing concentrations of Vn (up to 250 ng/well). After several washings with PBS, 0.5 μg of anti-Vn sheep IgG in BSA (1%, v/v) was added to the wells and incubated for 90 min.

The plates were washed and then incubated for 1 h with rabbit HRP-conjugated anti-sheep IgG diluted 1:1000. After washing, *o*-phenylenediamine dihydrochloride was added, and the absorbance at 490 nm was determined using an ELISA plate reader (Bio-Rad, CA USA).

Release of cell wall-anchored proteins from S. aureus and detection of Vn-binding activity

Lysostaphin digestion—To release cell wall-anchored proteins from *S. aureus*, bacteria were grown at 37 °C to exponential phase (OD_{600} of 0.4–0.6) or stationary phase, either in RPMI or BHI medium. Cells were harvested by centrifugation at 7000 × *g* at 4 °C for 15 min, washed three times with PBS, and resuspended to an A_{600} of 2.0 in lysis buffer (50 mM Tris-HCl, 20 mM $MgCl_2$, pH 7.5) supplemented with 30% raffinose. Cell wall proteins were solubilized from *S. aureus* by incubation with lysostaphin (200 μg/ml) at 37 °C for 20 min in the presence of protease inhibitors (Complete Mini; Sigma-Aldrich). Protoplasts were recovered by centrifugation at 6000 × *g* for 20 min, and the supernatants were taken as the wall fraction. The supernatant was concentrated by treatment with 20% (v/v) TCA at 4 °C for 30 min. The precipitated proteins were washed twice with ice-cold acetone and dried overnight.

SDS-PAGE and far Western blotting—Proteins released by lysostaphin digestion were boiled for 10 min in sample buffer (0.125 M Tris-HCl, 4% [w/v] SDS, 20% [v/v] glycerol, 10% [v/v] β-mercaptoethanol, 0.002% [w/v] bromphenol blue) and separated by 12.5% (w/v) SDS-PAGE. The gels were stained with Coomassie brilliant blue (Bio-Rad). For Western blotting, proteins were subjected to SDS-PAGE and electroblotted onto a nitrocellulose membrane (GE Healthcare). After blocking with 5% (w/v) skim milk (Sigma-Aldrich) in PBS overnight at 4 °C, the membrane was probed with 2 μg/ml of Vn in PBS for 1 h at 22 °C followed by anti-Vn sheep IgG (1:10,000) and with rabbit HRP-conjugated anti-sheep IgG (1:100). Finally, blots were developed using the ECL Advance Western blotting detection kit (GE Healthcare), and images of the bands were captured by an ImageQuantTM LAS 4000 mini-biomolecular imager (GE Healthcare).

MS analysis

Proteins released by lysostaphin digestion of bacterial cells were separated by 12.5% SDS-PAGE and stained with GelCode blue stain reagent (Thermo Fisher Scientific, Waltham, MA, USA). The band marked by the *red arrow* (Fig. 2) was excised from the gel using a sterile scalpel and protein contained in the gel digested with sequencing grade trypsin (Sigma-Aldrich). Tryptic peptides were mixed with CHCA (alpha-cyano-4-hydroxycinnamic acid) and spotted onto the target plate. The spectra were acquired with a TOF/TOF 5800 system (AB SCIEX, Framingham, MT) using TOF/TOF Series Explorer acquisition software version 4.1.0. MS spectra were recorded in Reflecton positive mode (settings: fixed laser intensity, 3200 units; pulse rate, 400 Hz; total shots/spectrum, 1000; mass range (Da), 1000–4000 *m*/*z*). Calibration was performed using Peptide calibration Mix4 (LaserBio Laboratory, Sophia-Antipolis Cedex, France). MS-MS spectra of the most intensive MS signals were recorded in MS-MS positive mode (settings: fixed laser intensity, 3500 units; laser pulse rate, 1000 Hz; total shots/spectrum, 5000). MS-MS spectra were analyzed with ProteinPilot™ 5.0 software (AB SCIEX, Framingham, MT, USA) against the UniProtKB database updated 2 August 2016 using the following analysis parameters: (*a*) sample type, identification; (*b*) digestion, trypsin; (*c*) detected protein threshold [unused Protscore (Conf)], >0.05 (10%); (*d*) cysteine alkylation, iodoacetamide; (*e*) ID focus, biological modifications, amino acid substitutions; (*f*) FDR analysis, no; (*g*) taxonomy, no species.

Determination of isdB gene expression by qRT-PCR

Total RNA was extracted from *S. aureus* SH1000 *spa* cells during the exponential (OD_{600} of 0.4–0.6) and stationary phases of growth in BHI and RPMI media. Cells were harvested and total RNA was stabilized with RNeasy Protect bacterial reagent (Qiagen, Hilden, Germany) according to the manufacturer's instructions. Total RNA was extracted using the Quick-RNA fungal/bacterial miniprep kit (Zymo Research, CA, USA) by following the manufacturer's recommendations. DNA was removed by DNase I treatment by using the TURBO DNA-free kit (Invitrogen, CA, USA). The RNA concentration was >100 ng/μl, and the A_{260}/A_{280} ratio was >1.8. qRT-PCR was performed with an iTAq Universal SYBR Green one-step kit (Bio-Rad) using 4 ng of RNA in 20-μl volumes carried out on three replicates, and all reactions were performed in 20-μl volumes according to the manufacturer's protocol. The cDNA was analyzed using primers relative to the *isdB* coding sequence (Table S1). The conditions for thermal cycling were 50 °C for 10 min and 95 °C for 1 min, 35–40 cycles with 95 °C for 10 s, and then 60 °C for 10–30 s, followed by a slow increase of temperature by 0.5 °C per cycle to 95 °C, with a continuous measurement of the fluorescence. 4 ng of total RNA from each sample was used in a qRT-PCR experiment performed using a CFX Connect real-

time PCR detection system (Bio-Rad) and an iTAq Universal SYBR Green one-step kit (Bio-Rad). Expression of *isdB* was analyzed using primers isdBF (GCAGGCGTTTTGTCTTTACC) and isdBR (GCCTAGCAAACCAACACCAT). Target gene expression was normalized using the reference gene *rpoC*, which was amplified using primers SAurpoCF (CCGCACCATCTGGTAAGATTAT) and SAurpoCR (GCTGTATCGGCAAGACCTTTA). No-template and no-RT controls were run for each assay, and the specificity of each amplification product was verified using dissociation curve analysis. Standard curves were generated from serial dilutions of chromosomal DNA spanning at least six orders of magnitude. All reactions proceeded with 90% to 110% efficiency. Gene expression analysis was performed using the CFX Manager software (Bio-Rad). Three technical replicates were performed for each experiment.

Determination of expression level of IsdB by Western immunoblotting

Material released by lysostaphin digestion of SH1000 *spa* grown either in BHI and RPMI media to both mid-exponential and stationary phases was subjected to SDS-PAGE and electroblotted onto nitrocellulose membrane, as reported above. After blocking with skim milk, the membrane was sequentially incubated with mouse IsdB antibody (1:5000) and HRP-conjugated rabbit anti-mouse IgG (1:10,000) and developed as described above.

Detection of the Vn-binding activity of IsdB-expressing L. lactis

Release of cell wall-anchored proteins from L. lactis transformants by mutanolysin/lysozyme digestion and far Western blotting—L. lactis was grown to late-exponential phase in BHI broth, washed twice in PBS, and concentrated to an A_{600} of 40 in 1 ml 26% raffinose (Sigma-Aldrich) in 20 mM Tris-HCl, pH 8, 10 mM $MgCl_2$. Cell wall-associated proteins were released by incubation at 37 °C with occasional shaking with 500 U mutanolysin/ml and 200 μg lysozyme/ml in the presence of protease inhibitors (Complete Mini; Sigma-Aldrich). Protoplasts were removed by centrifugation at 6000 × *g* for 20 min, and the supernatant was concentrated as reported above. The interaction of Vn with IsdB was detected by SDS-PAGE followed by far Western blotting as reported above.

Vn binding to L. lactis by ELISA—To investigate the binding of Vn to *L. lactis*, microtiter wells were coated overnight at 37 °C with 100 μl/well of bacterial cell suspensions (OD_{600} of 1) in PBS. After treating with BSA, the plates were incubated with 10 μg/well Vn. Proteins bound to the bacterial cells were detected as described above.

Binding of Vn to IsdB by ELISA

The ability of immobilized recombinant IsdB proteins to bind to soluble Vn was determined using ELISA. Microtiter wells were coated overnight at 4 °C with 0.2 μg/well of the appropriate IsdB protein in 0.1 M sodium carbonate, pH 9.5. The plates were washed with 0.5% (v/v) Tween 20 in PBS (PBST) and then treated for 1 h at 22 °C with BSA (2%, v/v) in PBS. The plates were incubated for 1 h with increasing concentrations of soluble Vn in PBS. Bound Vn was detected by sheep anti-Vn IgG followed by rabbit HRP-conjugated anti-sheep IgG.

To determine the effect of ionic strength on the Vn-IsdB interaction, microtiter wells coated with 200 ng of IsdB $NEAT_1$-$NEAT_2$ were incubated with 500 ng/well of Vn in PBS containing increasing concentrations of NaCl. Complex formation was detected by incubation of the wells with antibodies as described above.

The effect of heparin, chondroitin sulfate, and heparan sulfate on the IsdB $NEAT_1$-$NEAT_2$–Vn interaction was examined by incubating IsdB $NEAT_1$-$NEAT_2$ immobilized onto microtiter plates (0.2 μg/well) with 0.5 μg/well of purified Vn in the presence of increasing concentrations of heparin, chondroitin sulfate, or heparan sulfate. Vn bound to IsdB $NEAT_1$-$NEAT_2$ was detected with antibodies as reported above.

SPR

To estimate the affinity of the interaction between Vn and IsdB $NEAT_1$-$NEAT_2$ or its domain $NEAT_1$ or $NEAT_2$, surface plasmon resonance (SPR) analyses were carried out using a multicycle injection strategy on a multiple flow cell Biacore X100 instrument (GE-Healthcare). IsdB $NEAT_1$-$NEAT_2$, $NEAT_1$, or $NEAT_2$ was covalently immobilized on a dextran matrix CM5 sensor chip surface in three different flow cells by using a protein solution (50 μg/ml in 50 mM sodium acetate buffer, pH 4.5) in a 1:1 dilution with *N*-hydroxysuccinimide and 1-ethyl-3-(3-dimethylaminopropyl) carbodiimide hydrochloride. The excess of the active groups on the dextran matrix was blocked using 1 M ethanolamine, pH 8.5. On the fourth flow cell, the dextran matrix was treated as described above but without any ligand to provide an uncoated reference flow cell. The running buffer used was PBS containing 0.005%, v/v, Tween 20. A 2-fold linear dilution series of Vn, in running buffer, was passed over the ligand at a flow rate of 30 μl/min, and all the sensorgrams were recorded at 22 °C. Assay channel data were subtracted from reference flow cell data. The response units at the steady state were plotted as a function of Vn concentration and fitted to the Langmuir equation to yield the K_D values.

Capture of Vn by S. aureus cells

Stationary *S. aureus* strain SH1000 or the *isdB* mutant (10^8 cells/ml) were mixed with 1 ml of fresh human plasma for 30 min. Bacteria were then harvested by centrifugation, washed with PBS, and treated with the extraction buffer (125 mM Tris-HCl, pH 7.0, containing 2% SDS) for 3 min at 95 °C and then centrifuged at 10,000 × *g* for 3 min. The supernatants were subjected to SDS-PAGE under reducing conditions, and the proteins were transferred to a nitrocellulose membrane. The membrane was sequentially probed for bound Vn with antibodies as described above. The band intensities were quantified with Quantity One software (Bio-Rad).

To analyze the capture of purified Vn by *S. aureus* SH1000 and its *spa* mutant, bacteria (1×10^8cells/ml) were grown either in BHI or RPMI medium in the absence/presence of 1 mM

$FeCl_3$ and then incubated with purified Vn for 60 min. Bacterium-bound proteins were released from the bacterial surface by extraction buffer and subjected to SDS-PAGE and far Western blotting as reported above.

Cell culture infection with staphylococci and blocking experiments

HeLa cells were cultured in 24-well plates until reaching confluence in DMEM supplemented with 10% FBS. HUVECs were cultured as previously reported (89).

24 h before adherence or invasion assays, the medium was removed from each culture and replaced with serum-free medium. Overnight cultures of *S. aureus* SH1000 WT or the *isdB* mutant grown either in BHI or RPMI medium were suspended in DMEM without antibiotics and FBS to 1×10^7cells/ml and added to the monolayers for 2 h at 37 ℃ in 5% CO_2. The effect of Vn on bacterial adhesion/invasion to monolayers was tested by pretreating the cells with 25 μg/ml of the protein 1 h prior to addition of the bacteria. To evaluate the role of $\alpha_v\beta_3$ integrin antibody and cilengitide on adhesion, monolayers were pretreated with Vn and then incubated with *S. aureus* SH1000 WT in the presence of 1 μg/ml of $\alpha_v\beta_3$ integrin LM609 mAb or 0.05 μM cilengitide. To determine bacterial adhesion, the infected cells were washed three times with Dulbecco's PBS, lysed, and plated on BHI agar for CFU counts. To enumerate internalized bacteria, the monolayers were further incubated for 2 h before cell lysis in medium supplemented with 100 μg/ml gentamicin to kill extracellular bacteria. Bacterial adherence and invasion are represented as recovered CFU/ml.

Statistical methods

Two group comparisons were performed by Student's *t test*. One-way analysis of variance, followed by Bonferroni's post hoc tests, was exploited for comparison of three or more groups. Analyses were performed using Prism 4.0 (GraphPad). Two-tailed *P* values of 0.05 were considered statistically significant.

Data availability

The MS proteomics data are available via ProteomeXchange with identifier PXD019371 (90). All other data supporting the findings of this study are available within the article and its supporting data.

Acknowledgments—We thank Giulia Barbieri, Department of Biology and Biotechnology, Pavia, Italy, for help with validation of *isdB* gene expression by qRT-PCR and cloning of recombinant fragments of IsdB. We thank PTS (Parco Tecnico Scientifico) of the University of Pavia and Polymerix srl, Pavia, Italy, for technical support with mass spectrometry.

Author contributions—G. P. conceptualization; G. P. resources; G. P., A. P., and M. J. A. data curation; G. P., A. P., and M. J. A. formal analysis; G. P., L. M., T. J. F., and P. S. supervision; G. P. funding acquisition; G. P., A. P., M. J. A., L. M., and P. S. validation; G. P., L. M., and P. S. visualization; G. P., A. P., M. J. A., L. M., and P. S. methodology; G. P., T. J. F., and P. S. writing-original draft; G. P. project administration; G. P., L. M., T. J. F., and P. S. writing-review and editing; A. P. and M. J. A. investigation; L. M. and P. S. software.

Funding and additional information—This research was funded by FFABR 2018, "Fondo di finanziamento per le attività base di ricerca," Ministero dell'Istruzione, dell'Università e della Ricerca (MIUR) to G. P.

Conflict of interest—The authors declare that they have no conflicts of interest with the contents of this article.

Abbreviations—The abbreviations used are: ECM, extracellular matrix; Aaa, autolysin/adhesin from S. aureus; Atl, autolysin; coll, collagen; EAP, extracellular adherence protein; Fn, fibronectin; Fbg, fibrinogen; Isd, iron-regulated surface determinant; Lpl, lipoprotein-like lipoprotein; NEAT, near iron transporter; MSCRAMM, microbial surface component recognizing adhesive matrix molecule; PLG, plasminogen; RU, response unit; SPR, surface plasmon resonance; Vn, vitronectin; OD, optical density; qRT-PCR, , quantitative RT-PCR; CWA, cell wall-anchored; BHI, brain heart infusion; RPMI, Roswell Park Memorial Institute; HUVEC, human umbilical vein endothelial cell.

References

1. Tong, S. Y., Davis, J. S., Eichenberger, E., Holland, T. L., and Fowler, V. G., Jr. (2015) *Staphylococcus aureus* infections: epidemiology, pathophysiology, clinical manifestations, and management. *Clin. Microbiol. Rev.* **28,** 603–661 CrossRef Medline
2. Hynes, R. O., and Naba, A. (2012) Overview of the matrisome—an inventory of extracellular matrix constituents and functions. *Cold Spring Harb. Perspect. Biol.* **4,** a004903 CrossRef Medline
3. Naba, A., Clauser, K. R., Ding, H., Whittaker, C. A., Carr, S. A., and Hynes, R. O. (2016) The extracellular matrix: tools and insights for the "omics" era. *Matrix Biol.* **49,** 10–24 CrossRef Medline
4. Foster, T. J., Geoghegan, J. A., Ganesh, V. K., and Höök, M. (2014) Adhesion, invasion and evasion: the many functions of the surface proteins of *Staphylococcus aureus*. *Nat. Rev. Microbiol.* **12,** 49–62 CrossRef Medline
5. Foster, T. J. (2019) The MSCRAMM family of cell-wall-anchored surface proteins of gram-positive cocci. *Trends Microbiol.* **27,** 927–941 CrossRef Medline
6. Preissner, K. T., and Seiffert, D. (1998) Role of vitronectin and its receptors in haemostasis and vascular remodeling. *Thromb Res.* **89,** 1–21 CrossRef Medline
7. Leavesley, D. I., Kashyap, A. S., Croll, T., Sivaramakrishnan, M., Shokoohmand, A., Hollier, B. G., and Upton, Z. (2013) Vitronectin—master controller or micromanager? *IUBMB Life* **65,** 807–818 CrossRef Medline
8. Boyd, N. A., Bradwell, A. R., and Thompson, R. A. (1993) Quantitation of vitronectin in serum: evaluation of its usefulness in routine clinical practice. *J. Clin. Pathol.* **46,** 1042–1045 CrossRef Medline
9. Chauhan, A. K., and Moore, T. L. (2006) Presence of plasma complement regulatory proteins clusterin (Apo J) and vitronectin (S40) on circulating immune complexes (CIC). *Clin. Exp. Immunol.* **145,** 398–406 CrossRef Medline
10. Berglund, L., Björling, E., Oksvold, P., Fagerberg, L., Asplund, A., Szigyarto, C. A., Persson, A., Ottosson, J., Wernérus, H., Nilsson, P., Lundberg, E., Sivertsson, A., Navani, S., Wester, K., Kampf, C., *et al.* (2008) A genecentric Human Protein Atlas for expression profiles based on antibodies. *Mol. Cell. Proteomics* **7,** 2019–2027 CrossRef Medline
11. Felding-Habermann, B., and Cheresh, D. A. (1993) Vitronectin and its receptors. *Curr. Opin. Cell Biol.* **5,** 864–868 CrossRef Medline

12. Schvartz, I., Seger, D., and Shaltiel, S. (1999) Vitronectin. *Int. J. Biochem. Cell Biol.* **31,** 539–544 CrossRef Medline
13. Stanley, K. K. (1986) Homology with hemopexin suggests a possible scavenging function for S-protein/vitronectin. *FEBS Lett.* **199,** 249–253 CrossRef Medline
14. Liang, O. D., Rosenblatt, S., Chhatwal, G. S., and Preissner, K. T. (1997) Identification of novel heparin-binding domains of vitronectin. *FEBS Lett.* **407,** 169–172 CrossRef Medline
15. Seiffert, D. (1995) Evidence that conformational changes upon the transition of the native to the modified form of vitronectin are not limited to the heparin binding domain. *FEBS Lett.* **368,** 155–159 CrossRef
16. Izumi, M., Yamada, K. M., and Hayashi, M. (1989) Vitronectin exists in two structurally and functionally distinct forms in human plasma. *Biochim. Biophys. Acta* **990,** 101–108 CrossRef Medline
17. Stockmann, A., Hess, S., Declerck, P., Timpl, R., and Preissner, K. T. (1993) Multimeric vitronectin. Identification and characterization of conformation-dependent self-association of the adhesive protein. *J. Biol. Chem.* **268,** 22874–22882 Medline
18. Zhuang, P., Li, H., Williams, J. G., Wagner, N. V., Seiffert, D., and Peterson, C. B. (1996) Characterization of the denaturation and renaturation of human plasma vitronectin. II. Investigation into the mechanism of formation of multimers. *J. Biol. Chem.* **271,** 14333–14343 CrossRef Medline
19. Lynn, G. W., Heller, W. T., Mayasundari, A., Minor, K. H., and Peterson, C. B. (2005) A model for the three-dimensional structure of human plasma vitronectin from small-angle scattering measurements. *Biochemistry* **44,** 565–574 CrossRef Medline
20. Seiffert, D., and Smith, J. W. (1997) The cell adhesion domain in plasma vitronectin is cryptic. *J. Biol. Chem.* **272,** 13705–13710 CrossRef Medline
21. Milis, L., Morris, C. A., Sheehan, M. C., Charlesworth, J. A., and Pussell, B. A. (1993) Vitronectin-mediated inhibition of complement: evidence for different binding sites for C5b-7 and C9. *Clin. Exp. Immunol.* **92,** 114–119 CrossRef Medline
22. Attia, A. S., Ram, S., Rice, P. A., and Hansen, E. J. (2006) Binding of vitronectin by the *Moraxella catarrhalis* UspA2 protein interferes with late stages of the complement cascade. *Infect. Immun.* **74,** 1597–1611 CrossRef Medline
23. Singh, B., Su, Y.-C., and Riesbeck, K. (2010) Vitronectin in bacterial pathogenesis: a host protein used in complement escape and cellular invasion. *Mol. Microbiol.* **78,** 545–560 CrossRef Medline
24. Bergmann, S., Lang, A., Rohde, M., Agarwal, V., Rennemeier, C., Grashoff, C., Preissner, K. T., and Hammerschmidt, S. (2009) Integrin-linked kinase is required for vitronectin-mediated internalization of *Streptococcus pneumoniae* by host cells. *J. Cell Sci.* **122,** 256–267 CrossRef Medline
25. Buommino, E., Di Domenico, M., Paoletti, I., Fusco, A., De Gregorio, V., Cozza, V., Rizzo, A., Tufano, M. A., and Donnarumma, G. (2014) AlphaV-Beta5 integrins mediates *Pseudomonas fluorescens* interaction with A549 cells. *Front. Biosci.* **19,** 408–415 CrossRef Medline
26. Heilmann, C., Hussain, M., Peters, G., and Götz, F. (1997) Evidence for autolysin-mediated primary attachment of *Staphylococcus epidermidis* to a polystyrene surface. *Mol. Microbiol.* **24,** 1013–1024 CrossRef Medline
27. Heilmann, C., Thumm, G., Chhatwal, G. S., Hartleib, J., Uekötter, A., and Peters, G. (2003) Identification and characterization of a novel autolysin (Aae) with adhesive properties from *Staphylococcus epidermidis*. *Microbiology* **149,** 2769–2778 CrossRef Medline
28. Hussain, M., Steinbacher, T., Peters, G., Heilmann, C., and Becker, K. (2015) The adhesive properties of the *Staphylococcus lugdunensis* multifunctional autolysin AtlL and its role in biofilm formation and internalization. *Int. J. Med. Microbiol.* **305,** 129–139 CrossRef Medline
29. Zoll, S., Schlag, M., Shkumatov, A. V., Rautenberg, M., Svergun, D. I., Götz, F., and Stehle, T. (2012) Ligand-binding properties and conformational dynamics of autolysin repeat domains in staphylococcal cell wall recognition. *J. Bacteriol.* **194,** 3789–3802 CrossRef Medline
30. Kohler, T. P., Gisch, N., Binsker, U., Schlag, M., Darm, K., Völker, U., Zähringer, U., and Hammerschmidt, S. (2014) Repeating structures of the major staphylococcal autolysin are essential for the interaction with human thrombospondin 1 and vitronectin. *J. Biol. Chem.* **289,** 4070–4082 CrossRef Medline
31. Hirschhausen, N., Schlesier, T., Schmidt, M. A., Götz, F., Peters, G., and Heilmann, C. (2010) A novel staphylococcal internalization mechanism involves the major autolysin Atl and heat shock cognate protein Hsc70 as host cell receptor. *Cell. Microbiol.* **12,** 1746–1764 CrossRef Medline
32. Hammer, N. D., and Skaar, E. P. (2011) Molecular mechanisms of *Staphylococcus aureus* iron acquisition. *Annu. Rev. Microbiol.* **65,** 129–147 CrossRef Medline
33. Mazmanian, S. K., Skaar, E. P., Gaspar, A. H., Humayun, M., Gornicki, P., Jelenska, J., Joachmiak, A., Missiakas, D. A., and Schneewind, O. (2003) Passage of heme-iron across the envelope of *Staphylococcus aureus*. *Science* **299,** 906–909 CrossRef Medline
34. Skaar, E. P., and Schneewind, O. (2004) Iron-regulated surface determinants (Isd) of *Staphylococcus aureus*: stealing iron from heme. *Microbes Infect.* **6,** 390–397 CrossRef Medline
35. Dryla, A., Gelbmann, D., Von Gabain, A., and Nagy, E. (2003) Identification of a novel iron regulated staphylococcal surface protein with haptoglobin-haemoglobin binding activity. *Mol. Microbiol.* **49,** 37–53 CrossRef Medline
36. Clarke, S. R., Wiltshire, M. D., and Foster, S. J. (2004) IsdA of *Staphylococcus aureus* is a broad spectrum, iron-regulated adhesin. *Mol. Microbiol.* **51,** 1509–1519 CrossRef Medline
37. Maresso, A. W., and Schneewind, O. (2006) Iron acquisition and transport in *Staphylococcus aureus*. *Biometals* **19,** 193–203 CrossRef Medline
38. Grigg, J. C., Ukpabi, G., Gaudin, C. F., and Murphy, M. E. (2010) Structural biology of heme binding in the *Staphylococcus aureus* Isd system. *J. Inorg. Biochem.* **104,** 341–348 CrossRef Medline
39. Pilpa, R. M., Fadeev, E. A., Villareal, V. A., Wong, M. L., Phillips, M., and Clubb, R. T. (2006) Solution structure of the NEAT (NEAr Transporter) domain from IsdH/HarA: the human hemoglobin receptor in *Staphylococcus aureus*. *J. Mol. Biol.* **360,** 435–447 CrossRef Medline
40. Zapotoczna, M., Heilbronner, S., Speziale, P., and Foster, T. J. (2012) Iron-regulated surface determinant (Isd) proteins of *Staphylococcus lugdunensis*. *J. Bacteriol.* **194,** 6453–6467 CrossRef Medline
41. Farrand, A. J., Haley, K. P., Lareau, N. M., Heilbronner, S., McLean, J. A., Foster, T., and Skaar, E. P. (2015) An iron-regulated autolysin remodels the cell wall to facilitate heme acquisition in *Staphylococcus lugdunensis*. *Infect. Immun.* **83,** 3578–3589 CrossRef Medline
42. Heilbronner, S., Monk, I. R., Brozyna, J. R., Heinrichs, D. E., Skaar, E. P., Peschel, A., and Foster, T. J. (2016) Competing for iron: duplication and amplification of the isd locus in *Staphylococcus lugdunensis* HKU09-01 provides a competitive advantage to overcome nutritional limitation. *PLoS Genet.* **12,** e1006246 CrossRef
43. Newton, S. M., Klebba, P. E., Raynaud, C., Shao, Y., Jiang, X., Dubail, I., Archer, C., Frehel, C., and Charbit, A. (2005) The svpA-srtB locus of *Listeria monocytogenes*: Fur-mediated iron regulation and effect on virulence. *Mol. Microbiol.* **55,** 927–940 CrossRef Medline
44. Skaar, E. P., Gaspar, A. H., and Schneewind, O. (2006) *Bacillus anthracis* IsdG, a heme-degrading monooxygenase. *J. Bacteriol.* **188,** 1071–1080 CrossRef Medline
45. Andrade, M. A., Ciccarelli, F. D., Perez-Iratxeta, C., and Bork, P. (2002) NEAT: a domain duplicated in genes near the components of a putative Fe^{3+} siderophore transporter from Gram-positive pathogenic bacteria. *Genome Biol.* **3,** research0047-1 CrossRef Medline
46. Clarke, S. R., Mohamed, R., Bian, L., Routh, A. F., Kokai-Kun, J. F., Mond, J. J., Tarkowski, A., and Foster, S. J. (2007) The *Staphylococcus aureus* surface protein IsdA mediates resistance to innate defenses of human skin. *Cell. Host Microbe* **1,** 199–212 CrossRef Medline
47. Visai, L., Yanagisawa, N., Josefsson, E., Tarkowski, A., Pezzali, I., Rooijakkers, S. H. M., Foster, T. J., and Speziale, P. (2009) Immune evasion by *Staphylococcus aureus* conferred by iron-regulated surface determinant protein IsdH. *Microbiology* **155,** 667–679 CrossRef
48. Zapotoczna, M., Jevnikar, Z., Miajlovic, H., Kos, J., and Foster, T. J. (2013) Iron-regulated surface determinant B (IsdB) promotes *Staphylococcus aureus* adherence to and internalization by non-phagocytic human cells. *Cell Microbiol.* **15,** 1026–1041 CrossRef Medline
49. Meenan, N. A., Visai, L., Valtulina, V., Schwarz-Linek, U., Norris, N. C., Gurusiddappa, S., Höök, M., Speziale, P., and Potts, J. R. (2007) The tandem β-zipper model defines high affinity fibronectin-binding repeats

within *Staphylococcus aureus* FnBPA. *J. Biol. Chem.* **282,** 25893–25902 CrossRef Medline

50. Geoghegan, J. A., Ganesh, V. K., Smeds, E., Liang, X., Höök, M., and Foster, T. J. (2010) Molecular characterization of the interaction of staphylococcal microbial surface components recognizing adhesive matrix molecules (MSCRAMM) ClfA and Fbl with fibrinogen. *J. Biol. Chem.* 285, 6208–6216 CrossRef Medline
51. Vazquez, V., Liang, X., Horndahl, J. K., Ganesh, V. K., Smeds, E., Foster, T. J., and Höök, M. (2011) Fibrinogen is a ligand for the *Staphylococcus aureus* microbial surface components recognizing adhesive matrix molecules (MSCRAMM) bone sialoprotein-binding protein (Bbp). *J. Biol. Chem.* 286, 29797–29805 CrossRef Medline
52. Ross, C. L., Liang, X., Liu, Q., Murray, B. E., Höök, M., and Ganesh, V. K. (2012) Targeted protein engineering provides insights into binding mechanism and affinities of bacterial collagen adhesins. *J. Biol. Chem.* **287,** 34856–34865 CrossRef Medline
53. Hare, S. A. (2017) Diverse structural approaches to haem appropriation by pathogenic bacteria. *Biochim. Biophys. Acta Proteins Proteom.* **1865,** 422–433 CrossRef Medline
54. Toida, T., Yoshida, H., Toyoda, H., Koshiishi, I., Imanari, T., Hileman, R. E., Fromm, J. R., and Linhardt, R. J. (1997) Structural differences and the presence of unsubstituted amino groups in heparan sulphates from different tissues and species. *Biochem. J.* **322,** 499–506 CrossRef
55. Johnson, M. B., Pang, B., Gardner, D. J., Niknam-Benia, S., Soundarajan, V., Bramos, A., Perrault, D. P., Banks, K., Lee, G. K., Baker, R. Y., Kim, G. H., Lee, S., Chai, Y., Chen, M., Li, W., Young-Kwong, H., *et al.* (2017) Topical fibronectin improves wound healing of irradiated skin. *Sci. Rep.* **7,** 1–10 CrossRef
56. Saravia-Otten, P., Müller, H. P., and Arvidson, S. (1997) Transcription of Staphylococcus aureus fibronectin-binding protein genes is negatively regulated by agr and an agr-independent mechanism. *J. Bacteriol.* **179,** 5259–5263 CrossRef Medline
57. Josse, J., Laurent, F., and Diot, A. (2017) Staphylococcal adhesion and host cell invasion: fibronectin-binding and other mechanisms. *Front. Microbiol.* **8,** 2433 CrossRef Medline
58. Bur, S., Preissner, K. T., Herrmann, M., and Bischoff, M. (2013) The *Staphylococcus aureus* extracellular adherence protein promotes bacterial internalization by keratinocytes independent of fibronectin-binding proteins. *J. Invest. Dermatol.* **133,** 2004–2012 CrossRef Medline
59. Tribelli, P. M., Luqman, A., Nguyen, M. T., Madlung, J., Fan, S. H., Macek, B., Sass, P., Bitschar, K., Schittek, B., Kretschmer, D., and Götz, F. (2020) *Staphylococcus aureus* Lpl protein triggers human host cell invasion via activation of Hsp90 receptor. *Cell. Microbiol.* **22,** e13111 CrossRef Medline
60. Kost, C., Stüber, W., Ehrlich, H. J., Pannekoek, H., and Preissner, K. T. (1992) Mapping of binding sites for heparin, plasminogen activator inhibitor-1, and plasminogen to vitronectin's heparin-binding region reveals a novel vitronectin-dependent feedback mechanism for the control of plasmin formation. *J. Biol. Chem.* **267,** 12098–12105 Medline
61. Miajlovic, H., Zapotoczna, M., Geoghegan, J. A., Kerrigan, S. W., Speziale, P., and Foster, T. J. (2010) Direct interaction of iron-regulated surface determinant IsdB of *Staphylococcus aureus* with the GPIIb/IIIa receptor on platelets. *Microbiology* **156,** 920–928 CrossRef Medline
62. McDevitt, D., Nanavaty, T., House-Pompeo, K., Bell, E., Turner, N., Mcintire, L., Foster, T., and Höök, M. (1997) Characterization of the interaction between the *Staphylococcus Aureus* clumping factor (ClfA) and fibrinogen. *Eur. J. Biochem.* **247,** 416–424 CrossRef Medline
63. Ganesh, V. K., Rivera, J. J., Smeds, E., Ko, Y. P., Bowden, M. G., Wann, E. R., Gurusiddappa, S., Fitzgerald, J. R., and Höök, M. (2008) A structural model of the *Staphylococcus aureus* ClfA-fibrinogen interaction opens new avenues for the design of anti-staphylococcal therapeutics. *PLoS Pathog.* 4, e1000226 CrossRef Medline
64. Hair, P. S., Ward, M. D., Semmes, O. J., Foster, T. J., and Cunnion, K. M. (2008) *Staphylococcus aureus* clumping factor A binds to complement regulator factor I and increases factor I cleavage of C3b. *J. Infect. Dis.* **198,** 125–133 CrossRef Medline
65. Hair, P. S., Echague, C. G., Sholl, A. M., Watkins, J. A., Geoghegan, J. A., Foster, T. J., and Cunnion, K. M. (2010) Clumping factor A interaction with complement factor I increases C3b cleavage on the bacterial surface of *Staphylococcus aureus* and decreases complement-mediated phagocytosis. *Infect. Immun.* **78,** 1717–1727 CrossRef Medline
66. Ní Eidhin, D., Perkins, S., Francois, P., Vaudaux, P., Höök, M., and Foster, T. J. (1998) Clumping factor B (ClfB), a new surface-located fibrinogen-binding adhesin of *Staphylococcus aureus*. *Mol. Microbiol.* **30,** 245–257 CrossRef Medline
67. Perkins, S., Walsh, E. J., Deivanayagam, C. C., Narayana, S. V., Foster, T. J., and Höök, M. (2001) Structural organization of the fibrinogen-binding region of the clumping factor B MSCRAMM of *Staphylococcus aureus*. *J. Biol. Chem.* **276,** 44721–44728 CrossRef Medline
68. O'Brien, L. M., Walsh, E. J., Massey, R. C., Peacock, S. J., and Foster, T. J. (2002) *Staphylococcus aureus* clumping factor B (ClfB) promotes adherence to human type I cytokeratin 10: implications for nasal colonization. *Cell. Microbiol.* **4,** 759–770 CrossRef Medline
69. Walsh, E. J., O'Brien, L. M., Liang, X., Hook, M., and Foster, T. J. (2004) Clumping factor B, a fibrinogen-binding MSCRAMM (microbial surface components recognizing adhesive matrix molecules) adhesin of *Staphylococcus aureus*, also binds to the tail region of type I cytokeratin 10. *J. Biol. Chem.* **279,** 50691–50699 CrossRef Medline
70. Mulcahy, M. E., Geoghegan, J. A., Monk, I. R., O'Keeffe, K. M., Walsh, E. J., Foster, T. J., and McLoughlin, R. M. (2012) Nasal colonisation by *Staphylococcus aureus* depends upon clumping factor B binding to the squamous epithelial cell envelope protein loricrin. *PLoS Pathog.* **8,** e1003092 CrossRef Medline
71. Vitry, P., Valotteau, C., Feuillie, C., Bernard, S., Alsteens, D., Geoghegan, J. A., and Dufrêne, Y. F. (2017) Force-induced strengthening of the interaction between Staphylococcus aureus clumping factor B and loricrin. *mBio* **8,** e01748-17 CrossRef
72. Bowden, C., Chan, A., Li, E., Arrieta, A. L., Eltis, L. D., and Murphy, M. (2018) Structure-function analyses reveal key features in *Staphylococcus aureus* IsdB-associated unfolding of the heme-binding pocket of human hemoglobin. *J. Biol. Chem.* **293,** 177–190 CrossRef Medline
73. Gianquinto, E., Moscetti, I., De Bei, O., Campanini, B., Marchetti, M., Luque, F. J., Cannistraro, S., Ronda, L., Bizzarri, A. R., Spyrakis, F., and Bettati, S. (2019) Interaction of human hemoglobin and semi-hemoglobins with the *Staphylococcus aureus* hemophore IsdB: a kinetic and mechanistic insight. *Sci. Rep.* **9,** 18629 CrossRef Medline
74. Stranger-Jones, Y. K., Bae, T., and Schneewind, O. (2006) Vaccine assembly from surface proteins of *Staphylococcus aureus*. *Proc. Natl. Acad. Sci. U S A* **103,** 16942–16947 CrossRef Medline
75. Kuklin, N. A., Clark, D. J., Secore, S., Cook, J., Cope, L. D., McNeely, T., Noble, L., Brown, M. J., Zorman, J. K., Wang, X. M., Pancari, G., Fan, H., Isett, K., Burgess, B., Bryan, J., *et al.* (2006) A novel *Staphylococcus aureus* vaccine: iron surface determinant B induces rapid antibody responses in rhesus macaques and specific increased survival in a murine *S. aureus* sepsis model. *Infect. Immun.* **74,** 2215–2223 CrossRef Medline
76. Kim, H. K., DeDent, A., Cheng, A. G., McAdow, M., Bagnoli, F., Missiakas, D. M., and Schneewind, O. (2010) IsdA and IsdB antibodies protect mice against *Staphylococcus aureus* abscess formation and lethal challenge. *Vaccine* **28,** 6382–6392 CrossRef Medline
77. Brown, M., Kowalski, R., Zorman, J., Wang, X. M., Towne, V., Zhao, Q., Secore, S., Finnefrock, A. C., Ebert, T., Pancari, G., Isett, K., Zhang, Y., Anderson, A. S., Montgomery, D., Cope, L., *et al.* (2009) Selection and characterization of murine monoclonal antibodies to *Staphylococcus aureus* iron-regulated surface determinant B with functional activity in vitro and in vivo. *Clin. Vaccine Immunol.* **16,** 1095–1104 CrossRef
78. Fowler, V. G., Allen, K. B., Moreira, E. D., Moustafa, M., Isgro, F., Boucher, H. W., Corey, G. R., Carmeli, Y., Betts, R., Hartzel, J. S., Chan, I. S., McNeely, T. B., Kartsonis, N. A., Guris, D., Onorato, M. T., *et al.* (2013) Effect of an investigational vaccine for preventing *Staphylococcus aureus* infections after cardiothoracic surgery: a randomized trial. *JAMA* **309,** 1368–1378 CrossRef Medline
79. Bagnoli, F., Bertholet, S., and Grandi, G. (2012) Inferring reasons for the failure of *Staphylococcus aureus* vaccines in clinical trials. *Front. Cell. Infect. Microbiol.* **2,** 16 CrossRef Medline
80. O'Halloran, D. P., Wynne, K., and Geoghegan, J. A. (2015) Protein A is released into the *Staphylococcus aureus* culture supernatant with an

unprocessed sorting signal. *Infect. Immun.* **83,** 1598–1609 CrossRef Medline

81. Patel, A. H., Nowlan, P., Weavers, E. D., and Foster, T. (1987) Virulence of protein A-deficient and alpha-toxin-deficient mutants of *Staphylococcus aureus* isolated by allele replacement. *Infect. Immun.* **55,** 3103–3110 CrossRef Medline
82. Higgins, J., Loughman, A., Van Kessel, K. P., Van Strijp, J. A., and Foster, T. J. (2006) Clumping factor A of *Staphylococcus aureus* inhibits phagocytosis by human polymorphonuclear leucocytes. *FEMS Microbiol. Lett.* **258,** 290–296 CrossRef Medline
83. Horsburgh, M. J., Aish, J. L., White, I. J., Shaw, L., Lithgow, J. K., and Foster, S. J. (2002) σB modulates virulence determinant expression and stress resistance: characterization of a functional rsbU strain derived from *Staphylococcus aureus* 8325-4. *J. Bacteriol.* **184,** 5457–5467 CrossRef Medline
84. Claro, T., Widaa, A., O'Seaghdha, M., Miajlovic, H., Foster, T. J., O'Brien, F. J., and Kerrigan, S. W. (2011) *Staphylococcus aureus* Protein A Binds to Osteoblasts and Triggers Signals That Weaken Bone in Osteomyelitis. *PLoS ONE* **6,** e18748 CrossRef Medline
85. De Ruyter, P. G., Kuipers, O. P., and De Vos, W. M. (1996) Controlled gene expression systems for *Lactococcus lactis* with the food-grade inducer nisin. *Appl. Environ. Microbiol.* **62,** 3662–3667 CrossRef Medline
86. Sambrook, J., Fritsch, E. F., and Maniatis, T. (1989) *Molecular cloning: a laboratory manual*, 2nd ed. Cold Spring Harbor Laboratory, Cold Spring Harbor, NY
87. Speziale, P., Visai, L., Rindi, S., and Di Poto, A. (2008) Purification of human plasma fibronectin using immobilized gelatin and Arg affinity chromatography. *Nat. Protoc.* **3,** 525–533 CrossRef Medline
88. Akiyama, S. K. (2013) Purification of vitronectin. *Curr. Protoc. Cell Biol.* **60,** Unit 10.6 CrossRef Medline
89. Viela, F., Prystopiuk, V., Leprince, A., Mahillon, J., Speziale, P., Pietrocola, G., and Dufrêne, Y. F. (2019) Binding of *Staphylococcus aureus* protein A to von Willebrand factor is regulated by mechanical force. *mBio* **10,** e00555-19 CrossRef
90. Perez-Riverol, Y., Csordas, A., Bai, J., Bernal-Llinares, M., Hewapathirana, S., Kundu, D. J., Inuganti, A., Griss, J., Mayer, G., Eisenacher, M., Pérez, E., Uszkoreit, J., Pfeuffer, J., Sachsenberg, T., Yilmaz, S., *et al.* (2019) The PRIDE database and related tools and resources in 2019: improving support for quantification data. *Nucleic Acids Res.* **47,** D442–D450 CrossRef Medline

NANO LETTERS

pubs.acs.org/NanoLett Letter

Single-Molecule Analysis Demonstrates Stress-Enhanced Binding between *Staphylococcus aureus* Surface Protein IsdB and Host Cell Integrins

Marion Mathelié-Guinlet, Felipe Viela, Mariangela Jessica Alfeo, Giampiero Pietrocola, Pietro Speziale, and Yves F. Dufrêne*

Cite This: *Nano Lett.* 2020, 20, 8919−8925 Read Online

ACCESS | Metrics & More | Article Recommendations | Supporting Information

ABSTRACT: Binding of *Staphylococcus aureus* surface proteins to endothelial cell integrins plays essential roles in host cell adhesion and invasion, eventually leading to life-threatening diseases. The staphylococcal protein IsdB binds to β3-containing integrins through a mechanism that has never been thoroughly investigated. Here, we identify and characterize at the nanoscale a previously undescribed stress-dependent adhesion between IsdB and integrin $\alpha_V\beta_3$. The strength of single IsdB−$\alpha_V\beta_3$ interactions is moderate (∼100 pN) under low stress, but it increases dramatically under high stress (∼1000−2000 pN) to exceed the forces traditionally reported for the binding between integrins and Arg-Gly-Asp (RGD) sequences. We suggest a mechanism where high mechanical stress induces conformational changes in the integrin from a low-affinity, weak binding state to a high-affinity, strong binding state. This single-molecule study highlights that direct adhesin−integrin interactions represent potential targets to fight staphylococcal infections.

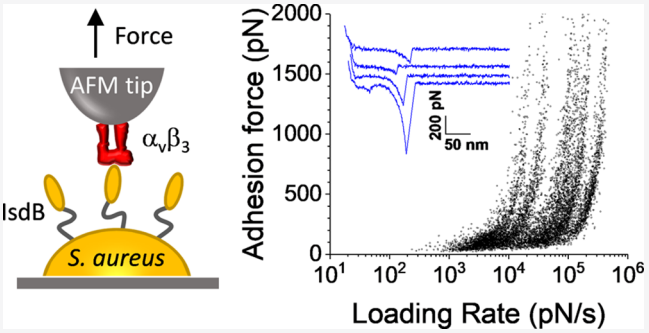

KEYWORDS: *staphylococcal adhesion, IsdB, $\alpha_V\beta_3$ integrins, single-molecule, binding strength, catch bond*

Staphylococcus aureus is an opportunistic pathogen which can lead to life-threatening diseases, such as bloodstream infections.[1−3] Mostly known for its role in nosocomial infections and for its ability to resist methicillin, *S. aureus* is now considered as a worldwide clinical problem.[4] *S. aureus* expresses and uses a range of cell wall-anchored (CWA) proteins to mediate adhesion to extracellular matrix (ECM) components of endothelial cells. While it has long been thought to be an extracellular pathogen, there is now compelling evidence that this pathogen uses such CWA proteins to support invasion of epithelial and endothelial cells.[5−8]

Integrins are heterodimeric mammalian transmembrane receptors mediating adhesion to the ECM or to other cells.[9] Ligand binding provides mechanical cues and triggers biochemical signals to regulate a number of physiological functions such as cell development, cytoskeleton organization, and surface receptor clustering. Fibronectin-binding proteins (FnBPs) of *S. aureus* interact with $\alpha_5\beta_1$ integrins indirectly through fibronectin (Fn) of the ECM, which acts as a molecular bridge tethering the pathogen to the target cell and promoting its internalization.[8,10,11] Similarly, vascular endothelial dysfunction has been attributed to the ability of *S. aureus* clumping factor A (ClfA) to adhere to $\alpha_V\beta_3$ integrins expressed on endothelial cells, with a critical role of fibrinogen (Fg).[12] Though less investigated, some pathogens can also interact directly with host integrins, as exemplified by enteropathogenic *Yersinia pseudotuberculosis* adhering and invading epithelial cells via β_1 integrins binding to invasin YadA.[13,14] As integrins are potential targets to treat *S. aureus* bloodstream infections, understanding their interactions with adhesins is an important topic.

The surface determinant IsdB protein binds to hemoglobin and provides *S. aureus* bacteria with a source of iron.[15] It has also been shown to promote the adhesion to platelets via direct binding to $\alpha_{IIb}\beta_3$ and potentially to some other β3-containing integrins.[16−19] Among them, $\alpha_V\beta_3$ is the major integrin expressed on endothelial cells.[9] These integrins promote bacterial adhesion to the ECM thanks to their multiligand binding activities (Vitronectin, Fn, Fg).[20] Vitronectin is notably known to form a molecular bridge between surface-exposed IsdB and $\alpha_V\beta_3$ integrins, but invasion of HeLa and

Received: October 7, 2020
Revised: November 16, 2020
Published: November 25, 2020

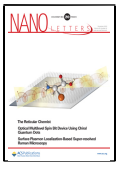

https://dx.doi.org/10.1021/acs.nanolett.0c04015
Nano Lett. 2020, 20, 8919−8925

HUVEC cells by *S. aureus* also occurs, though with lower probability, in the absence of vitronectin, suggesting that a direct adhesin−integrin interaction might occur and contribute to *S. aureus* pathogenesis.[21] Here, we use single-molecule experiments to demonstrate direct binding of IsdB to $\alpha_V\beta_3$ and to decipher the molecular forces and dynamics guiding such interactions. The mechanical stability of the IsdB−$\alpha_V\beta_3$ complex is low under low stress conditions (150 pN at a loading rate < 10^2 pN/s) but is strongly increased by mechanical tension (up to 2000 pN at a loading rate of 10^5 pN/s). Reminiscent of a catch bond behavior, this force-enhanced binding of IsdB to $\alpha_V\beta_3$ integrin might help the pathogen to firmly attach to host cells and resist fluid shear stress conditions that, in turn, translate into higher tensile loads on adhesive bonds.

RESULTS AND DISCUSSION

IsdB Supports Bacterial Adhesion to Immobilized $\alpha_V\beta_3$ Integrins. We first determined the adhesion forces between single *S. aureus* WT bacteria (exposing IsdB adhesins) and $\alpha_V\beta_3$-coated substrates. Figure 1A shows the maximum adhesion forces and rupture lengths histograms obtained for three representative cells. High binding probability was frequently observed between WT cells and $\alpha_V\beta_3$ surfaces (40 ± 5% from those three representative cells) with adhesion forces exhibiting a widely spread distribution, from 50 pN to 1500 pN (Figure 1A). Only specific adhesive events, showing defined single peaks, well fitted by the worm-like chain model, were considered in the analysis; this means that non-specific adhesion arising, e.g., from other proteins or biomolecules unspecifically interacting with integrins were discarded. All cells showed major adhesion forces below 500 pN, with a mean force of 153 ± 106 pN (mean ± s.d. on n = 291 adhesive curves from 3 cells; frequency of 74%). Larger forces up to 1500 pN were also observed in 26% of the cases. It is noteworthy that we observed rupture lengths of 112 ± 55 nm (n = 392 events from 3 cells). Given that the IsdB adhesin is made of ∼600 residues and that each amino acid contributes to 0.36 nm of the contour length, the fully unfolded protein should be ∼215 nm, larger than the reported rupture lengths. Consequently, the observed bonds break before the complete unfolding of IsdB, highlighting the mechanical stability of those *S. aureus* adhesins.

The specificity of interaction was tested by measuring the forces between IsdB$^-$ cells lacking IsdB and $\alpha_V\beta_3$-coated substrates (Figure 1B). There was a significant drop in adhesion probability, from 35 ± 7% (14 WT cells, Figure 3A) to 22 ± 9% (12 IsdB$^-$ cells, Figure 3A), and only low forces of 142 ± 87 pN (n = 155 adhesive events from 3 independent cells) were observed, suggesting that IsdB plays a critical role in the measured interaction forces. The residual adhesion still observed for IsdB$^-$ cells might arise from other surface receptors. Nonetheless, as reported below, the single molecule configuration leads to almost no adhesion for mutant cells, confirming our hypothesis on the critical and specific role of IsdB in driving binding to $\alpha_V\beta_3$ integrin. Moreover, there was a strong reduction of adhesion when blocking the integrin with either anti-$\alpha_V\beta_3$ antibodies or cilengitide, with low and high forces still being observed (Figure 1C and D, Figure 3A). The binding probability dropped from 35 ± 7% for WT cells to 15 ± 6% (16 cells) and 23 ± 9% (13 cells) for WT cells treated with antibodies and cilengitide, respectively. The substantial drop in adhesion confirms the overall blocking of the interaction between IsdB and αVβ3, though residual specific binding can still occur.

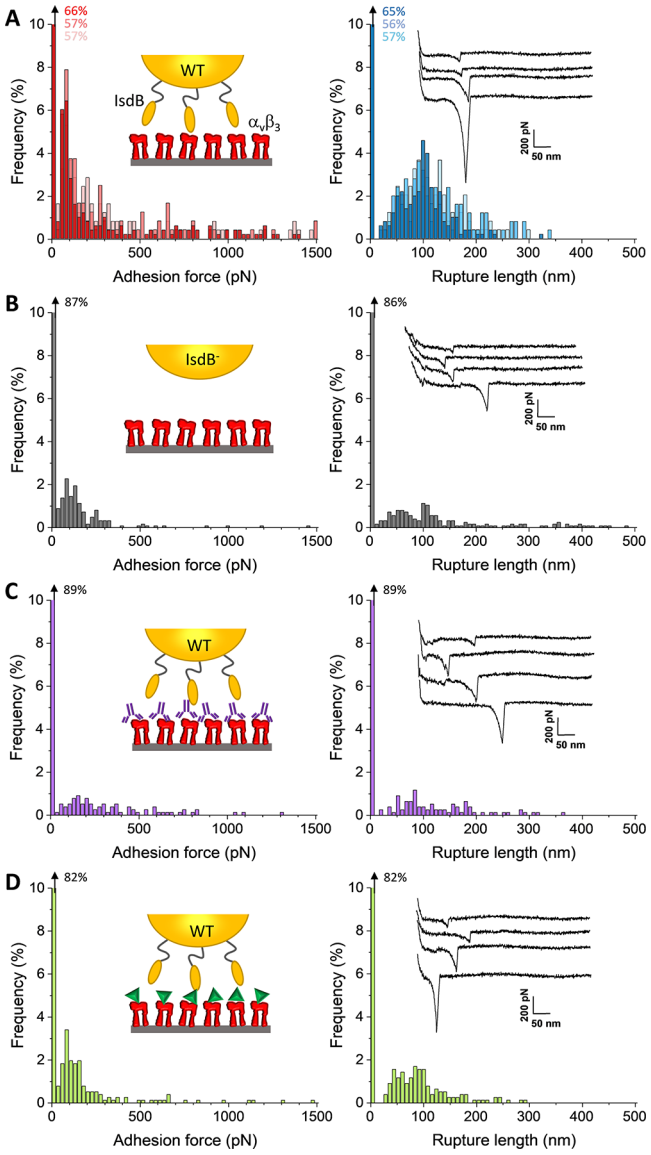

Figure 1. Single-cell force spectroscopy identifies IsdB as a mediator for *S. aureus* adhesion to $\alpha_V\beta_3$ surfaces. (A) Adhesion force (left) and rupture length (right) histograms obtained between three representative WT cells and $\alpha_V\beta_3$−substrates interacting in PBS (color-coded). (B) Data obtained between IsdB$^-$ cells (3 merged cells), lacking the IsdB adhesins, and $\alpha_V\beta_3$−substrates. (C, D) Data obtained between WT cells (3 merged cells) and $\alpha_V\beta_3$−substrates blocked with anti-$\alpha_V\beta_3$ antibodies LM 609 and cilengitide, respectively. For each panel, the left inset represents a scheme of the setup and the right inset shows representative retraction profiles. A contact time of 500 ms, a maximum applied force of 250 pN, and approach and retraction speeds of 1000 nm/s were used to record force−distance curves from which adhesion forces and rupture lengths were extracted.

Strength of Single IsdB−$\alpha_V\beta_3$ Interactions. To further quantify the strength of single IsdB−$\alpha_V\beta_3$ interactions, we measured the forces between $\alpha_V\beta_3$ integrins grafted on the AFM tip and *S. aureus* WT bacteria (Figure 2A). Similar to single-cell measurements, we observed the most probable adhesion forces below 500 pN, centered at 175 ± 121 pN (mean ± s.d., from n = 193 adhesive events from 3

https://dx.doi.org/10.1021/acs.nanolett.0c04015
Nano Lett. 2020, 20, 8919−8925

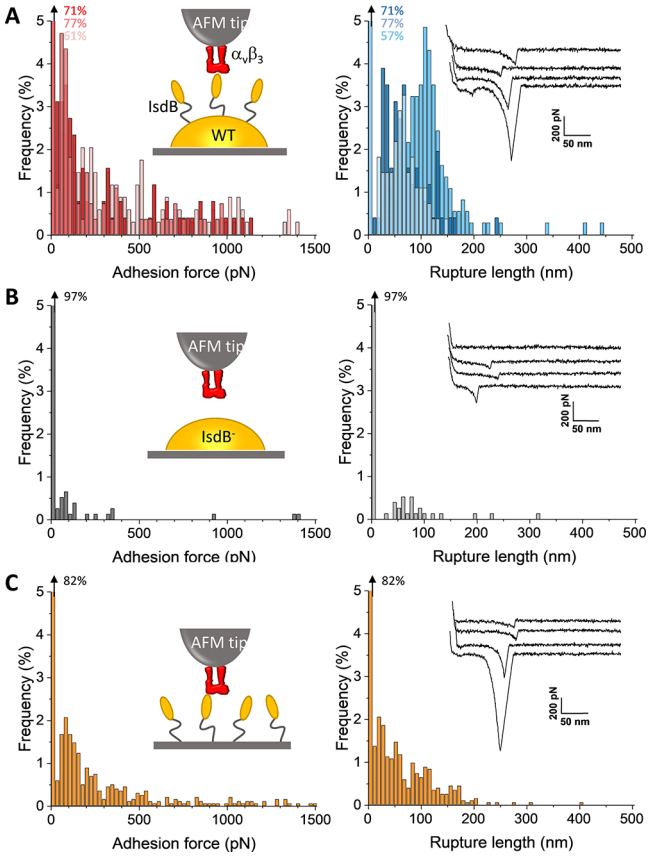

Figure 2. Single-molecule force spectroscopy captures the binding strength of $\alpha_V\beta_3$ interacting with single IsdB adhesin expressed on *S. aureus*. (A) Adhesion force (left) and rupture length (right) histograms obtained on three representative WT cells probed with $\alpha_V\beta_3$-functionalized AFM tips (color-coded). (B) The same data on IsdB$^-$ cells (3 cells merged). (C) The same data obtained between AFM tips labeled with $\alpha_V\beta_3$ integrins and IsdB-coated N1−N2 substrates. For each panel, the left inset represents a scheme of the setup and the right inset shows representative retraction profiles. A contact time of 500 ms, a maximum applied force of 250 pN, and approach and retraction speeds of 1000 nm/s were used to record force−distance curves from which adhesion forces and rupture lengths were extracted.

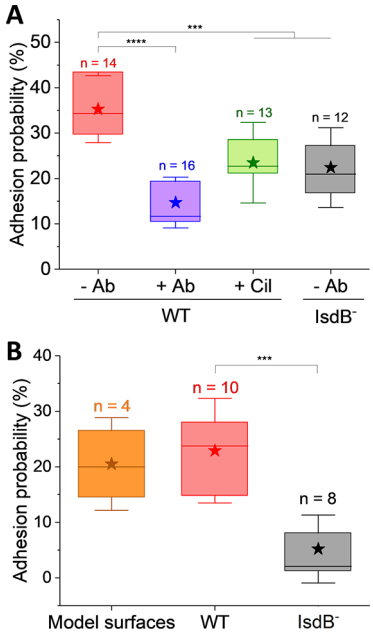

Figure 3. Single-cell and single-molecule force spectroscopy experiments reveal the specific binding between IsdB and $\alpha_V\beta_3$. (A) Box plots of the adhesion probability obtained between bacteria, either WT or mutant cells (n cells), and $\alpha_V\beta_3$ immobilized on solid substrates, in single-cell experiments. Cil. stands for the blocking experiments performed with cilengitide and Ab for antibodies. (B) Adhesion probability for both strains and model surfaces obtained in single-molecule experiments over n independent samples. Stars account for the mean values, boxes the 25−75% quartiles, and whiskers the standard deviation. Student's t-tests: ****$p < 0.0001$ and ***$p < 0.001$.

representative independent cells), in agreement with the strength of single integrins.

Again, we also observed higher forces up to 1500 pN at a frequency of 29%. Similar features, though with lower adhesion probability, were obtained when decreasing the density of integrins grafted on the tip (1% vs 10% carboxyl-terminated thiols) (Supplementary Figure S1A and S1B), suggesting that such differences in strength cannot be accounted for multiple bonds breaking in parallel but rather by intrinsic properties of the formed IsdB−$\alpha_V\beta_3$ complex. Both weak and strong interactions were abolished when probing IsdB$^-$ cells (5% vs 23% for WT cells, Figure 3B; Figure 2B), confirming that IsdB interacts specifically with $\alpha_V\beta_3$ integrins.

Also, recombinant IsdB N1−N2 region proteins showed the same binding features as WT cells when probed against $\alpha_V\beta_3$ tips (Figure 2C, Figure 3B), supporting the idea that IsdB was the only surface molecule involved in the interaction.

IsdB−$\alpha_V\beta_3$ Interaction Is Strengthened by Mechanical Force. It has been recently shown that staphylococcal adhesive interactions can be reinforced by mechanical stress.[22−25] When the bacteria adhere to a surface through the specific interaction between an adhesin and its ligand, this interaction is under tensile load due to the diverse flow conditions encountered in the environment. Increasing shear stress thus translates into increasing tensile load on the bond. Therefore, we used dynamic force spectroscopy (DFS) to measure the rupture force (F) between $\alpha_V\beta_3$ tips and WT cells, when the complex is pulled at different speeds, i.e., at different loading rates (LRs) assessed from the force versus time curves (Figure 4). Increasing the retraction speed from 0.5 μm/s to 10 μm/s led to a shift toward higher forces, with a progressive depletion of the main force population at ∼100 pN and an increase in the amount of higher forces both below and above 500 pN (Figure 4A), suggesting a force-enhanced interaction. Figure 4B shows the resulting dynamic force spectroscopy plot pooled from four independent cells. Clearly, a nonlinear behavior was observed with forces rising up to 2000 pN at LRs higher than 10^4 pN/s. Overall, the whole set of forces could not be fitted by the Bell−Evans or the Friddle−Noy−de Yoreo (FNdeY) models.[26,27] Nonetheless, the low force regime at ∼100 pN could be described by a FNdeY model, but the sudden increase in force and the increasing proportion of forces higher than 500 pN at higher loading rates were beyond the expectation of this model. This led us to believe that such strong bonds arised from a force-induced deformation and conformational change in the complex. We analyzed the distribution of binding forces over discrete ranges of LRs (Figure 4C, n = 7774 adhesion events over four cells; see also Supplementary Figure S2). The lowest LRs ($10^3 < LR < 3 \times 10^3$ pN/s) showed only weak forces of 100−200 pN while the highest LRs ($10^5 < LR < 3 \times$

https://dx.doi.org/10.1021/acs.nanolett.0c04015
Nano Lett. 2020, 20, 8919−8925

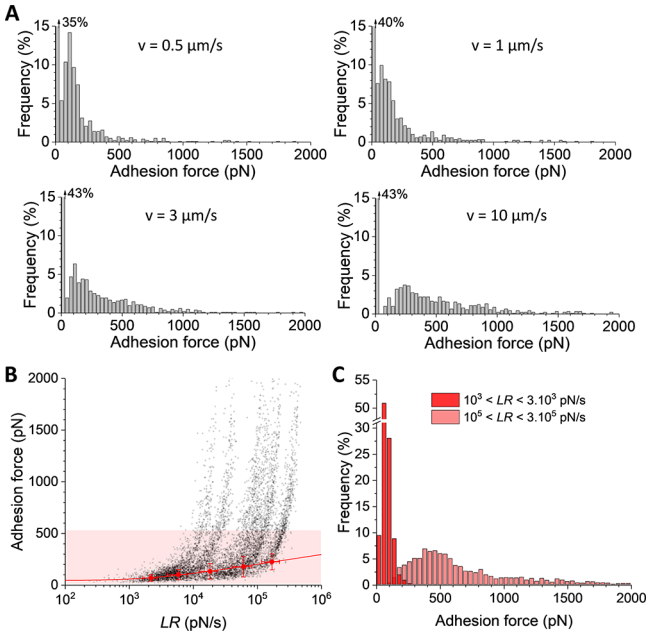

Figure 4. Mechanical load enhances the IsdB-$\alpha_V\beta_3$ interaction strength. (A) Adhesion force histograms, obtained at different retraction speeds, by recording force curves on one representative WT cell using AFM tips labeled with $\alpha_V\beta_3$ integrins. (B) Dynamic force spectroscopy plot (force, *F*, vs loading rate, *LR*) for the IsdB−$\alpha_V\beta_3$ interaction on four independent cells (pooled from n = 7774 adhesive events). The red zone indicates the threshold between the low force regime (F < 500 pN) and the high regime (F > 500 pN). Shown in red is a Friddle−Noy−de Yoreo fit, with an equilibrium force F_{eq} = 44 ± 15 pN, a transition energetic barrier at x_β = 0.100 ± 0.002, and an off-rate constant of dissociation k_{off}^0 = 30.6 ± 18.4 s^{-1}. (C) Adhesion force histograms obtained by sorting the DFS data in discrete *LR* ranges.

10^5 pN/s) featured stronger forces in the 500 pN range and up to 2000 pN. At intermediate LRs, both populations of forces were observed in different proportions depending on the LR (Supplementary Figure S2). The DFS plot obtained while lowering the integrin density on the tip exhibited similar features with forces up to 2000 pN at LRs higher than 10^4 pN/s and had both increasing proportion of higher forces and stronger forces with increasing LRs (Supplementary Figure S1C). Consequently, it is rather unlikely that multiple cumulative bonds could explain such high forces never reported before for a direct adhesin−integrin binding.

Staphylococci have evolved dedicated mechanisms to mediate strong attachment to host cells under shear stress, chiefly mediated by surface-exposed proteins specifically binding to host receptors or ECM proteins.[28,29] We have shown here that the direct interaction between IsdB and $\alpha_V\beta_3$ integrin is stress sensitive, becoming extraordinarily strong (1000−2000 pN) under high stress conditions. Such interaction strength is equivalent to that of a covalent bond and is thus much higher than that of classical ligand−integrin bonds studied so far, in the range of ∼100 pN.[30−32]

Earlier studies have revealed the capacity of integrins to form such force-enhanced complexes with, e.g., Fn, inducing a strengthening of cellular adhesion. Notably, based on single-molecule experiments, Kong et al. observed an increase in bond lifetimes with forces ranging from 10 to 30 pN for a Fn fragment in complex with an integrin fusion protein.[33] Also, Strohmeyer et al. found that fibroblasts initiate binding to Fn through adhesive complexes with $\alpha_5\beta_1$ integrins that are strengthened, in terms of force and lifetime, to resist shear conditions.[34] While these studies provide compelling evidence that integrin-mediated adhesion of mammalian cells is modulated by mechanical force, whether this occurs directly between integrins and bacterial adhesins was not known. Solving this question is yet critical to the development of new integrin inhibitors to treat *S. aureus* infections. Unique to our study is that IsdB directly binds to $\alpha_V\beta_3$, in the absence of any ligands of the ECM, and that the interaction is extraordinarily strong under high stress conditions (loading rate of 10^5 pN/s). This strong adhesion could not be described by the Friddle−Noy−de Yoreo model, pointing to an unusual force-activated binding mechanism. Our force-strengthened adhesion is comparable with that reported for dock, lock, and latch (DLL) complexes[35,36] such as staphylococci SdrG, ClfA, and ClfB adhesins[37−40] that can resist extreme forces ∼2 nN because of an intricate hydrogen-bonding network formed by the locked peptide and the adhesin binding pocket.[39] Though involving a different binding mechanism, such a force-dependent hydrogen-bonding network might contribute to the ultrastrong IsdB−$\alpha_V\beta_3$ interaction observed here.

Moreover, our force-enhanced IsdB−$\alpha_V\beta_3$ interaction is reminiscent of the catch bond behavior exhibited by the blood proteins selectins[41] and the bacterial adhesin FimH,[42−44] which become longer lived with increasing shear stress. This phenomenon has also been previously reported for some ligand−integrin complexes that, in turn, strengthen cellular adhesion under stress.[45−49] Interestingly, theoretical analyses have revealed that external load could induce an increase in the lifetime of hydrogen bonds, formed in the binding pocket between a receptor and its ligand, leading to a catch bond behavior,[50] a finding that also explains how structurally unrelated integrin−Fn and/or actomyosin complexes bind.

Although the molecular origin of IsdB−$\alpha_V\beta_3$ interaction remains unclear, we suggest a model in which force-induced structural changes upshift the integrins to a high affinity state. This notion is supported by previous works showing that *S. aureus* adheres to platelets through the binding of IsdB to the high affinity form of platelet integrins $\alpha_{IIb}\beta_3$, without the need of an extra ECM protein.[16,17] Inhibition of $\alpha_V\beta_3$ adhesion by cilengitide observed in this work also highlights that the integrin binding site for cilengitide and IsdB must be close and that this proximity reduces binding of IsdB, as IsdB does not contain any RGD sequence. In addition, it is possible that force acting on integrins is transmitted to the IsdB binding site, leading to a conformational change of the adhesin and creating a new hydrogen-bonding network that stabilizes the complex. Overall, our single-molecule approach on purified integrins provides a crucial initial understanding of the molecular mechanism underlying the direct binding of bacterial adhesins to such targets, without the requirement of ECM proteins. Further work is needed to confirm whether similar direct IsdB−$\alpha_V\beta_3$ interaction occurs on endothelial cells. The force-enhanced adhesion between IsdB and integrins might be one among many mechanisms staphylococci have developed to efficiently colonize and/or invade their hosts while resisting shear forces encountered in various environments upon infection.[51]

METHODS

Bacterial Strains and Growth Conditions. *S. aureus* SH1000 WT (expressing IsdB) and IsdB⁻ mutant (lacking the

https://dx.doi.org/10.1021/acs.nanolett.0c04015
Nano Lett. 2020, 20, 8919−8925

adhesin) cells were cultured in brain heart infusion (BHI) broth overnight at 37 °C and under shaking at 200 rpm. When the stationary phase was reached, bacteria were diluted 100× and grown in RPMI (Roswell Park Memorial Institute medium, usually used for mammalian cell culture) overnight (37 °C, 200 rpm) to create iron-restricted conditions. Cells were finally harvested three times by centrifugation at 3000*g* for 5 min. They were diluted 100× in PBS and used directly for AFM experiments.

AFM Tips and Gold Surfaces Functionalization with Integrin $\alpha_V\beta_3$. Gold-coated glass coverslips and gold-coated OMCL-TR4 AFM cantilevers (Olympus, Ltd., Tokyo, Japan) were immersed overnight in an ethanolic solution containing 16-mercaptododecahexanoic acid (0.1 mM) and 1-mercapto-1-undecanol (0.9 mM). They were then washed with ethanol and dried under a stream of N_2. Substrates and AFM cantilevers were then immersed for 30 min in a solution of *N*-hydroxysuccinimide (NHS, 10 mg/mL) and 1-ethyl-3-(3-dimethylaminopropyl)-carbodiimide (EDC, 25 mg/mL). The resulting NHS−carboxyl ester-exposing cantilevers and substrates were rinsed with ultrapure water and incubated with $\alpha_V\beta_3$ integrin (0.1 mg/mL; Sigma) for 1 h. Finally, they were rinsed with PBS buffer and stored in PBS before AFM experiments.

Single-Cell Force Spectroscopy Experiments. The preparation of colloidal probes for single-cell experiments was described previously, and the cell viability, after attachment to the probe, was validated.[52] Thanks to an optical microscope coupled to the AFM instrument (Nanowizard III and IV atomic force microscopes, JPK Instruments), a triangular tipless cantilever (NP-O10, Bruker) was gently immersed in a thin layer of UV-curable glue (NOA 63, Norland Edmund Optics) and was then brought in contact with a single silica bead (6.1 μm diameter, Bangs Laboratories) for it to attach. The resulting colloidal probes were exposed to UV light for 15 min to cure the glue. They were then coated with dopamine for 1 h by immersion in Tris-buffered saline (TBS; Tris, 50 mM; NaCl, 150 mM; pH 8.5) containing 4 mg/mL dopamine hydrochloride (Sigma-Aldrich) and further rinsed in three baths of TBS. The spring constant of the probe cantilever was determined, before attachment of the bacteria, by the thermal noise method and gave an average value of 0.085 N/m. For single-cell experiments, 50 μL of a diluted suspension of bacteria was dropped on a polystyrene Petri dish for 20 min before being rinsed with PBS. An integrin $\alpha_V\beta_3$-coated substrate was placed right next to the bacteria spot, and the Petri dish was finally covered with 3 mL of PBS. One bacterium was caught electrostatically by gently approaching the colloidal probe toward an isolated cell, and verifying, on the optical cliché, its absence when the cantilever was retracted from its position. The cell probe was then brought into contact with the $\alpha_V\beta_3$-coated substrate to record multiple force curves (maps of 16 × 16 pixels) on different spots (5 μm × 5 μm), with an applied force of 250 pN, approach and retraction speeds of 1 μm/s, and a contact time of 500 ms. For blocking experiments, we used commercially available cilengitide (Sigma), and anti $\alpha_v\beta_3$ antibody LM 609 (Abcam), 150 μL of which were incubated on the $\alpha_V\beta_3$− surface for 1 h at a concentration of 0.1 mg/mL. All experiments were performed at room temperature.

Single-Molecule Force Spectroscopy Experiments. For single-molecule experiments, bacteria were first immobilized on a polystyrene Petri dish; a 50 μL drop of diluted bacterial suspension was deposited on the center of the dish and let sit for 20 min before being rinsed with PBS and immersed in 3 mL of PBS. Gold-coated OMCL-TR4 AFM cantilevers were initially calibrated on the bare polystyrene with the thermal noise method and gave an average value of $k \sim 0.05$ N/m. Finally, the AFM-functionalized tip was brought in contact with an isolated bacterium, and adhesion maps were recorded on top of the cell (500 nm × 500 nm, 32 × 32 pixels) with an applied force of 250 pN, a constant approach and retraction speed of 1 μm/s, and a contact time of 500 ms. In some experiments, gold surfaces coated with recombinant IsdB were probed. To this end, recombinant IsdB N2−N3 (residues 48−480) was expressed from pQE30 (Qiagen, Hilden, Germany) in *E. coli* XL1-Blue (Agilent Technologies, CA, USA) and purified by Ni^{2+}-affinity chromatography on a HiTrap chelating column (GE Healthcare, Buckinghamshire, UK) as reported in ref 21. The retraction speed was varied from 0.5 to 10 μm/s for loading rate experiments. All experiments were performed at room temperature.

Single-Cell and Single-Molecule Data Analysis. We used the JPK data processing software to analyze the data. The adhesion force and rupture distance of the last specific adhesion peak for each curve were determined and then plotted as histograms in Origin. A specific adhesive event is defined as an event, occurring far from the contact point, and where the retraction segment of the force curve shows a variation in the slope (representing the stretching of the molecular complex) before the rupture point. The frequency of those specific adhesion events, recorded in a map on a 500 nm × 500 nm area, is defined as the adhesion probability. Those specific adhesive events, mainly showing a single defined peak, were well fitted with the worm-like chain model during the analysis process. Loading rate was calculated from the linear slope immediately preceding the rupture event on the force versus time curves. Student's *t*-test was used to estimate the statistical differences among the obtained results; *p* values are provided in figure captions when appropriate.

■ ASSOCIATED CONTENT

Supporting Information

The Supporting Information is available free of charge at https://pubs.acs.org/doi/10.1021/acs.nanolett.0c04015.

Supplementary Figures S1 and S2 (PDF)

■ AUTHOR INFORMATION

Corresponding Author

Yves F. Dufrêne − *Louvain Institute of Biomolecular Science and Technology, UCLouvain, B-1348 Louvain-la-Neuve, Belgium;* orcid.org/0000-0002-7289-4248; Email: yves.dufrene@uclouvain.be

Authors

Marion Mathelié-Guinlet − *Louvain Institute of Biomolecular Science and Technology, UCLouvain, B-1348 Louvain-la-Neuve, Belgium;* orcid.org/0000-0001-9023-3470

Felipe Viela − *Louvain Institute of Biomolecular Science and Technology, UCLouvain, B-1348 Louvain-la-Neuve, Belgium*

Mariangela Jessica Alfeo − *Department of Molecular Medicine, Unit of Biochemistry, University of Pavia, 27100 Pavia, Italy*

https://dx.doi.org/10.1021/acs.nanolett.0c04015
Nano Lett. 2020, 20, 8919−8925

Giampiero Pietrocola − *Department of Molecular Medicine, Unit of Biochemistry, University of Pavia, 27100 Pavia, Italy;* orcid.org/0000-0002-7069-8155

Pietro Speziale − *Department of Molecular Medicine, Unit of Biochemistry, University of Pavia, 27100 Pavia, Italy*

Complete contact information is available at: https://pubs.acs.org/10.1021/acs.nanolett.0c04015

Author Contributions

M.M.G., F.V., M.J.A., G.P., P.S., and Y.F.D. designed the experiments and wrote the article. M.M.G. and F.V. collected the data. M.M.G., F.V., and Y.F.D. analyzed the data.

Notes

The authors declare no competing financial interest.

■ ACKNOWLEDGMENTS

Work at the Université catholique de Louvain was supported by the European Research Council (ERC) under the European Union's Horizon 2020 research and innovation programme (693630), the National Fund for Scientific Research (FNRS), and the Research Department of the Communauté française de Belgique (Concerted Research Action). Y.F.D. is a Research Director at the FNRS.

■ REFERENCES

(1) Foster, T. J. The *Staphylococcus aureus* "Superbug". *J. Clin. Invest.* **2004**, *114* (12), 1693−1696.

(2) Parlet, C. P.; Brown, M. M.; Horswill, A. R. Commensal Staphylococci Influence *Staphylococcus aureus* Skin Colonization and Disease. *Trends Microbiol.* **2019**, *27* (6), 497−507.

(3) Thomer, L.; Schneewind, O.; Missiakas, D. Pathogenesis of *Staphylococcus aureus* Bloodstream Infections. *Annu. Rev. Pathol.: Mech. Dis.* **2016**, *11*, 343−364.

(4) Chambers, H. F.; Deleo, F. R. Waves of Resistance: *Staphylococcus aureus* in the Antibiotic Era. *Nat. Rev. Microbiol.* **2009**, *7* (9), 629−641.

(5) Ogawa, S. K.; Yurberg, E. R.; Hatcher, V. B.; Levitt, M. A.; Lowy, F. D. Bacterial Adherence to Human Endothelial Cells in Vitro. *Infect. Immun.* **1985**, *50* (1), 218−224.

(6) Menzies, B. E.; Kourteva, I. Internalization of *Staphylococcus aureus* by Endothelial Cells Induces Apoptosis. *Infect. Immun.* **1998**, *66* (12), 5994−5998.

(7) Dziewanowska, K.; Patti, J. M.; Deobald, C. F.; Bayles, K. W.; Trumble, W. R.; Bohach, G. A. Fibronectin Binding Protein and Host Cell Tyrosine Kinase Are Required for Internalization of *Staphylococcus aureus* by Epithelial Cells. *Infect. Immun.* **1999**, *67* (9), 4673−4678.

(8) Sinha, B.; François, P. P.; Nüsse, O.; Foti, M.; Hartford, O. M.; Vaudaux, P.; Foster, T. J.; Lew, D. P.; Herrmann, M.; Krause, K. H. Fibronectin-Binding Protein Acts as *Staphylococcus aureus* Invasin via Fibronectin Bridging to Integrin $\alpha_5\beta_1$. *Cell. Microbiol.* **1999**, *1* (2), 101−117.

(9) Hynes, R. O. Integrins: Bidirectional, Allosteric Signaling Machines. *Cell* **2002**, *110* (6), 673−687.

(10) Sinha, B.; Herrmann, M. Mechanism and Consequences of Invasion of Endothelial Cells by *Staphylococcus aureus*. *Thromb. Haemostasis* **2005**, *94* (2), 266−277.

(11) Edwards, A. M.; Potts, J. R.; Josefsson, E.; Massey, R. C. *Staphylococcus aureus* Host Cell Invasion and Virulence in Sepsis Is Facilitated by the Multiple Repeats within FnBPA. *PLoS Pathog.* **2010**, *6* (6), No. e1000964.

(12) McDonnell, C. J.; Garciarena, C. D.; Watkin, R. L.; McHale, T. M.; McLoughlin, A.; Claes, J.; Verhamme, P.; Cummins, P. M.; Kerrigan, S. W. Inhibition of Major Integrin $\alpha_V\beta_3$ Reduces *Staphylococcus aureus* Attachment to Sheared Human Endothelial Cells. *J. Thromb. Haemostasis* **2016**, *14* (12), 2536−2547.

(13) Dersch, P.; Isberg, R. R. A Region of the *Yersinia pseudotuberculosis* Invasin Protein Enhances Integrin-Mediated Uptake into Mammalian Cells and Promotes Self-Association. *EMBO J.* **1999**, *18* (5), 1199−1213.

(14) Dersch, P.; Isberg, R. R. An Immunoglobulin Superfamily-Like Domain Unique to the *Yersinia pseudotuberculosis* Invasin Protein Is Required for Stimulation of Bacterial Uptake via Integrin Receptors. *Infect. Immun.* **2000**, *68* (5), 2930−2938.

(15) Mazmanian, S. K.; Skaar, E. P.; Gaspar, A. H.; Humayun, M.; Gornicki, P.; Jelenska, J.; Joachmiak, A.; Missiakas, D. M.; Schneewind, O. Passage of Heme-Iron across the Envelope of *Staphylococcus aureus*. *Science* **2003**, *299* (5608), 906−909.

(16) Miajlovic, H.; Zapotoczna, M.; Geoghegan, J. A.; Kerrigan, S. W.; Speziale, P.; Foster, T. J. Direct Interaction of Iron-Regulated Surface Determinant IsdB of *Staphylococcus aureus* with the GPIIb/IIIa Receptor on Platelets. *Microbiology (London, U. K.)* **2010**, *156* (3), 920−928.

(17) Zapotoczna, M.; Jevnikar, Z.; Miajlovic, H.; Kos, J.; Foster, T. J. Iron-Regulated Surface Determinant B (IsdB) Promotes *Staphylococcus aureus* Adherence to and Internalization by Non-Phagocytic Human Cells. *Cell. Microbiol.* **2013**, *15* (6), 1026−1041.

(18) Ma, Y.-Q.; Qin, J.; Plow, E. F. Platelet Integrin $\alpha_{IIb}\beta_3$: Activation Mechanisms. *J. Thromb. Haemostasis* **2007**, *5* (7), 1345−1352.

(19) Eliceiri, B. P.; Cheresh, D. A. The Role of αv Integrins during Angiogenesis: Insights into Potential Mechanisms of Action and Clinical Development. *J. Clin. Invest.* **1999**, *103* (9), 1227−1230.

(20) Plow, E. F.; Haas, T. A.; Zhang, L.; Loftus, J.; Smith, J. W. Ligand Binding to Integrins. *J. Biol. Chem.* **2000**, *275* (29), 21785−21788.

(21) Pietrocola, G.; Pellegrini, A.; Alfeo, M. J.; Marchese, L.; Foster, T. J.; Speziale, P. The Iron-Regulated Surface Determinant B (IsdB) Protein from *Staphylococcus aureus* Acts as a Receptor for the Host Protein Vitronectin. *J. Biol. Chem.* **2020**, *295* (29), 10008−10022.

(22) Milles, L. F.; Gaub, H. E. Extreme Mechanical Stability in Protein Complexes. *Curr. Opin. Struct. Biol.* **2020**, *60*, 124−130.

(23) Mathelié-Guinlet, M.; Viela, F.; Viljoen, A.; Dehullu, J.; Dufrêne, Y. F. Single-Molecule Atomic Force Microscopy Studies of Microbial Pathogens. *Curr. Opin. Biomed. Eng.* **2019**, *12*, 1−7.

(24) Viljoen, A.; Mignolet, J.; Viela, F.; Mathelié-Guinlet, M.; Dufrêne, Y. F. How Microbes Use Force To Control Adhesion. *J. Bacteriol.* **2020**, *202* (12), 1.

(25) Viela, F.; Mathelié-Guinlet, M.; Viljoen, A.; Dufrêne, Y. F. What Makes Bacterial Pathogens so Sticky? *Mol. Microbiol.* **2020**, *113*, 683.

(26) Friddle, R. W.; Noy, A.; De Yoreo, J. J. Interpreting the Widespread Nonlinear Force Spectra of Intermolecular Bonds. *Proc. Natl. Acad. Sci. U. S. A.* **2012**, *109* (34), 13573−13578.

(27) Evans, E. Probing the Relation between Force−Lifetime−and Chemistry in Single Molecular Bonds. *Annu. Rev. Biophys. Biomol. Struct.* **2001**, *30*, 105−128.

(28) Foster, T. J.; Geoghegan, J. A.; Ganesh, V. K.; Höök, M. Adhesion, Invasion and Evasion: The Many Functions of the Surface Proteins of *Staphylococcus aureus*. *Nat. Rev. Microbiol.* **2014**, *12* (1), 49−62.

(29) Dufrêne, Y. F.; Persat, A. Mechanomicrobiology: How Bacteria Sense and Respond to Forces. *Nat. Rev. Microbiol.* **2020**, *18*, 227−240.

(30) Viela, F.; Speziale, P.; Pietrocola, G.; Dufrêne, Y. F. Mechanostability of the Fibrinogen Bridge between Staphylococcal Surface Protein ClfA and Endothelial Cell Integrin $\alpha_V\beta_3$. *Nano Lett.* **2019**, *19* (10), 7400−7410.

(31) Li, F.; Redick, S. D.; Erickson, H. P.; Moy, V. T. Force Measurements of the $\alpha_5\beta_1$ Integrin-Fibronectin Interaction. *Biophys. J.* **2003**, *84* (2), 1252−1262.

(32) Bharadwaj, M.; Strohmeyer, N.; Colo, G. P.; Helenius, J.; Beerenwinkel, N.; Schiller, H. B.; Fässler, R.; Müller, D. J. αV-Class Integrins Exert Dual Roles on α5β1 Integrins to Strengthen Adhesion to Fibronectin. *Nat. Commun.* **2017**, *8* (1), 14348.

(33) Kong, F.; García, A. J.; Mould, A. P.; Humphries, M. J.; Zhu, C. Demonstration of Catch Bonds between an Integrin and Its Ligand. *J. Cell Biol.* **2009**, *185* (7), 1275−1284.
(34) Strohmeyer, N.; Bharadwaj, M.; Costell, M.; Fässler, R.; Müller, D. J. Fibronectin-Bound $\alpha5\beta1$ Integrins Sense Load and Signal to Reinforce Adhesion in Less than a Second. *Nat. Mater.* **2017**, *16* (12), 1262−1270.
(35) Ponnuraj, K.; Bowden, M. G.; Davis, S.; Gurusiddappa, S.; Moore, D.; Choe, D.; Xu, Y.; Hook, M.; Narayana, S. V. L. A "Dock, Lock, and Latch" Structural Model for a Staphylococcal Adhesin Binding to Fibrinogen. *Cell* **2003**, *115* (2), 217−228.
(36) Bowden, M. G.; Heuck, A. P.; Ponnuraj, K.; Kolosova, E.; Choe, D.; Gurusiddappa, S.; Narayana, S. V. L.; Johnson, A. E.; Höök, M. Evidence for the "Dock, Lock, and Latch" Ligand Binding Mechanism of the Staphylococcal Microbial Surface Component Recognizing Adhesive Matrix Molecules (MSCRAMM) SdrG. *J. Biol. Chem.* **2008**, *283* (1), 638−647.
(37) Herman, P.; El-Kirat-Chatel, S.; Beaussart, A.; Geoghegan, J. A.; Foster, T. J.; Dufrêne, Y. F. The Binding Force of the Staphylococcal Adhesin SdrG Is Remarkably Strong. *Mol. Microbiol.* **2014**, *93* (2), 356−368.
(38) Herman-Bausier, P.; Labate, C.; Towell, A. M.; Derclaye, S.; Geoghegan, J. A.; Dufrêne, Y. F. *Staphylococcus aureus* Clumping Factor A Is a Force-Sensitive Molecular Switch That Activates Bacterial Adhesion. *Proc. Natl. Acad. Sci. U. S. A.* **2018**, *115* (21), 5564−5569.
(39) Milles, L. F.; Schulten, K.; Gaub, H. E.; Bernardi, R. C. Molecular Mechanism of Extreme Mechanostability in a Pathogen Adhesin. *Science* **2018**, *359* (6383), 1527−1533.
(40) Vitry, P.; Valotteau, C.; Feuillie, C.; Bernard, S.; Alsteens, D.; Geoghegan, J. A.; Dufrêne, Y. F. Force-Induced Strengthening of the Interaction between *Staphylococcus aureus* Clumping Factor B and Loricrin. *mBio* **2017**, *8* (6), No. e01748.
(41) Marshall, B. T.; Long, M.; Piper, J. W.; Yago, T.; McEver, R. P.; Zhu, C. Direct Observation of Catch Bonds Involving Cell-Adhesion Molecules. *Nature* **2003**, *423* (6936), 190−193.
(42) Le Trong, I.; Aprikian, P.; Kidd, B. A.; Forero-Shelton, M.; Tchesnokova, V.; Rajagopal, P.; Rodriguez, V.; Interlandi, G.; Klevit, R.; Vogel, V.; Stenkamp, R. E.; Sokurenko, E. V.; Thomas, W. E. Structural Basis for Mechanical Force Regulation of the Adhesin FimH via Finger Trap-like β Sheet Twisting. *Cell* **2010**, *141* (4), 645−655.
(43) Yakovenko, O.; Sharma, S.; Forero, M.; Tchesnokova, V.; Aprikian, P.; Kidd, B.; Mach, A.; Vogel, V.; Sokurenko, E.; Thomas, W. E. FimH Forms Catch Bonds That Are Enhanced by Mechanical Force Due to Allosteric Regulation. *J. Biol. Chem.* **2008**, *283* (17), 11596−11605.
(44) Thomas, W. E.; Trintchina, E.; Forero, M.; Vogel, V.; Sokurenko, E. V. Bacterial Adhesion to Target Cells Enhanced by Shear Force. *Cell* **2002**, *109* (7), 913−923.
(45) Zhu, C.; Chen, W. Catch Bonds of Integrin/Ligand Interactions. In *Single-molecule Studies of Proteins*; Oberhauser, A. F., Ed.; Springer, 2013; pp 77−96.
(46) Zhu, C.; Chen, Y.; Ju, L. A. Dynamic Bonds and Their Roles in Mechanosensing. *Curr. Opin. Chem. Biol.* **2019**, *53*, 88−97.
(47) Prezhdo, O. V.; Pereverzev, Y. V. Theoretical Aspects of the Biological Catch Bond. *Acc. Chem. Res.* **2009**, *42* (6), 693−703.
(48) Thomas, W. E.; Vogel, V.; Sokurenko, E. Biophysics of Catch Bonds. *Annu. Rev. Biophys.* **2008**, *37* (1), 399−416.
(49) Sokurenko, E. V.; Vogel, V.; Thomas, W. E. Catch-Bond Mechanism of Force-Enhanced Adhesion: Counterintuitive, Elusive, but ... Widespread? *Cell Host Microbe* **2008**, *4* (4), 314−323.
(50) Chakrabarti, S.; Hinczewski, M.; Thirumalai, D. Plasticity of Hydrogen Bond Networks Regulates Mechanochemistry of Cell Adhesion Complexes. *Proc. Natl. Acad. Sci. U. S. A.* **2014**, *111* (25), 9048−9053.
(51) Otto, M. Physical Stress and Bacterial Colonization. *FEMS Microbiol. Rev.* **2014**, *38* (6), 1250−1270.
(52) Beaussart, A.; El-Kirat-Chatel, S.; Sullan, R. M. A.; Alsteens, D.; Herman, P.; Derclaye, S.; Dufrêne, Y. F. Quantifying the Forces Guiding Microbial Cell Adhesion Using Single-Cell Force Spectroscopy. *Nat. Protoc.* **2014**, *9* (5), 1049−1055.

https://dx.doi.org/10.1021/acs.nanolett.0c04015
Nano Lett. 2020, 20, 8919−8925

Fibronectin-binding protein B (FnBPB) from *Staphylococcus aureus* protects against the antimicrobial activity of histones

Received for publication, September 5, 2018, and in revised form, December 17, 2018 Published, Papers in Press, January 8, 2019, DOI 10.1074/jbc.RA118.005707

Giampiero Pietrocola[‡1], Giulia Nobile[‡], Mariangela J. Alfeo[‡], Timothy J. Foster[§], Joan A. Geoghegan[¶], Vincenzo De Filippis[‖], and Pietro Speziale[‡2]**

*From the [‡]Department of Molecular Medicine, Unit of Biochemistry, University of Pavia, 27100 Pavia, Italy, the [§]Microbiology Department, Trinity College Dublin, Dublin 2, Ireland, the [¶]Department of Microbiology, Moyne Institute of Preventive Medicine, School of Genetics and Microbiology, Trinity College, Dublin, Dublin 2, Ireland, the [‖]Laboratory of Protein Chemistry and Molecular Hematology, Department of Pharmaceutical and Pharmacological Sciences, University of Padua, 36131 Padova, Italy, and the **Department of Industrial and Information Engineering, University of Pavia, 27100 Pavia, Italy*

Edited by Roger J. Colbran

Staphylococcus aureus **is a Gram-positive bacterium that can cause both superficial and deep-seated infections. Histones released by neutrophils kill bacteria by binding to the bacterial cell surface and causing membrane damage. We postulated that cell wall–anchored proteins protect *S. aureus* from the bactericidal effects of histones by binding to and sequestering histones away from the cell envelope. Here, we focused on *S. aureus* strain LAC and by using an array of biochemical assays, including surface plasmon resonance and ELISA, discovered that fibronectin-binding protein B (FnBPB) is the main histone receptor. FnBPB bound all types of histones, but histone H3 displayed the highest affinity and bactericidal activity and was therefore investigated further. H3 bound specifically to the A domain of recombinant FnBPB with a K_D of 86 nM, ~20-fold lower than that for fibrinogen. Binding apparently occurred by the same mechanism by which FnBPB binds to fibrinogen, because FnBPB variants defective in fibrinogen binding also did not bind H3. An FnBPB-deletion mutant of *S. aureus* LAC bound less H3 and was more susceptible to its bactericidal activity and to neutrophil extracellular traps, whereas an FnBPB-overexpressing mutant bound more H3 and was more resistant than the WT. FnBPB bound simultaneously to H3 and plasminogen, which after activation by tissue plasminogen activator cleaved the bound histone. We conclude that FnBPB provides a dual immune-evasion function that captures histones and prevents them from reaching the bacterial membrane and simultaneously binds plasminogen, thereby promoting its conversion to plasmin to destroy the bound histone.**

Staphylococcus aureus is a leading cause of diverse infections ranging from mild skin diseases such as impetigo, cellulitis, and skin abscesses to serious invasive diseases, including sepsis, endocarditis, osteomyelitis, toxic shock syndrome, and necrotizing pneumoniae (1, 2). Strains that are resistant to multiple antibiotics are a major problem in healthcare settings in developed countries (3). These are referred to as hospital-associated methicillin-resistant *S. aureus* (MRSA)[3] and occur in individuals with pre-disposing risk factors, such as surgical wounds and indwelling medical devices (4, 5). Recently, there has been a dramatic increase in the incidence of community-associated MRSA infections that occur in otherwise healthy individuals (6, 7). Community-associated MRSA strains, exemplified by the USA300 clone (8), express a low level of resistance to β-lactam antibiotics and cause serious skin and soft tissue infections (9–11).

S. aureus expresses a plethora of virulence factors, including both secreted and cell wall-anchored (CWA) proteins. The latter mediate adherence to the extracellular matrix, promote invasion of and survival within host cells, neutralize phagocytes, and modulate the immune response (12). CWA proteins are covalently anchored to peptidoglycan via a conserved C-terminal sorting signal mediated by the membrane-associated sortase A (13). Fibronectin-binding proteins FnBPA and FnBPB are CWA proteins belonging to the microbial surface components recognizing adhesive matrix molecules (MSCRAMMs) family. The N-terminal A domain of FnBPs comprises three separately folded subdomains N1, N2, and N3 (14, 15). The minimum ligand-binding region of the A domain (N2–N3) comprises two IgG-like folded subdomains that bind fibrinogen (FBG) by the dock, lock, and latch mechanism (DLL) (15, 16) in a similar fashion to clumping factor A (ClfA) (17). Between the N2 and N3 subdomains lies a wide hydrophobic trench that accommodates the ligand, in the case of ClfA, FnBPA, and FnBPB the extreme C terminus of the γ-chain of FBG. According to this mechanism, the ligand first docks into the trench, and this is followed by a conformational change and redirection

This work was supported by Fondazione CARIPLO Grant Vaccines 2009-3546 (to P. S.) and in part by PRAT-2015 Grant (to V. D. F.). The authors declare that they have no conflicts of interest with the contents of this article.

[1] To whom correspondence may be addressed: Dept. of Molecular Medicine, Unit of Biochemistry, University of Pavia, Viale Taramelli 3/b, 27100 Pavia, Italy. E-mail: giampiero.pietrocola@unipv.it.

[2] To whom correspondence may be addressed: Dept. of Molecular Medicine, Unit of Biochemistry, University of Pavia, Viale Taramelli 3/b, 27100 Pavia, Italy. E-mail: pspeziale@unipv.it.

[3] The abbreviations used are: MRSA, methicillin-resistant *S. aureus*; Bbp, bone sialoprotein-binding protein; ClfA, clumping factor; CNA, collagen adhesin; CTH, calf thymus histone; CWA, cell wall–associated protein; FBG, fibrinogen; FnBPA, fibronectin-binding protein A; FnBPB, fibronectin-binding protein B; MBC, minimum bactericidal concentration; NEM, *N*-ethylmaleimide; NET, neutrophil extracellular trap; MSCRAMM, microbial surface component recognizing adhesive matrix molecule; PLG, plasminogen; PBST, PBS containing Tween 20; Pls, plasmin-sensitive protein; t-PA, tissue plasminogen activator; PMA, phorbol 12-myristate 13-acetate; DLL, dock, lock, and latch; HRP, horseradish peroxidase; BHI, brain heart infusion.

of the disordered C-terminal extension of the N3 subdomain resulting in its folding over the bound ligand to lock it in place. In the final latching step, the complex is stabilized by inserting the "latch" region in the N3 extension into the N2 subdomain through a β-strand complementation (18, 19). The N2–N3 subdomains of both FnBPA and FnBPB each comprise seven distinct isoforms (14, 20), also bind elastin (21) and plasminogen (PLG) (22), and promote biofilm formation by homophilic interactions (23). The C terminus of FnBPs comprises 10/11 tandemly repeated fibronectin-binding domains that bind type I modules of fibronectin by the tandem β-zipper mechanism (24, 25).

In eukaryotes, DNA is wrapped around a core complex of the histones H2A, H2B, H3, and H4 to form the nucleosome. Histones are the most abundant proteins in neutrophil extracellular traps (NETs), which are released by neutrophils as part of the innate defenses against infecting bacteria (26). In addition to histones, NETs contain nuclear DNA and proteases (*e.g.* elastase). Histones are also released into the bloodstream during severe sepsis (27). The potent antimicrobial activity of histones is due to characteristics akin to cationic antimicrobial peptides such as cathelicidins. Besides NETs, other myeloid cell lineages such as basophils (28), eosinophils (29), and macrophages (30) can deploy histones within DNA-based extracellular traps. In addition, histones can induce production of chemokines and elicit leukocyte recruitment (31).

Histones are classified as lysine-rich (H1, H2A, and H2B) and arginine-rich (H3 and H4) (32). H2A, H3, and H4 have been shown to have anti-staphylococcal activity (33), but the mechanistic basis differs. H3 and H4 cause membrane damage with blebbing and pore formation, whereas H2B disrupts the integrity of the cell without obvious morphological changes (33).

In Gram-positive (34, 35) and Gram-negative (36) bacteria, surface components can bind histones and provide protection from bactericidal effects. Lipoteichoic acid (37), the cell wall–anchored M1 protein (35), and the secreted protein SIC of *Streptococcus pyogenes* (38) bind to and promote resistance to histones. In the Gram-negative *Klebsiella pneumoniae* and *Shigella flexneri*, the polysaccharide O-antigen of lipopolysaccharide in the outer membrane can contribute to resistance to histones (36).

In this study, we have investigated the molecular basis of resistance to histones in *S. aureus* and found that FnBPB is the major surface component responsible. We studied the mechanism of histone binding by FnBPB and identified the most potent anti-staphylococcal histone as H3.

Results

Cell wall–anchored proteins bind histones

S. aureus is known to bind to histones, but the bacterial components responsible have not been characterized. To determine whether CWA proteins contribute to histone binding, the USA 300 strain LAC (8) and a sortase A-deficient mutant (*srtA*) (39) lacking CWA proteins were tested for their ability to adhere to a surface-coated with pooled calf thymus histones (CTH). WT LAC adhered about three times more strongly than the *srtA* mutant, which suggests that one or more CWA proteins are dominant histone binders (Fig. 1). The residual binding by the *srtA* mutant could be due to other surface components such as lipoteichoic acid (33, 37).

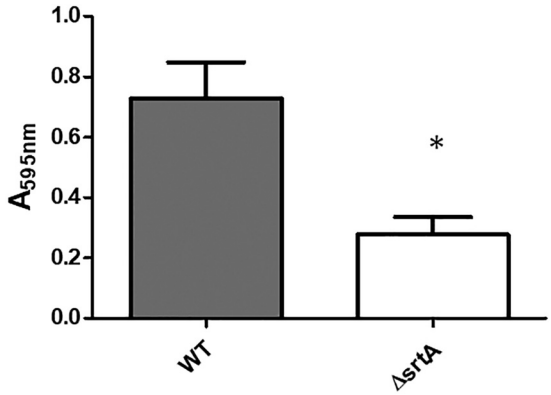

Figure 1. Adherence of bacteria to CTH-coated microtiter wells. Microtiter wells coated with CTH were incubated with *S. aureus* USA 300 LAC cells. After washing with PBS, adherent cells were fixed and stained with crystal violet, and the absorbance at 595 nm was measured using an ELISA plate reader. Means and S.D. of the results of two independent experiments, each performed in triplicate, are indicated. A statistically significant difference is indicated (Student's *t* test; *, $p < 0.05$).

Recombinant FnBPB binds histones

Purified recombinant ligand-binding domains of several CWA proteins were tested for binding to immobilized CTH in an ELISA-type assay. In particular, subdomains N2–N3 of isoform I of FnBPB, comprising residues 163–480 (FnBPB(163–480)), bound strongly to the histone mixture, whereas the N-terminal ligand-binding domains of isoform I of FnBPA, clumping factors A and B, the collagen-binding protein CNA, and also Bbp and Pls, did not bind detectably (Fig. 2*A*). Control experiments showed that the anti-His tag antibody used in these ELISA experiments recognize all recombinant proteins similarly.

The specificity of FnBPB binding to histones was confirmed by performing dose-response binding assays with immobilized CTH. FnBPB(163–480) bound dose-dependently and saturably, whereas no binding of FnBPA(194–511) was observed (Fig. 2*B*).

The ability of recombinant FnBPB(163–480) to bind to individual histones was next measured by ELISA and far-Western blotting. FnBPB(163–480) bound H1 and H3 the strongest (Fig. 3, *A* and *B*). It was decided to focus on binding to H3 rather than H1 because the former exhibited stronger anti-bacterial activity (see below).

The A domain of FnBPB binds to FBG by the dock, lock, and latch (DLL) mechanism (16). To investigate whether DLL is involved in histone binding, variants of the recombinant A domain lacking the ability to bind FBG were tested for histone binding. A truncate lacking the 17 residues involved in the locking and latching steps of DLL(464–480) and a mutant with substitutions of Asn-312 and Phe-314 located in the peptide binding trench, neither of which bound FBG, were also defective in binding to histone H3. Furthermore, neither single recombinant subdomains N2(163–308) nor N3(309–480) bound FBG or histone H3 (Fig. 3*C*). These data suggest that histones could bind FnBPB by the DLL mechanism.

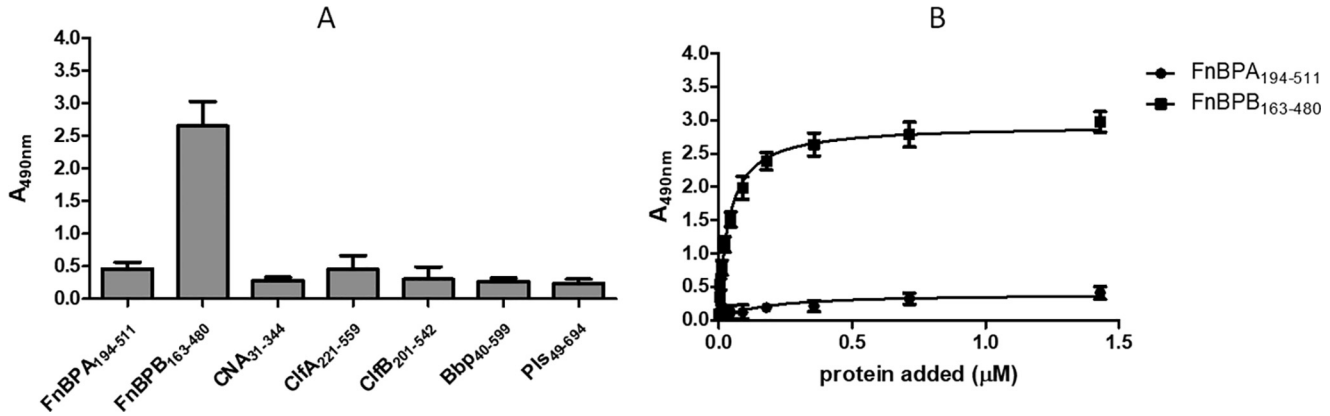

Figure 2. Binding of recombinant CWA proteins to immobilized CTH. *A,* microtiter wells coated with CTH were incubated with purified recombinant A domains of the indicated CWA proteins of *S. aureus*. Bound proteins were detected with mouse anti-hexahistidine mAb 7E8 followed by HRP-conjugated rabbit anti-mouse IgG. *B,* microtiter wells coated with CTH were incubated with increasing concentrations of purified recombinant N2N3 domains of FnBPA (FnBPA(194–511)) or FnBPB (FnBPB(163–480)). Bound proteins were detected as described above. The data points are the means (±S.D.) of two independent experiments, each performed in triplicate.

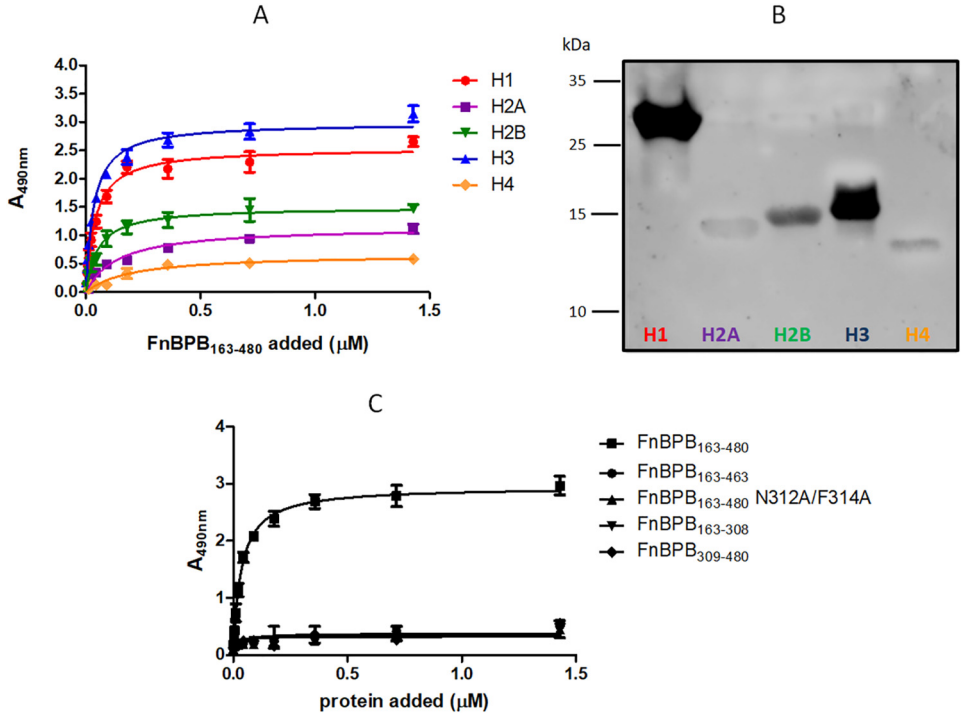

Figure 3. FnBPB(163–480) binding to different histone subtypes. *A,* microtiter wells coated with different histone subtypes were incubated with increasing concentrations of recombinant FnBPB(163–480) domain. Bound protein was detected with rabbit FnBPB(163–480) polyclonal antibody followed by HRP-conjugated goat anti-rabbit IgG. Means and S.D. of results of two independent experiments, each performed in triplicate, are presented. *B,* different histone subtypes were subjected to SDS-PAGE and transferred to a nitrocellulose membrane. The membrane was probed with FnBPB(163–480) followed by a rabbit anti-FnBPB(163–480) polyclonal IgG and HRP-conjugated goat anti-rabbit IgG. *C,* microtiter wells coated with histone H3 were incubated with increasing concentrations of recombinant variants of FnBPB A domain. Bound proteins were detected with mouse anti-hexahistidine mAb 7E8 followed by HRP-conjugated rabbit anti-mouse IgG. The data points are the means (±S.D.) of two independent experiments, each performed in triplicate.

Analysis of complex formation between FnBPB(163–480) and H3 by gel-filtration chromatography

To determine whether FnBPB(163–480) forms a complex with H3 in solution, equimolar amounts of the two proteins were mixed and subjected to gel-filtration chromatography (Fig. 4). The two proteins alone eluted with distribution constants (K_{av}) corresponding to their molecular masses, *i.e.* ~15 kDa for H3 and 35 kDa for FnBPB(163–480) (Fig. 4, *inset*), whereas co-incubation of the two proteins yielded a fast running peak of ~50 kDa, in agreement with the predicted molecular mass of FnBPB(163–480)/H3 complex. In contrast, the nonhistone-binding trench mutant failed to form the 50-kDa complex. This shows that FnBPB(163–480) can form a stable complex with H3 in solution and that residues in the FBG-binding trench are crucially important.

Measurement of the affinity and ionic strength-dependence of H3–FnBPB(163–480) interaction

Surface plasmon resonance—The affinity of FnBPB for human H3 was measured by surface plasmon resonance. Recombinant

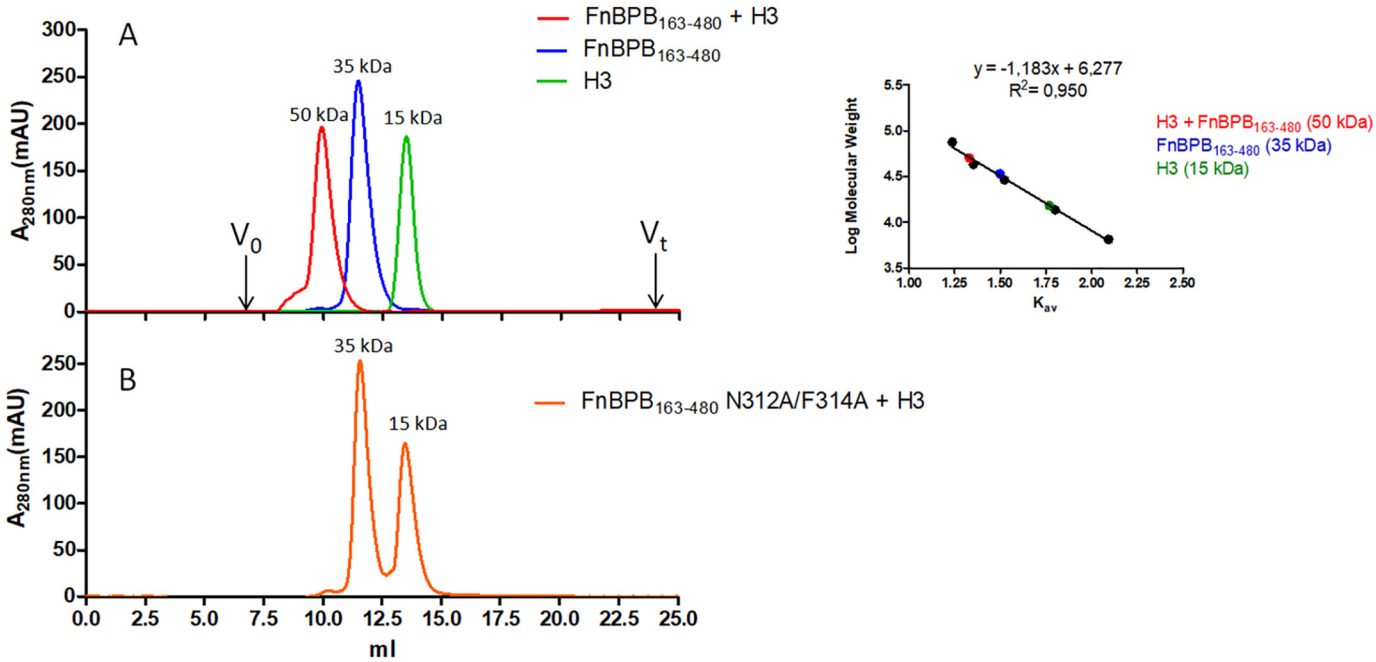

Figure 4. Size-exclusion chromatography analysis of the interaction of FnBPB(163–480) with histone H3. *A*, elution profiles of FnBPB(163–480), histone H3 alone, and a mixture of a co-incubated, equimolar concentrations of FnBPB and H3 loaded onto a Superdex 75 10/300 GL gel-filtration chromatography column. *B*, elution profile of a mixture of co-incubated, equimolar concentrations of FnBPB(163–480) trench mutant variant (N312A/F314A) and histone H3 loaded onto the gel-filtration chromatography column as indicated in *A*. In the *inset*, a calibration curve relating the K_{av} of standard proteins to their molecular mass is reported. The figure is representative of three independent experiments. *mAU*, milli-absorbance units.

FnBPB(163–480) was passed over human H3 immobilized on the surface of a dextran chip in concentrations ranging from 3.9 to 500 nM. The equilibrium dissociation constant, K_D, for the interaction was estimated as 86.0 ± 12.5 nM, an affinity that is ~20-fold higher than that reported for the interaction between FnBPB and FBG (Fig. 5*A*) (20). No signal was detected when the FnBPB(163–480) trench mutant was analyzed (Fig. 5*B*). These data show that FnBPB(163–480) has a high affinity for H3 in solution and that the interaction most likely occurs by the DLL mechanism.

Nature of the interaction between FnBPB(163–480) and H3—The FnBPB(163–480) protein has a hypothetical pI of 5.62 indicating that the protein is anionic at physiological pH, whereas H3 is highly positive (pI 12.5). To further investigate the nature of interaction of H3 with FnBPB(163–480), surface-coated H3 was incubated with FnBPB(163–480) in the presence of increasing amounts of NaCl. At a NaCl concentration of 500 mM, binding of FnBPB(163–480) was reduced by more than 80%. No FnBPB(163–480) binding was observed at higher NaCl concentrations, suggesting that hydrophobic forces are not involved in the interaction and that FnBPB(163–480) binding to H3 is an ionic strength-dependent process (Fig. 5*C*).

Interaction of H3 with FnBPB isoforms

There are seven isoforms of FnBPB with amino acid sequence identities ranging from 61 to 85% (20). Each of the isoforms bind FBG, fibronectin, elastin, and PLG. To determine whether all isoforms bind H3, increasing concentrations of the recombinant N2–N3 subdomains were tested for their ability to bind surface-coated H3 in an ELISA-type assay (Fig. 6). Isoforms II, III, and VI bound similarly to isoform I with dissociation constants in the range of 50–185 nM, whereas the isoforms IV, V, and VII showed a lower binding affinity, with apparent K_D values ranging from 270 to 830 nM (Fig. 6*A*, *inset*).

FnBPB promotes binding of S. aureus to H3

To investigate whether FnBPB expressed on the surface of *S. aureus* mediates binding to H3, WT *S. aureus* LAC, a deletion mutant lacking the *fnbA* and *fnbB* genes (40), and the mutant expressing isoform I FnBPA or FnBPB from a multicopy plasmid (40) were tested for their ability to adhere to immobilized H3 and to capture soluble H3 onto the cell surface. The Δ*fnbAfnbB* mutant lacked the ability to adhere to immobilized H3, compared with the parental strain. In contrast, the mutant expressing FnBPB adhered more strongly than the WT strain, whereas the mutant expressing FnBPA did not adhere (Fig. 7*A*).

Bacteria were incubated with soluble H3 and washed, and the bound H3 was eluted by incubating with extraction buffer containing SDS. Released H3 was detected by SDS-PAGE/Western immunoblotting and measured by ELISA. In both experiments, WT *S. aureus* LAC captured H3, whereas the Δ*fnbAfnbB* mutant did not bind H3 detectably. In contrast, the mutant expressing FnBPB captured ~40% more H3 than the WT, most likely due to overexpression of FnBPB from the multicopy plasmid (Fig. 7, *B* and *C*). These data are consistent with results obtained above with recombinant proteins and show that FnBPB is the major surface protein involved in binding H3.

Histone bactericidal activity and resistance to killing promoted by FnBPB

It has been widely reported that soluble histones kill many species of Gram-negative and Gram-positive bacteria and that

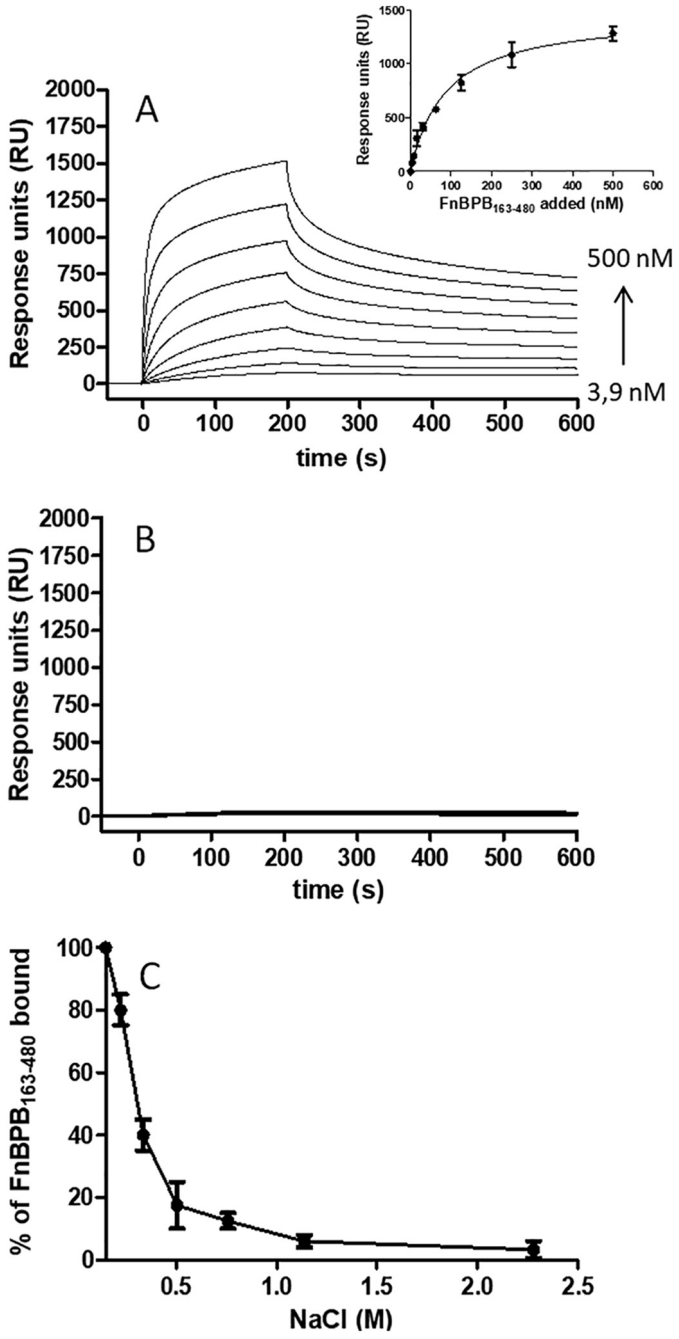

Figure 5. Affinity and ionic strength–dependence of interaction of the H3–FnBPB(163–480). *A,* representative sensorgrams display binding of FnBPB(163–480) to and dissociation from CM5 chip-coated histone H3. The affinity was calculated from curve fitting to a plot of the response unit values at the steady state (RU_{max}) against increasing concentrations of FnBPB(163–480) (*inset*). *B,* representative sensorgrams display binding of FnBPB(163–480) trench mutant variant (N312A/F314A) to and dissociation from H3. The figure shown is representative of three independent experiments. *C,* FnBPB(163–480) bound to H3 was analyzed under increasing concentrations of NaCl. FnBPB(163–480) bound to immobilized H3 was detected using a specific anti-FnBPB antibody.

they are often more potent than cationic antimicrobial defensin peptides. The minimum bactericidal concentration (MBC) required to kill >99.9% of a standard suspension of *S. aureus* cells was measured and used to compare the potency of different histones toward WT *S. aureus* LAC. Histones H3 and H4 had significantly lower MBC values compared with H1, H2A, and H2B indicating that they have more potent bactericidal activity (Fig. 8*A*).

The MBC of histone H3 toward the variants of *S. aureus* LAC described above were measured. The MBC of H3 for the Δ*fnbAfnbB* mutant was ~3-fold lower than the WT LAC, whereas the mutant overexpressing FnBPB from a multicopy plasmid had an ~7-fold higher MBC than the mutant, which is consistent with the overexpressed FnBPB protein providing enhanced protection from the bactericidal activity of H3 (Fig. 8*B*). The MBC of H3 measured for the *clfA* mutant was similar to that for WT LAC, indicating that a mutation in a gene encoding a CWA protein other than *fnbB* does not affect the killing activity of H3 (Fig. 8*B*). Consistent with a significantly reduced binding to histones (Fig. 1), the *srtA* mutant showed a high susceptibility to H3 killing, as indicated by an ~4-fold lower MBC value than the WT LAC (Fig. 8*B*). To further demonstrate the specificity of H3 binding to FnBPB, we also measured the MBC values of histone H4 for the LAC WT, the Δ*fnbAfnbB* mutant, the mutant overexpressing FnBPA or FnBPB, the *srtA* mutant, and the *clfA* mutant. As shown in Fig. 8*C*, the MBC values of H4 for the WT and the *fnb* mutants and complemented strains were very similar. In contrast, the MBC of H4 for *srtA* mutant was 4-fold lower than WT, indicating a higher susceptibility of the mutant to H4.

Soluble recombinant FnBPB(163–480) was added to a suspension of LAC Δ*fnbAfnbB* mutant cells to determine whether the protein protected susceptible bacteria from the bactericidal activity of H3. WT FnBPB(163–480) promoted survival of the mutant, whereas proteins defective in the ability to bind FBG and H3 failed to offer any protection. These data are consistent with FnBPB binding to soluble H3 and neutralizing its bactericidal activity (Fig. 9*A*).

S. pyogenes, also known as group A *Streptococcus*, is a Gram-positive bacterium for which the bactericidal action of histones has been previously demonstrated (34, 35). Thus, we asked whether soluble FnBPB(163–480) could competitively neutralize the bactericidal activity of H3 for this bacterium. The MBC value of H3 for the *S. pyogenes* serotype M1 strain 71-695 was ~75 μg/ml, and exogenous addition of 5 μM FnBPB(163–480) to the MBC assay resulted in a 2-fold increase in resistance to the killing activity of H3. In a similar experimental approach, the MBC for *S. aureus* LAC was ~6 μg/ml, and a 3-fold increase of MBC was produced when *S. aureus* WT LAC was incubated with H3 in the presence of 1 μM FnBPB(163–480) (Fig. 9*B*). Together, these data demonstrate that in both bacterial species soluble FnBPB(163–480) can confer resistance to H3-mediated killing.

To determine whether FnBPBs expressed by different strains of *S. aureus* also protected bacteria from the bactericidal effects of histones, the MBCs of H3 toward strains BH1CC (4), 8325-4 (42), and SH1000 (43) that express isoform I FnBPB and P1 (44) that expresses isoform IV FnBPB were very similar, although mutants lacking FnBPs (4, 21, 22, 45) were ~3-fold more susceptible. This shows that both isoform I and isoform IV of FnBPB protect different strains of *S. aureus* to a similar degree despite isoform IV binding H3 less strongly than isoform I *in vitro* (Fig. 9*C*).

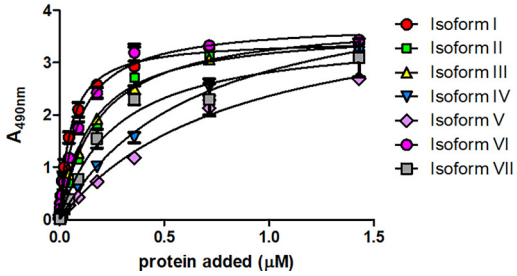

FnBPB isoform	K_D (nM)
I	52,3 ± 5,4
II	185,6 ± 13,1
III	152,1 ± 10,2
IV	636,7 ± 62,8
V	832,0 ± 99,4
VI	93,4± 6,4
VII	268,1 ± 49,4

Figure 6. Dose-dependent binding of FnBPB isoforms to surface-coated histone H3. Histone H3 was immobilized onto microtiter wells and tested for binding to recombinant N2–N3 domains of isoforms I–VII of FnBPB. Bound isoforms were detected with mouse anti-His mAb 7E8 followed by HRP-conjugated rabbit anti-mouse IgG. In the *inset,* the K_D values of each isoform are reported. The data points are the means ± S.D. of three independent experiments each performed in triplicate.

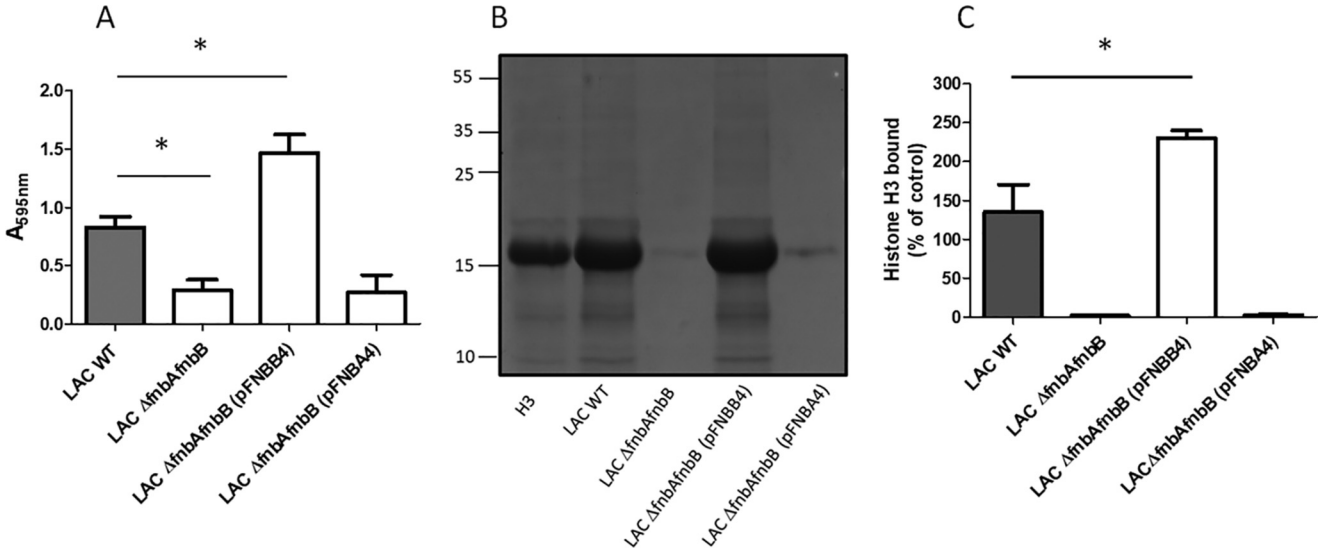

Figure 7. Interaction of *S. aureus* USA 300 LAC with histone H3. *A,* microtiter wells coated with histone H3 were incubated with cells of the indicated bacteria. Wells were washed with PBS, fixed with formaldehyde, and stained with crystal violet, and the absorbance at 595 nm was measured in an ELISA plate reader. Means and S.D. of results of two independent experiments, each performed in triplicate, are presented. Statistically significant differences is indicated (Student's *t* test; *, $p < 0.05$). *B, S. aureus* strain USA 300 LAC, the double mutant Δ*fnbAfnbB,* or the mutant overexpressing FnBPB or FnBPA was incubated with histone H3. After several washings, proteins bound to the cell surface were released by extraction buffer, separated by SDS-PAGE under nonreducing conditions, and transferred to a nitrocellulose membrane. The membrane was sequentially probed with rabbit anti-histone IgG and HRP-conjugated goat anti-rabbit IgG. The figure is representative of two independent experiments. *C,* densitometric analysis of histone H3 binding to *S. aureus* LAC and its mutants as reported in *B*. The band intensity was quantified relative to a sample of pure histone H3 (5 μg, 100 intensity). The reported data are the mean values ± S.D. from two independent experiments. Statistically significant differences are indicated (Student's *t* test; *, $p < 0.05$).

FnBPB expression protects S. aureus from NETs

To determine whether histones released when neutrophils undergo NETosis exert bactericidal activity toward *S. aureus,* human neutrophils were stimulated to release NETs using a protein kinase C agonist and then incubated with the *S. aureus* LAC variants described previously. The Δ*fnbAfnbB* mutant survived less well than WT LAC, whereas the mutant overexpressing FnBPB survived much better than the mutant or indeed the WT. Strains expressing FnBPA were not protected (Fig. 10*A*). Treatment of the NETs with protease-free DNase allowed the Δ*fnbAfnbB* mutant and the mutant expressing FnBPA to survive to the same degree as WT LAC and the FnBPB-overexpressing strain (Fig. 10*B*). This indicates that bacteria must be entrapped within the DNA of the NETs for maximum bactericidal activity. Degradation of the NETs is likely to cause bactericidal proteins to be dissipated and diluted. Incubation of the NET with anti-histone antibody also restored survival of the Δ*fnbAfnbB* mutant and the mutant expressing FnBPA to the same level as WT and the mutant expressing FnBPB, which suggests that histones are the major bactericidal factors acting against *S. aureus* in NETs (Fig. 10*C*).

Activated plasminogen captured by FnBPB cleaves H3 and enhances bacterial survival

We previously showed that FnBPs expressed on the surface of *S. aureus* can capture PLG, which can be activated by PLG activators to cleave FBG (22). Hence, we investigated whether recombinant FnBPB could simultaneously bind PLG and histone H3. FnBPB(163–480) was immobilized in microtiter plate wells and tested for binding of histone H3 in the presence of saturating amounts of PLG in an ELISA-type assay. The level of bound PLG remained the same (as detected with a specific antibody) in increasing concentrations of H3 (Fig. 11*A*). A similar result was obtained when increasing concentrations of PLG were added in the presence of a saturating concentration of H3 (Fig. 11*B*). Together, these data indicate that PLG and H3 bind to distinct sites on FnBPB consistent with H3 binding by the DLL mechanism.

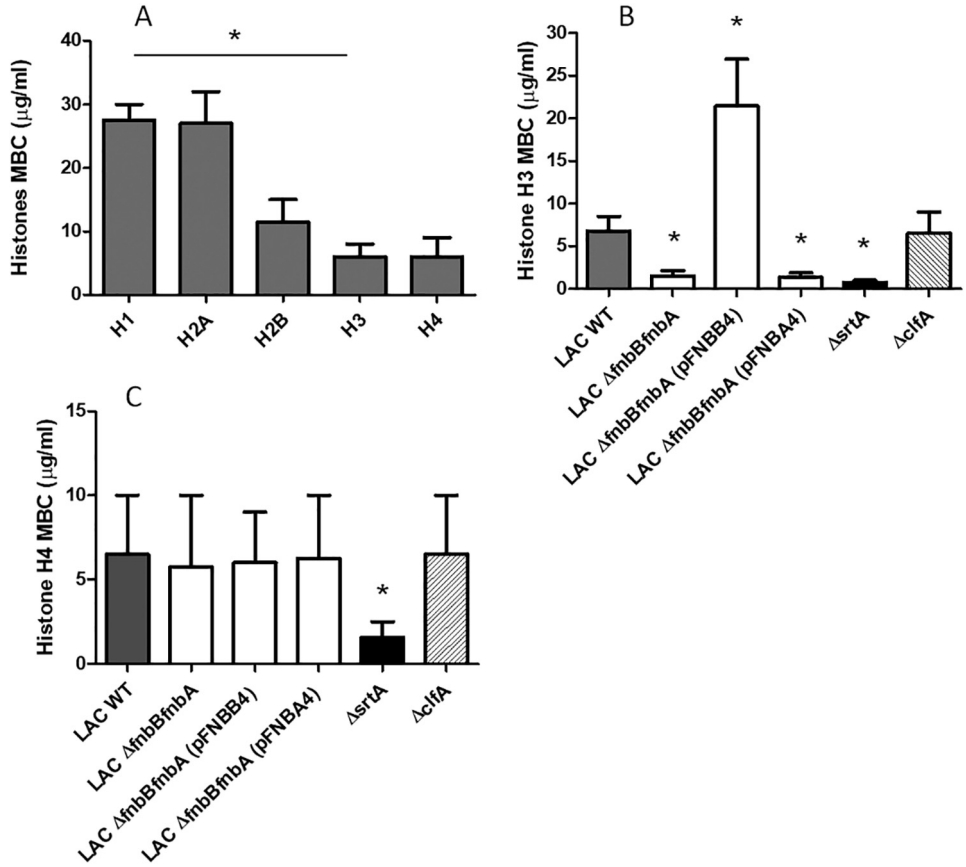

Figure 8. FnBPB expression on the surface of *S. aureus* LAC cells protects against the killing activity of histones. *A,* to determine the MBC of histones, cells of *S. aureus* LAC were incubated with the indicated increasing amounts of individual histones. After incubation, cell mixtures were plated on BHI agar, and colony counts were determined. Cells of *S. aureus* LAC, the Δ*fnbAfnbB* mutant, the mutant overexpressing FnBPA or FnBPB, and *clfA* and the *srtA* mutants were tested in the MBC assay with histone H3 in *B* or histone H4 in *C*. After incubation, serial dilutions of the cell mixtures were plated onto BHI agar and colony counts determined.

To determine whether bacteria-bound PLG can be activated by tissue plasminogen activator (t-PA) and can cleave H3, *S. aureus* LAC Δ*fnbAfnbB* cells expressing high levels of FnBPB from a multicopy plasmid were immobilized and incubated with PLG. After washing, both H3 and t-PA were added and incubated for different times. SDS-PAGE analysis revealed that H3 was rapidly degraded, whereas no cleavage of H3 was seen in controls incubated with PLG or t-PA alone. Interestingly, as reported previously (22), PLG bound to Δ*fnbAfnbB* mutant cells, and when activated to plasmin, it degraded H3 (Fig. 12*A*). In any case, it remains to be established whether activated PLG preferentially degrades bacteria-bound H3 rather than free H3 (or both).

In support of specific plasmin generation on the surface of bacterial cells, the serine protease inhibitor aprotinin was found to inhibit H3 degradation. In contrast, complete cleavage of H3 was observed when the incubation was carried out in the presence of the cysteine protease inhibitor *N*-ethylmaleimide (NEM) (Fig. 12*B*). To investigate the possibility that activated PLG also degraded surface-expressed FnBPB, immobilized cells of *S. aureus* LAC Δ*fnbAfnbB* expressing (p-FnBPB) were incubated with PLG, and the complex was activated with t-PA. No signal was detected when the supernatant obtained from the incubation mixture was analyzed for the presence of FnBPB digestion products by Western immunoblotting, suggesting that FnBPB is not cleaved by bacteria-bound PLG (data not shown).

Next, the ability of activated PLG to protect *S. aureus* from the bactericidal activity of histone H3 was investigated. *S. aureus* LAC Δ*fnbAfnbB* cells expressing high levels of FnBPB from a multicopy plasmid were incubated with PLG and t-PA, and the MBC of H3 was found to be ~50 μg/ml. For bacteria incubated with PLG without t-PA, the MBC was ~2-fold lower. An almost identical MBC value was obtained even in the presence of equimolar concentrations of FBG, suggesting that H3 preferentially binds to FnBPB and cleaved by PLG (Fig. 12*C*).

Discussion

Histones are constituents of the nucleosome in the nucleus of mammalian cells where they act to compact DNA and regulate gene expression. However, it is becoming apparent that histones also occur outside the nucleus, for example in granules of phagocytic cells or mucosal surfaces, including the human stomach, and are released into the bloodstream at elevated levels during sepsis. Histones are also secreted by sebocytes of the sebaceous gland in the skin and are thought to have antimicrobial activity against commensals living in the skin such *S. aureus* (46).

Several reports indicate that *S. aureus* can bind histones, but virtually nothing is known about the factors involved or the

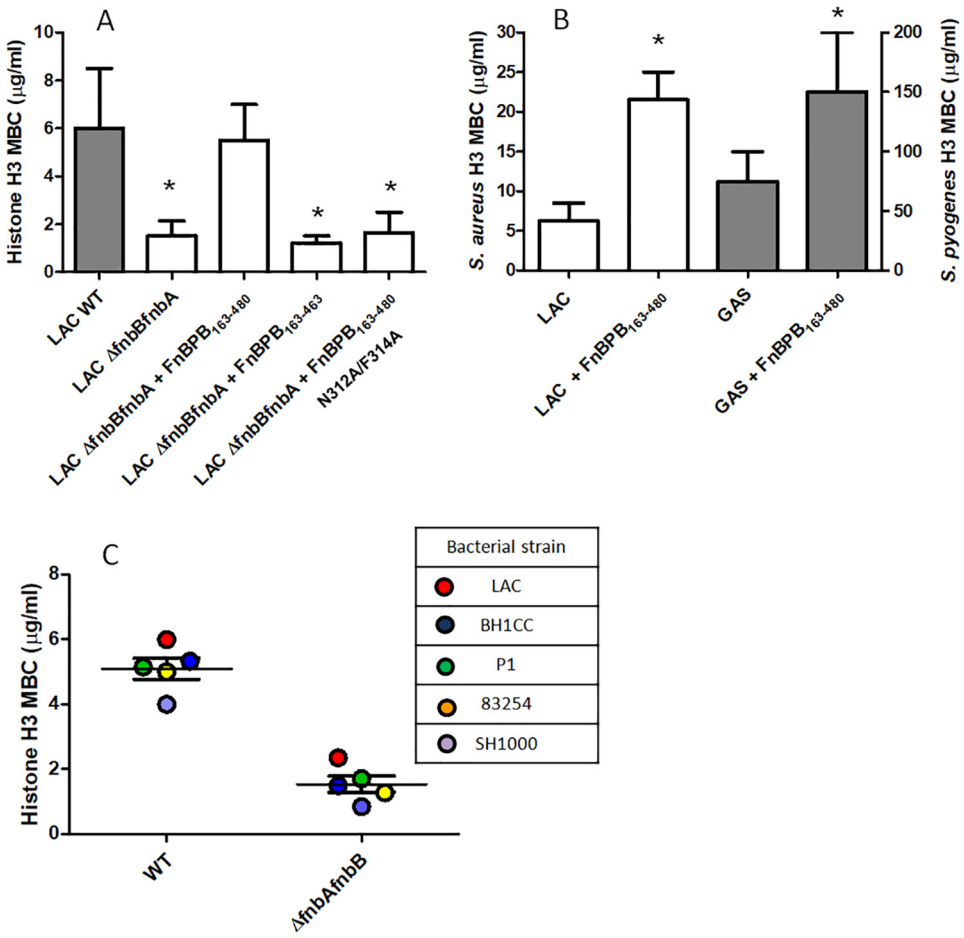

Figure 9. Comparison of MBC values of H3 for *S. pyogenes* and *S. aureus* strains. *A,* to evaluate the potential attenuation of microbicidal activity of histone H3 by soluble FnBPB(163–480), cells of *S. aureus* Δ*fnbAfnbB* mutant were tested in the MBC assay for killing by H3 in the presence of recombinant FnBPB(163–480) or its variants. After incubation, serial dilutions of the cell mixtures were plated on BHI agar and colonies counted. The MBC for WT is reported as control. Data are the mean values ± S.D. from three independent experiments. Statistically significant differences compared with the WT are indicated (Student's *t* test; *, $p < 0.05$). *B,* to determine the neutralizing effect of soluble FnBPB(163–480) on the bactericidal effect of H3 for *S. pyogenes* 71-695 and *S. aureus* LAC, bacteria were incubated in the presence/absence of FnBPB(163–480). Following incubation, serial dilutions of the mixtures were plated on BHI agar and colonies counted. Data shown are the mean values ± S.D. from three independent experiments. Statistically significant differences compared with the untreated WT are indicated (Student's *t* test; *, $p < 0.05$). *C,* protective effect of FnBPB expression against cytotoxicity of histone H3 was assessed by evaluating the MBC against different *S. aureus* strains and their *fnb* mutants.

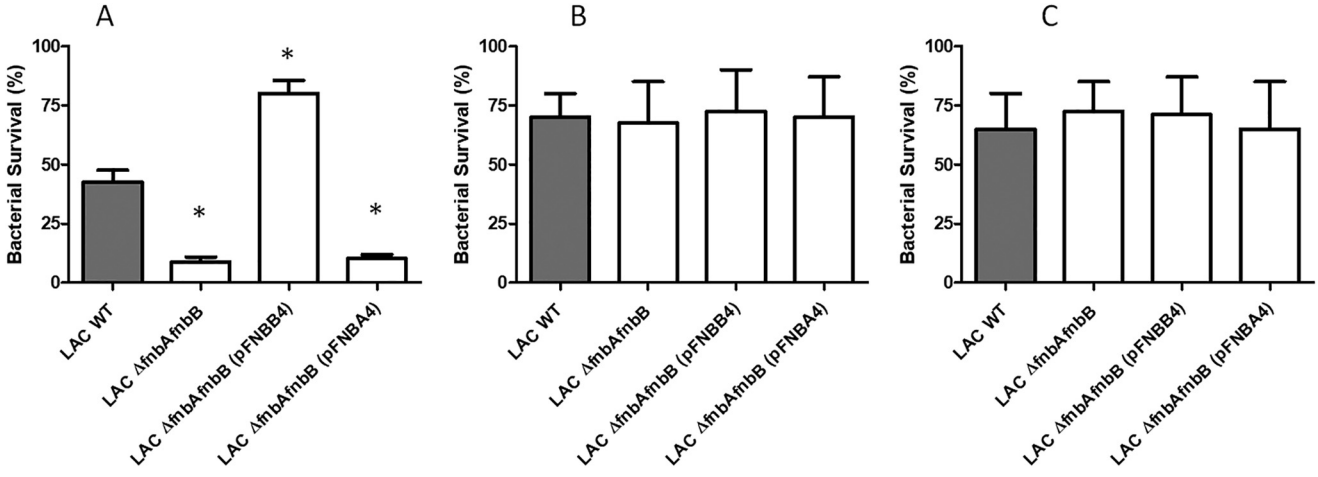

Figure 10. FnBPB protein protects against histones released from neutrophils. *A,* neutrophils were stimulated with PMA to induce NETs and then incubated with *S. aureus* LAC, the Δ*fnbAfnbB* mutant, and the complemented mutant overexpressing FnBPA or FnBPB. After incubation, dilutions were plated on BHI agar and the colony counts determined. *B,* NETs treated with DNase I. *C,* NETs treated with anti-histone antibodies prior to infection. Surviving colony-forming units were calculated relative to initial inoculum incubated with untreated NETs.

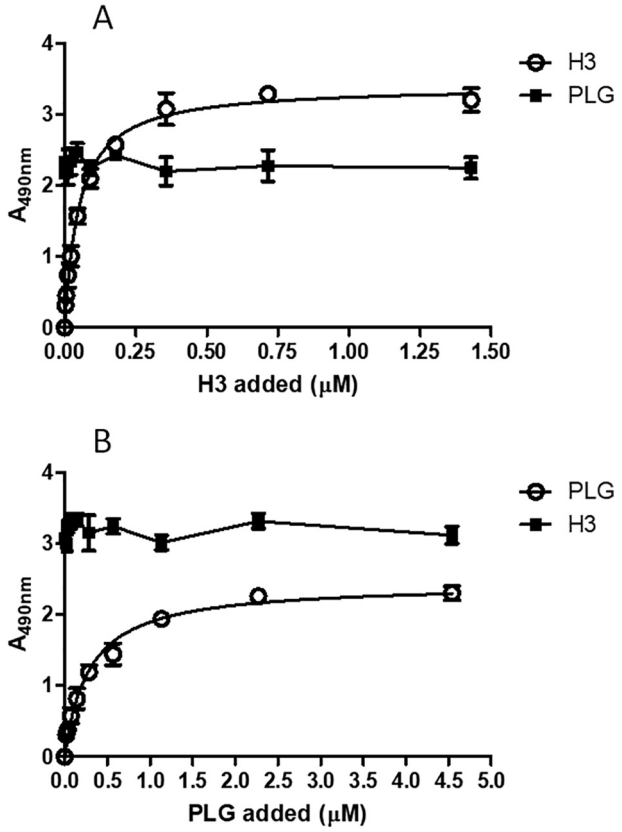

Figure 11. Binding of FnBPB to H3 in the presence of PLG. *A,* recombinant FnBPB(163–480) was immobilized on the surface of microtiter wells. Saturating concentrations of PLG were added along with increasing concentrations of H3. Bound PLG was detected with rabbit anti-PLG IgG followed by HRP-conjugated goat anti-rabbit IgG (*solid squares*). In the same panel, binding of increasing amounts of H3 to the wells is also reported (*open circles*). Bound H3 was detected with rabbit anti-histone antibodies followed by HRP-conjugated goat anti-rabbit IgG. *B,* ELISA-type assay with rFnBPB immobilized on the surface of microtiter wells. Saturating concentrations of H3 were added along with increasing amounts of PLG. Bound H3 was detected with rabbit anti-histones IgG followed by HRP-conjugated goat anti-rabbit IgG (*solid squares*). The *panel* shows binding of increasing amounts of PLG to the wells (*open circles*). Bound proteins were detected with specific antibodies as in *A*. The data points reported in the panels are the means ±S.D. of three independent experiments each performed in triplicate.

mechanism of bactericidal action (33). This study began by showing that a sortase mutant bound a lower level of histones than the WT, and we were able to show that a single CWA protein, FnBPB, was responsible for this interaction. The N2–N3 region of FnBPB bound specifically to CTH *in vitro*, although the most closely related surface proteins, such as FnBPA and ClfA, did not. When FnBPB binding to individual histones was tested, it was found that all types could bind but that H3 displayed the highest binding and bactericidal activity. We found that H3 binds to the N2N3 region of FnBPB, most likely by the dock, lock, and latch mechanism used to bind FBG (Fig. 13), because variants lacking the ability to bind FBG were also defective in H3 binding. To prove that the DLL mechanism is involved in the binding of FnBPB to H3, co-crystallization of FnBPB(163–480) in complex with H3 could be carried out. Notably, FnBPB has a 20-fold higher affinity for H3 than FBG suggesting that in plasma or other environments where FBG is present, FnBPB would bind H3 preferentially. Furthermore, increasing ionic strength had a dramatic effect on FnBPB binding to H3, indicating that H3/FnBPB complex formation is mainly driven by electrostatic interactions.

The specificity of the interaction between FnBPB(163–480) and H3 was demonstrated by capture ELISA, gel filtration, and surface plasmon resonance, which together indicate that the proteins form a complex even in the fluid phase. The almost identical susceptibility of *S. aureus* LAC and its *fnbB* mutants to the treatment with H4 suggests a specific role of FnBPB in the protection of bacteria by H3. The data obtained with *srtA* mutant also showed that H4 interacts with a bacterial surface component other than FnBPB and exhibits a toxicity for staphylococcal cells at a level equivalent to H3. This effect is consistent with the finding that histone H4 is an important component of the antimicrobial action of human sebocytes against *S. aureus* (46).

Seven different isoforms of FnBPB can bind to H3, but some have a higher affinity than others. This paper focused on *S. aureus* strain LAC, which expresses isoform I FnBPB. This isoform binds H3 strongly *in vitro* (K_D of 50 nM). It is noteworthy that strain P1 that expresses the apparently weaker binding FnBPB isoform IV (apparent K_D of 636.7 nM as estimated from ELISA) is protected to the same extent as LAC from the bactericidal activity. With respect with this point, it would be interesting to compare mutants of strains expressing other isoforms.

FnBPB can also bind to PLG at a site that does not overlap that of FBG. Indeed, FnBPB can bind both ligands independently (22). In a similar fashion, FnBPB can bind PLG to the same extent in the presence of H3 as in its absence. Indeed, bound PLG could be activated to plasmin by t-PA and rapidly degraded H3.

Previously, we showed that the double Δ*fnbAfnbB* mutant of *S. aureus* LAC still binds to PLG, which indicates that additional surface components can bind PLG (22). Consistent with this, we found that PLG captured by the Δ*fnbAfnbB* mutant efficiently digests H3 proving that, whatever the staphylococcal receptor, PLG retains its proteolytic potential. Importantly, cleavage of H3 by PLG was not affected by the presence of FBG, suggesting that even in closer physiological conditions H3 is degraded by PLG.

Summing up, we propose that FnBPB contributes to protection of *S. aureus* (i) by capturing/scavenging histones and preventing them from reaching the membrane and (ii) by promoting their degradation by binding PLG, which is activated by exogenously or endogenously expressed PLG activators (Fig. 13). It is unknown whether these mechanisms are operational *in vivo*. Thus, definition of the role of FnBPB and PLG as inhibitors of the bactericidal activity of H3 in animal models may be worth exploring.

In a study by Nitzsche *et al.* (34), *S. pyogenes* serotype M49 has been shown to protect itself from histone-killing through PLG acquisition and activation by streptokinase. However, the question was not addressed whether the M49 protein is directly involved in PLG and/or histone binding (34). Along this line, *Finegoldia magna*, a Gram-positive commensal of the skin and mucous membranes, binds histones extracted from human skin through the surface protein FAF (*F. magna* adhesion factor), and histones were found to be degraded by SufA (subtilase of *F. magna*), a subtilisin-like extracellular serine protease of

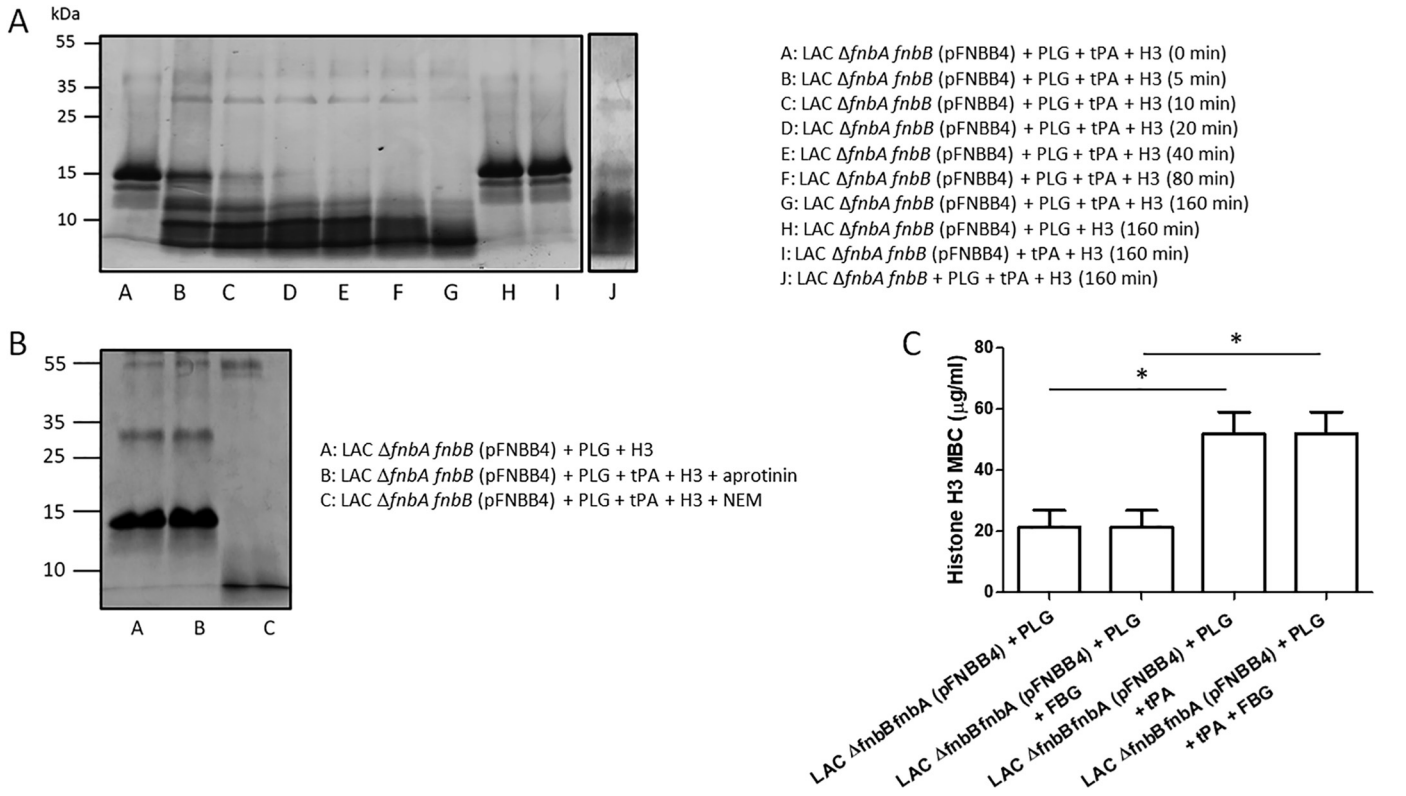

Figure 12. Specificity of H3 cleavage by bacteria-bound plasmin. *A,* cells of *S. aureus* LAC Δ*fnbAfnbB* mutant overexpressing FnBPB were immobilized on the surface of microtiter plates and then incubated with human PLG. After washing, t-PA and histone H3 were added to the wells and incubated for increasing periods of time. Supernatants were subjected to SDS-PAGE and the gels stained with Coomassie Blue. Controls made of mixtures without PLG or t-PA are reported. The effect of activated PLG captured by the Δ*fnbAfnbB* mutant cells on H3 cleavage is also reported. The figure is representative of two independent experiments. *B,* to demonstrate the specificity of proteolysis, immobilized bacteria were incubated with PLG, and t-PA and H3 were added and further incubated in the presence of aprotinin or NEM. Supernatants were then analyzed for H3 cleavage by SDS-PAGE. *C,* cells of the *S. aureus* LAC Δ*fnbAfnbB* mutant overexpressing FnBPB were mixed with human PLG, added to serial 1.3-fold diluted histone H3 in the presence/absence of t-PA, and incubated for additional periods of time. The MBC of histone H3 was determined by plating serial dilutions of bacteria on BHI agar. To analyze the effect of FBG on H3 cleavage by activated PLG, bacteria preincubated with PLG were mixed with equimolar concentrations of H3 and FBG and processed as above. The reported data are the mean values ± S.D. from three independent experiments. Statistically significant differences are indicated (Student's *t* test; *, $p < 0.05$).

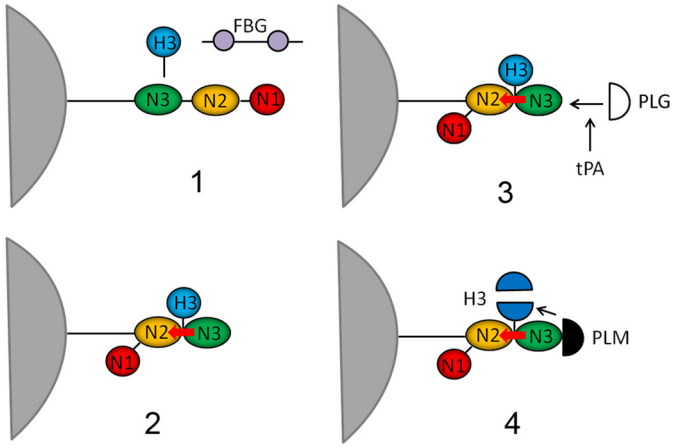

Figure 13. Proposed model of FnBPB in binding and inactivation of histone H3. The figure shows a sequence of events (numbered from *1* to *4*) involving FnBPB expressed on the surface of *S. aureus.* At first, in preference to fibrinogen, H3 binds to the trench between the N2 and N3 subdomains of FnBPB, and once in place it induces a conformational change that enables C-terminal residues of the N3 extension (*red arrow*) to be inserted into the trench and to stabilize the complex (dock, lock, and latch mechanism). Then, plasminogen (*PLG*) (*open semicircle*) binds to a site on N3 subdomain and once activated by t-PA to plasmin (*PLM*) (*solid semicircle*) cleaves FnBPB-bound H3.

F. magna (47). Thus, different bacterial species, including *S. aureus,* may use similar strategies to neutralize the antibacterial activity of histones.

It is clear that FnBPB is the major histone-binding cell wall–anchored surface protein expressed by *S. aureus* LAC under the *in vitro* growth conditions employed here. By using genetically manipulated strains, FnBPB expression was shown to be responsible for binding H3 and protecting *S. aureus* from the bactericidal effects of H3 or the total histones released by neutrophils when NETs were formed. Effects were severely reduced in the Δ*fnbAfnbB* mutant and, importantly, were enhanced to a greater extent than in the WT strain when FnBPB was expressed at enhanced levels from a multicopy plasmid. Loss of FnBPB reduced the bactericidal effect of H3 toward several other *S. aureus* strains. It could be argued that protecting *S. aureus* cells from traps extruded from the myeloid cell is the most important function of the A region of FnBPB given the high affinity of FnBPB for histones.

The WT LAC is efficiently killed by a relatively low dose of H3 (MBC: 5 μg/ml). Additionally, as reported previously, histones are expressed and extruded in NETs in abundant amounts, estimated at 2.5 $\mu g/10^6$ neutrophils, such that his-

Table 1
Bacterial strains
Abbreviations used are as follows: *Erm*^{r}, erythromycin resistance; *Tc*^{r}, tetracycline resistance.

Bacterial strains	Relevant properties	Refs.
S. aureus LAC	Community-associated MRSA of USA300 lineage	8
S. aureus LAC *srtA*	Constructed by the transduction of *srtA::Erm*^{r} from Newman *srtA* (39) using bacteriophage 85	This study
S. aureus LAC *clfA*	Constructed by the transduction of *clfA::Erm*^{r} from Newman *clfA* (51) using bacteriophage 85	This study
S. aureus LAC Δ*fnbAfnbB*	Deletion of *fnbA* and *fnbB* genes isolated by allelic exchange	40
S. aureus LAC Δ*fnbAfnbB* (pFNBA4)	Mutant transformed with plasmid-expressing FnBPA	40
S. aureus LAC Δ*fnbAfnbB* (pFNBB4)	Mutant transformed with plasmid-expressing FnBPB	40
S. aureus BH1CC	Hospital-associated MRSA	4
S. aureus BH1CC Δ*fnbAfnbB*	*fnbA::Tc*^{r} *fnbB::Erm*^{r} mutations transduced from 8325-4 *fnbA fnbB*	4
S. aureus P1	Rabbit passaged strain derived from ATCC25923	44
S. aureus P1 Δ*fnbAfnbB*	*fnbA::Tc*^{r} *fnbB::Er20m*^{r} mutations transduced from 8325-4 *fnbAfnbB*	21
S. aureus 8325-4	NCTC8325 cured of three prophages	42
S. aureus 8325-4 Δ*fnbAfnbB*	*fnbA::Tc*^{r} *fnbB::Erm*^{r} mutations isolated by allelic exchange	45
S. aureus SH1000	rbsU restored in 8325-4	43
S. aureus SH1000 Δ*fnbAfnbB*	*fnbA::Tc*^{r} *fnbB::Erm*^{r}mutations transduced from 8325-4 *fnbA fnbB*	22

tones comprise more than two-thirds of the protein content within the NET structure (48). This information raises the question whether inhibition by FnBPB of histone-mediated bacterial killing is biologically significant. Notably, data reported here show that FnBPB protects staphylococci from killing by NETs, demonstrating that FnBPB-mediated resistance is important when H3 is present in a biologically relevant milieu. It is possible that other factors present in the NETs could down-regulate the bactericidal activity of histones. Among these, entrapment of histones by DNA might contribute to the reduction of bioavailability of histones in NETs and facilitate the histone-scavenging activity of FnBPB. Consideration should be also given to the fact that H3 is a fractional component (20%) of the total amount of histones in the NETs (48), and this could enhance the efficacy of the neutralizing activity of FnBPB.

Recently, it has been demonstrated that *S. aureus* extracellular protein Eap shows a neutrophil serine protease inhibitor activity in association with NET functions (49) and binds and aggregates DNA, thus blocking neutrophil extracellular trap formation (50). With this study, FnBPB is added to the list of potential factors that inhibit this important mechanism of host innate defense.

Other bacterial species block the killing activity of NETs through the neutralization of histones. For example, Dörhmann *et al.* (35) have shown the antimicrobial activity of histones against group A streptococci belonging to different serotypes. In particular, the surface-expressed M1 protein, a classical virulence factor of this pathogen, was required to bind and inactivate extracellular histones in NETs, deploying an FnBPB-like evasion strategy (35). Interestingly, soluble FnBPB(163–480) neutralized the ability of H3 to interact with and subsequently kill *S. aureus* as well as *S. pyogenes*. Hence, one can envisage the development of therapeutic derivatives of this protein.

In conclusion, we have shown that FnBPB is the dominant binding protein for capturing histone H3 by *S. aureus* and conferring resistance to the bacterium against the antimicrobial activity of histones. We have also investigated the molecular details of the histones binding to such an important virulence factor.

Experimental procedures

Bacterial strains and culture conditions

All strains are listed in Table 1. *S. aureus* was grown in Brain Heart Infusion broth (VWR International Srl, Milan, Italy) to mid-exponential phase (OD = 0.4) at 37 °C with shaking. The *S. pyogenes* serotype M1 strain 71-675 was received from Professor Bernd Kreikemeyer (Rostock, Germany). Bacteria were cultured in Todd-Hewitt broth supplemented with yeast extract at 37 °C with shaking.

In those experiments, where a defined number of cells were used, bacteria were harvested from the cultures by centrifugation, washed, suspended in PBS, and counted in a Petroff-Hausser chamber. *Escherichia coli* TOPP3 transformed with vector pQE30 (Stratagene, La Jolla, CA) or derivatives was grown in Luria agar and Luria broth (VWR International Srl, Milan, Italy) containing 100 μg/ml ampicillin. *S. aureus* LAC *srtA* was constructed by the transduction of *srtA::Erm*^{r} from Newman *srtA* (39) using bacteriophage 85. *S. aureus* LAC *clfA* was constructed by the transduction of *clfA::Erm*^{r} from Newman *clfA* using bacteriophage 85 (51).

DNA manipulation

DNA manipulation was performed as previously reported (22).

Expression and purification of recombinant proteins

Recombinant proteins FnBPB(163–308), FnBPB(309–480), and FnBPB(163–463) latch-truncated were expressed from pQE30 (Qiagen, Chatsworth, CA) in *E. coli* TOPP3 (Stratagene), as reported previously (22).

Recombinant FnBPB isotypes (20), FnBPB(163–480) N312A/F314A trench mutant (16), FnBPA(194–511) (15), CNA(31–344) (52), ClfA(221–559) (53), ClfB(201–542) (54), Bbp(40–599) (55), and Pls(49–694) (56), were each previously expressed with His_6 N-terminal affinity tags using *E. coli* vectors and purified on a HiTrap chelating column (GE Healthcare, Buckinghamshire, UK) by Ni^{2+}-chelate chromatography as described above. Protein purity was assessed to be 98% by SDS-PAGE, Coomassie Brilliant Blue staining, and densitometry analysis. A bicinchoninic acid protein assay (Pierce) was used to measure concentrations of purified proteins.

Proteins and reagents

Protease-free DNase I, BSA (BSA), skim milk, CTH, and human histones H1, H2A, H2B, H3, and H4 were purchased from Sigma.

Antibodies

Rabbit anti-mouse and goat anti-rabbit horseradish peroxidase (HRP)-conjugated secondary antibodies were purchased from Dako Cytomation (Glostrup, Denmark). Anti-human histone antibody was purchased from USBiological (Salem, MA). Polyclonal antiserum against FnBPB(163–480) was raised in a rabbit by routine immunization procedure using purified FnBPB(163–480) as antigen.

7E8 is an in-house–generated murine mAb recognizing recombinant His-tagged proteins. To validate ELISAs, where different His-tagged bacterial proteins were assessed for reactivity to antibody 7E8, increasing amounts of His-tagged CWA proteins, variants of FnBPB(163–480), or isoforms of FnBPB(163–480) were immobilized, and bound 7E8 was detected using HRP-conjugated rabbit anti-mouse IgG.

ELISA type solid-phase binding assays

The ability of soluble recombinant *S. aureus* proteins to bind to immobilized CTH or individual histones was determined using ELISA-type assays. Microtiter wells were coated overnight at 4 °C with 0.5 μg/well of CTH or individual histones in 0.1 M sodium carbonate, pH 9.5. The plates were washed with 0.5% (v/v) Tween 20 in PBS (PBST). To block additional protein-binding sites, the wells were treated for 1 h at 22 °C with bovine serum albumin (BSA) 2% (v/v) in PBS. The plates were then incubated for 1 h with 0.5 μmol of each ligand. After several washes with PBST, 0.5 μg of the specific mouse anti-hexahistidine tag mAb 7E8 in BSA (1% v/v) was added to the wells and incubated for 90 min. The plates were washed and incubated for 1 h with HRP-conjugated rabbit anti-mouse IgG diluted 1:1000. After washing, *o*-phenylenediamine dihydrochloride was added, and the absorbance at 490 nm was determined using an ELISA plate reader.

In some ELISA-type assays, a primary rabbit antibody binding was detected incubating the wells with HRP-conjugated goat anti-rabbit IgG secondary antibody. To calculate the relative affinity association constant (K_A), values of each FnBPB isoform for H3 histone, the data were fitted using Equation 1,

$$A = A_{max}[L]K_A/(1 + K_A[L]) \quad \text{(Eq. 1)}$$

where [L] is the molar concentration of isoform. The reported dissociation constants (K_D values) were calculated as reciprocals of the K_A values.

To determine the effect of ionic strength on the H3–FnBPB interaction, microtiter wells coated with 500 ng of H3 were incubated with 1 μg/well of FnBPB(163–480) diluted in a phosphate buffer containing increasing concentrations of NaCl (0.15–2.3 M). Complex formation was detected by incubation of the wells with a rabbit anti-FnBPB antibody, followed by HRP-conjugated goat anti-rabbit secondary antibody.

Adherence of bacteria to surface-coated CTH or histone H3 was performed by incubating immobilized histones (2 μg/well) with log-phase *S. aureus* cells (10^8) for 2 h at 37 °C. After several washings with PBS, adherent cells were fixed with 2.5% formaldehyde for 30 min and stained with 1% crystal violet for 1 min. After washing with PBS, 100 μl of 10% acetic acid was added to the wells, and absorbance at 595 nm was recorded in an ELISA plate reader.

Size-exclusion chromatography analysis of the interaction of FnBPB(163–480) with histone H3

Samples of FnBPB(163–480), histone H3, and mixtures of co-incubated equimolar amounts of FnBPB(163–480) (or FnBPB(163–480) trench mutant variant (N312A/F314A)) and H3 were loaded onto a 75 10/300 GL gel-filtration chromatography column of Superdex (Vt = 24 ml). The column, equilibrated with PBS, was eluted with the same buffer at a flow rate of 0.75 ml/min. To calibrate the column, standard proteins (GE Healthcare) were allowed to pass through the column, and their partition coefficient K_{av} was plotted against the logarithm of the molecular weight.

Cleavage of histone H3 (or FnBPB) by S. aureus-associated activated plasminogen

5×10^7 cells of log-phase *S. aureus* LAC Δ*fnbAfnbB* (pFNBB4) or double Δ*fnbAfnbB* mutant were immobilized on the surface of microtiter plates and then incubated with human PLG (1 μg/well) for 1 h at 37 °C. After several washes, cell-coated wells were added with 27 nM t-PA and histone H3 (5 μg/well), and the mixtures were incubated at 22 °C for increasing periods of time (5–160 min). Supernatants containing cleaved histone H3 were subjected to 15% SDS-PAGE, and the gels were stained with Coomassie Brilliant Blue (see below).

To assess the specific activation of PLG to plasmin, surface-coated *S. aureus* LAC Δ*fnbAfnbB* (pFNBB4) was incubated with PLG, t-PA, and H3 in the presence of 5 μg/ml aprotinin or 100 μM NEM for 160 min, and the supernatants were subjected to 15% SDS-PAGE, as reported above.

To evaluate the possible cleavage of surface-expressed FnBPB by bacteria-bound plasmin, immobilized *S. aureus* cells were incubated with PLG and t-PA for 160 min, as reported above. Supernatant containing released material was subjected to 12.5% SDS-PAGE, and the proteins were transferred to a nitrocellulose membrane. The membrane was sequentially probed with a rabbit anti-FnBPB IgG and HRP-conjugated goat anti-rabbit IgG.

Capture of histone H3 by S. aureus cells

Log-phase *S. aureus* strain USA 300 LAC, the double mutant Δ*fnbAfnbB,* or the mutants transformed with plasmid overexpressing FnBPB or FnBPA (10^8 cells/ml) were mixed with 10 μg of histone H3 for 10 min. Bacteria were then harvested by centrifugation, washed with PBS, and treated with the extraction buffer (125 mM Tris-HCl, pH 7.0, containing 2% SDS) for 3 min at 95 °C and then centrifuged at 10,000 × *g* for 3 min. The supernatants were subjected to SDS-PAGE under nonreducing conditions, and the proteins were transferred to a nitrocellulose membrane. The membrane was sequentially probed with rabbit anti-histone IgG and HRP-conjugated goat anti-rabbit IgG (see below).

SDS-PAGE, Western immunoblotting, and far Western immunoblotting

Digestion products of histone H3 were boiled for 3 min in sample buffer (0.125 M Tris-HCl, 4% (w/v) SDS, 20% (v/v) glycerol, 10% (v/v) β-mercaptoethanol, 0.002% (w/v) bromphenol blue) and separated by 15% (w/v) SDS-PAGE. The gels were stained with Coomassie Brilliant Blue (Bio-Rad, Milan, Italy).

For Western immunoblotting, histone H3 captured and released from the bacterial cell surface was subjected to 15% SDS-PAGE and electroblotted onto a nitrocellulose membrane (GE Healthcare), and the membrane was blocked overnight at 4 °C with 5% (w/v) skim milk (Sigma) in PBS. Blotted proteins were probed with rabbit polyclonal anti-histone (1:5000) for 1 h at 22 °C. Following washes with PBST, the membrane was incubated for 1 h with HRP-conjugated goat anti-rabbit IgG (1:10,000). Finally, the blot was developed using the ECL Advance Western blotting detection kit (GE Healthcare), and an ImageQuant™ LAS 4000 mini-biomolecular imager (GE Healthcare) was used to capture images of the bands. The band intensities were quantified relative to the histone H3 (5 μg, 100% intensity) with the Quantity One software (Bio-Rad).

For far Western immunoblotting, the individual histones were subjected to 15% SDS-PAGE and electroblotted onto a nitrocellulose membrane (GE Healthcare), and the membrane was blocked overnight at 4 °C with 5% (w/v) skim milk in PBS. The membrane was probed with 1 μg/ml FnBPB(163–480) for 1 h at 22 °C followed by rabbit anti-FnBPB(163–480) polyclonal antibody (1:5000) and with HRP-conjugated goat anti-rabbit IgG (1:10,000), and the complexes were detected as reported above.

Surface plasmon resonance analysis of FnBPB binding to histone H3

To estimate the affinity of the interaction between H3 and FnBPB(163–480), surface plasmon resonance was conducted using a BIAcore X-100 instrument (GE Healthcare). Histone H3 was covalently immobilized on dextran matrix CM5 sensor chip surface by using a histone H3 solution (30 μg/ml in 50 mM sodium acetate buffer, pH 5) in a 1:1 dilution with *N*-hydroxysuccinimide and 1-ethyl-3-(3-dimethylaminopropyl) carbodiimide hydrochloride. The excess of active groups on the dextran matrix was blocked using 1 M ethanolamine, pH 8.5. On another flow cell, the dextran matrix was treated as described above but without any ligand to provide an uncoated reference flow cell. The running buffer used was PBS containing 0.005% (v/v) Tween 20. A 2-fold linear dilution series (3.9–500 nM) of FnBPB(163–480), in running buffer, was passed over the ligand at the flow rate of 10 μl/min, and all the sensorgrams were recorded at 22 °C. Assay channel data were subtracted from reference flow cell data. The response units at steady state were plotted as a function of FnBPB(163–480) concentration and fitted to the Langmuir equation to yield the K_D values.

Isolation of neutrophils

Neutrophils were isolated from healthy donors using PolyMorphPrep solution (ThermoFisher Scientific) as described by Kristian *et al.* (57). Viability of neutrophils was assessed using 0.004% trypan blue staining by light microscopy.

NET-mediated killing of bacteria

Killing of bacteria by NETs was performed as reported previously (41). Briefly, 10^5 neutrophils were seeded into a 96-well plate and stimulated with 25 nM PMA for 4 h to induce NETosis. Log-phase bacteria were washed twice and added to neutrophils at a multiplicity of infection of 1 and incubated for 15 min at 37 °C, 5% CO_2. To evaluate the role of DNA in NET-mediated killing of bacteria, NETs were degraded prior to infection with 2 units of DNase I for 10 min at 37 °C. The bactericidal activity of histones was blocked prior to infection with 2 μg/ml anti-human histone antibody for 30 min. In both cases, neutrophils were washed once prior to challenge. Colony-forming units were enumerated by plating onto brain heart infusion (BHI) the cells suspension. Bacterial survival was calculated as percentage of the initial inoculum.

Determination of histone minimal bactericidal concentrations

Resistance of *S. aureus* USA 300 LAC to individual histones was determined in a minimum bactericidal concentration (MBC) assay incubating bacteria (1×10^8) with 1.3-fold diluted histone starting from 60 to 0.93 μg/ml. The MBC value of H3 for *S. pyogenes* strain 71-675 was determined by using 1.3-fold dilution of histone starting from 400 to 29 μg/ml. After 2 h of incubation at 37 °C, serial dilutions of cell mixtures were plated on BHI agar, and bacterial colonies counts were determined the day after. The MBC was calculated by determining the lowest concentration of each histone that reduced the viability of the initial bacterial *inoculum* by ≥99.9%. The MBC of H4 for WT LAC and its mutants was evaluated as reported above. To determine the neutralizing effect of soluble FnBPB(163–480) and its mutated variants on killing by H3, the MBC of H3 for *S. aureus* Δ*fnbAfnbB* was determined in the presence of 1 μM FnBPB proteins. A similar experimental protocol was used to measure the effect of FnBPB(163–480) on MBC of H3 for *S. pyogenes* strain 71-675 in the presence of 5 μM FnBPB(163–480).

Determination of the protective effect of plasminogen on S. aureus from the bactericidal activity of histone H3

Log-phase cells of *S. aureus* LAC Δ*fnbAfnbB* (pFNBB4) (2×10^5/ml) were incubated with human PLG (10 μg) for 1 h. Cells were harvested by centrifugation, washed with PBS, and then incubated with serial 1.3-fold diluted histone H3 (from 100 to 0.78 μg/ml) in the presence/absence of t-PA (27 nM) for 2 h at 37 °C. In those experiments where the effect of fibrinogen on H3 cleavage by activated PLG captured by staphylococci was assessed, equimolar concentrations of H3 and fibrinogen were incubated with PLG captured by staphylococci, and the mixtures were processed as above.

To determine the MBC of histone H3, serial dilutions of the mixtures were plated on BHI agar and incubated at 37 °C overnight. Bacterial counts were determined the day after.

Statistical methods

Continuous data were expressed as means and standard deviations. Two group comparisons were performed by Student's *t* test. One-way analysis of variance, followed by Bonferroni's post hoc tests, was exploited for comparison of three

or more groups. Analyses were performed using Prism 4.0 (GraphPad). Two-tailed p values of 0.05 were considered statistically significant.

Author contributions—G. P., T. J. F., J. A. G., V. D. F., and P. S. conceptualization; G. P. and P. S. resources; G. P. and P. S. data curation; G. P., G. N., M. J. A., and P. S. formal analysis; G. P. and P. S. supervision; G. P., G. N., and P. S. validation; G. P., M. J. A., and P. S. investigation; G. P. and P. S. visualization; G. P., G. N., M. J. A., T. J. F., and P. S. methodology; G. P., V. D. F., and P. S. writing-original draft; G. P., T. J. F., J. A. G., V. D. F., and P. S. writing-review and editing; V. D. F. and P. S. funding acquisition.

Acknowledgments—We thank Dara P. O'Halloran for constructing the LAC srtA mutant and Leanne M. Hays for constructing the LAC clfA mutant.

References

1. Chambers, H. F. (2005) Community-associated MRSA-resistance and virulence converge. *N. Engl. J. Med.* **352,** 1485–1487 CrossRef Medline
2. Lowy, F. D. (1998) *Staphylococcus aureus* infections. *N. Engl. J. Med.* **339,** 520–532 CrossRef Medline
3. Noskin, G. A., Rubin, R. J., Schentag, J. J., Kluytmans, J., Hedblom, E. C., Smulders, M., Lapetina, E., and Gemmen, E. (2005) The burden of *Staphylococcus aureus* infections on hospitals in the United States: an analysis of the 2000 and 2001 Nationwide Inpatient Sample Database. *Arch. Intern. Med.* **165,** 1756–1761 CrossRef Medline
4. O'Neill, E., Pozzi, C., Houston, P., Humphreys, H., Robinson, D. A., Loughman, A., Foster, T. J., and O'Gara, J. P. (2008) A novel *Staphylococcus aureus* biofilm phenotype mediated by the fibronectin-binding proteins, FnBPA and FnBPB. *J. Bacteriol.* **190,** 3835–3850 CrossRef Medline
5. Vergara-Irigaray, M., Valle, J., Merino, N., Latasa, C., García, B., Ruiz de Los Mozos, I., Solano, C., Toledo-Arana, A., Penadés, J. R., and Lasa, I. (2009) Relevant role of fibronectin-binding proteins in *Staphylococcus aureus* biofilm-associated foreign-body infections. *Infect. Immun.* **77,** 3978–3991 CrossRef Medline
6. Fridkin, S. K., Hageman, J. C., Morrison, M., Sanza, L. T., Como-Sabetti, K., Jernigan, J. A., Harriman, K., Harrison, L. H., Lynfield, R., Farley, M. M., and Active Bacterial Core Surveillance Program of the Emerging Infections Program Network. (2005) Methicillin-resistant *Staphylococcus aureus* disease in three communities. *N. Engl. J. Med.* **352,** 1436–1444 CrossRef Medline
7. Moran, G. J., Krishnadasan, A., Gorwitz, R. J., Fosheim, G. E., McDougal, L. K., Carey, R. B., Talan, D. A., and EMERGEncy ID Net Study Group. (2006) Methicillin-resistant *S. aureus* infections among patients in the emergency department. *N. Engl. J. Med.* **355,** 666–674 CrossRef Medline
8. Diep, B. A., Gill, S. R., Chang, R. F., Phan, T. H., Chen, J. H., Davidson, M. G., Lin, F., Lin, J., Carleton, H. A., Mongodin, E. F., Sensabaugh, G. F., and Perdreau-Remington, F. (2006) Complete genome sequence of USA300, an epidemic clone of community-acquired methicillin-resistant *Staphylococcus aureus*. *Lancet* **367,** 731–739 CrossRef Medline
9. Otto, M. (2013) Community-associated MRSA: what makes them special? *Int. J. Med. Microbiol.* **303,** 324–330 CrossRef Medline
10. Foster, T. J. (2017) Antibiotic resistance in *Staphylococcus aureus.* Current status and future prospects. *FEMS Microbiol. Rev.* **41,** 430–449 CrossRef Medline
11. Foster, T. J. (2019) Can β-lactam antibiotics be resurrected to combat MRSA? *Trends Microbiol.* **27,** 26–38 CrossRef Medline
12. Foster, T. J., Geoghegan, J. A., Ganesh, V. K., and Höök, M. (2014) Adhesion, invasion and evasion: the many functions of the surface proteins of *Staphylococcus aureus*. *Nat. Rev. Microbiol.* **12,** 49–62 CrossRef Medline
13. Marraffini, L. A., Dedent, A. C., and Schneewind, O. (2006) Sortases and the art of anchoring proteins to the envelopes of Gram-positive bacteria. *Microbiol. Mol. Biol. Rev.* **70,** 192–221 CrossRef Medline
14. Loughman, A., Sweeney, T., Keane, F. M., Pietrocola, G., Speziale, P., and Foster, T. J. (2008) Sequence diversity in the A domain of *Staphylococcus aureus* fibronectin-binding protein A. *BMC Microbiol.* **8,** 74 CrossRef Medline
15. Keane, F. M., Loughman, A., Valtulina, V., Brennan, M., Speziale, P., and Foster, T. J. (2007) Fibrinogen and elastin bind to the same region within the A domain of fibronectin binding protein A, an MSCRAMM of *Staphylococcus aureus*. *Mol. Microbiol.* **63,** 711–723 Medline
16. Burke, F. M., Di Poto, A., Speziale, P., and Foster, T. J. (2011) The A domain of fibronectin-binding protein B of *Staphylococcus aureus* contains a novel fibronectin binding site. *FEBS J.* **278,** 2359–2371 CrossRef Medline
17. Deivanayagam, C. C., Wann, E. R., Chen, W., Carson, M., Rajashankar, K. R., Höök, M., and Narayana, S. V. (2002) A novel variant of the immunoglobulin fold in surface adhesins of *Staphylococcus aureus*: crystal structure of the fibrinogen-binding MSCRAMM, clumping factor A. *EMBO J.* **21,** 6660–6672 CrossRef Medline
18. Ponnuraj, K., Bowden, M. G., Davis, S., Gurusiddappa, S., Moore, D., Choe, D., Xu, Y., Hook, M., and Narayana, S. V. (2003) A "dock, lock, and latch" structural model for a staphylococcal adhesin binding to fibrinogen. *Cell* **115,** 217–228 CrossRef Medline
19. Bowden, M. G., Heuck, A. P., Ponnuraj, K., Kolosova, E., Choe, D., Gurusiddappa, S., Narayana, S. V., Johnson, A. E., and Höök, M. (2008) Evidence for the "dock, lock, and latch" ligand binding mechanism of the staphylococcal microbial surface component recognizing adhesive matrix molecules (MSCRAMM) SdrG. *J. Biol. Chem.* **283,** 638–647 CrossRef Medline
20. Burke, F. M., McCormack, N., Rindi, S., Speziale, P., and Foster, T. J. (2010) Fibronectin-binding protein B variation in *Staphylococcus aureus*. *BMC Microbiol.* **10,** 160 CrossRef Medline
21. Roche, F. M., Downer, R., Keane, F., Speziale, P., Park, P. W., and Foster, T. J. (2004) The N-terminal A domain of fibronectin-binding proteins A and B promotes adhesion of *Staphylococcus aureus* to elastin. *J. Biol. Chem.* **279,** 38433–38440 CrossRef Medline
22. Pietrocola, G., Nobile, G., Gianotti, V., Zapotoczna, M., Foster, T. J., Geoghegan, J. A., and Speziale, P. (2016) Molecular interactions of human plasminogen with fibronectin-binding protein B (FnBPB), a fibrinogen/fibronectin-binding protein from *Staphylococcus aureus*. *J. Biol. Chem.* **291,** 18148–18162 CrossRef Medline
23. Geoghegan, J. A., Monk, I. R., O'Gara, J. P., and Foster, T. J. (2013) Subdomains N2N3 of fibronectin binding protein A mediate *Staphylococcus aureus* biofilm formation and adherence to fibrinogen using distinct mechanisms. *J. Bacteriol.* **195,** 2675–2683 CrossRef Medline
24. Schwarz-Linek, U., Werner, J. M., Pickford, A. R., Gurusiddappa, S., Kim, J. H., Pilka, E. S., Briggs, J. A., Gough, T. S., Höök, M., Campbell, I. D., and Potts, J. R. (2003) Pathogenic bacteria attach to human fibronectin through a tandem β-zipper. *Nature* **423,** 177–181 CrossRef Medline
25. Meenan, N. A., Visai, L., Valtulina, V., Schwarz-Linek, U., Norris, N. C., Gurusiddappa, S., Höök, M., Speziale, P., and Potts, J. R. (2007) The tandem β-zipper model defines high affinity fibronectin-binding repeats within *Staphylococcus aureus* FnBPA. *J. Biol. Chem.* **282,** 25893–25902 CrossRef Medline
26. Sollberger, G., Tilley, D. O., and Zychlinsky, A. (2018) Neutrophil extracellular traps: the biology of chromatin externalization. *Dev. Cell* **44,** 542–553 CrossRef Medline
27. Xu, J., Zhang, X., Pelayo, R., Monestier, M., Ammollo, C. T., Semeraro, F., Taylor, F. B., Esmon, N. L., Lupu, F., and Esmon, C. T. (2009) Extracellular histones are major mediators of death in sepsis. *Nat. Med.* **15,** 1318–1321 CrossRef Medline
28. Schorn, C., Janko, C., Latzko, M., Chaurio, R., Schett, G., and Herrmann, M. (2012) Monosodium urate crystals induce extracellular DNA traps in neutrophils, eosinophils, and basophils but not in mononuclear cells. *Front. Immunol.* **3,** 277 Medline
29. Ueki, S., Melo, R. C., Ghiran, I., Spencer, L. A., Dvorak, A. M., and Weller, P. F. (2013) Eosinophil extracellular DNA trap cell death mediates lytic release of free secretion-competent eosinophil granules in humans. *Blood* **121,** 2074–2083 CrossRef Medline

30. Chow, O. A., von Köckritz-Blickwede, M., Bright, A. T., Hensler, M. E., Zinkernagel, A. S., Cogen, A. L., Gallo, R. L., Monestier, M., Wang, Y., Glass, C. K., and Nizet, V. (2010) Statins enhance formation of phagocyte extracellular traps. *Cell Host Microbe* **8,** 445–454 CrossRef Medline
31. Westman, J., Papareddy, P., Dahlgren, M. W., Chakrakodi, B., Norrby-Teglund, A., Smeds, E., Linder, A., Mörgelin, M., Johansson-Lindbom, B., Egesten, A., and Herwald, H. (2015) Extracellular histones Induce chemokine production in whole blood *ex vivo* and leukocyte recruitment *in vivo*. *PLoS Pathog.* **11,** e1005319 CrossRef Medline
32. DeLange, R. J., and Smith, E. L. (1971) Histones: structure and function. *Annu. Rev. Biochem.* **40,** 279–314 CrossRef Medline
33. Morita, S., Tagai, C., Shiraishi, T., Miyaji, K., and Iwamuro, S. (2013) Differential mode of antimicrobial actions of arginine-rich and lysine-rich histones against Gram-positive *Staphylococcus aureus*. *Peptides* **48,** 75–82 CrossRef Medline
34. Nitzsche, R., Köhler, J., Kreikemeyer, B., and Oehmcke-Hecht, S. (2016) *Streptococcus pyogenes* escapes killing from extracellular histones through plasminogen binding and activation by streptokinase. *J. Innate Immun.* **8,** 589–600 CrossRef Medline
35. Döhrmann, S., LaRock, C. N., Anderson, E. L., Cole, J. N., Ryali, B., Stewart, C., Nonejuie, P., Pogliano, J., Corriden, R., Ghosh, P., and Nizet, V. (2017) Group A streptococcal M1 protein provides resistance against the antimicrobial activity of histones. *Sci. Rep.* **7,** 43039 CrossRef Medline
36. Chaput, C., Spindler, E., Gill, R. T., and Zychlinsky, A. (2013) O-antigen protects Gram-negative bacteria from histone killing. *PLoS ONE* **8,** e71097 CrossRef Medline
37. Rose-Martel, M., and Hincke, M. T. (2014) Antimicrobial histones from chicken erythrocytes bind bacterial cell wall lipopolysaccharides and lipoteichoic acids. *Int. J. Antimicrob. Agents* **44,** 470–472 CrossRef Medline
38. Westman, J., Chakrakodi, B., Snäll, J., Mörgelin, M., Bruun Madsen, M., Hyldegaard, O., Neumann, A., Frick, I. M., Norrby-Teglund, A., Björck, L., and Herwald, H. (2018) Protein SIC secreted from *Streptococcus pyogenes* forms complexes with extracellular histones that boost cytokine production. *Front. Immunol.* **9,** 236 CrossRef Medline
39. Mazmanian, S. K., Liu, G., Ton-That, H., and Schneewind, O. (1999) *Staphylococcus aureus* sortase, an enzyme that anchors surface proteins to the cell wall. *Science* **285,** 760–763 CrossRef Medline
40. McCourt, J., O'Halloran, D. P., McCarthy, H., O'Gara, J. P., and Geoghegan, J. A. (2014) Fibronectin-binding proteins are required for biofilm formation by community-associated methicillin-resistant *Staphylococcus aureus* strain LAC. *FEMS Microbiol. Lett.* **353,** 157–164 CrossRef Medline
41. Corriden, R., Hollands, A., Olson, J., Derieux, J., Lopez, J., Chang, J. T., Gonzalez, D. J., and Nizet, V. (2015) Tamoxifen augments the innate immune function of neutrophils through modulation of intracellular ceramide. *Nat. Commun.* **6,** 8369 CrossRef Medline
42. Novick, R. (1967) Properties of a cryptic high-frequency transducing phage in *Staphylococcus aureus*. *Virology* **33,** 155–166 CrossRef Medline
43. Horsburgh, M. J., Aish, J. L., White, I. J., Shaw, L., Lithgow, J. K., and Foster, S. J. (2002) σB modulates virulence determinant expression and stress resistance: characterization of a functional rsbU strain derived from *Staphylococcus aureus* 8325-4. *J. Bacteriol.* **184,** 5457–5467 CrossRef Medline
44. Sherertz, R. J., Carruth, W. A., Hampton, A. A., Byron, M. P., and Solomon, D. D. (1993) Efficacy of antibiotic-coated catheters in preventing subcutaneous *Staphylococcus aureus* infection in rabbits. *J. Infect. Dis.* **167,** 98–106 CrossRef Medline
45. Greene, C., McDevitt, D., Francois, P., Vaudaux, P. E., Lew, D. P., and Foster, T. J. (1995) Adhesion properties of mutants of *Staphylococcus aureus* defective in fibronectin-binding proteins and studies on the expression of *fnb* genes. *Mol. Microbiol.* **17,** 1143–1152 CrossRef Medline
46. Lee, D. Y., Huang, C. M., Nakatsuji, T., Thiboutot, D., Kang, S. A., Monestier, M., and Gallo, R. L. (2009) Histone H4 is a major component of the antimicrobial action of human sebocytes. *J. Invest. Dermatol.* **129,** 2489–2496 CrossRef Medline
47. Murphy, E. C., Mohanty, T., and Frick, I. M. (2014) FAF and SufA: proteins of *Finegoldia magna* that modulate the antibacterial activity of histones. *J. Innate Immun.* **6,** 394–404 CrossRef Medline
48. Urban, C. F., Ermert, D., Schmid, M., Abu-Abed, U., Goosmann, C., Nacken, W., Brinkmann, V., Jungblut, P. R., and Zychlinsky, A. (2009) Neutrophil extracellular traps contain calprotectin, a cytosolic protein complex involved in host defense against *Candida albicans*. *PLoS Pathog.* **5,** e1000639 CrossRef Medline
49. Stapels, D. A., Ramyar, K. X., Bischoff, M., von Köckritz-Blickwede, M., Milder, F. J., Ruyken, M., Eisenbeis, J., McWhorter, W. J., Herrmann, M., van Kessel, K. P., Geisbrecht, B. V., and Rooijakkers, S. H. (2014) *Staphylococcus aureus* secretes a unique class of neutrophil serine protease inhibitors. *Proc. Natl. Acad. Sci. U.S.A.* **111,** 13187–13192 CrossRef Medline
50. Eisenbeis, J., Saffarzadeh, M., Peisker, H., Jung, P., Thewes, N., Preissner, K. T., Herrmann, M., Molle, V., Geisbrecht, B. V., Jacobs, K., and Bischoff, M. (2018) The *Staphylococcus aureus* extracellular adherence protein Eap is a DNA binding protein capable of blocking neutrophil extracellular trap formation. *Front. Cell. Infect. Microbiol.* **8,** 235 CrossRef Medline
51. McDevitt, D., Francois, P., Vaudaux, P., and Foster, T. J. (1994) Molecular characterization of the clumping factor (fibrinogen receptor) of *Staphylococcus aureus*. *Mol. Microbiol.* **11,** 237–248 CrossRef Medline
52. Zong, Y., Xu, Y., Liang, X., Keene, D. R., Höök, A., Gurusiddappa, S., Höök, M., and Narayana, S. V. (2005) A "Collagen Hug" model for *Staphylococcus aureus* CNA binding to collagen. *EMBO J.* **24,** 4224–4236 CrossRef Medline
53. O'Connell, D. P., Nanavaty, T., McDevitt, D., Gurusiddappa, S., Höök, M., and Foster, T. J. (1998) The fibrinogen-binding MSCRAMM (clumping factor) of *Staphylococcus aureus* has a Ca^{2+}-dependent inhibitory site. *J. Biol. Chem.* **273,** 6821–6829 CrossRef Medline
54. Mulcahy, M. E., Geoghegan, J. A., Monk, I. R., O'Keeffe, K. M., Walsh, E. J., Foster, T. J., and McLoughlin, R. M. (2012) Nasal colonization by *Staphylococcus aureus* depends upon clumping factor B binding to the squamous epithelial cell envelope protein loricrin. *PLoS Pathog.* **8,** e1003092 CrossRef Medline
55. Vazquez, V., Liang, X., Horndahl, J. K., Ganesh, V. K., Smeds, E., Foster, T. J., and Hook, M. (2011) Fibrinogen is a ligand for the *Staphylococcus aureus* microbial surface components recognizing adhesive matrix molecules (MSCRAMM) bone sialoprotein-binding protein (Bbp). *J. Biol. Chem.* **286,** 29797–29805 CrossRef Medline
56. Roche, F. M., Meehan, M., and Foster, T. J. (2003) The *Staphylococcus aureus* surface protein SasG and its homologues promote bacterial adherence to human desquamated nasal epithelial cells. *Microbiology* **149,** 2759–2767 CrossRef Medline
57. Kristian, S. A., Datta, V., Weidenmaier, C., Kansal, R., Fedtke, I., Peschel, A., Gallo, R. L., and Nizet, V. (2005) D-Alanylation of teichoic acids promotes group a streptococcus antimicrobial peptide resistance, neutrophil survival, and epithelial cell invasion. *J. Bacteriol.* **187,** 6719–6725 CrossRef Medline